2mit

CR-~~133454~~
134184

C-5A/ORBITER WIND TUNNEL TESTING AND ANALYSIS

— PIGGYBACK FERRY —

(NASA-CR-~~133484~~) C-5A/ORBITER WIND TUNNEL TESTING AND ANALYSIS: PIGGYBACK FERRY Final Report (Lockheed-Georgia Co.) ~~239~~ 243 p HC $14.00 CSCL 01C

N74-15717

Unclas G3/02 28801

Final Report
LG73ER0193
December 1973

by

K. H. Tomlin
W. T. Blackerby
A. C. Hughes
E. G. Husband
J. H. Paterson

Prepared under Contract NAS9-13702
for the
NATIONAL AERONAUTICS AND SPACE ADMINISTRATION
JOHNSON SPACECRAFT CENTER
Houston, Texas

by the

LOCKHEED-GEORGIA COMPANY
A Division of Lockheed Aircraft Corporation
Marietta, Georgia 30063

Lockheed Georgia Company

C-5A/ORBITER WIND TUNNEL TESTING AND ANALYSIS

— PIGGYBACK FERRY —

Final Report
LG73ER0193
December 1973

by

K. H. Tomlin
W. T. Blackerby
A. C. Hughes
E. G. Husband
J. H. Paterson

Prepared under Contract NAS9-13702
for the
NATIONAL AERONAUTICS AND SPACE ADMINISTRATION
JOHNSON SPACECRAFT CENTER
Houston, Texas

by the

LOCKHEED-GEORGIA COMPANY
A Division of Lockheed Aircraft Corporation
Marietta, Georgia 30063

Lockheed Georgia Company

CONTENTS

CONTENTS (Continued)

LIST OF FIGURES

LIST OF FIGURES (Continued)

LIST OF FIGURES (Continued)

SUMMARY

Wind tunnel testing and analytical studies of the feasibility of ferrying the NASA Shuttle Orbiter on the C-5A in a piggyback mode have been accomplished by the Lockheed-Georgia Company in response to NASA contract NAS9-13702. The study was managed by J. H. Paterson of the Flight Sciences Division. Testing was conducted in the Lockheed-California Company 8 x 12 foot low speed wind tunnel using an existing Air Force 0.0399 scale C-5A model in conjunction with a NASA 0.0405 scale Orbiter model. Six component force and moment data were measured over a range of pitch and yaw angles to determine lift and drag characteristics, lateral/directional stability characteristics and longitudinal and directional control powers.

Appendix A contains a description of the wind tunnel test program with a run schedule and the complete plotted data for all the test runs. Initial emphasis was given to determining the effects of the Orbiter above the C-5A and the optimum location for minimum interference on C-5A characteristics. A comprehensive series of cruise configurations were tested including a range of Orbiter longitudinal and vertical locations, incidences, and afterbody fairings. Subsequently, a series of configurations were devised during the test program to determine means of recovering directional stability degradation due to Orbiter interference.

Extensions to the present C-5 vertical stabilizer were designed as were twin fins to be located at the tips of the horizontal stabilizer. Analytical studies subsequent to the test and based on test results indicate that these exterior changes should not be necessary as automatic flight controls provide satisfactory flying qualities.

Performance studies of the C-5A/Orbiter Piggyback show that the drag penalty of the Orbiter on the C-5A does not preclude non-stop, unrefueled ferry missions up to 2500 nautical miles. Some flight restrictions for the Piggyback are unavoidable; however these are not considered unreasonable for the special nature of the mission. In short, ferrying the Shuttle Orbiter in a Piggyback mode on top of a C-5A appears feasible with minimum modifications to the basic C-5A.

1.0 INTRODUCTION

Recent interest by NASA and Rockwell International in alternatives to the present Orbiter Airbreathing Propulsion System for ferry and flight test of the Space Shuttle Orbiter has led to a series of proposals, analytical studies and wind tunnel tests to determine the feasibility of alternate systems. The Lockheed-Georgia Company has actively participated in these studies because of the suitability of Lockheed's C-5A as a carrier system for the Orbiter and in an attempt to apply Lockheed's "big airplane" talents and knowledge to this program.

In response to NASA RFP 9-BC451-M6-4-4P, regarding the feasibility of ferrying the Orbiter piggyback on top of a C-5A, Lockheed-Georgia submitted a proposal and subsequently was awarded NASA contract NAS9-13702 for a low speed wind tunnel test and analytical study of a C-5A/Orbiter Piggyback configuration. This report constitutes the final report for this contract work. Analysis of the wind tunnel test results and the feasibility of the C-5A Piggyback concept are contained in the main part of the report. Appendix A contains the final plotted results from the wind tunnel test.

2.0 ANALYSIS OF EXPERIMENTAL RESULTS

2.1 STABILITY AND CONTROL

2.1.1 Effects of Orbiter, Cruise Configuration

The small effect of the Orbiter on the C-5 longitudinal stability is demonstrated in Figure 1. These data are for the forward, low position of the Orbiter where maximum interaction of the two wings should occur. A negative shift in C_M of 0.04 occurs at all angles of attack. Minor modifications of the medium angle of attack pitching moment, in the destabilizing sense, is apparent for the Orbiter configuration without a fairing due to wake impingement on the horizontal tail. At high angles of attack, beyond stall, the typical C-5 initial pitch up followed by a strong nose down pitch is modified by both Orbiter configurations in such a manner that the net result should be almost imperceptible to the pilot.

An increase in lift curve slope due to the presence of the Orbiter, as well as a small increase in $C_{L_{MAX}}$, is demonstrated in Figure 2. A small further improvement in $C_{L_{MAX}}$ due to the aft fairing is shown. The C_M-C_L curves demonstrate the negative C_{M_O} shift and negligible change in neutral point due to the Orbiter. The C_{M_O} shift is the equivalent of less than one degree of stabilizer angle.

The effect of the higher vertical center of gravity due to the Orbiter, approximately 60 inches, will result in a slight decrease in speed stability that will be most apparent in the landing approach mode. It is anticipated that this effect will require little more than pilot familiarization with the new pitch response to engine power since the current aircraft already has a vertical c.g. range of 51 inches.

The major effect of the Orbiter on the C-5 aerodynamic data is the reduction of weathercock stability as reflected by C_{N_β}. Figure 3 demonstrates this effect for the most critical configuration forward and low with a negative shuttle incidence. This loss of directional stability is primarily a result of the Orbiter's influence on the air flow at the C-5 vertical tail. There is also a secondary destabilizing effect with

this Orbiter location due to Orbiter side area that is ahead of the C-5 center of gravity. The prime effect, however, occurs because of the flow bending, caused by the Orbiter body. As a result, the C-5 vertical tail does not experience the full yaw angle seen by the forward fuselage. This reduction in yaw angle, as seen by the fin is approximately 30% of the nominal value. As shown in Figure 3, the afterbody fairing resulted in an improvement in stability at high sideslip angles but delayed the turnover point.

Lateral stability, represented by dihedral effect, is little affected by the Orbiter as shown in Figure 4. A small reduction in C_{ℓ_β} occurs through 15° of sideslip accompanied by a linearization of the higher sideslip angle data due to the Orbiter wing configuration effect on the C-5 wing. The aft fairing causes further increases in C_{ℓ_β} at high sideslip angles due to the fin effectiveness.

Figure 5 shows that a large increase in C_{Y_β} occurs due to the presence of the Orbiter as a result of the side area increase, as would be expected. The aft fairing causes a small increase in sideforce at sideslip angles greater than 15° and no effect at lesser angles. It is somewhat surprising that more sideforce does not result from the added side area of the fairing. Apparently this area is not effective in sideforce due to the very thick boundary layer or there is a compensating flow change at the fin, or both.

2.1.2 Effect of Orbiter Position, Cruise Configuration

The effect on longitudinal stability of Orbiter fore and aft and vertical position relative to the C-5 is demonstrated in Figure 6. This comparison is made with the Gelac fairing No. 1 on the Orbiter and with the Orbiter at an incidence of 0.5 degrees. The destabilizing effect of the Orbiter in the forward high position is due to the combined effect of the Orbiter lifting moment and the interference with the flow at the C-5 horizontal stabilizer. The aft low position represents a significant improvement; showing a small negative ΔC_M shift that remains constant until the stall is reached. The pitch down tendency beyond stall of the basic C-5 has been reduced slightly. A small reduction in stability occurs in the aft high position with more pitch up at the

stall than that for the low position due to the increased stabilizer interference: however, the stability change relative to the basic C-5, below stall is negligible.

Figure 7 shows that Orbiter position has little effect on the lift curve slope and only a small effect on $C_{L_{MAX}}$: the highest $C_{L_{MAX}}$ occurs with the Orbiter in the aft high position. From a longitudinal stability point of view it is apparent that the aft low position would be the best with the aft high position a second choice.

The effect of Orbiter position on directional stability is very pronounced as shown in Figure 8. The major change that occurs with aft movement is due to the tail-off stability increase as the body side area is moved aft of the reference c.g. A small stabilizing change in fin effectiveness occurs with aft movement of the Orbiter. Again these data demonstrate the ability of the Orbiter body to reduce the local flow angle at the fin relative to the free stream angle through $\pm$ 15 degrees. The sensitivity of the C-5 weathercock stability to the presence of the Orbiter is largely due to the equal magnitudes of tail-off instability and tail-on stability. Thus, a 50 percent loss of fin effectiveness will cause a 100 percent loss of stability. The aft, high position of the Orbiter has the best directional stability characteristic but is still slightly unstable through small sideslip angles.

A significant change in dihedral effect occurs as a function of Orbiter position as shown in Figure 9. The major effect is due to Orbiter height above the C-5, showing larger $C_{\hat{\ell}_\beta}$ for increased height. Fore and aft position does not appear to have much influence, showing a small increase in C_{ℓ_β} for aft movement of the Orbiter. It would appear that the major effect on C_{ℓ_β} is probably due to the freeing effect of moving the wings apart thus allowing full development of the normal lift change due to sideslip on both wings.

Orbiter position has a negligible effect on the net sideforce due to sideslip as shown in Figure 10. A large increase in C_{Y_β} is, of course, present due to the side area of the Orbiter configuration.

Page intentionally left blank

2.1.3 Effect of Orbiter Incidence, Cruise Configuration

The effect of Orbiter incidence on the C-5 pitching moment is shown in Figure 11 for the aft, high position of the Orbiter with the aft fairing (Test Fairing No. 3). Increasing the Orbiter incidence relative to the C-5 reduced the pitching moment shift through nominal angles of attack, and at high angles of attack, increased the pitch up with a slightly less stable pitch out.

Small shifts in α_{OL} with no change in lift curve slope due to Orbiter incidence are shown in Figure 12. Increasing Orbiter incidence results in small increases in net C_{LMAX}. The $C_M - C_L$ data reflect the expected shift in C_{MO} with essentially no change in neutral point.

Insignificant changes in directional stability resulted from Orbiter incidence variation as shown in Figure 13. The basic configuration for the Orbiter was the aft, high position with the No. 3 fairing.

Only minor changes in C_{l_β} occur due to Orbiter incidence as shown in Figure 14. A small increase in C_{l_β} at the higher sideslip angles, as Orbiter incidence increases, is apparent.

No change in C_{Y_β} due to Orbiter incidence is apparent, as shown in Figure 15.

2.1.4 Effect of After-body Fairing, Cruise Configuration

The effect of various after-body fairing changes on pitching moment is shown in Figure 16. These fairing modifications were aimed at improving directional stability characteristics and have little direct influence on longitudinal stability other than through the drag changes.

C_{N_β} is unstable through small angles for C-5 Orbiter combinations with both the Gelac No. 1 fairing and the Rockwell fairing. Attempts to reshape the aft fairing to improve the flow field at the vertical tail are shown in Figure 17. Small improvements

were obtained with fairing No. 2 and 3 but are not sufficient in themselves to cure the problem.

The effects of after-body shape on C_{l_β} and C_{Y_β} are negligible, demonstrating the lack of load producing area in the aft body region.

2.1.5 Effect of Orbiter, Landing Configuration

The effect of the Orbiter on the longitudinal characteristics of the C-5A in the landing mode is similar to that of the clean configuration. A larger negative pitching moment shift due to the Orbiter is apparent - Figure 18. (The Orbiter is in high aft position.) A slight increase in stability is also noted.

Little or no change in lift curve slope occurs, as shown in Figure 19. A small neutral point shift in the stable sense is predictable from the $C_M - C_L$ curves of this figure. These data were obtained without the uprigged spoilers normally used for the C-5 landing configuration, however, little or no influence is expected.

In the landing configuration, the airflow at the C-5 vertical tail is not as restricted as in the clean configuration due to the large downflow, away from the fin, caused by the flaps. As shown in Figure 20, the net result is a more stable C_{N_β} level than for the clean airplane even though a small "flat spot" still occurs at small sideslip angles. The shape of the basic C-5 curve is predicated by fin stall at large sideslip angles. Since the air flow at the fin is restricted by the Orbiter in the Piggyback mode, the fin never experiences stall in the tested sideslip range, hence the more linear yawing moment at large angles.

The major effect of the Orbiter on C_{Y_β} is to delay the fin stall at high sideslip angles so that an increase in rolling moment occurs. This effect is shown in Figure 21. Little or no effect on C_{l_β} in the small sideslip angle range is noted.

The effect of the Orbiter on C_{Y_β} parallels that obtained in the clean configuration and the levels at each sideslip angle are almost identical.

2.1.6 Vertical Tail Development

The effects of the addition of a central fin to the C-5 horizontal tail bullet and the addition of tip fins to the horizontal tail are demonstrated in Figure 22. The Orbiter position is aft and high with the #3 aft fairing. This position results in a negligible change in tail-off C_{N_β} except at the higher sideslip angles, since the Orbiter fin-body area is well aft of the c.g.

The addition of a center fin above the C-5 tail produces sufficient stability beyond 5^o of sideslip but is influenced by the Orbiter body effect at smaller angles. The addition of twin fins at the horizontal stabilizer tips successfully achieves the same stability level as the basic C-5 throughout the small angle range, and a much increased level at the higher sideslip angles.

The additional sideforce developed in sideslip by tip and center fins required for directional stability is shown in Figure 23. These large values are not desirable because of gust response and turn coordination, especially in light of the already large increase in sideforce due to the Orbiter.

As shown earlier, the directional stability in the landing configuration in the presence of the Orbiter, is better than that for the clean configuration. As a result the fins, as sized, represent an excess capability as shown in Figure 24.

The sideforce due to sideslip is approximately the same as for the clean configuration shown in Figure 25.

The effectiveness of the center and tip fins, without the Orbiter, are shown in Figure 26. The center fin retains its effectiveness at high sideslip angles to a higher degree than the tip fins. They are equally effective at small angles.

Similar data for the sideforce characteristics are shown in Figure 27.

2.1.7 Effect of Orbiter on Longitudinal Trim

The Orbiter, in the aft high position, has a negligible influence on the dynamic pressure of the airflow at the C-5 horizontal stabilizer and only a minor influence on the downwash. The net effect is shown in Figure 28 for the cruise configuration. It may be noted that the "Orbiter on" data of this figure also have the vertical center fin whereas the "Orbiter-off" data do not. Although not shown here, the data in the appendix demonstrates that there is no effect in pitch due to the center fin, thus the comparison is valid.

Data are not available for the landing configuration. The influence of the Orbiter on trim effectiveness is anticipated to be even less than that for the cruise configuration because of the downward depression of the wing wake, away from the tail, caused by the flaps.

A small loss in dynamic pressure at the fin occurs due to the presence of the Orbiter and a reduction of local yaw angle relative to the free stream yaw in steady sideslip, as previously demonstrated. The net effect on rudder power for trim is shown in Figure 29. The Orbiter on data also include the effects of a center fin extension as discussed in 2.1.6.

The incremental effectiveness of the rudder in yaw is not anticipated to be affected by flap deflection.

2.2 DRAG CHARACTERISTICS

2.2.1 Effect of Orbiter

Figure 30 illustrates the magnitude of the effect of the Orbiter on C-5 drag. At a cruise C_L of 0.5, the drag of the Piggyback configuration is 70% greater than the basic C-5 level. By enclosing the bluff aft end of the Orbiter, the drag level of the

Piggyback is reduced to a level about 40% above that of the C-5 at $C_L = 0.5$. Undoubtedly, the skin friction drag of this very long fairing offsets some of the potential reduction in Orbiter base drag.

2.2.2 Effect of Orbiter Position

The effect on Piggyback cruise configuration drag of Orbiter location is shown by Figure 31. In general, the drag is seen to be insensitive to position for the locations tested, except for the aft - low position, which carries slightly lower drag up to a C_L of 0.6. The drag of the aft high position is about the same as that of the forward positions at all C_L's. These results indicate that interference drag is a very small contributor to total drag.

2.2.3 Effect of Afterbody Fairing

Figure 32 compares drag for the various afterbodies tested. Not a great deal of significance can be attached to these results. As expected, the increased afterbody fineness ratio of Gelac fairing #1 improved the flow relative to a blunter Rockwell fairing, however, the increased skin friction drag due to additional wetted area almost negates this as the decrease in cruise drag is only about 2 percent.

2.2.4 Effect of Orbiter Incidence

Figure compares drag results for the two Orbiter incidence angles and substantiates no change in Piggyback drag due to incidence over the range from -1.5° to 0.5°.

3.0 ASSESSMENT OF FULL SCALE FLIGHT FEASIBILITY

3.1 STABILITY AND CONTROL

3.1.1 Comparison of Wind Tunnel and Full Scale Directional Stability

The wind tunnel data, obtained from this test, are compared with the published, full-scale, levels for the C-5A to establish the base for the incremental data obtained in the presence of the Orbiter. The full-scale data are based upon the correlation of flight test data, obtained during the C-5A development program and the design wind tunnel data.

The cruise data for yaw due to sideslip are shown in Figure 34. The major change from the wind tunnel data is an extension of the fin sideforce capability to a higher yaw angle and a slightly more effective fin. There is also a more linear continuation of the tail-off yawing moment through high sideslip angles.

The landing flap data, shown in Figure 35, demonstrate further differences from the wind tunnel data. These differences are largely due to a change in the aft body interference with flaps down, that resulted in a less stable airplane than predicted by the wind tunnel. As may be noted, the net fin effectiveness, full scale, is considerably less than the wind tunnel level. These data are for landing flaps with the gear up. When the gear is down a higher C_{N_β} is realized due to the effect of the gear on the afterbody interference.

3.1.2 Predicted Full-Scale Directional Stability

Using incremental tail-off and tail-on data for the effect of the Orbiter, the full-scale predicted levels of weathercock stability are shown in Figure 36 compared with the basic C-5 in the cruise configuration. As may be noted, the Orbiter/C-5 combination is neutrally stable through $\pm$ 15 degrees of sideslip.

The full-scale prediction for the landing configuration, gear up, is shown in Figure 37.

These data reflect the low full-scale fin effectiveness discussed in the previous paragraph. The configuration is predicted to be neutrally stable through $\pm 2^{o}$ of sideslip and lightly stable at higher angles. Although not shown here, the gear-down landing configuration will be more stable.

3.2 FLYING QUALITIES

The wind tunnel test results have shown that the present C-5A longitudinal aerodynamic characteristics would not be critically affected by the piggyback shuttle installation. Evidently such would not be the case for the lateral-directional characteristics, particularly in the cruise configuration. The C-5A with the Orbiter in position exhibits an increase in sideforce due to sideslip, $C_{y_\beta} = -1.39$/radian compared to -0.80/radian for the C-5A. The directional stability level is reduced to nil, $C_{n_\beta} = 0$ composed with 0.0728/radian for the basic airplane. These predicted characteristics pertain to the M=0.52 at 20,000 feet flight condition. A cursory analysis was completed to assess the impact of these aerodynamic changes on C-5A flying qualities.

Pertinent flight vehicle data are tabulated in Figure 38. The reference gross weight is 704,626 pounds, which represents a 550,000 -pound airplane (no payload) with either a 154,626-pound cargo or the present design piggyback installation of the Orbiter vehicle. The Orbiter center of mass is considered to be 11.55 feet behind and 28.02 feet above the C-5A mass center.

Modal response data are presented in Figure 39. The aerodynamic changes due to the Orbiter installation result in a re-distribution of the total airplane damping due to C_{y_β}, C_{ℓ_p} and C_{n_r}. The spiral mode is more stable, now characterized by a 15.2 second time constant. The dutch roll mode is now unstable and the period of these oscillations is doubled, $\zeta_d = -.023$ and $T_d = 18.3$ seconds. The C-5A airplane incorporates a full-time stability augmentation system (SAS) on roll and yaw axes, and thus this unstable condition would not be experienced in flight. The Orbiter ferry mission may be completed with the autopilot also operative in cruise.

Flight vehicle response data were obtained using a digital computer program to evaluate responses to a 30KTAS lateral gust disturbance and a 10.0-degree lateral control wheel input. The program considers the solution of the three lateral equations of motion with respect to the usual linear assumptions. SAS and pertinent autopilot functions were included on a simple gain basis. The various high-order filters and the 0.25-second servo time constants were neglected such that the problem reduced to the control loop closures indicated in Figure 40. It is noted that the autopilot control command loops are excluded. The lateral stability functions have been included to enable an evaluation of flight vehicle response to external gust disturbances. Bank angles are presumed to be less than 7.0 degrees and thus the heading stability elements of the autopilot may also be excluded.

Figure 41 presents sideslip and bank angle responses to a continuous step gust of 30 KTAS. The lack of directional stability with the piggyback Orbiter installation results in a reluctance of the flight vehicle to naturally crab into the wind. Figure 42 provides a comparison of flight vehicle responses to control wheel throw. The excellent turn coordination characteristics of the basic C-5A airplane are somewhat degraded by the Orbiter installation. It is evident from the foregoing material that the aerodynamic changes associated with Orbiter installation may require a re-tuning of the basic C-5A stability augmentation system gains for cruise flight. The autopilot will probably be activated for the cruise condition of the Orbiter ferry mission. These would be an associated tightening of the lateral stability loop for the autopilot operative mode. The data presented in Figure 43 indicate that the flight vehicle responses to lateral gust disturbances would be stabilized, although still greater than for the basic C-5A airplane.

As stated earlier, the present analysis was of a cursory nature. The guarded conclusion is that the ferry cruise of the piggyback C-5A/Orbiter flight vehicle may not require significant C-5A flight control modifications. A continuation of studies to a greater depth than those described herein is recommended. The effects of flight vehicle vertical center of gravity location should receive attention. It is acknowledged that

an upward shift of the flight vehicle mass center will result in a reduction of the effective dihedral. The impact of c.g position on longitudinal characteristics should also be evaluated. Low speed, flaps-down, flight should also receive analytical attention.

3.3 PERFORMANCE

3.3.1 Full-Scale Drag Characteristics

Figure 44 compares estimated and wind tunnel drag for the C-5/Orbiter Piggyback. Test results on the isolated C-5 have been summed with wind tunnel data for an isolated Orbiter at the same test Reynolds number. The addition was accomplished at constant angle of attack. The excellent agreement between these two drag polars implies an absence of any net interference drag in the cruise configuration. Therefore, for purposes of this analysis, full-scale drag at flight Reynolds number for the Piggyback configuration has been defined by summing the estimated full-scale drag of an isolated Orbiter with C-5 flight test correlated drag. Resulting lift-to-drag ratios for the Piggyback at a typical cruise Mach number of 0.6 are shown compared with the C-5 in Figure 45.

Figure 46 shows a drag comparison, similar to Figure 44, for the landing configuration. The net interference drag in this case is seen to be equal to about 75% of the isolated Orbiter drag. Therefore, the low-speed, flaps-down drag data used for airport performance analyses reported herein have been increased to account for this effect.

3.3.2 Airfield Performance

Figures 47 and 48 show the takeoff and landing distances for the C-5/Orbiter Piggyback at varying gross weights. These data represent standard C-5 takeoff and land distances increased slightly to account for drag due to the Orbiter. Runway conditions for an airfield pressure altitude of 2000 feet and standard-day temperatures have been used for these as well as all other airfield performance data presented.

Takeoff flap setting for the C-5A is 16 degrees with a takeoff speed of 1.2 V_{STALL}.

For a long-range ferry mission takeoff gross weight of 700,000 pounds, takeoff ground roll is seen to be 7230 feet with a total distance of 8640 feet to clear a 50-foot obstacle. Engine-out climb capability of the C-5 Piggyback configuration may restrict operations at these conditions such that increased takeoff speeds and distances may be required. However, operation from airfields with runway lengths of 10,000 feet should not be prohibited.

Landing flaps for the C-5A are set at 40 degrees and approach speeds are normally 1.3 V_{STALL}. For an aborted mission after takeoff at 700,000 pounds, a landing ground roll of 3250 feet is indicated by Figure 48. Normal ferry mission landing weights would be approximately 550,000 pounds, for which a landing ground roll of 2200 feet and total landing distance from a 50-foot obstacle of 3580 feet would be expected.

3.3.3 Climb and Cruise Performance

One-engine-inoperative climb gradients for the C-5 Piggyback at several takeoff speeds and with the landing gear retracted are shown in Figure 49 for standard-day, 2000-foot pressure altitude conditions. Since Piggyback climb gradients are reduced relative to those of the basic C-5A, consideration has been given to increasing the takeoff speeds to improve climbout performance. As can be seen, an increase from 1.2 V_{STALL} to 1.3 V_{STALL} increases the gradient by about 0.35 percent, or for a constant climb gradient, the takeoff weight is increased by about 23,000 pounds. This amounts to approximately a 10 percent increase in fuel for long-range ferry missions.

Cruise ceilings for the C-5 Piggyback are shown in Figure 50 for several rates of climb. Long-range cruise performance calculated for the ferry mission is based on the altitudes for the 300-feet-per-minute ceiling shown for normal rated thrust (NRT). The cruise ceilings with military rated thrust (MRT) are useful for determining maximum speed-altitude capability of the C-5 Piggyback.

Figure 51 summarizes the speed-altitude capability at MRT of the Piggyback for weights corresponding to both an empty and fully loaded Orbiter. Also shown are data for the case of an Orbiter configuration without an afterbody fairing. At 25,000 feet, the maximum speed attainable is 259 KEAS with a faired afterbody, fully loaded Orbiter and 266.5 KEAS with an empty Orbiter.

3.3.4 Orbiter Ferry Capability

Figure 52 summarizes the capability of the C-5A to ferry the Orbiter in the Piggyback mode as a function of military critical field length and takeoff ground roll. These data are shown for takeoff speeds of 1.2, 1.25 and 1.3 times the stall speed and for three values of one-engine inoperative climb gradient. A climb gradient of 2.3% is the current minimum allowable gradient for the C-5A. Reducing the climb gradient to 1.8% improves the range by 240 miles while increasing takeoff distance by less than 1000 feet. Similarly, increasing takeoff speed from 1.2 to 1.3 V_{STALL} increases range by 160 miles but increases takeoff distance by 2500 feet.

For a special-purpose airplane it appears quite reasonable to accept lower climb gradients as a means of increasing range, provided there are no obstacles in the take-off path. Alternately, it is not necessary to resort to lower climb gradients, since the C-5A's inflight refueling capabilities make its range essentially unlimited.

3.4 FLIGHT RESTRICTIONS

Flight restrictions for the Piggyback are summarized in Figure 53 for two configurations, the C-5 with and without tail modifications. As discussed previously in subsection 3.2, ferry flight without any extension modifications to the C-5 tail can be accomplished with reliance on automatic flight controls, and flight restrictions listed here are given only as a matter of interest.

These restrictions have been established such that no structural modification to the C-5A is necessary other than that required to mount the Orbiter. The "fuselage fuel"

included in the weights breakdown represents an amount of ballast required for the Orbiter mounted in the aft position. This position in 10 feet aft relative to the base-line location, and the ballast is required to bring the c.g. within the current aft limit of the C-5A. The operating weights shown include the weight of the fuselage fuel tank.

Flight restrictions for the C-5/Orbiter Piggyback are compared with those of the Super Guppy in Figure 54. As can be seen, they are quite comparable. The only condition in which the C-5A is restricted more than the Super Guppy is in touchdown rate of sink. This is insignificant, since the design weights can be lowered somewhat and still allow the ferry-range performance shown in subsection 3.3.4. Design speeds and gust weights are naturally considerably greater for the C-5A as represented by the 300 KCAS level-flight maximum speed for the C-5A/Orbiter Piggyback, compared with 219 KCAS for the Super Guppy, and a maximum gross weight of 865,000 pounds for the Piggyback compared with 162,000 pounds for the Super Guppy. Maneuver-load factors for cruise are about the same: 2.0 for the Piggyback and 2.2 for the Super Guppy.

4.0 CONCLUSIONS AND RECOMMENDATIONS

Wind tunnel testing of the C-5A/Orbiter Piggyback configuration has demonstrated that the major effect of the Orbiter on the aerodynamics of the C-5A is a loss of directional stability due primarily to airflow losses at the vertical tail, and to an increase in overall side area and side forces. The effects of the Orbiter on longitudinal stability are almost negligible as evidenced by a C_{m_o} shift due to the Orbiter equivalent to less than one degree of horizontal stabilizer incidence. The effect on drag, as expected, is significant, but the drag level of the Piggyback configuration can be reduced to a level about 40% above C-5A cruise configuration drag with an Orbiter afterbody fairing. Interference effects from a drag standpoint appear from the test results to be insignificant for the ferry cruise configuration.

Variations in Orbiter longitudinal and vertical locations showed that the aft high position was the best, primarily because the losses in directional stability were minimized by moving the side areas aft of the reference c.g. The effects of varying the Orbiter incidence relative to the C-5A were, from any viewpoint, inconsequential for the range tested (-1.5° and 0.5°). A Lockheed-Georgia afterbody designed for the Orbiter to improve the flow at the empennage and the directional stability proved insufficient, although a slight drag reduction was noticed for the Lockheed-Georgia fairing.

During the wind tunnel test, several empennage modifications were designed and tested to remedy the directional stability problems. These modifications included a control fin addition above the present horizontal stabilizer, and twin fin additions to the horizontal stabilizer tip.

These were successful in restoring the stability level of the Piggyback to that of the basic C-5A so that, if desired, external modifications could be defined that would provide satisfactory flying qualities. Cursory analytical studies indicate that the C-5A automatic controls can be modified to fly the Piggyback configuration in a ferry operation without external modifications and with only minor modifications to the flight control systems.

Performance analyses revealed the feasibility of trans-continental unrefueled distances for the C-5A ferrying the Shuttle Orbiter. Airfield performance assures operation from fields of less than 10,000 feet where minimum takeoff climbout gradients can be tolerated. In total, the feasibility of the C-5A/Orbiter Piggyback ferry concept appears excellent and the following recommendations are respectfully submitted:

- Development of the C-5A ferry vehicle should be initiated as soon as possible.
- A wind tunnel test program of the airlaunch configuration should be initiated.
- Studies of airlaunch concepts and separation trajectory analyses should be made in conjunction with the wind tunnel program.
- More detailed, flying-qualities studies of the C-5/Orbiter Piggyback configuration should be conducted to identify potential modifications of the C-5A automatic flight control systems.

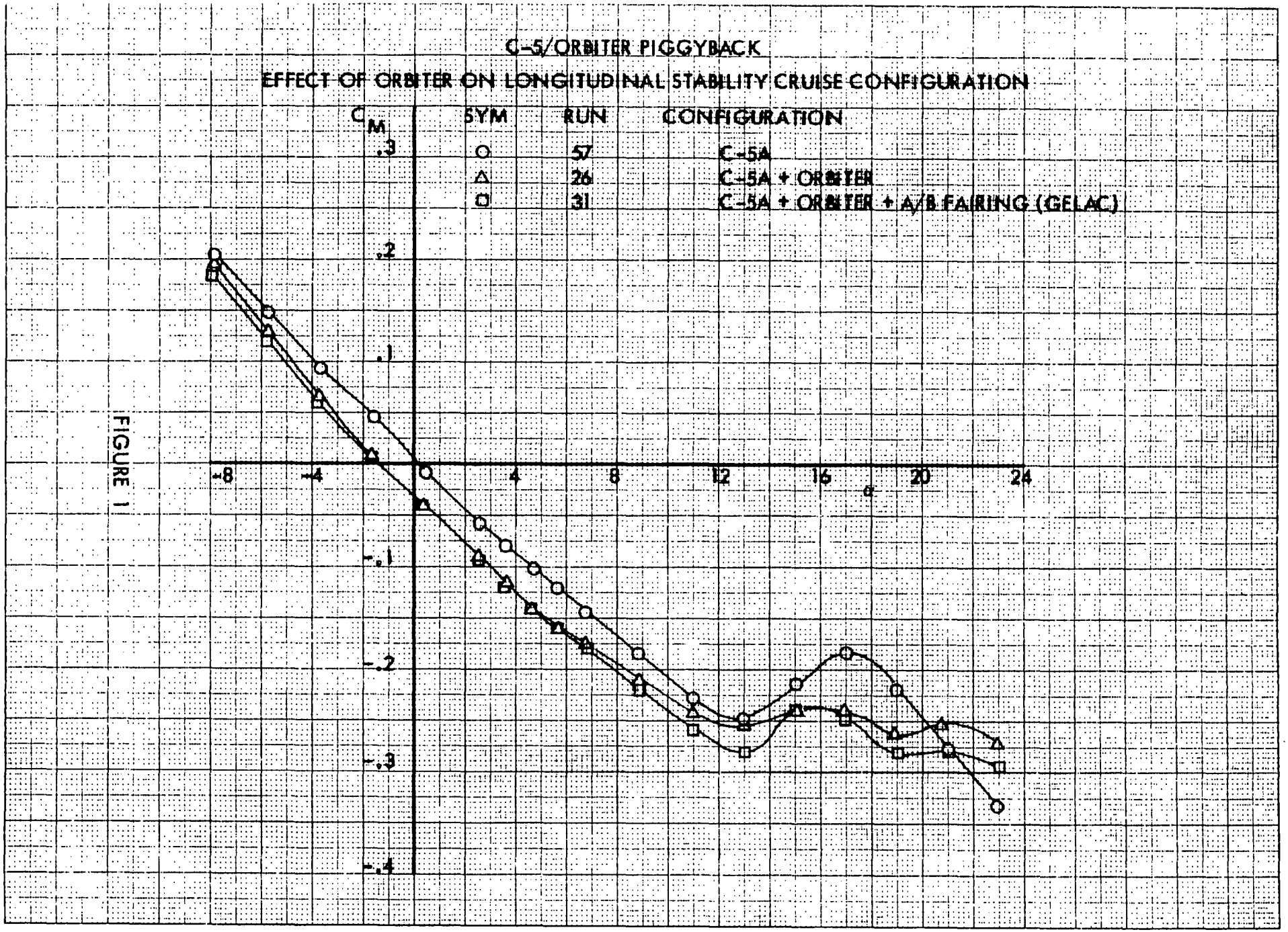
C-5/ORBITER PIGGYBACK
EFFECT OF ORBITER ON LONGITUDINAL STABILITY CRUISE CONFIGURATION
C_M
SYM
RUN
CONFIGURATION
57
C-5A
26
C-5A + ORBITER
31
C-5A + ORBITER + A/B FAIRING (GELAC)
.3
.2
.1
-.1
-.2
-.3
-.4
-8
-4
4
8
12
16
20
24
α

FIGURE 1

C-5A/ORBITER PIGGYBACK

EFFECT OF ORBITER ON LONGITUDINAL STABILITY CRUISE CONFIGURATION

SYM	RUN	CONFIGURATION
○	57	C-5A
△	26	C-5A + ORBITER
□	31	C-5A + ORBITER + A/B Fairing (GELAC)

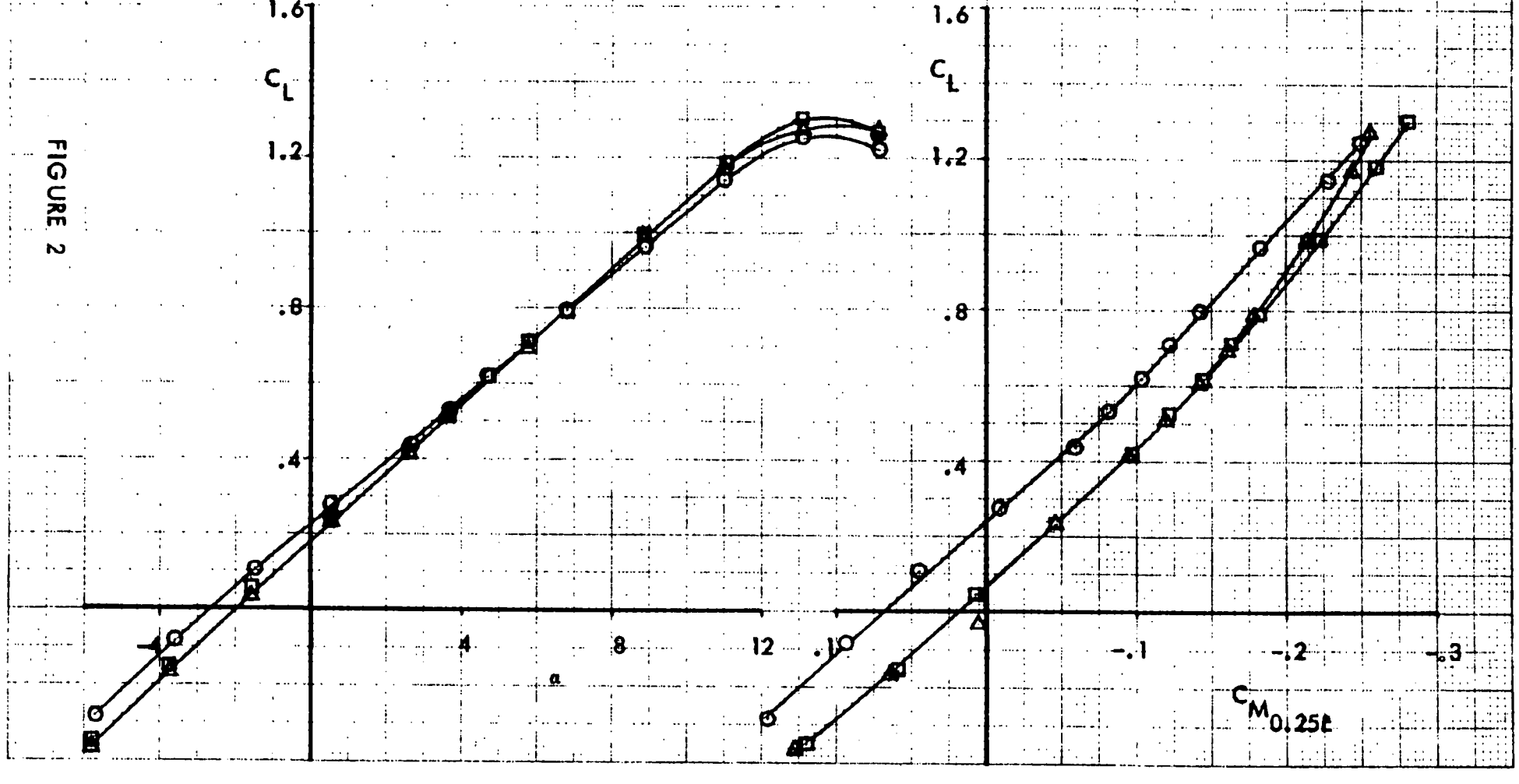

FIGURE 2

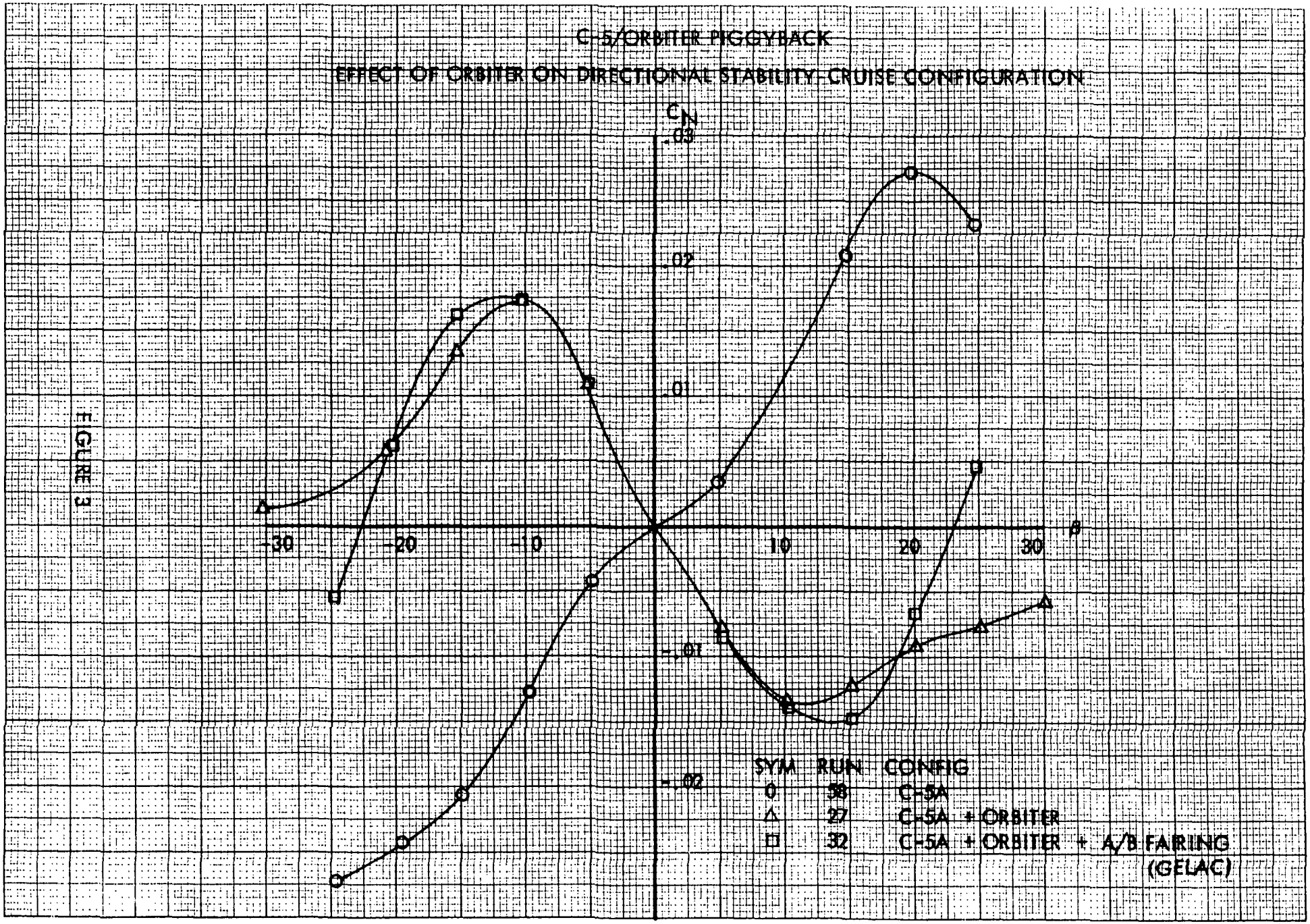
C-5/ORBITER PIGGYBACK
EFFECT OF ORBITER ON DIRECTIONAL STABILITY-CRUISE CONFIGURATION
C_N
.03
.02
.01
-.01
-.02
-30
-20
-10
10
20
30
β
SYM RUN CONFIG
0 38 C-5A
△ 27 C-5A + ORBITER
□ 32 C-5A + ORBITER + A/B FAIRING (GELAC)

FIGURE 3

C-5A/ORBITER PIGGYBACK

EFFECT OF ORBITER ON LATERAL STABILITY CRUISE CONFIGURATION

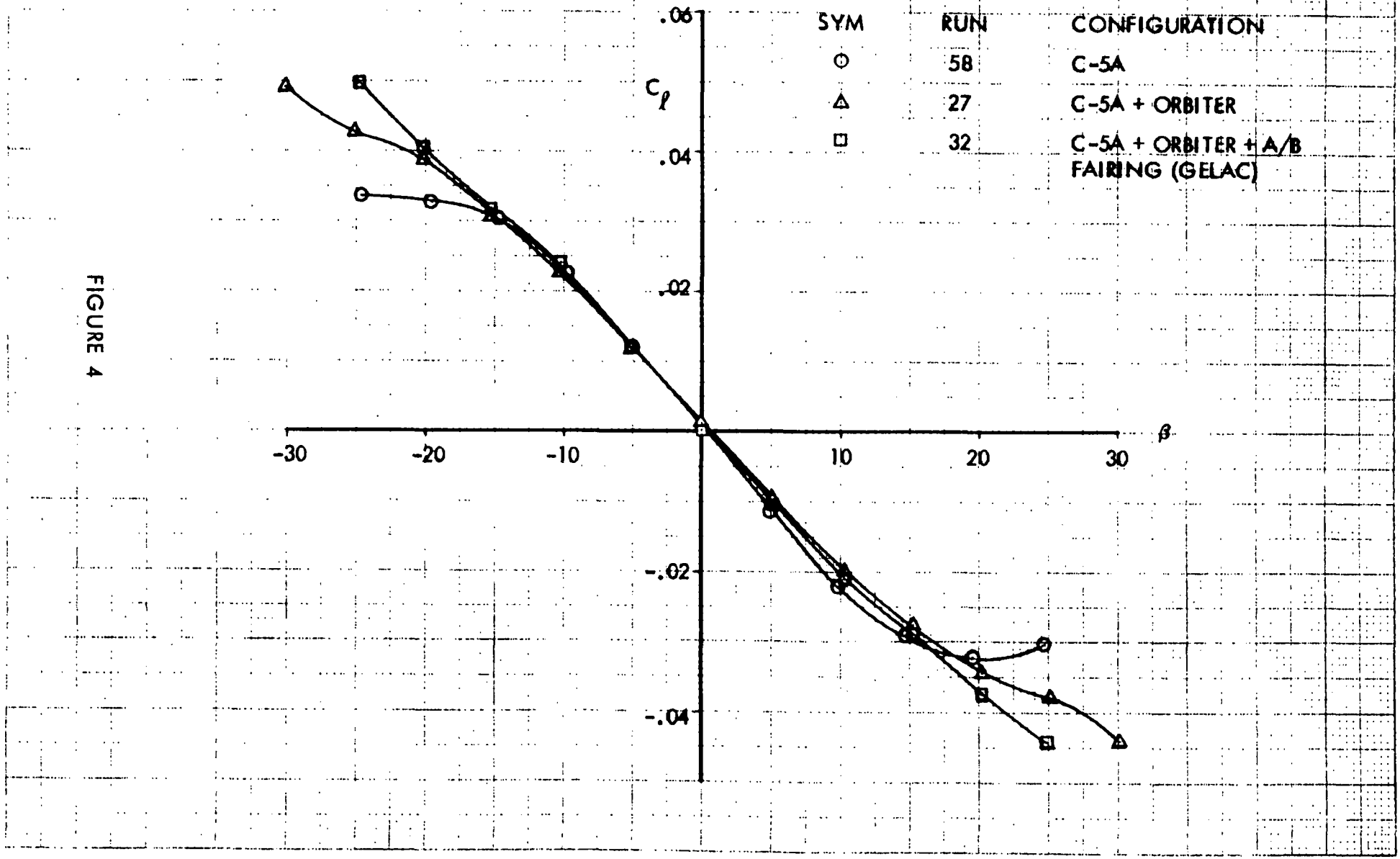

FIGURE 4

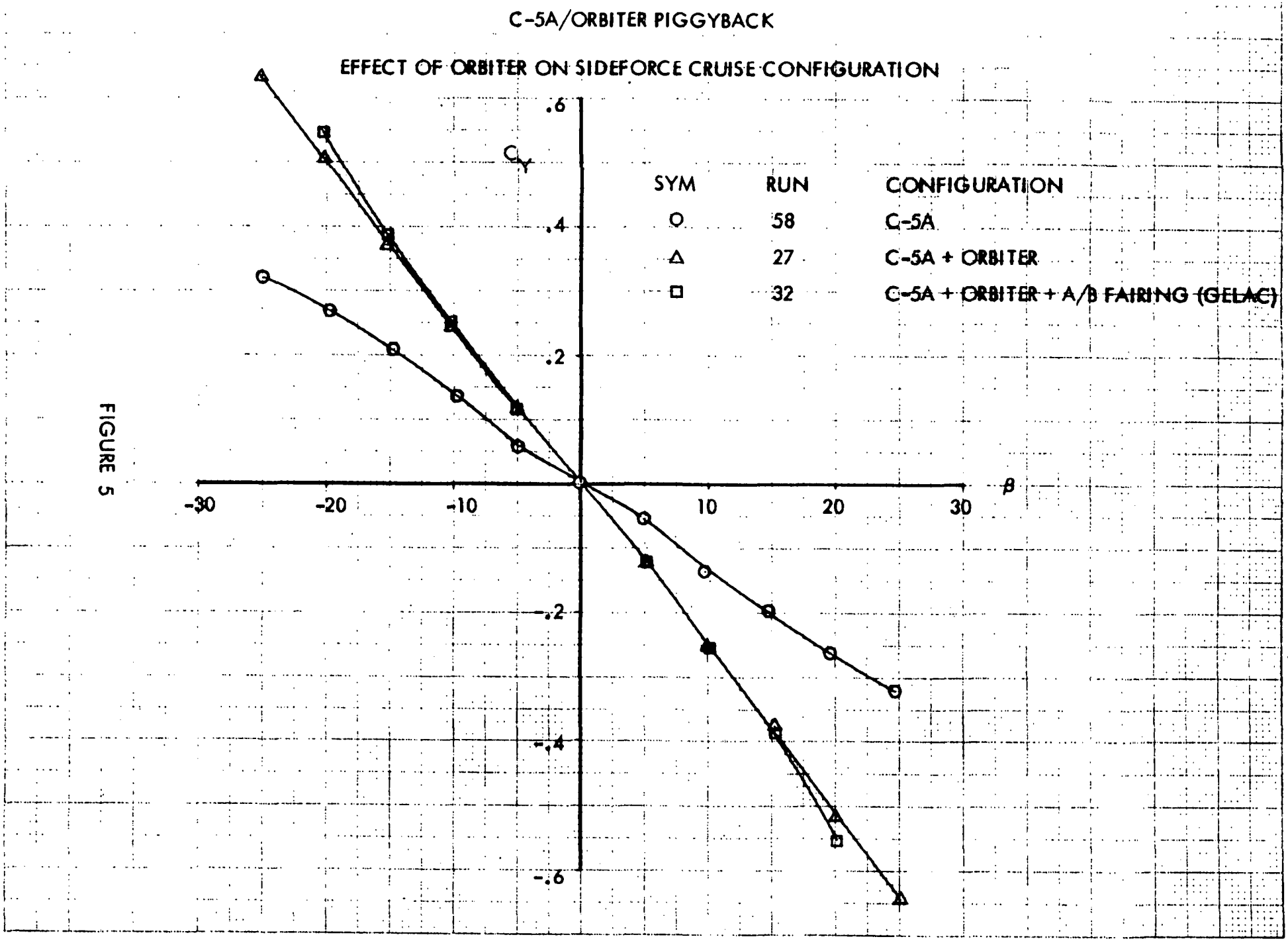
C-5A/ORBITER PIGGYBACK
EFFECT OF ORBITER ON SIDEFORCE CRUISE CONFIGURATION
C_Y
.6
.4
.2
-.2
-.4
-.6
-30
-20
-10
10
20
30
β
SYM
RUN
CONFIGURATION
58
C-5A
27
C-5A + ORBITER
32
C-5A + ORBITER + A/B FAIRING (GELAC)

FIGURE 5

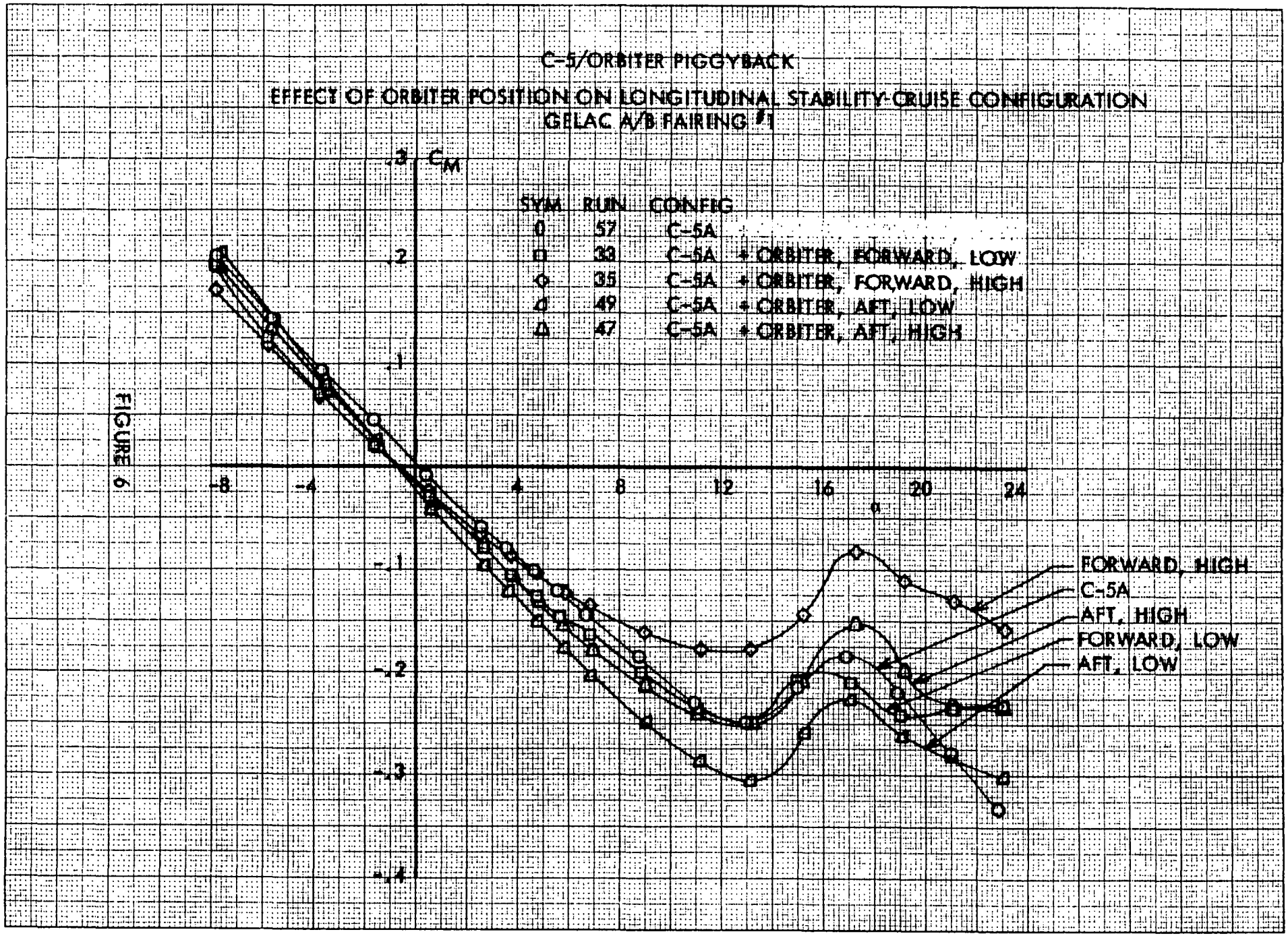
C-5/ORBITER PIGGYBACK
EFFECT OF ORBITER POSITION ON LONGITUDINAL STABILITY-CRUISE CONFIGURATION
GELAC A/B FAIRING #1
C_M
SYM RUN CONFIG
0 57 C-5A
□ 33 C-5A + ORBITER, FORWARD, LOW
◇ 35 C-5A + ORBITER, FORWARD, HIGH
◁ 49 C-5A + ORBITER, AFT, LOW
△ 47 C-5A + ORBITER, AFT, HIGH
.3
.2
.1
-.1
-.2
-.3
-.4
-8
-4
4
8
12
16
20
24
α
FORWARD, HIGH
C-5A
AFT, HIGH
FORWARD, LOW
AFT, LOW

FIGURE 6

C-5A/ORBITER PIGGYBACK

EFFECT OF ORBITER POSITION ON LONGITUDINAL STABILITY CRUISE CONFIGURATION

GELAC A/B FAIRING # 1

SYM	RUN	CONFIGURATION
○	57	C-5A
□	33	C-5A + ORBITER, FWD LOW
△	35	C-5A + ORBITER, FWD HIGH
◇	49	C-5A + ORBITER, AFT LOW
△	47	C-5A + ORBITER, AFT HIGH

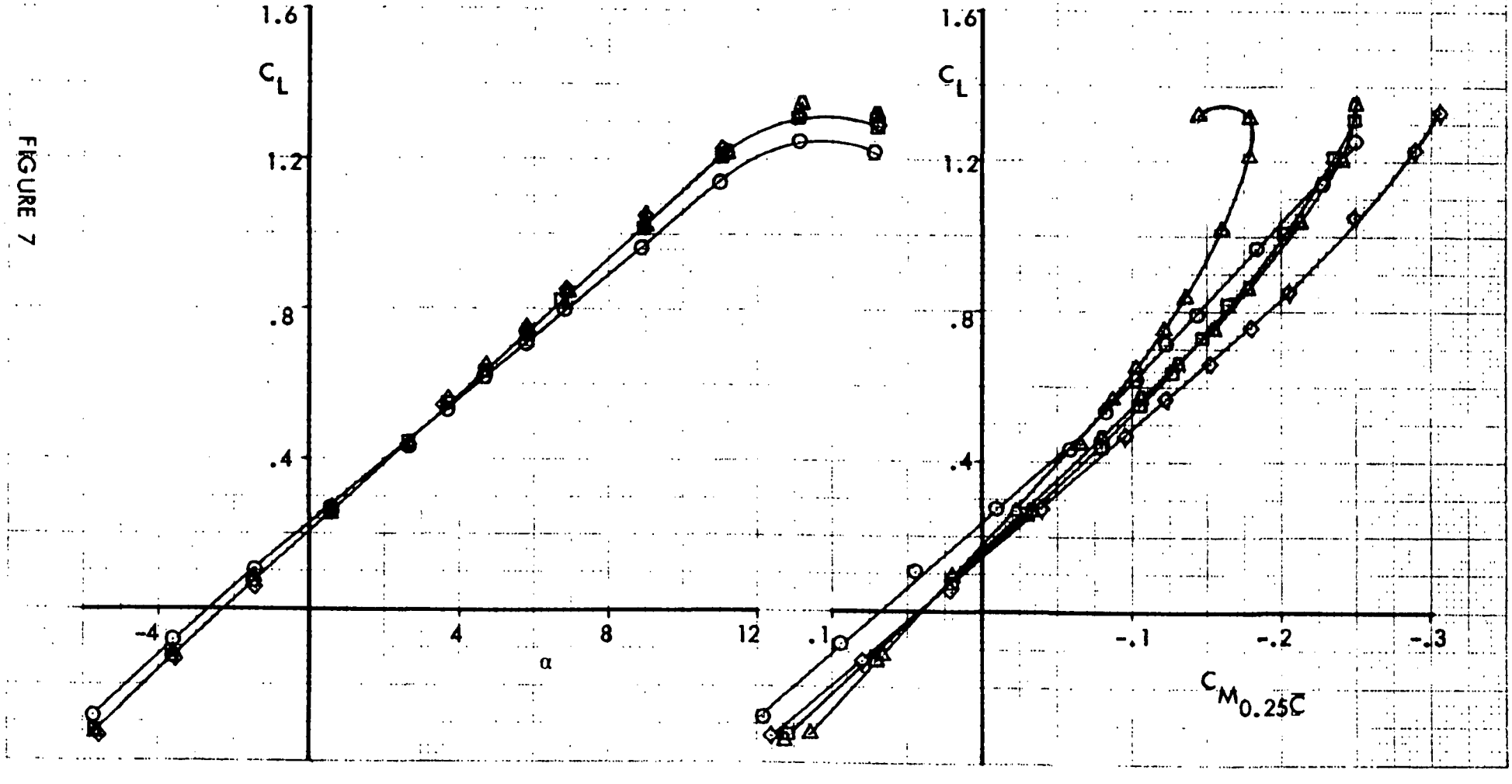

FIGURE 7

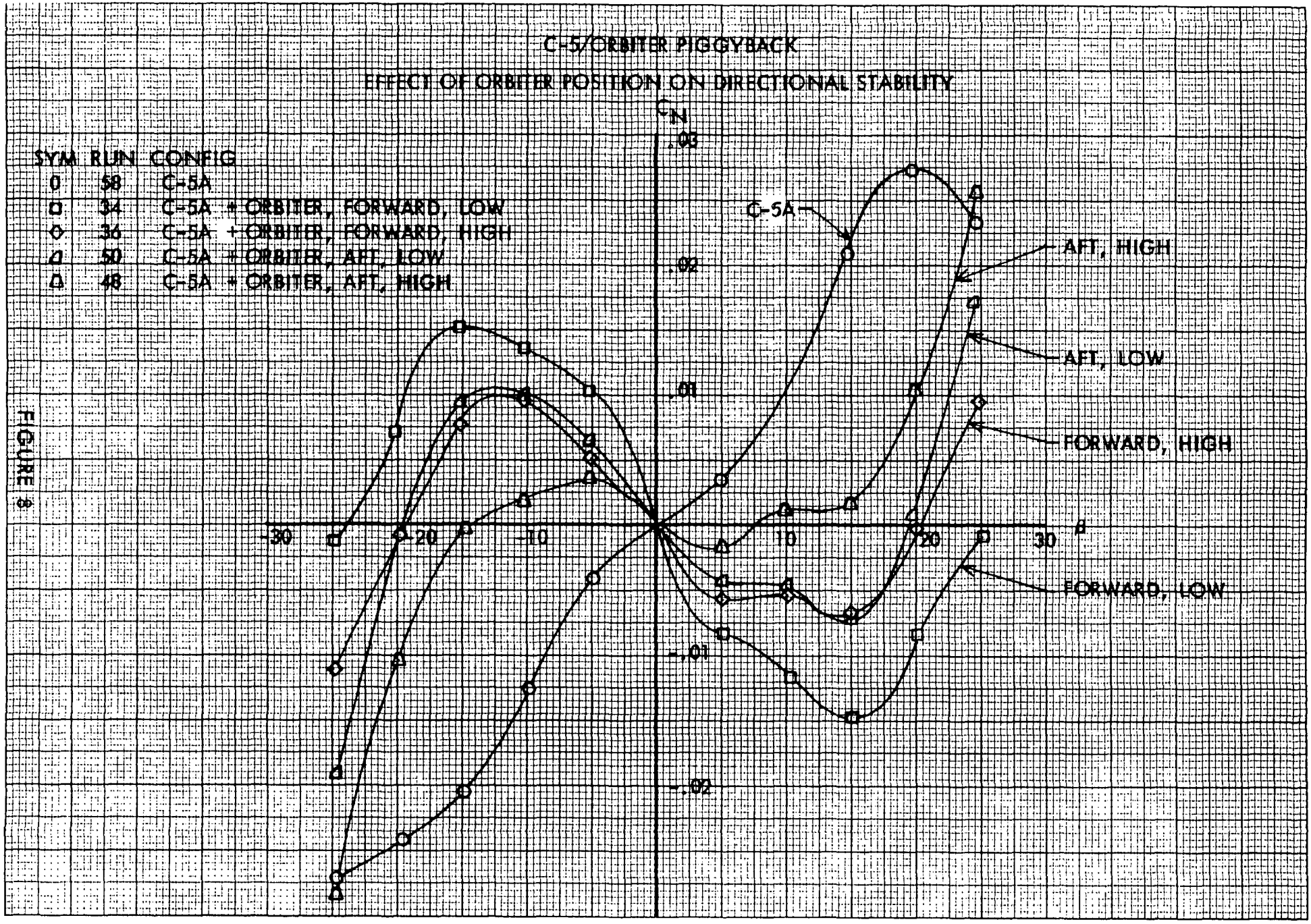
C-5/ORBITER PIGGYBACK
EFFECT OF ORBITER POSITION ON DIRECTIONAL STABILITY
SYM RUN CONFIG
0 58 C-5A
□ 34 C-5A + ORBITER, FORWARD, LOW
◇ 36 C-5A + ORBITER, FORWARD, HIGH
△ 50 C-5A + ORBITER, AFT, LOW
△ 48 C-5A + ORBITER, AFT, HIGH
C_N
.03
.02
.01
-.01
-.02
-30
-20
-10
10
20
30
β
C-5A
AFT, HIGH
AFT, LOW
FORWARD, HIGH
FORWARD, LOW

FIGURE 8

C-5/ORBITER PIGGYBACK

EFFECT OF ORBITER POSITION ON LATERAL STABILITY CRUISE CONFIGURATION

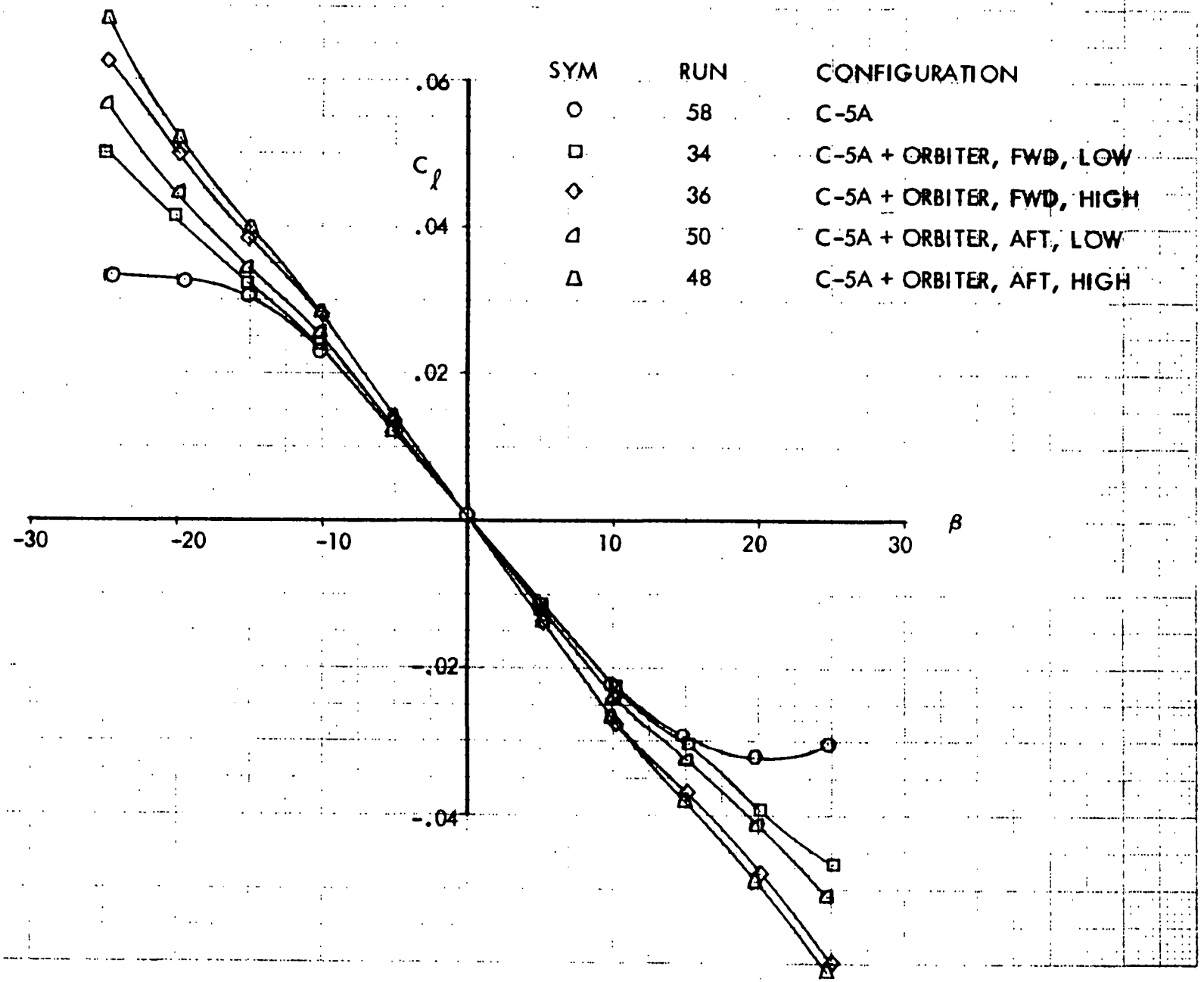

FIGURE 9

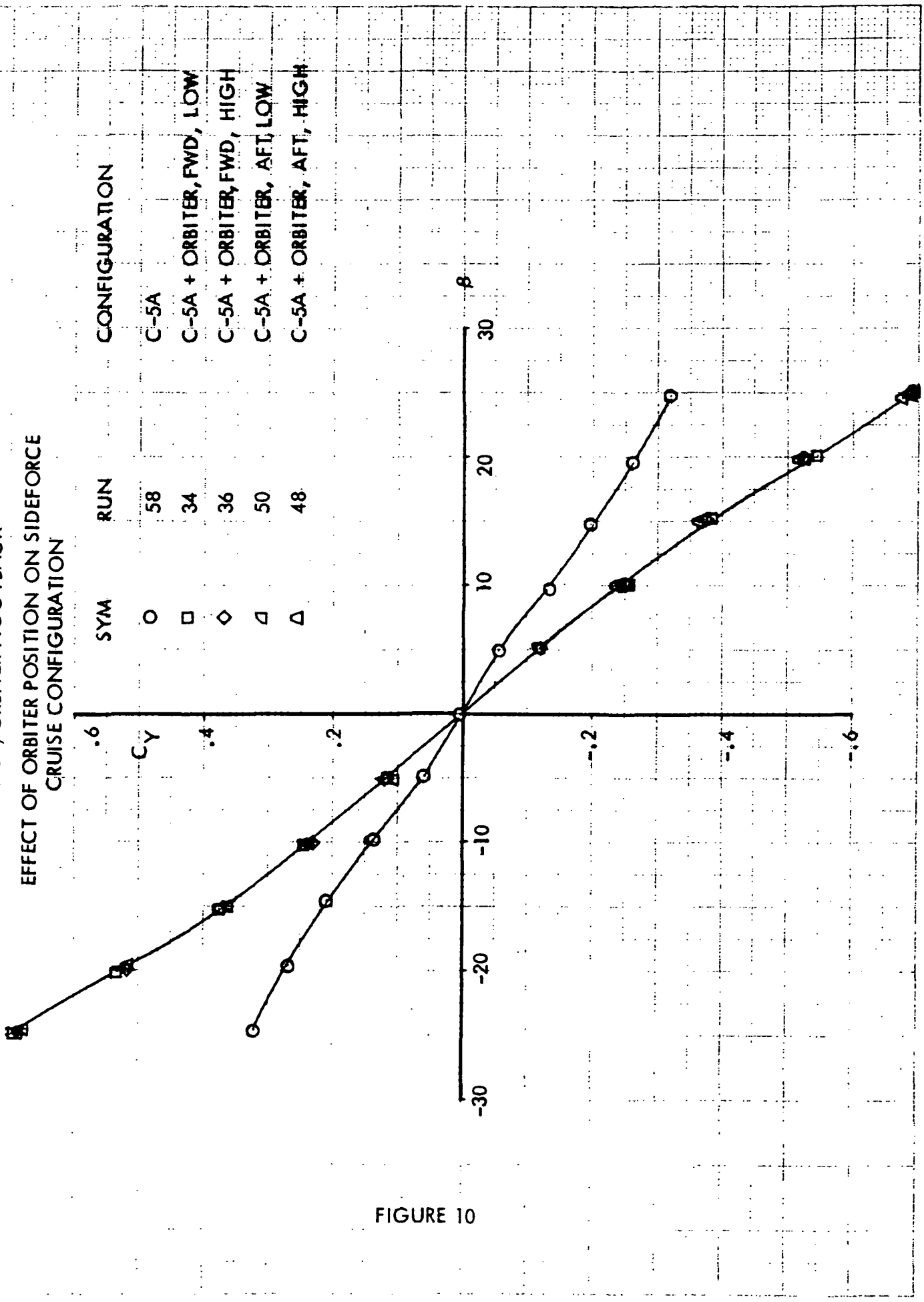
C-5A/ORBITER PIGGYBACK
EFFECT OF ORBITER POSITION ON SIDEFORCE
CRUISE CONFIGURATION
SYM
RUN
CONFIGURATION
C-5A
58
C-5A + ORBITER, FWD, LOW
34
C-5A + ORBITER, FWD, HIGH
36
C-5A + ORBITER, AFT, LOW
50
C-5A + ORBITER, AFT, HIGH
48
C_Y
.6
.4
.2
-.2
-.4
-.6
β
30
20
10
-10
-20
-30

FIGURE 10

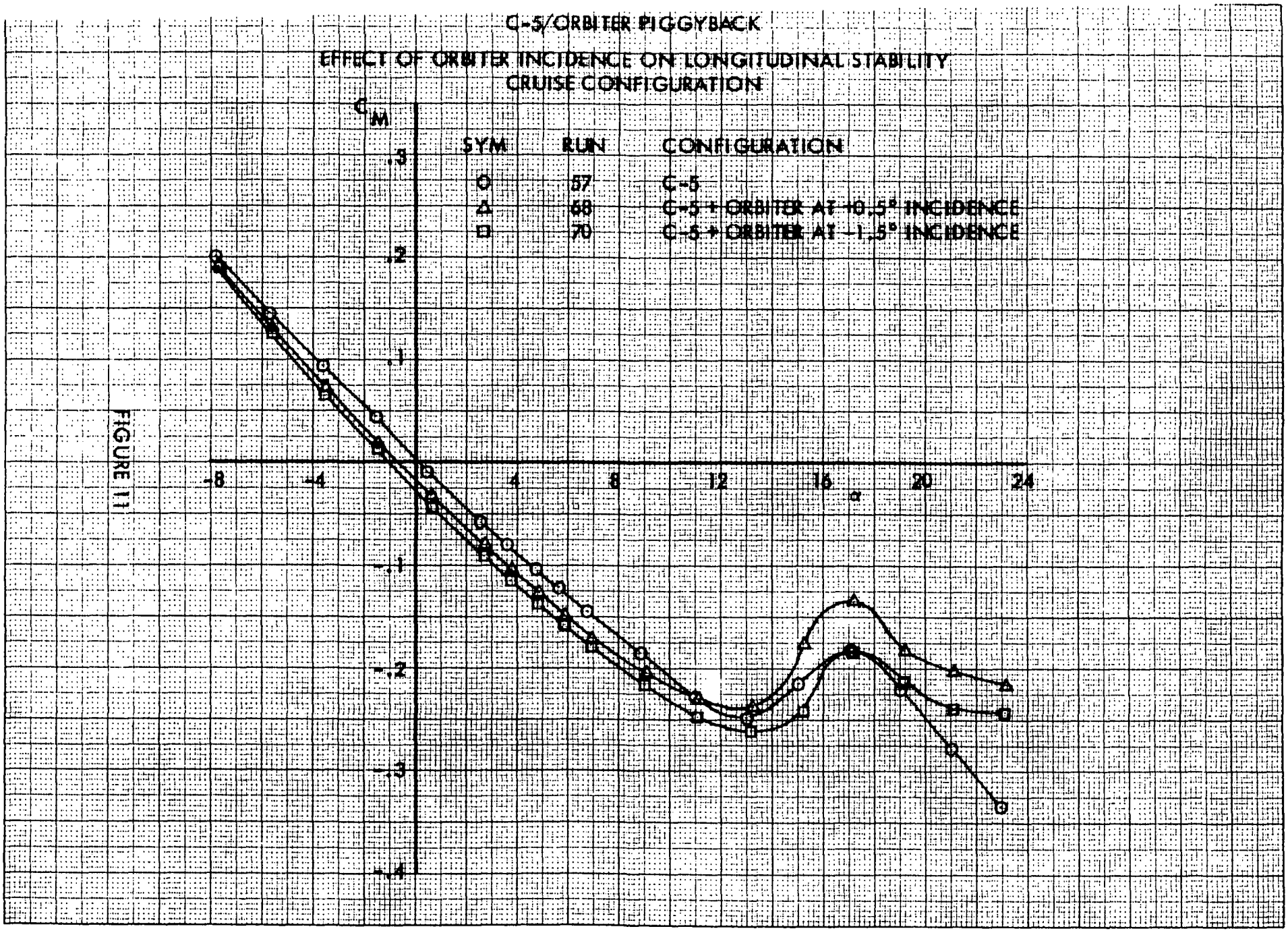
C-5/ORBITER PIGGYBACK
EFFECT OF ORBITER INCIDENCE ON LONGITUDINAL STABILITY
CRUISE CONFIGURATION
C_M
SYM RUN CONFIGURATION
57 C-5
68 C-5 + ORBITER AT +0.5° INCIDENCE
70 C-5 + ORBITER AT -1.5° INCIDENCE
.3
.2
.1
-.1
-.2
-.3
-.4
-8
-4
4
8
12
16
20
24
α

FIGURE 11

C-5A/ORBITER PIGGYBACK

EFFECT OF ORBITER INCIDENCE ON LONGITUDINAL STABILITY CRUISE CONFIGURATION

SYM	RUN	CONFIGURATION
○	57	C-5A
△	68	C-5A + ORBITER AT 0.5° INCIDENCE
□	70	C-5A + ORBITER AT - 1.5° INCIDENCE

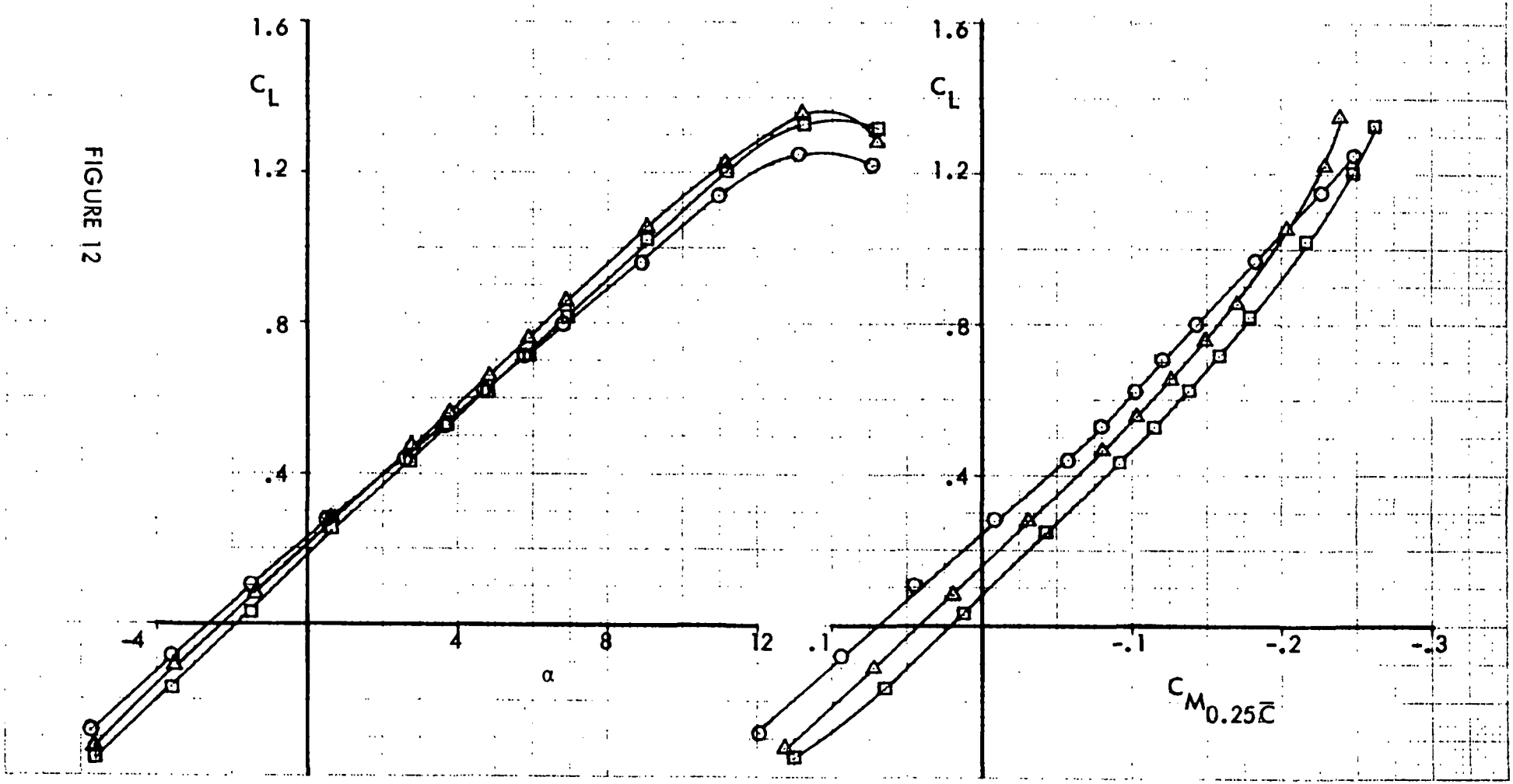

FIGURE 12

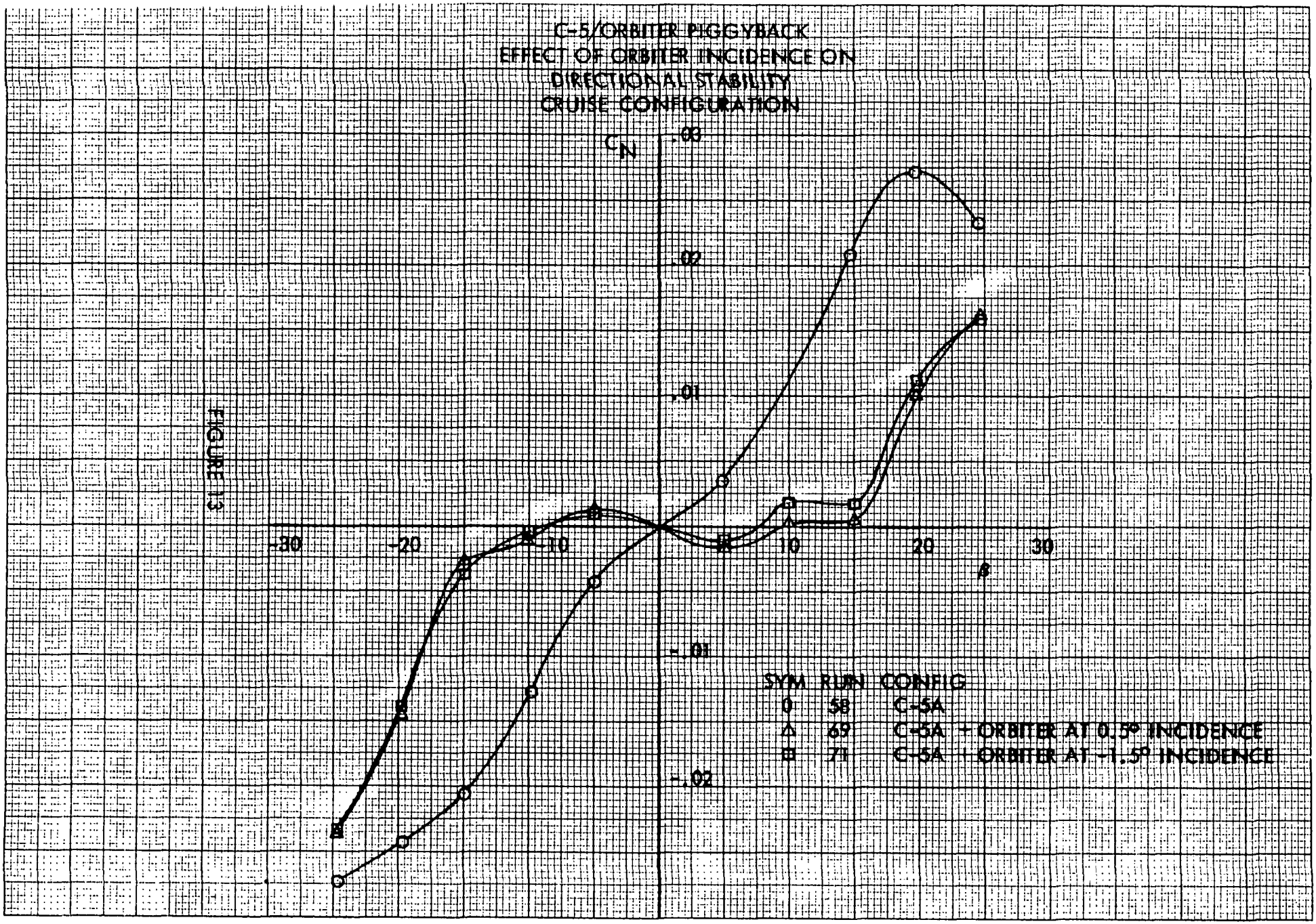
C-5/ORBITER PIGGYBACK
EFFECT OF ORBITER INCIDENCE ON
DIRECTIONAL STABILITY
CRUISE CONFIGURATION
C_N
.03
.02
.01
-.01
-.02
-30
-20
-10
10
20
30
β
SYM RUN CONFIG
0 58 C-5A
△ 69 C-5A + ORBITER AT 0.5° INCIDENCE
⊞ 71 C-5A + ORBITER AT -1.5° INCIDENCE

FIGURE 13

C-5A/ORBITER PIGGYBACK

EFFECT OF ORBITER INCIDENCE ON LATERAL STABILITY CRUISE CONFIGURATION

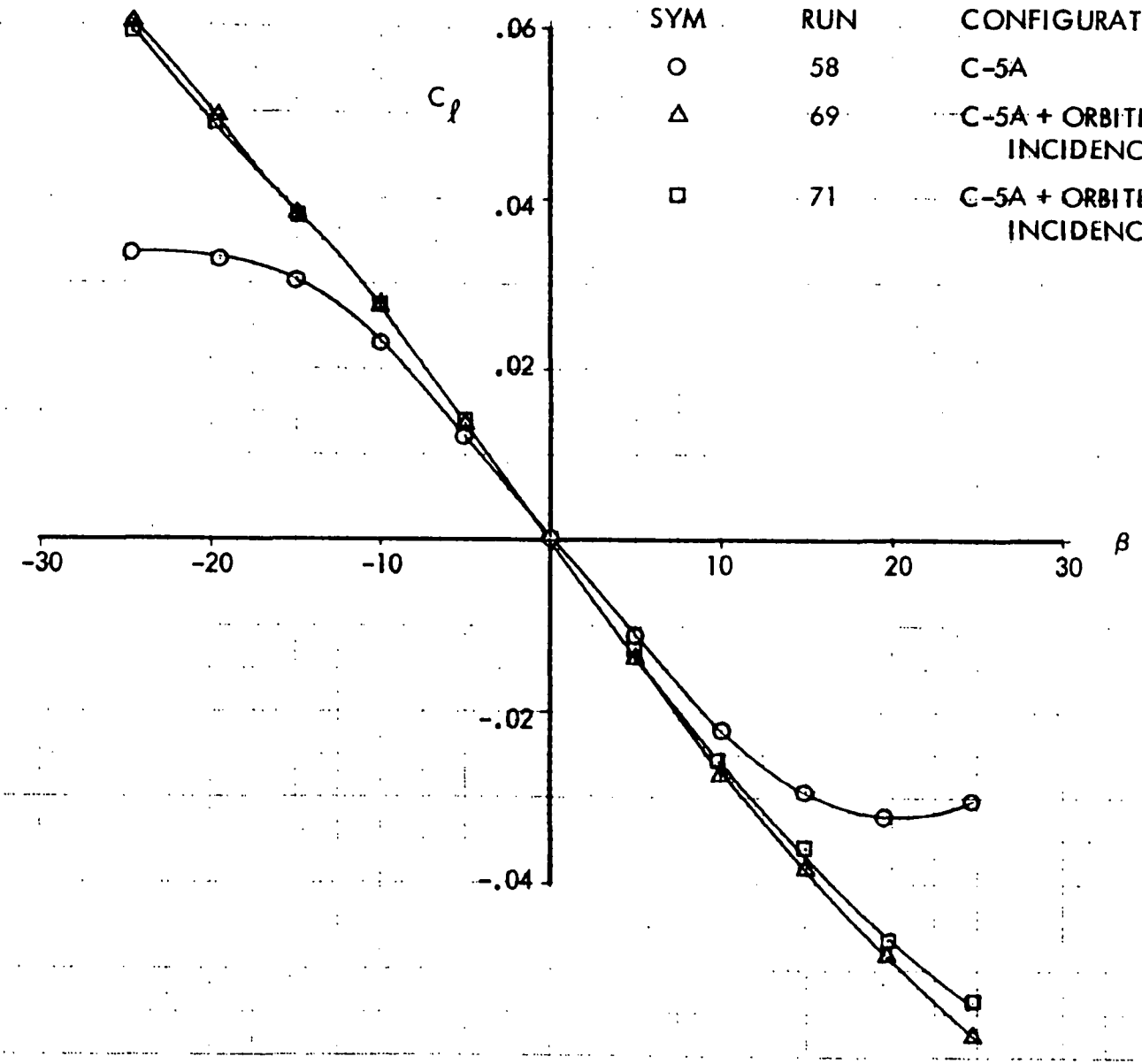

FIGURE 14

C-5A/ORBITER PIGGYBACK

EFFECT OF ORBITER INCIDENCE ON SIDEFORCE
CRUISE CONFIGURATION

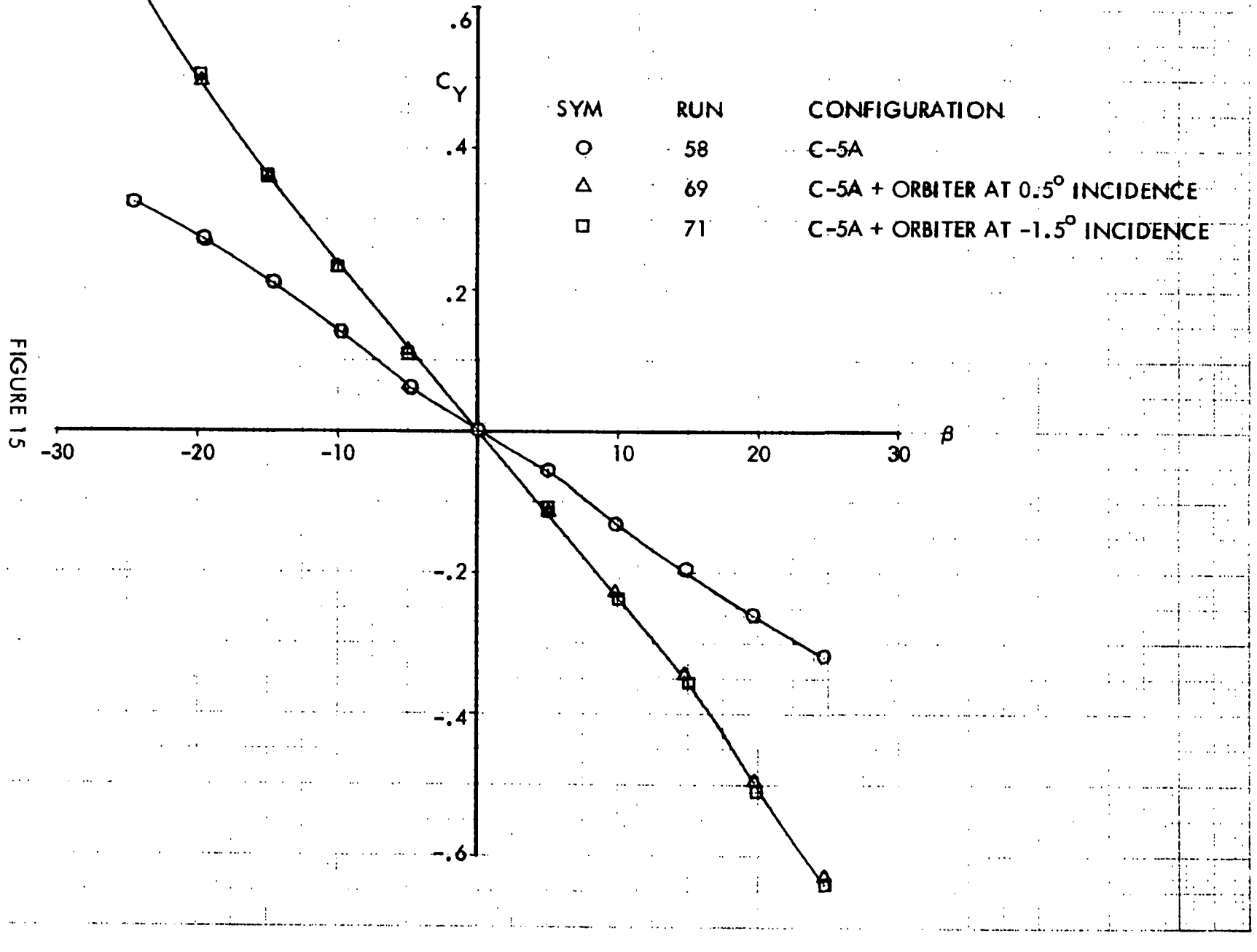

FIGURE 15

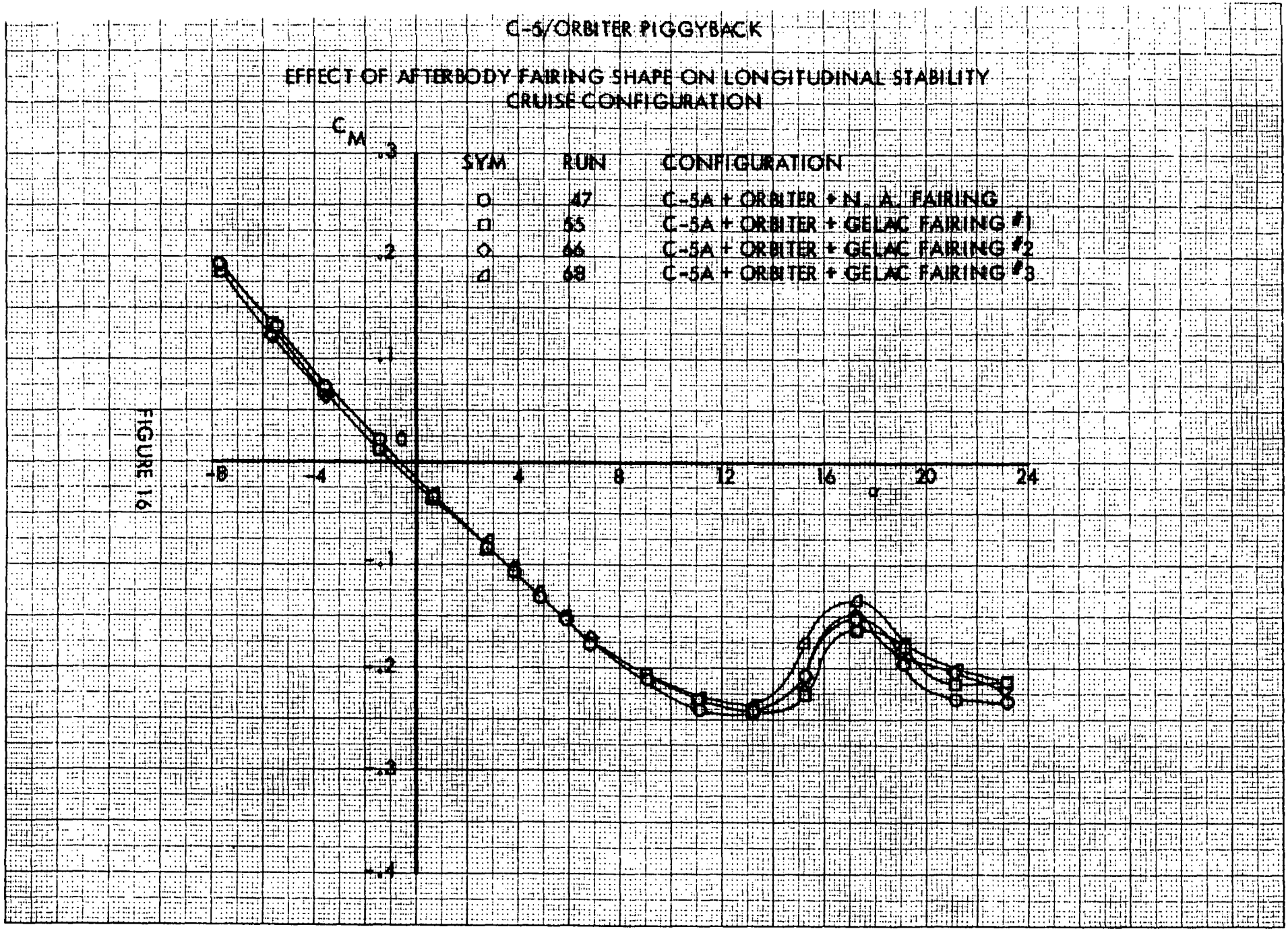
C-5/ORBITER PIGGYBACK
EFFECT OF AFTERBODY FAIRING SHAPE ON LONGITUDINAL STABILITY
CRUISE CONFIGURATION
C_M
SYM RUN CONFIGURATION
47 C-5A + ORBITER + N. A. FAIRING
55 C-5A + ORBITER + GELAC FAIRING #1
66 C-5A + ORBITER + GELAC FAIRING #2
68 C-5A + ORBITER + GELAC FAIRING #3
-8 -4 4 8 12 16 20 24 α
.3 .2 .1 0 -.1 -.2 -.3 -.4

FIGURE 16

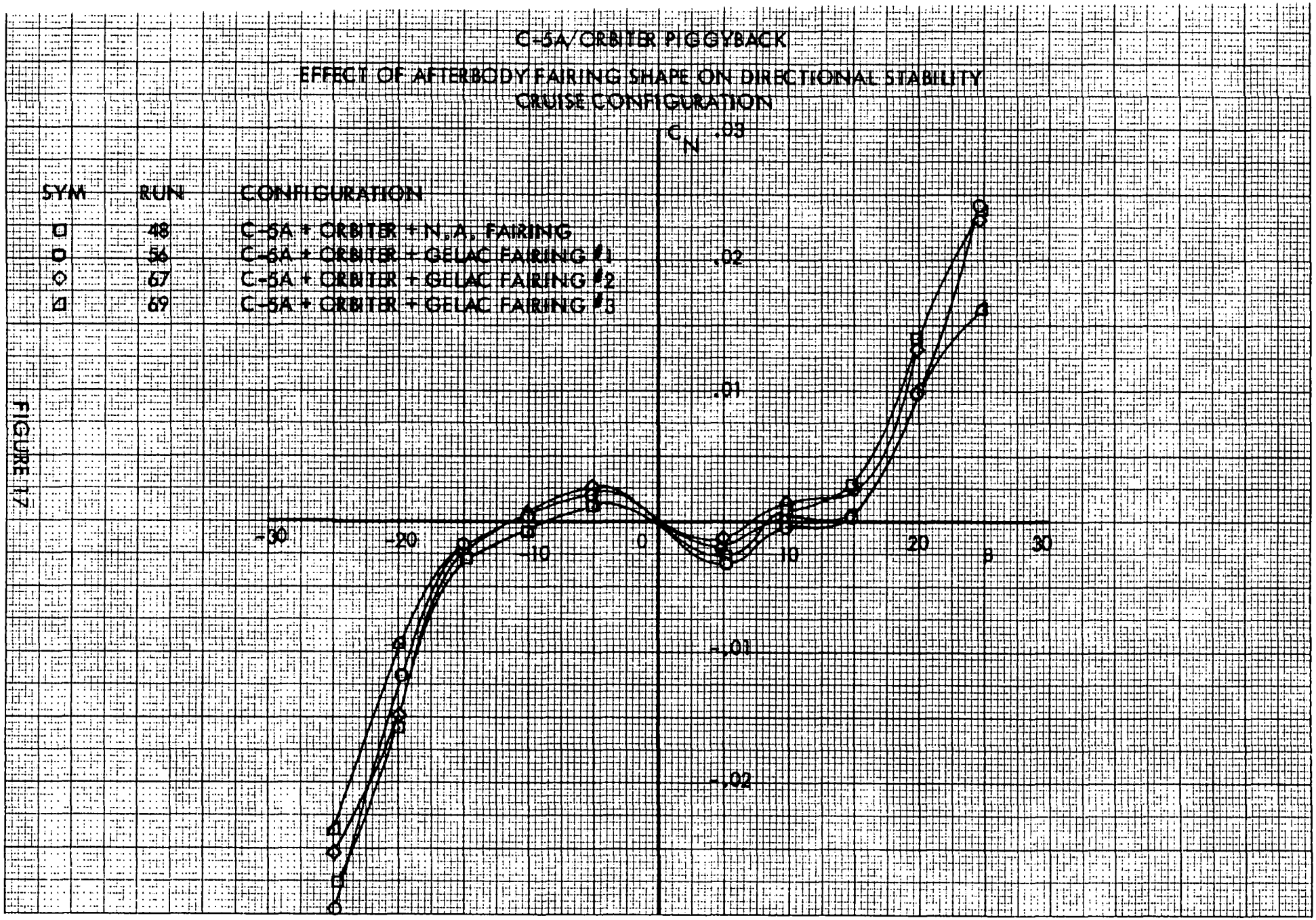
C-5A/ORBITER PIGGYBACK
EFFECT OF AFTERBODY FAIRING SHAPE ON DIRECTIONAL STABILITY
CRUISE CONFIGURATION
C_N
.03
.02
.01
-.01
-.02
-30
-20
-10
0
10
20
30
SYM
RUN
CONFIGURATION
48
C-5A + ORBITER + N.A. FAIRING
56
C-5A + ORBITER + GELAC FAIRING #1
67
C-5A + ORBITER + GELAC FAIRING #2
69
C-5A + ORBITER + GELAC FAIRING #3

FIGURE 17

EFFECT OF ORBITER ON LONGITUDINAL STABILITY
LANDING CONFIGURATION

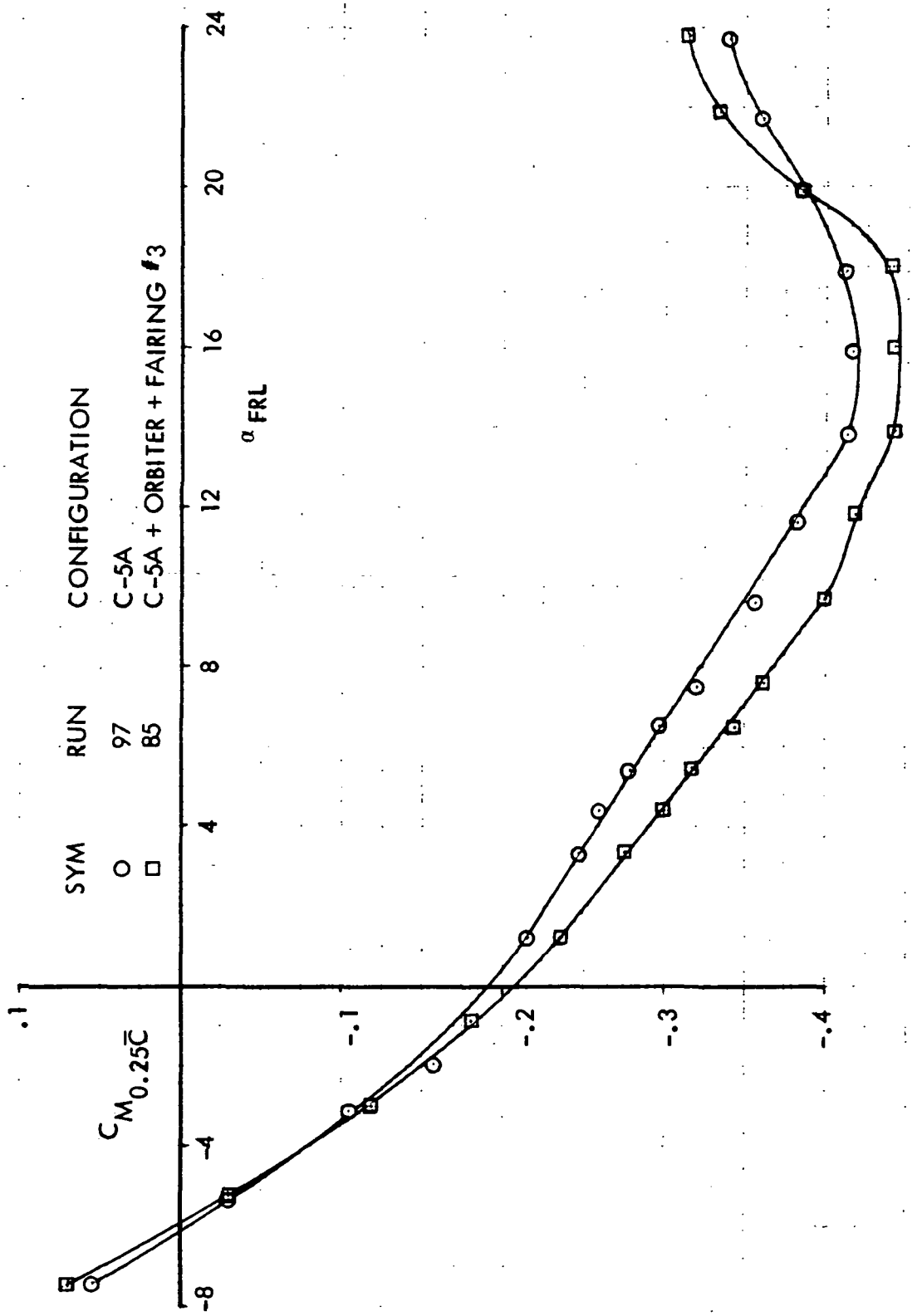

FIGURE 18

EFFECT OF ORBITER ON LONGITUDINAL STABILITY
LANDING CONFIGURATION

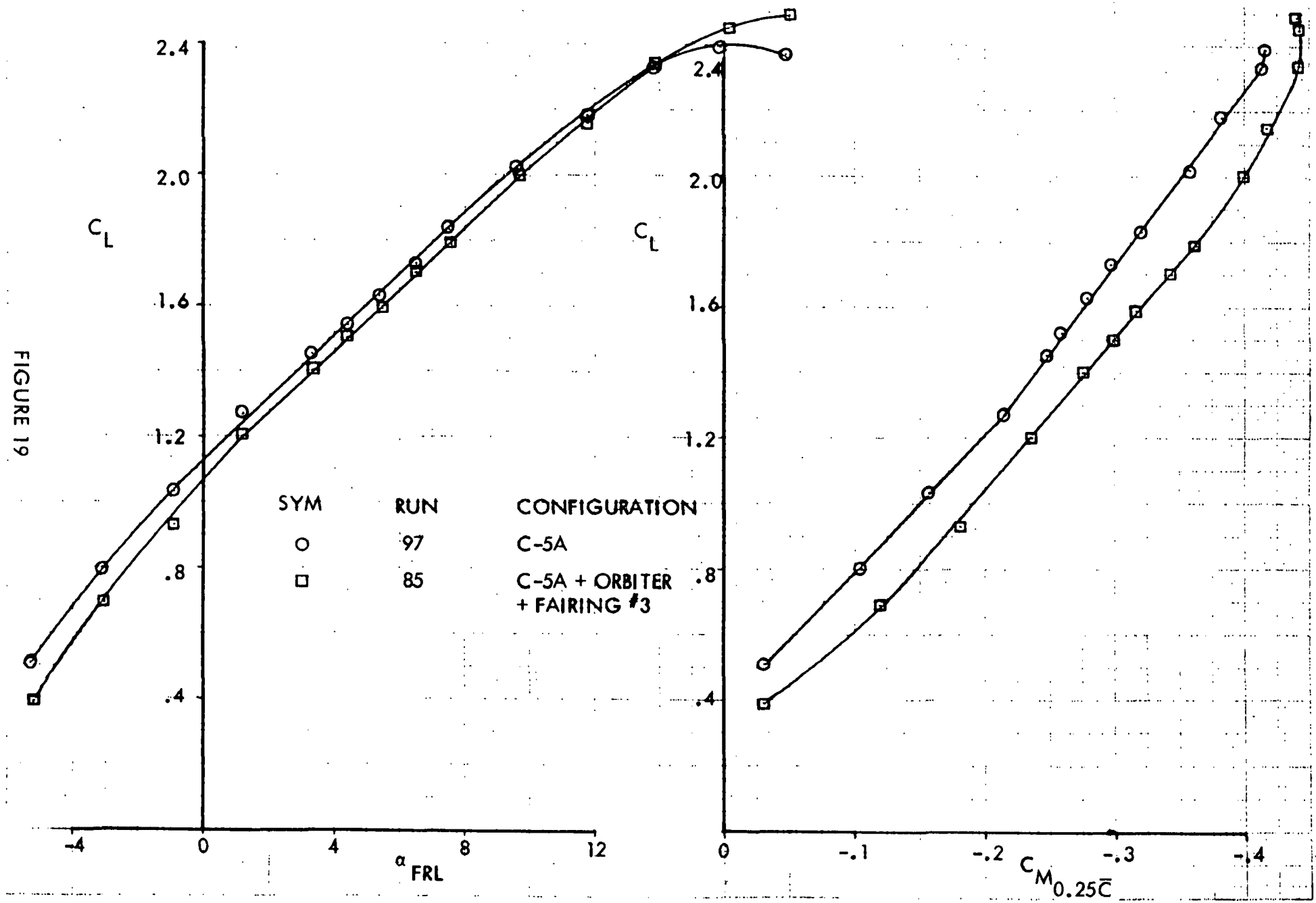

FIGURE 19

C-5A/PIGGYBACK ORBITER

EFFECT OF ORBITER ON DIRECTIONAL STABILITY
LANDING CONFIGURATION

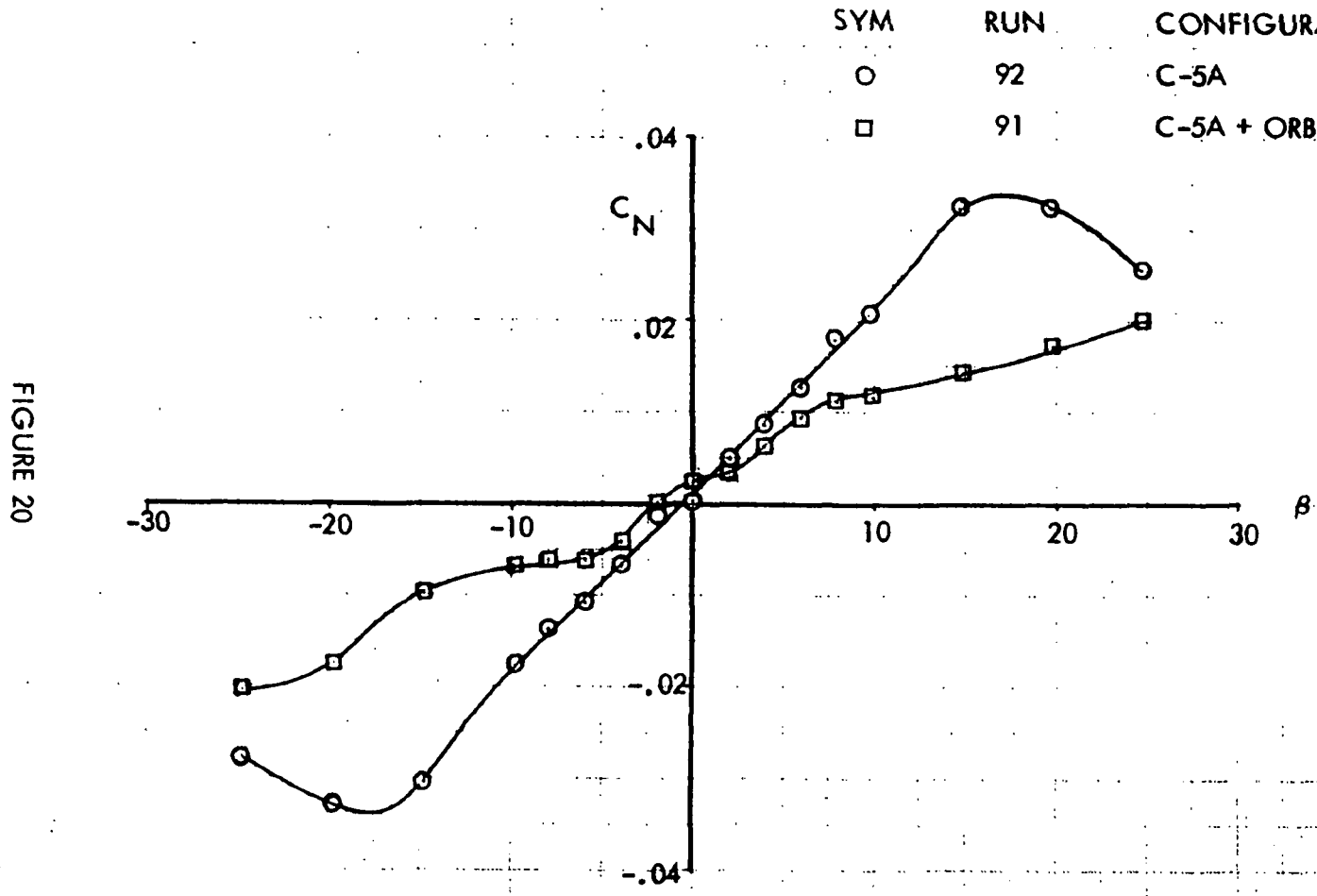

FIGURE 20

C-5A/ORBITER PIGGYBACK

EFFECT OF ORBITER ON LATERAL STABILITY
LANDING CONFIGURATION

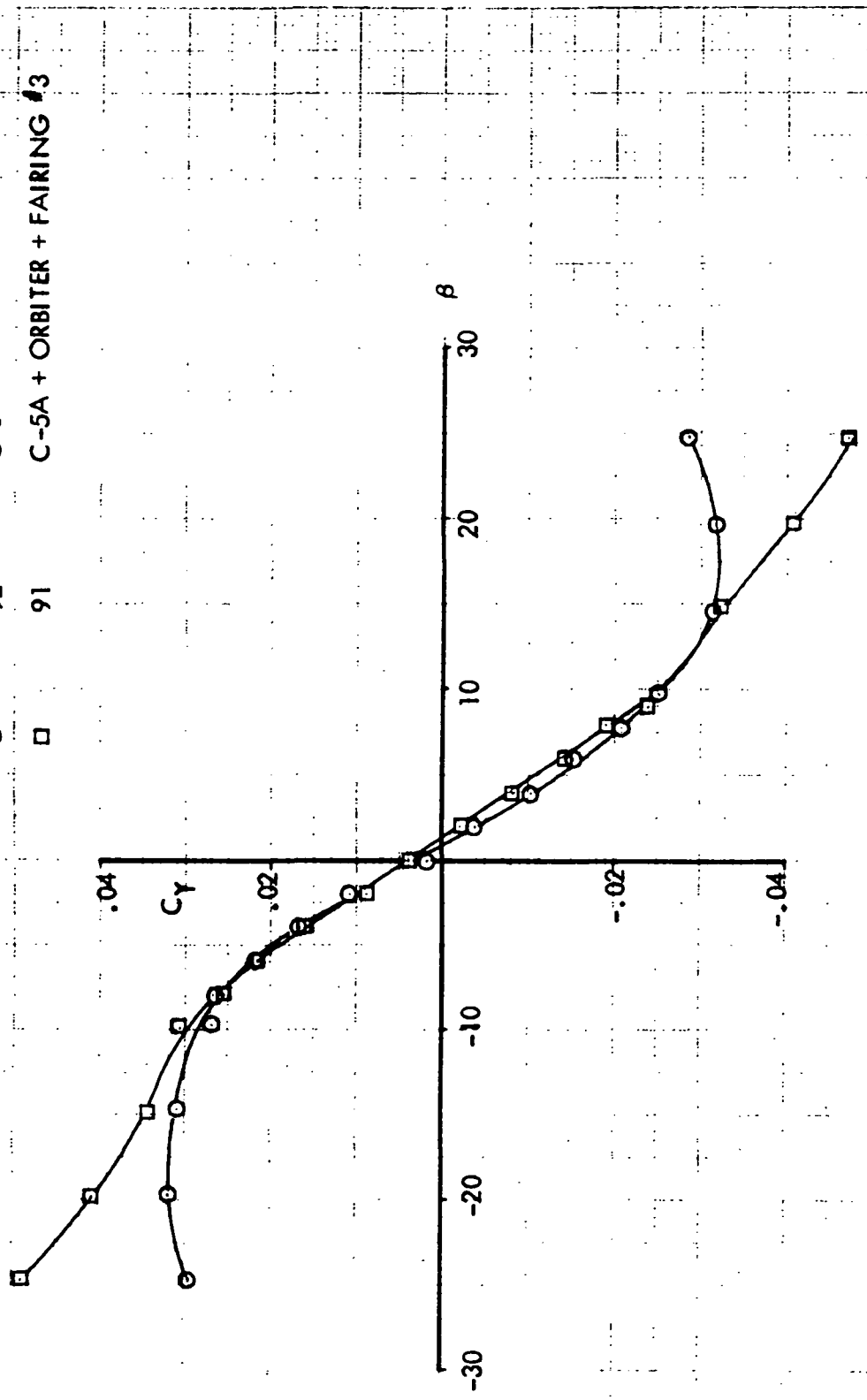

FIGURE 21

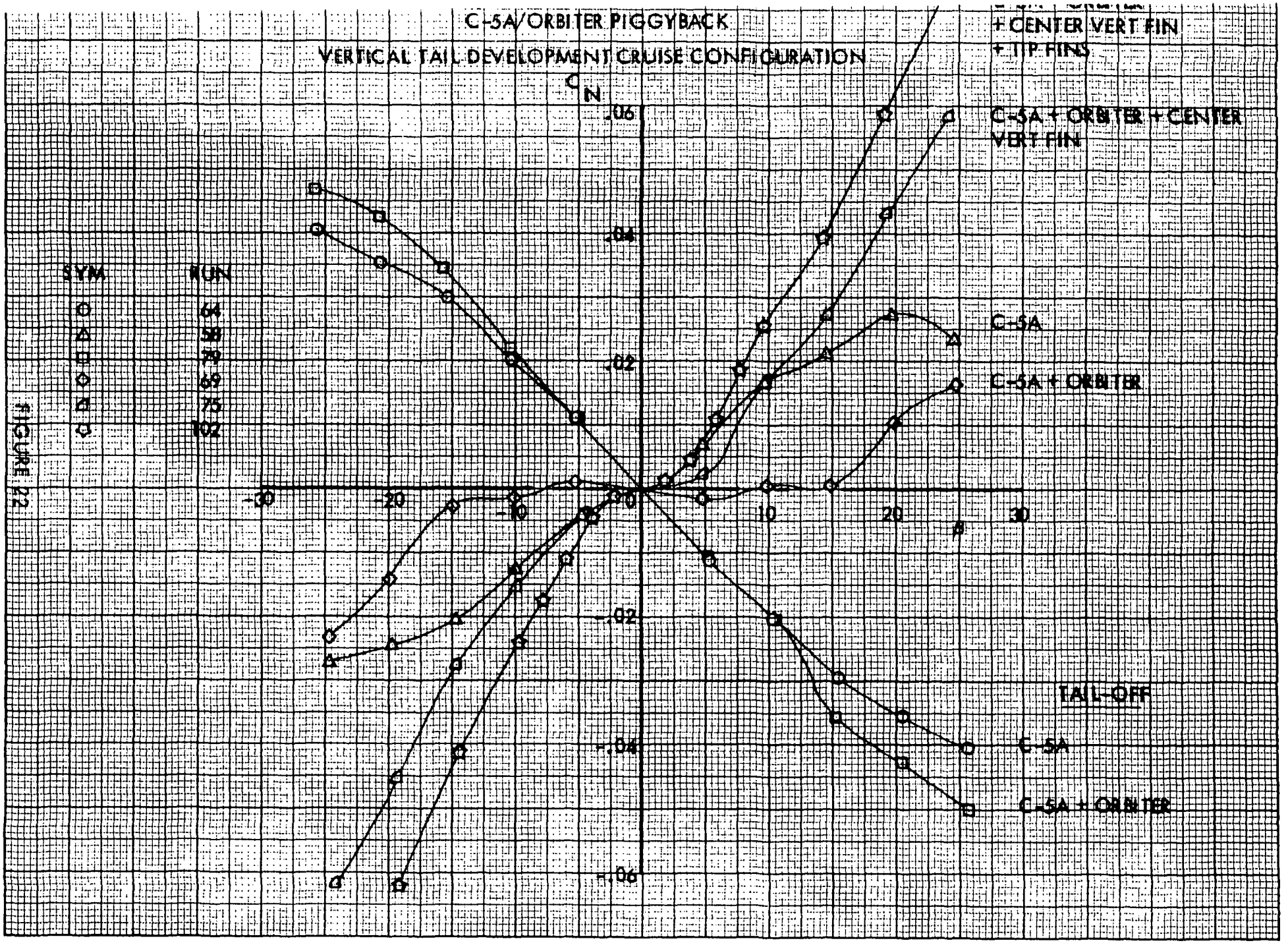
C-5A/ORBITER PIGGYBACK
VERTICAL TAIL DEVELOPMENT CRUISE CONFIGURATION
+ CENTER VERT FIN
+ TIP FINS
C_N
.06
.04
.02
-.02
-.04
-.06
-30
-20
-10
0
10
20
30
β
C-5A + ORBITER + CENTER VERT FIN
C-5A
C-5A + ORBITER
TAIL-OFF
C-5A
C-5A + ORBITER
SYM
RUN
64
58
79
69
75
102

FIGURE 22

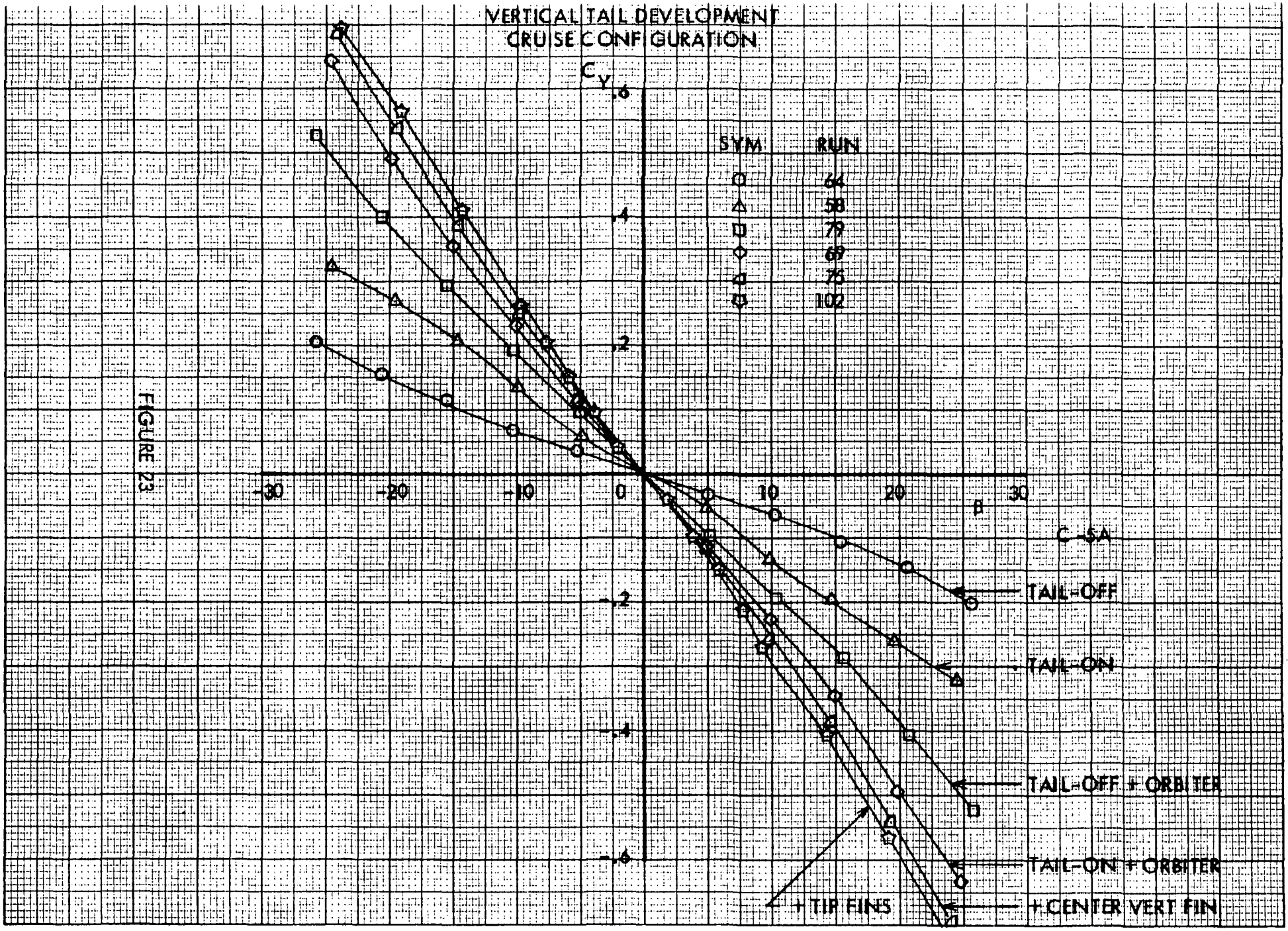
VERTICAL TAIL DEVELOPMENT
CRUISE CONFIGURATION
C_{Y_β}
SYM
RUN
64
58
79
69
76
102
.4
.2
-.2
-.4
-.6
-30
-20
-10
0
10
20
30
β
C-5A
TAIL-OFF
TAIL-ON
TAIL-OFF + ORBITER
TAIL-ON + ORBITER
+ TIP FINS
+ CENTER VERT FIN

FIGURE 23

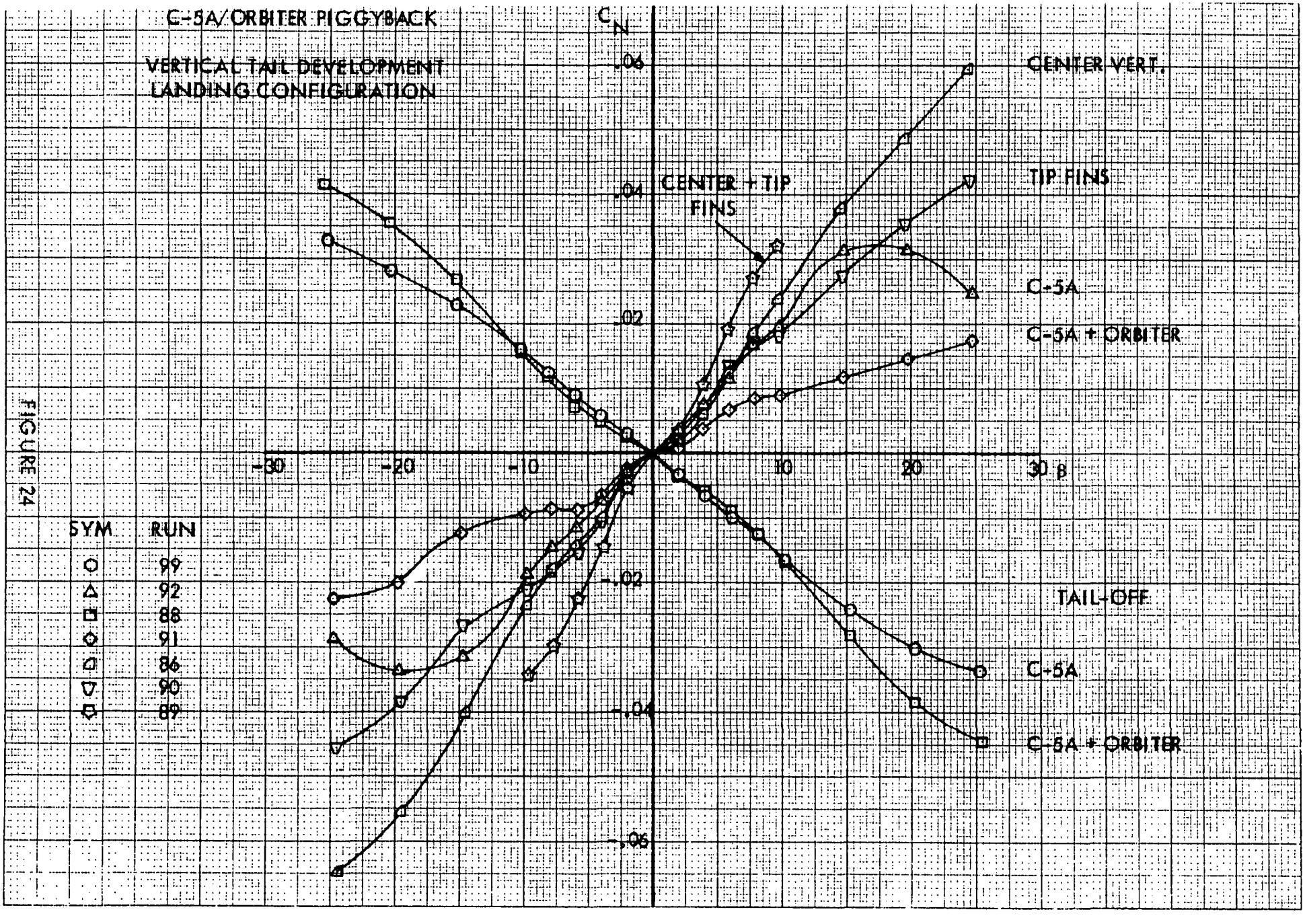
C-5A/ORBITER PIGGYBACK
VERTICAL TAIL DEVELOPMENT
LANDING CONFIGURATION
C_N
.06
.04
.02
-.02
-.04
-.06
-30
-20
-10
10
20
30 β
CENTER VERT.
CENTER + TIP FINS
TIP FINS
C-5A
C-5A + ORBITER
TAIL-OFF
C-5A
C-5A + ORBITER
SYM RUN
99
92
88
91
86
90
89

FIGURE 24

C-5A/ORBITER PIGGYBACK
VERTICAL TAIL DEVELOPMENT LANDING CONFIGURATION
C_{Y_β}
C-5A
TAIL-OFF
TAIL-ON
+ ORBITER TAIL-OFF
+ ORBITER TAIL-ON
+ CENTER VERT. FIN
+ TIP FINS
+ CENTER + TIP FINS
SYM
RUN
-30
-20
-10
0
10
20
30
-.6
-.4
-.2
.2
.4
.6

FIGURE 25

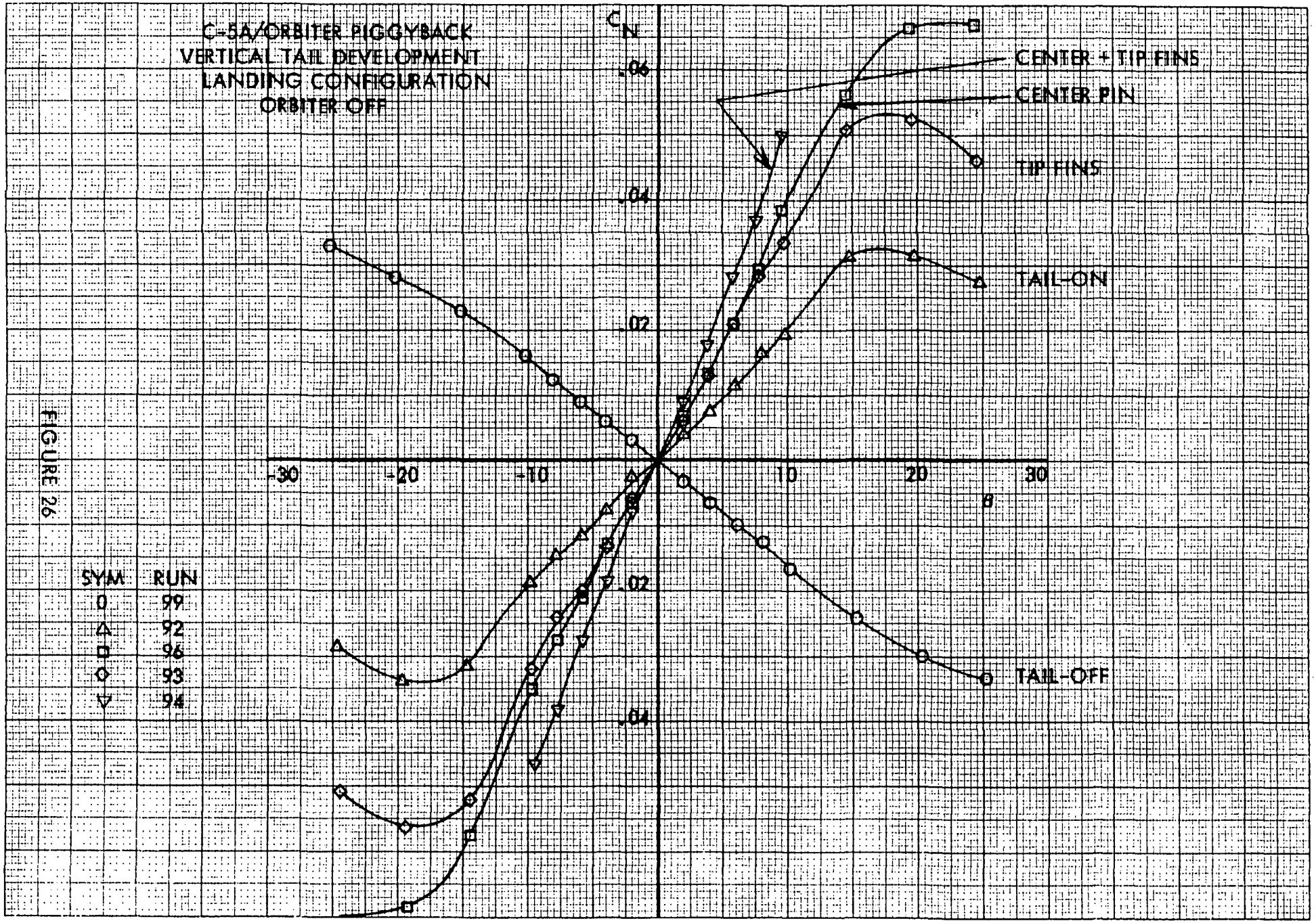
C-5A/ORBITER PIGGYBACK
VERTICAL TAIL DEVELOPMENT
LANDING CONFIGURATION
ORBITER OFF
C_N
.06
.04
.02
-.02
-.04
-30
-20
-10
10
20
30
β
CENTER + TIP FINS
CENTER FIN
TIP FINS
TAIL-ON
TAIL-OFF
SYM RUN
0 99
△ 92
□ 96
◇ 93
▽ 94

FIGURE 26

C-5A/ORBITER PIGGYBACK
VERTICAL TAIL DEVELOPMENT
LANDING CONFIGURATION
ORBITER OFF
SYM RUN
99
92
96
93
94
C_Y
.4
.2
-.2
-.4
30
20
10
-10
-20
-30
4
TAIL-OFF
TAIL-ON
TAIL-ON + TIP FINS
TAIL-ON + CENTER FIN
TAIL-ON + CENTER FIN + TIP FINS

FIGURE 27

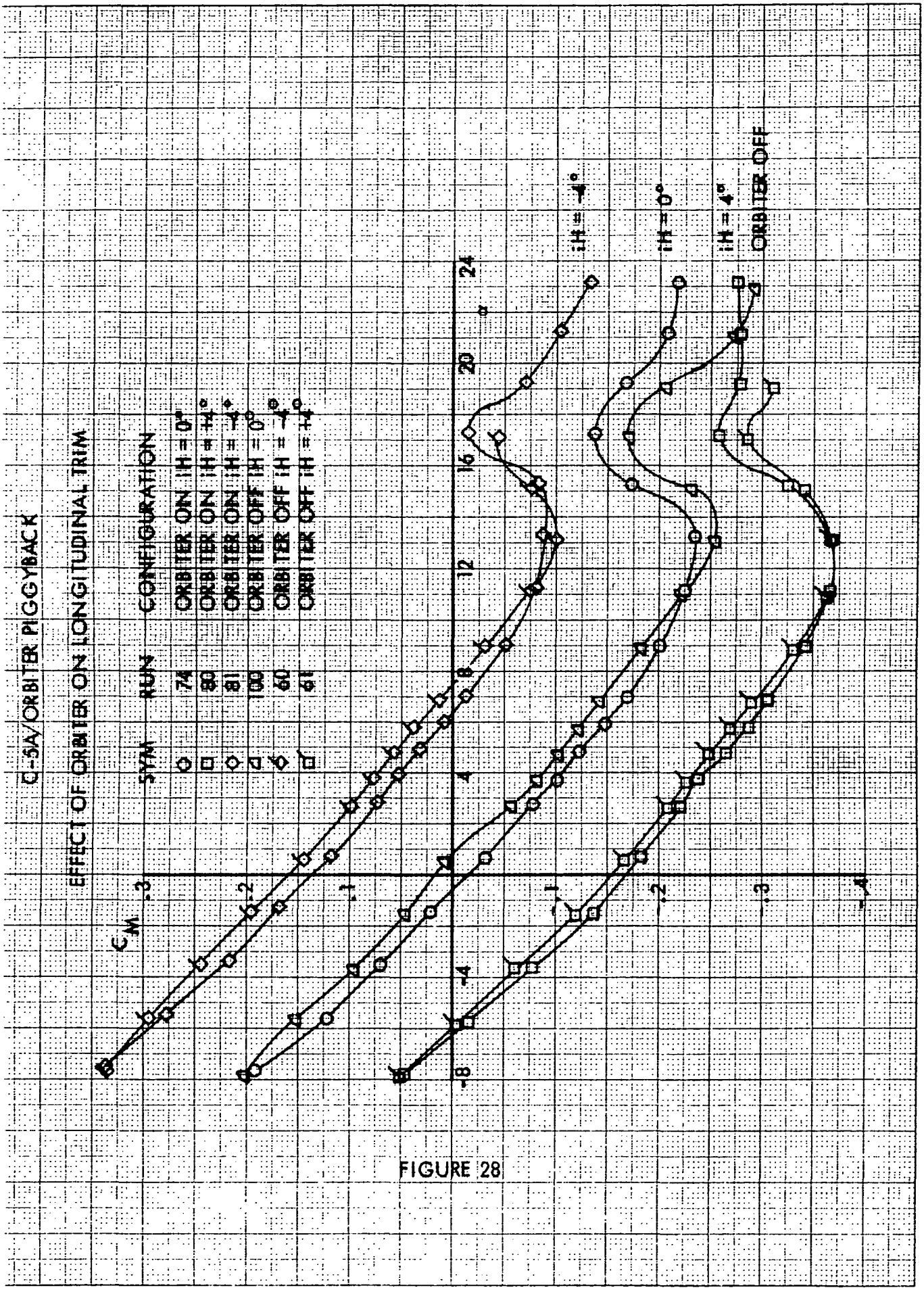
C-5A/ORBITER PIGGYBACK
EFFECT OF ORBITER ON LONGITUDINAL TRIM
C_M
SYM RUN CONFIGURATION
74 ORBITER ON iH = 0°
80 ORBITER ON iH = +4°
81 ORBITER ON iH = -4°
100 ORBITER OFF iH = 0°
60 ORBITER OFF iH = -4°
61 ORBITER OFF iH = +4°
iH = -4°
iH = 0°
iH = 4°
ORBITER OFF
α
24
20
16
12
8
4
-4
-8
.3
.2
.1
-.1
-.2
-.3
-.4

FIGURE 28

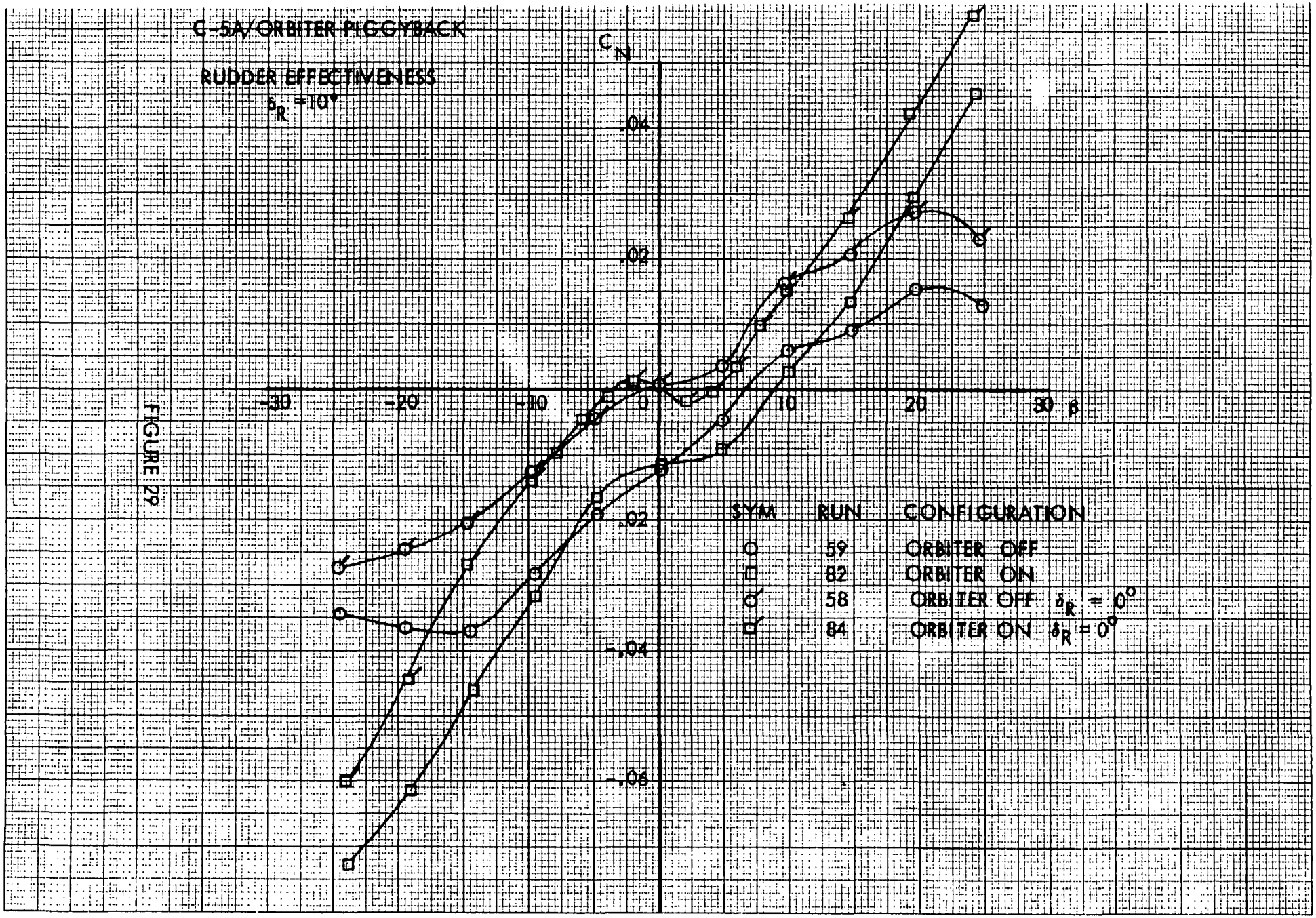
C-5A/ORBITER PIGGYBACK
RUDDER EFFECTIVENESS
δ_R =10°
C_N
.04
.02
-.02
-.04
-.06
-30
-20
-10
0
10
20
30
β
SYM
RUN
CONFIGURATION
59
ORBITER OFF
82
ORBITER ON
58
ORBITER OFF $\delta_R = 0°$
84
ORBITER ON $\delta_R = 0°$

FIGURE 29

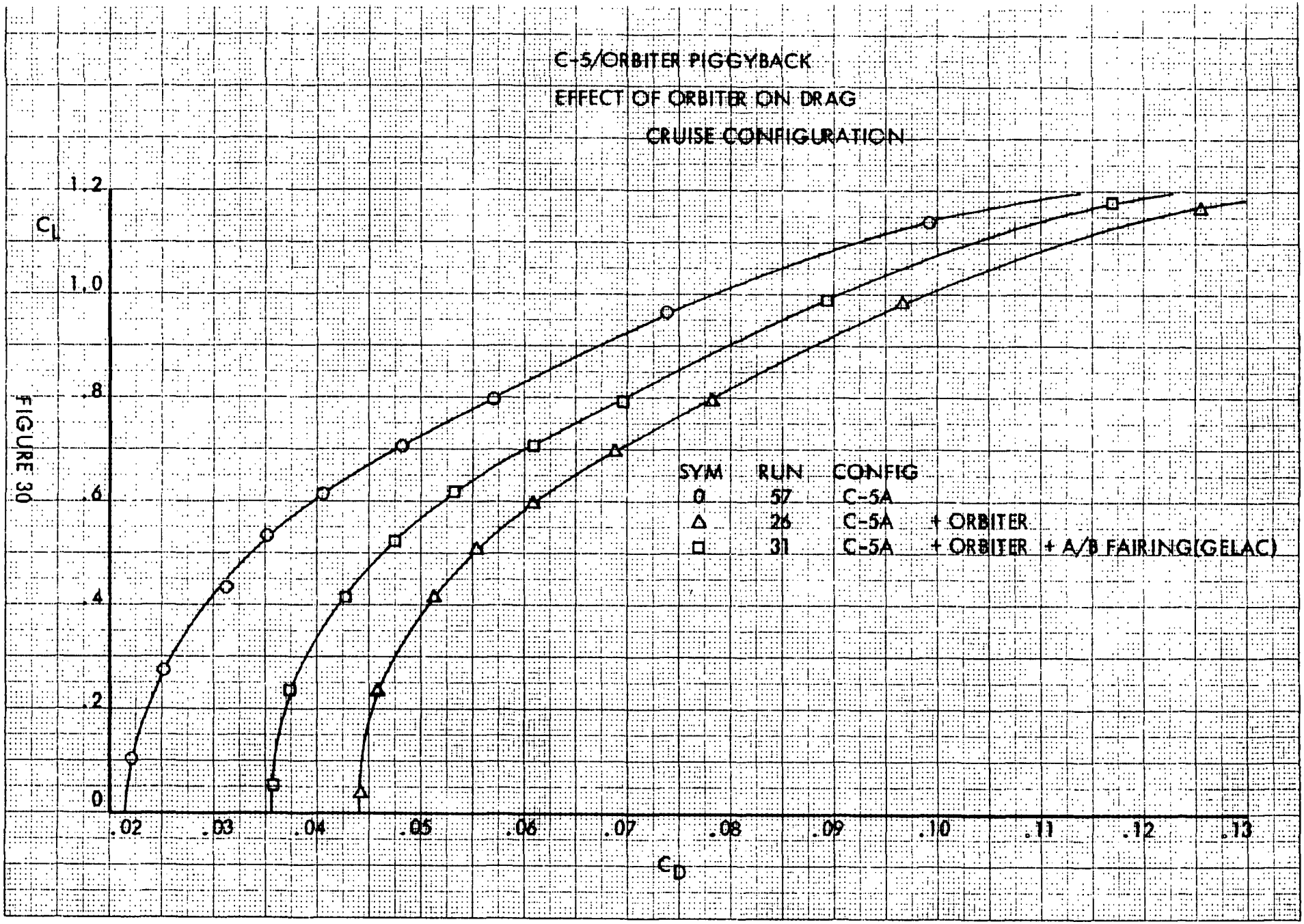
C-5/ORBITER PIGGYBACK
EFFECT OF ORBITER ON DRAG
CRUISE CONFIGURATION
C_L
1.2
1.0
.8
.6
.4
.2
0
.02
.03
.04
.05
.06
.07
.08
.09
.10
.11
.12
.13
C_D
SYM RUN CONFIG
○ 57 C-5A
△ 26 C-5A + ORBITER
□ 31 C-5A + ORBITER + A/B FAIRING(GELAC)

FIGURE 30

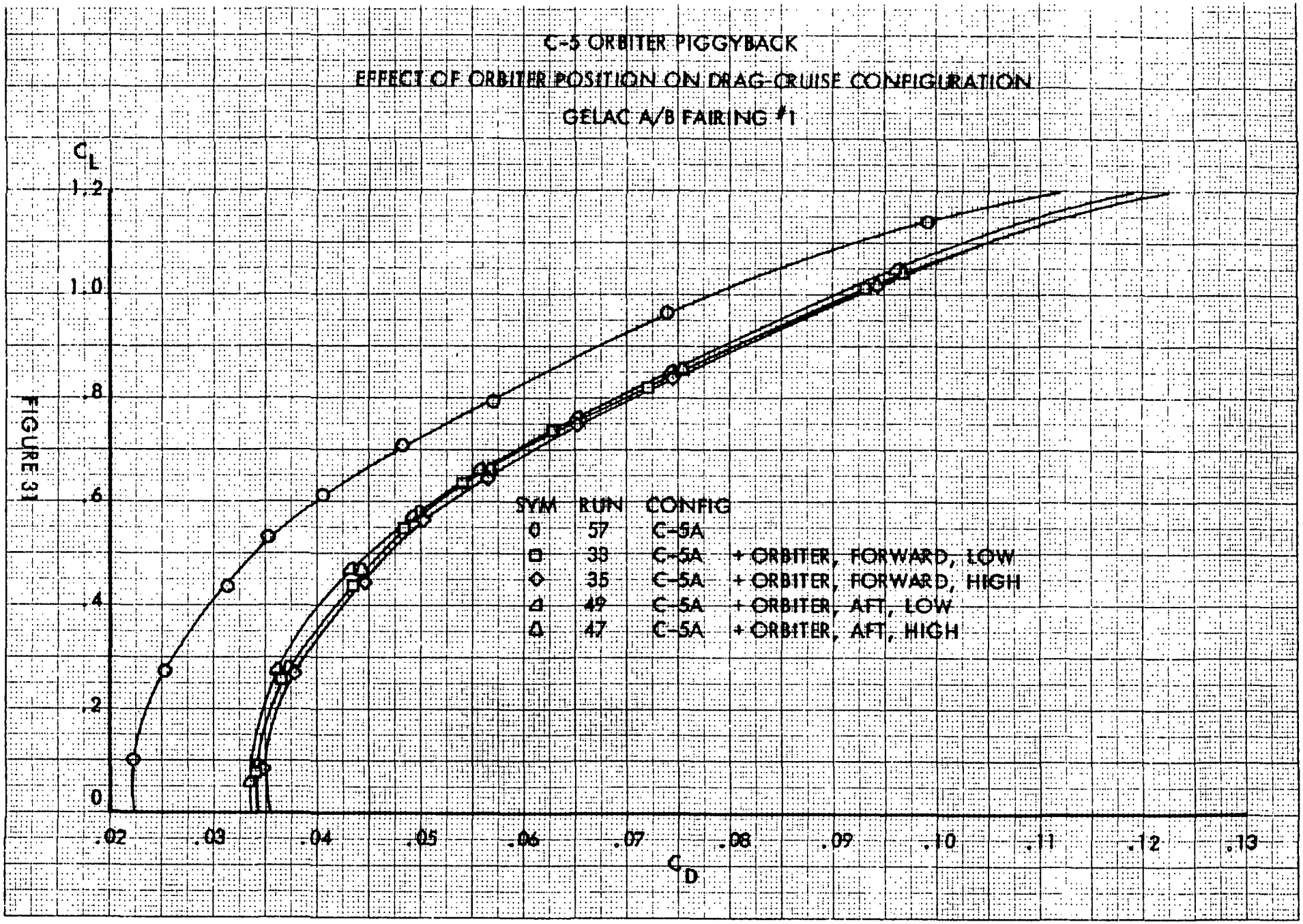
C-5 ORBITER PIGGYBACK
EFFECT OF ORBITER POSITION ON DRAG-CRUISE CONFIGURATION
GELAC A/B FAIRING #1
C_L
1.2
1.0
.8
.6
.4
.2
0
.02
.03
.04
.05
.06
.07
.08
.09
.10
.11
.12
.13
C_D
SYM RUN CONFIG
0 57 C-5A
□ 38 C-5A + ORBITER, FORWARD, LOW
◇ 35 C-5A + ORBITER, FORWARD, HIGH
△ 49 C-5A + ORBITER, AFT, LOW
△ 47 C-5A + ORBITER, AFT, HIGH

FIGURE 31

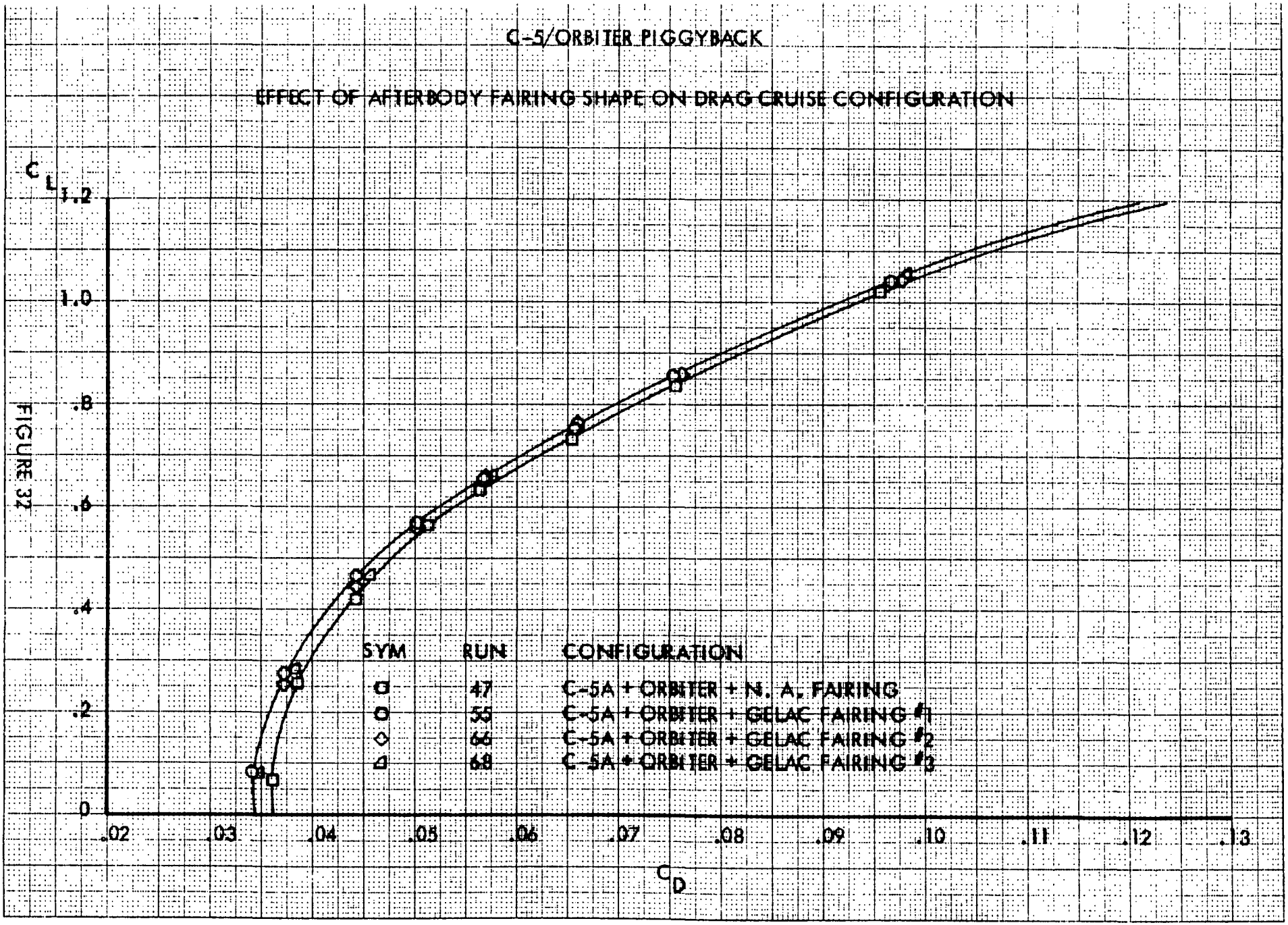
C-5/ORBITER PIGGYBACK
EFFECT OF AFTERBODY FAIRING SHAPE ON DRAG CRUISE CONFIGURATION
C_L
1.2
1.0
.8
.6
.4
.2
0
.02
.03
.04
.05
.06
.07
.08
.09
.10
.11
.12
.13
C_D
SYM RUN CONFIGURATION
47 C-5A + ORBITER + N. A. FAIRING
55 C-5A + ORBITER + GELAC FAIRING #1
66 C-5A + ORBITER + GELAC FAIRING #2
68 C-5A + ORBITER + GELAC FAIRING #3

FIGURE 32

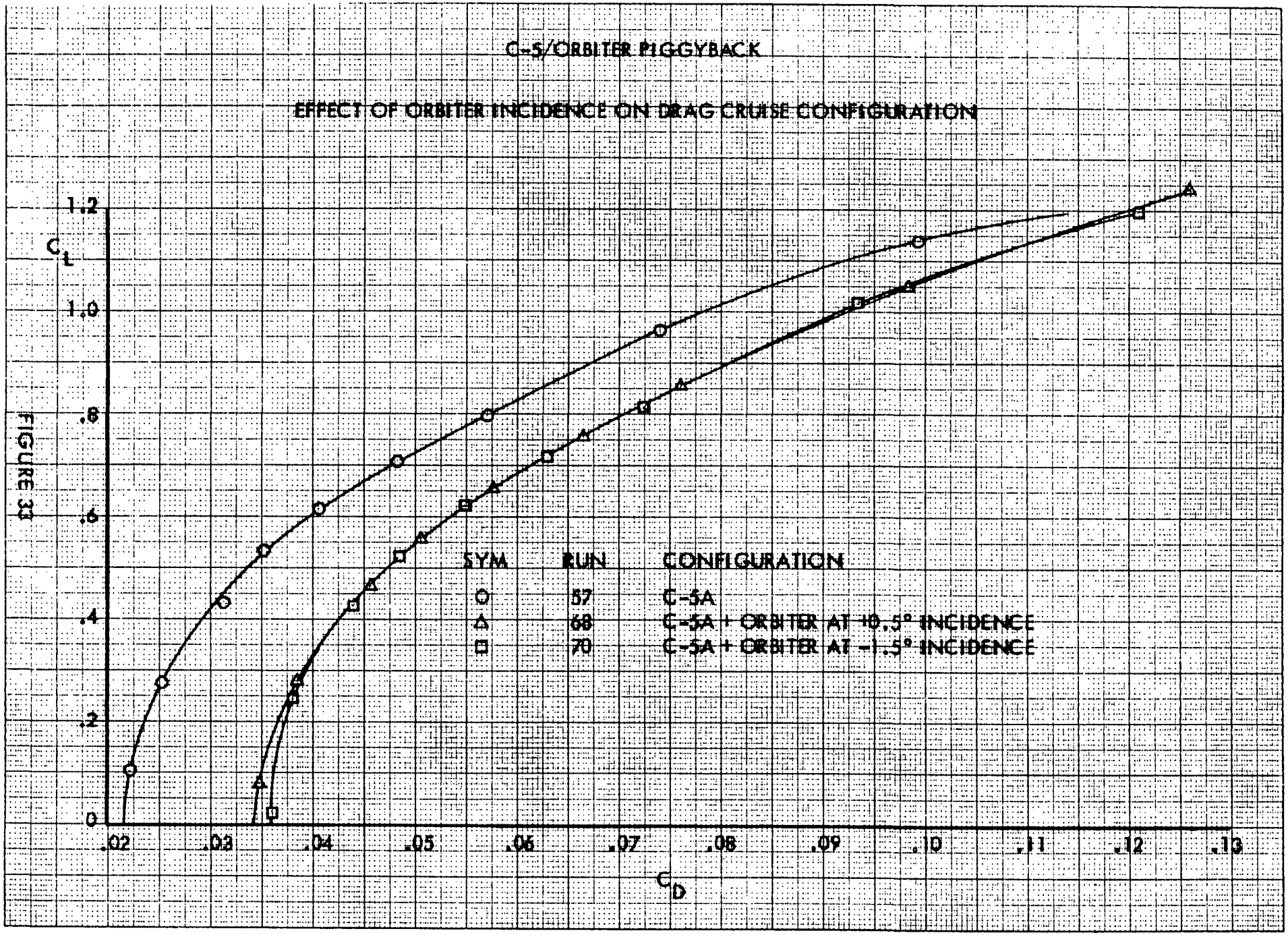
C-5/ORBITER PIGGYBACK
EFFECT OF ORBITER INCIDENCE ON DRAG CRUISE CONFIGURATION
C_L
1.2
1.0
.8
.6
.4
.2
0
.02
.03
.04
.05
.06
.07
.08
.09
.10
.11
.12
.13
C_D
SYM
RUN
CONFIGURATION
57
C-5A
68
C-5A + ORBITER AT +0.5° INCIDENCE
70
C-5A + ORBITER AT -1.5° INCIDENCE

FIGURE 33

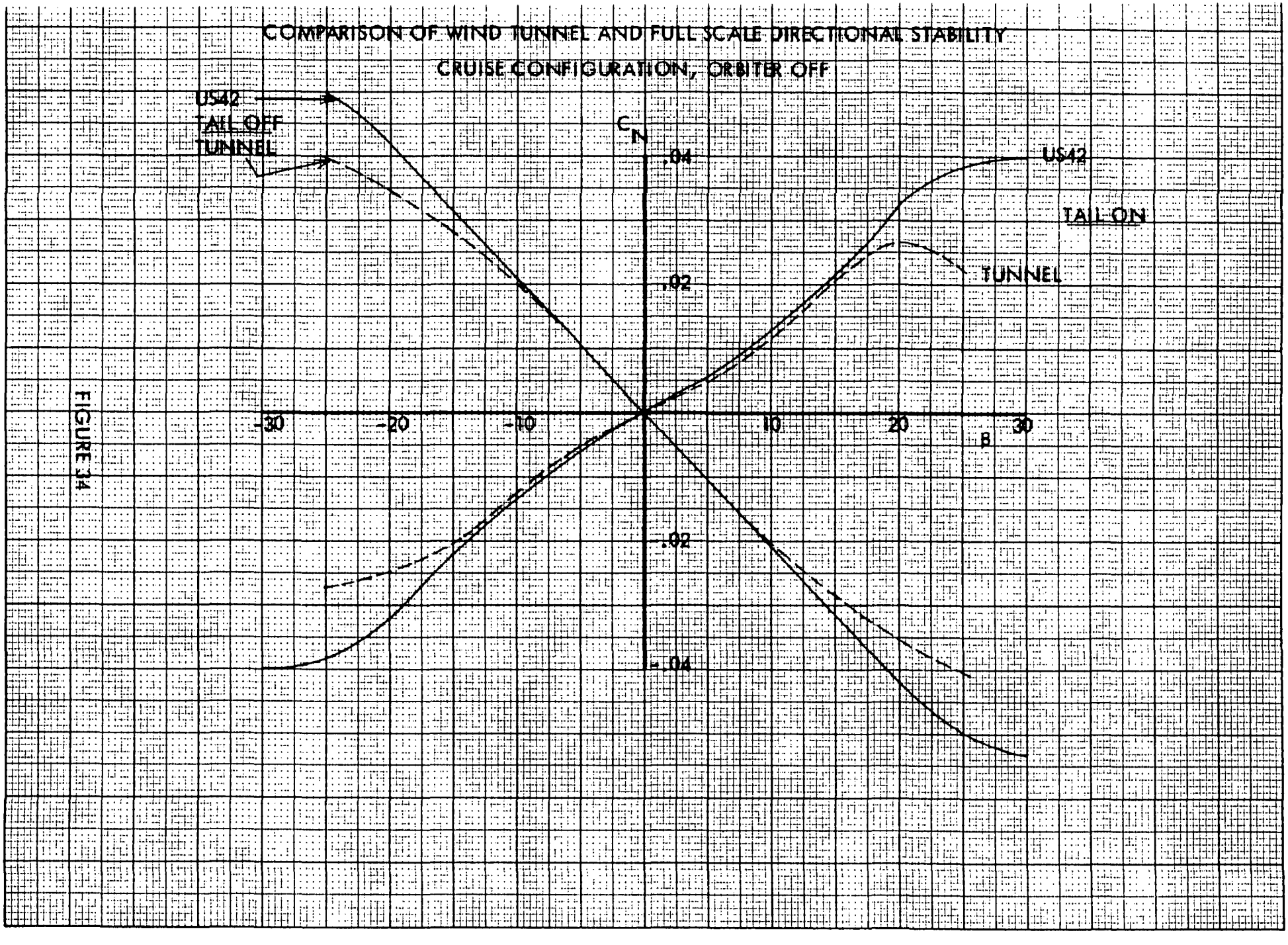
COMPARISON OF WIND TUNNEL AND FULL SCALE DIRECTIONAL STABILITY
CRUISE CONFIGURATION, ORBITER OFF
US42
TAIL OFF
TUNNEL
C_N
.04
.02
-.02
-.04
US42
TAIL ON
TUNNEL
-30
-20
-10
10
20
30
β

FIGURE 34

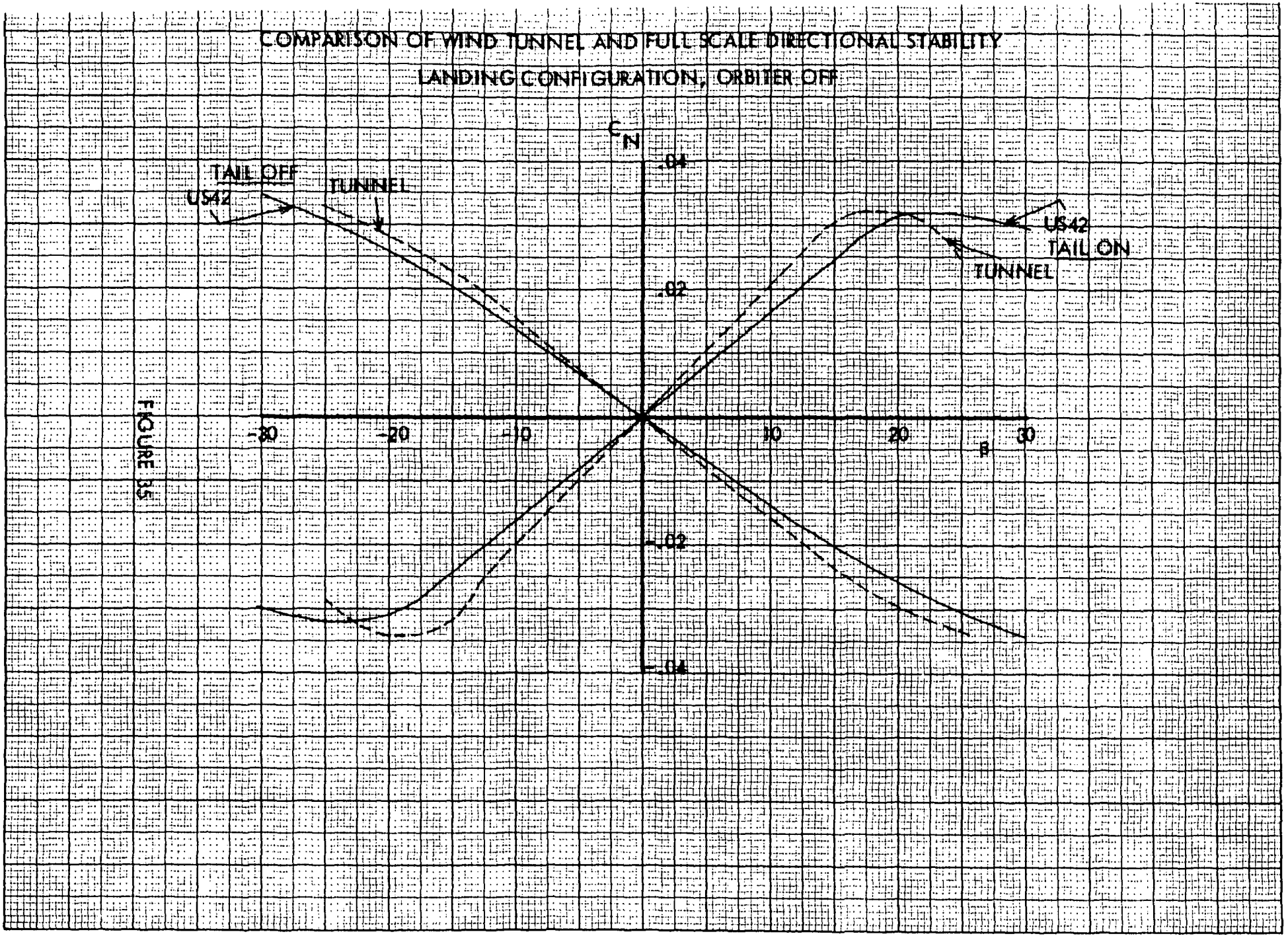
COMPARISON OF WIND TUNNEL AND FULL SCALE DIRECTIONAL STABILITY
LANDING CONFIGURATION, ORBITER OFF
C_{YN}
.04
.02
-.02
-.04
-30
-20
-10
10
20
30
β
TAIL OFF
US42
TUNNEL
US42
TAIL ON
TUNNEL

FIGURE 35

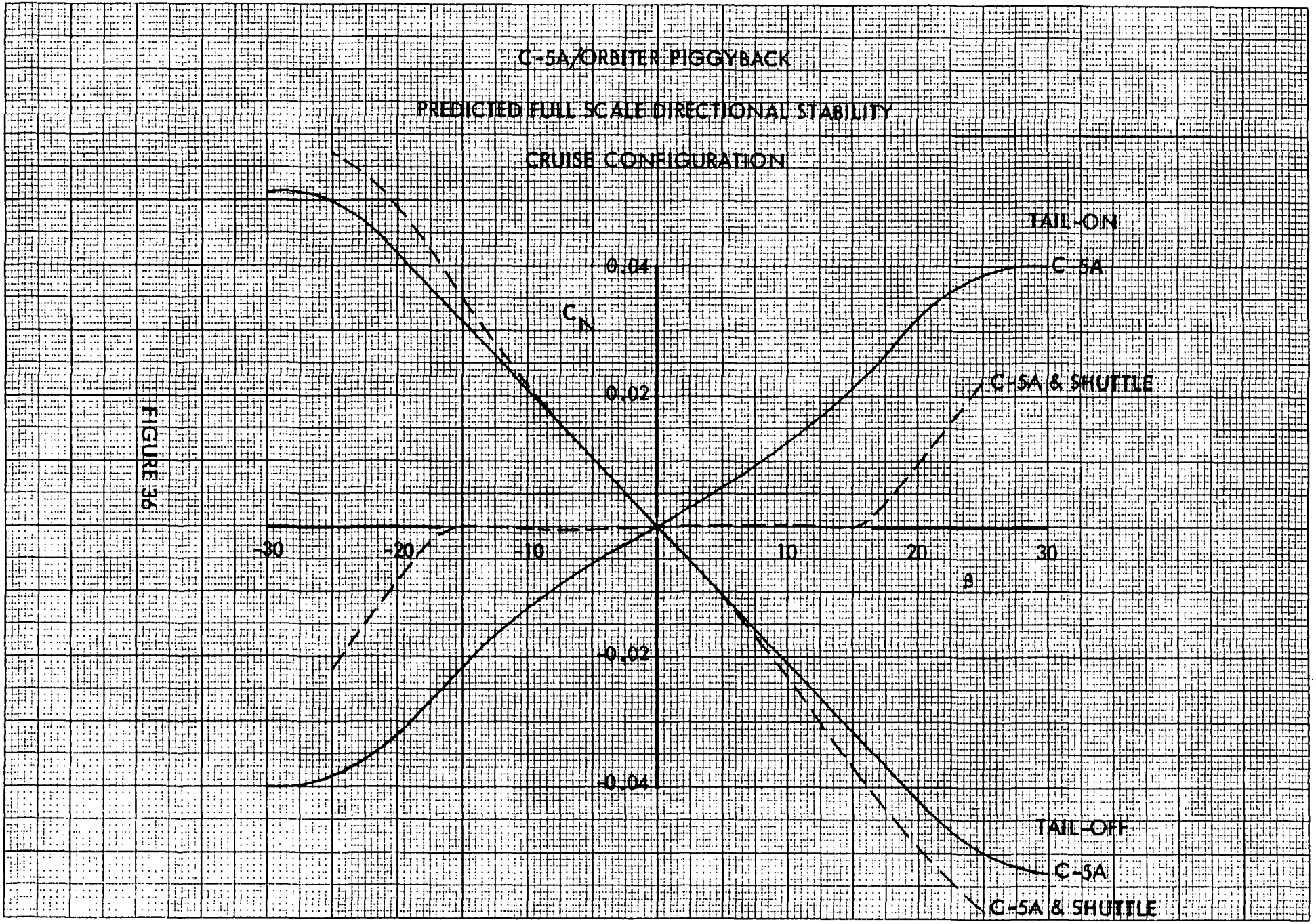
C-5A/ORBITER PIGGYBACK
PREDICTED FULL SCALE DIRECTIONAL STABILITY
CRUISE CONFIGURATION
TAIL-ON
C-5A
C-5A & SHUTTLE
C_N
0.04
0.02
-0.02
-0.04
-30
-20
-10
10
20
30
β
TAIL-OFF
C-5A
C-5A & SHUTTLE

FIGURE 36

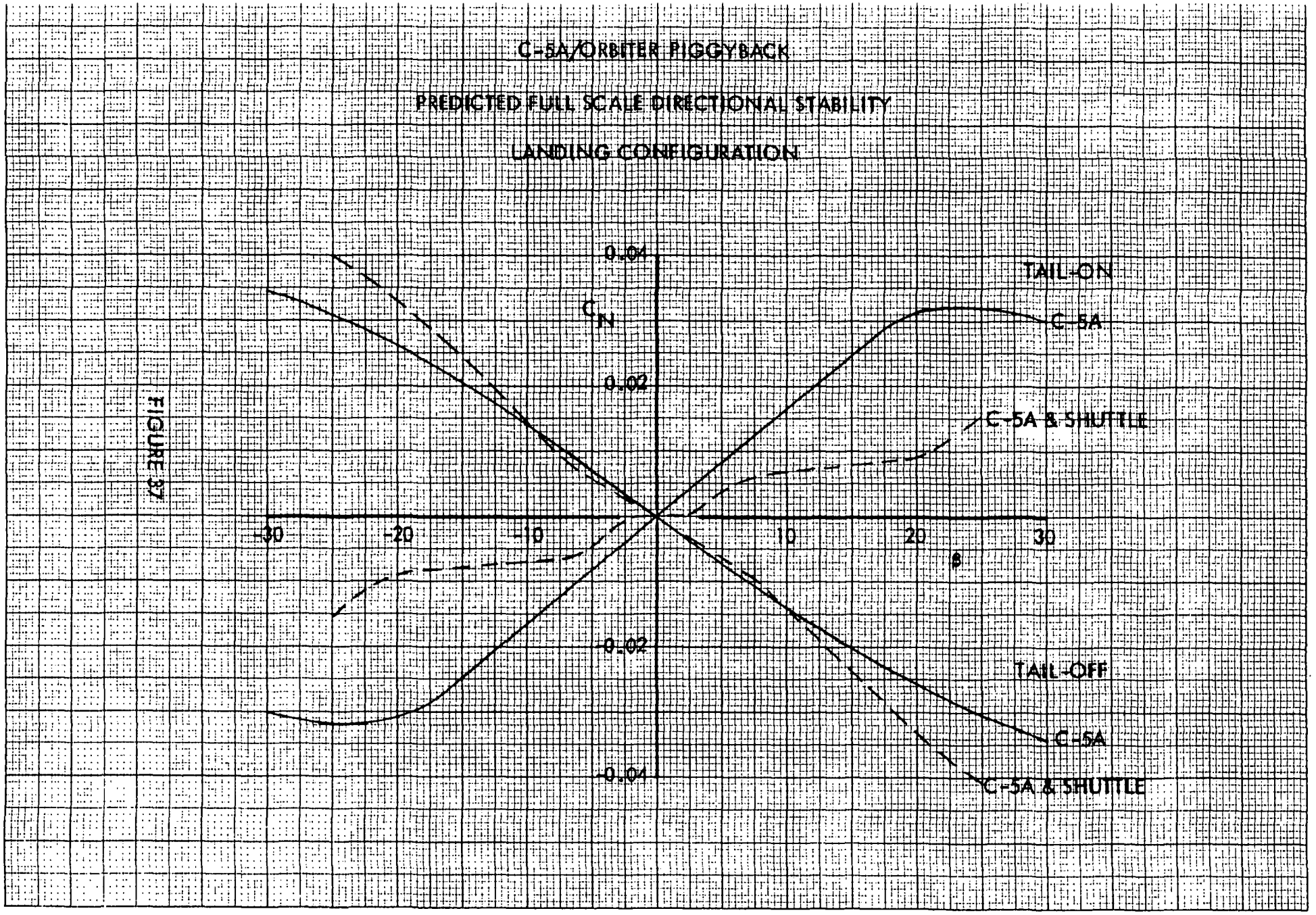
C-5A/ORBITER PIGGYBACK
PREDICTED FULL SCALE DIRECTIONAL STABILITY
LANDING CONFIGURATION
0.04
C_N
0.02
-0.02
-0.04
-30
-20
-10
10
20
30
β
TAIL-ON
C-5A
C-5A & SHUTTLE
TAIL-OFF
C-5A
C-5A & SHUTTLE

FIGURE 37

C-5A/ORBITER PIGGYBACK FLIGHT VEHICLE DATA

M = 0.52 @ 20,000 ft V_T = 319 KTAS

Wing area, S = 6200 ft^2 Wing span, b = 219 ft

FLIGHT CASE		#1	#2	#3
Gross Weight ~ lbs		550,000	704,626	704,626
I_{xx} ~ slugs $ft^2 \times 10^{-6}$		3.43	3.45	3.89
I_{zz} ~ slugs $ft^2 \times 10^{-6}$		5.48	6.07	6.11
I_{xz} ~ slugs $ft^2 \times 10^{-6}$		2.20	2.42	3.97
Stability and Control Derivatives				
Sideslip	C_{y_β} ~ /rad.	-.802	-.802	-1.34
	C_{ℓ_β} ~ /rad.	-.0771	-.0997	-.0997
	C_{n_β} ~ /rad.	.0728	.0728	0
Roll rate	C_{ℓ_p} ~ /rad.	-.390	-.390	-.390
	C_{n_p} ~/rad.	-.081	-.081	-.081
Yaw rate	C_{y_r} ~/rad.	.510	.500	.500
	C_{ℓ_r} ~/rad.	.177	.199	.199
	C_{n_r} ~/rad.	-.180	-.180	-.180
Aileron angle	$C_{\ell_{\delta_a}}$ ~/rad.	-.0319	-.0319	-.0319
	$C_{n_{\delta_a}}$ ~/rad.	0	0	0
Rudder angle	$C_{y_{\delta_r}}$ ~ /rad.	.2006	.2006	.2006
	$C_{\ell_{\delta_r}}$ ~ /rad.	.0210	.0181	.0181
	$C_{n_{\delta_r}}$ ~/rad.	-.1031	-.1031	-.1031
Spoiler angle	$C_{y_{\delta_s}}$ ~/rad.	-.0573	-.0573	-.0573
	$C_{\ell_{\delta_s}}$ ~/rad.	.0268	.0268	.0268
	$C_{n_{\delta_s}}$ ~/rad.	.0057	.0057	.0057

FIGURE 38

LATERAL-DIRECTIONAL RESPONSE MODE DATA

Characteristic Equation:

$$(s^2 + 2\zeta_d w_d s + w_d^2)(s + 1/\tau_R)(s + 1/\tau_s) = 0$$

Item or Parameter	Case #1	Case #2	Case #3
G.W. (no payload)	550,000#	550,000#	550,000#
cargo weight	-	154,626#	-
orbiter weight	-	-	154,626#
gross weight	550,000#	704,626#	704,626#
Dutch Roll Mode			
frequency, w_d - rad/sec	.634	.620	.344
damping ratio, ζ_d	.118	.076	-.023
period, T_d - secs.	9.98	10.2	18.3
time to 1/2-ampl, $t_{1/2}$ - secs.	9.18	14.6	-89
cycles 1/2-ampl, $C_{1/2}$	.92	1.44	-4.9
Roll Convergence Mode			
time constant, τ_R - secs	1.45	1.42	1.35
time to 1/2-ampl, $t_{1/2}$ - secs	1.0	.98	.93
Spiral Mode			
time constant, τ_s - secs	694	216	15.2
time to 1/2-ampl, $t_{1/2}$ - secs	479	149	10.5

NOTE: Negative values signify an unstable dutch roll mode.

FIGURE 39

C-5A STABILITY AUGMENTATION &

AUTOPILOT SYSTEMS APPROXIMATIONS

Stability Augmentation Elements

Aileron: $\delta_a = 0.055\ (\phi)$

Spoiler: $\delta_s = 0$

Rudder: $\delta_r = -.482(p) - .101(\phi) + 1.0\ (r)$

Incremental Elements for Autopilot Operative*

Aileron: $\Delta\delta_a = 2.25\ (p) + 3.22\ (\phi)$

Spoiler: $\Delta\delta_s = -.786\ (\phi)$

Rudder: $\Delta\delta_r = 0$

* Control command and heading stability ($\phi < 7^{\circ}$) elements are excluded.

FIGURE 40

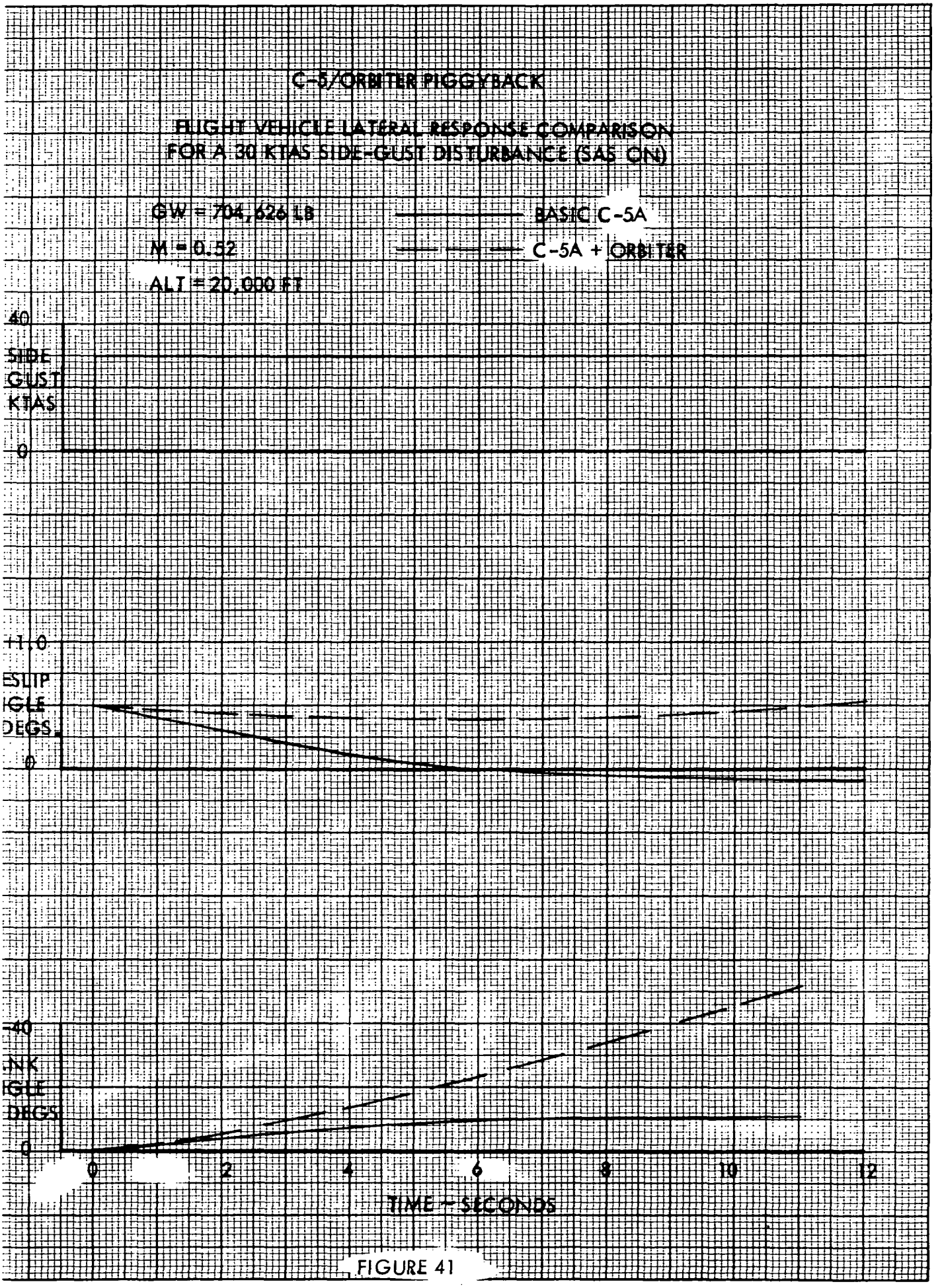
C-5/ORBITER PIGGYBACK
FLIGHT VEHICLE LATERAL RESPONSE COMPARISON
FOR A 30 KTAS SIDE-GUST DISTURBANCE (SAS ON)
GW = 704,626 LB
M = 0.52
ALT = 20,000 FT
BASIC C-5A
C-5A + ORBITER
40
SIDE
GUST
KTAS
0
+1.0
ESLIP
IGLE
DEGS
0
-40
INK
IGLE
DEGS
0
0
2
4
6
8
10
12
TIME - SECONDS

FIGURE 41

C-5A/ORBITER PIGGYBACK

FLIGHT VEHICLE RESPONSE COMPARISON FOR
CONTROL WHEEL INPUT OF 10 DEGREES (SAS ON)

G.W. = 704,626 LB. ——————— BASIC C-5A

M = 0.52 ——————— C-5A + ORBITER

ALT = 20,000 FT.

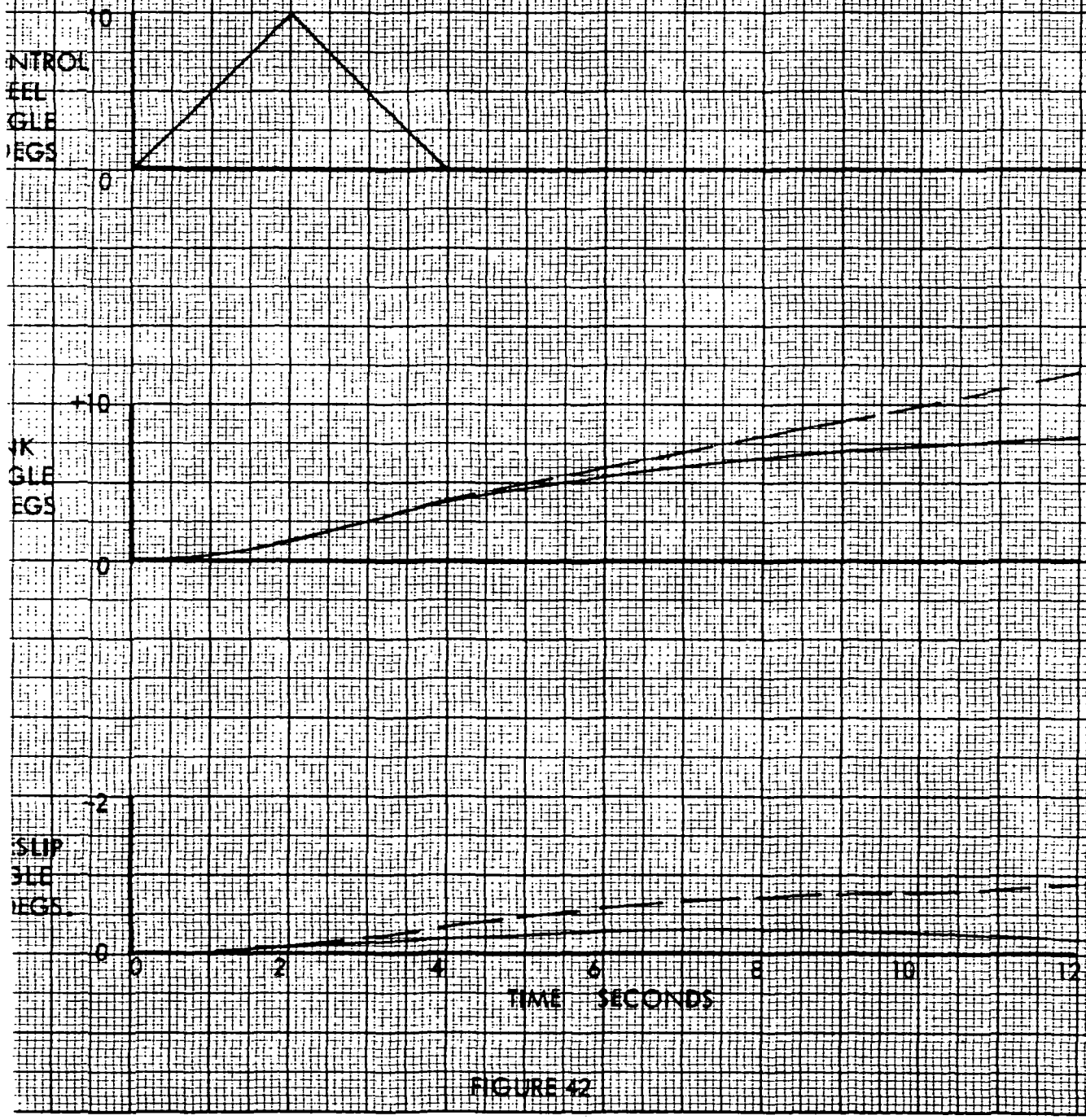

FIGURE 42

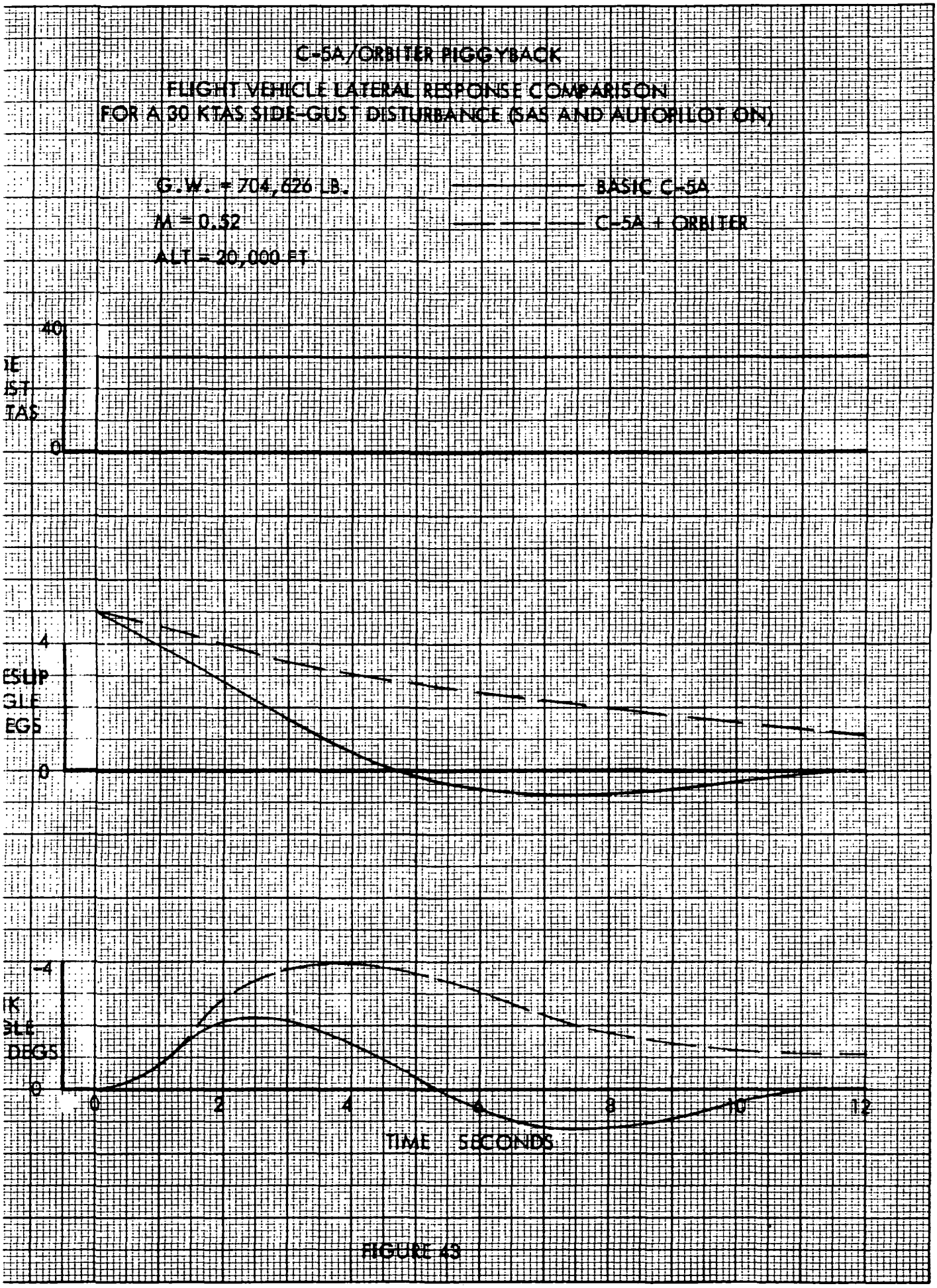
C-5A/ORBITER PIGGYBACK
FLIGHT VEHICLE LATERAL RESPONSE COMPARISON
FOR A 30 KTAS SIDE-GUST DISTURBANCE (SAS AND AUTOPILOT ON)
G.W. = 704,626 LB.
M = 0.52
ALT = 20,000 FT
BASIC C-5A
C-5A + ORBITER
40
0
4
0
-4
0
0
2
4
6
8
10
12
TIME SECONDS

FIGURE 43

C-5/ORBITER PIGGYBACK

COMPARISON OF ESTIMATED AND WIND TUNNEL TEST DRAG POLARS

CRUISE CONFIGURATION

TEST $R_N = 1.4 \times 10^6$/FT

○ RUN 57, CLEAN CONFIGURATION C-5

□ RUN 31, C-5 PLUS ORBITER

——— ESTIMATED C-5 PLUS ORBITER

NOTE: ESTIMATED DRAG = RUN 57 DATA PLUS $\Delta C_{D_{ORB}}$ FROM PUBLISHED ORBITER ALONE TEST DATA

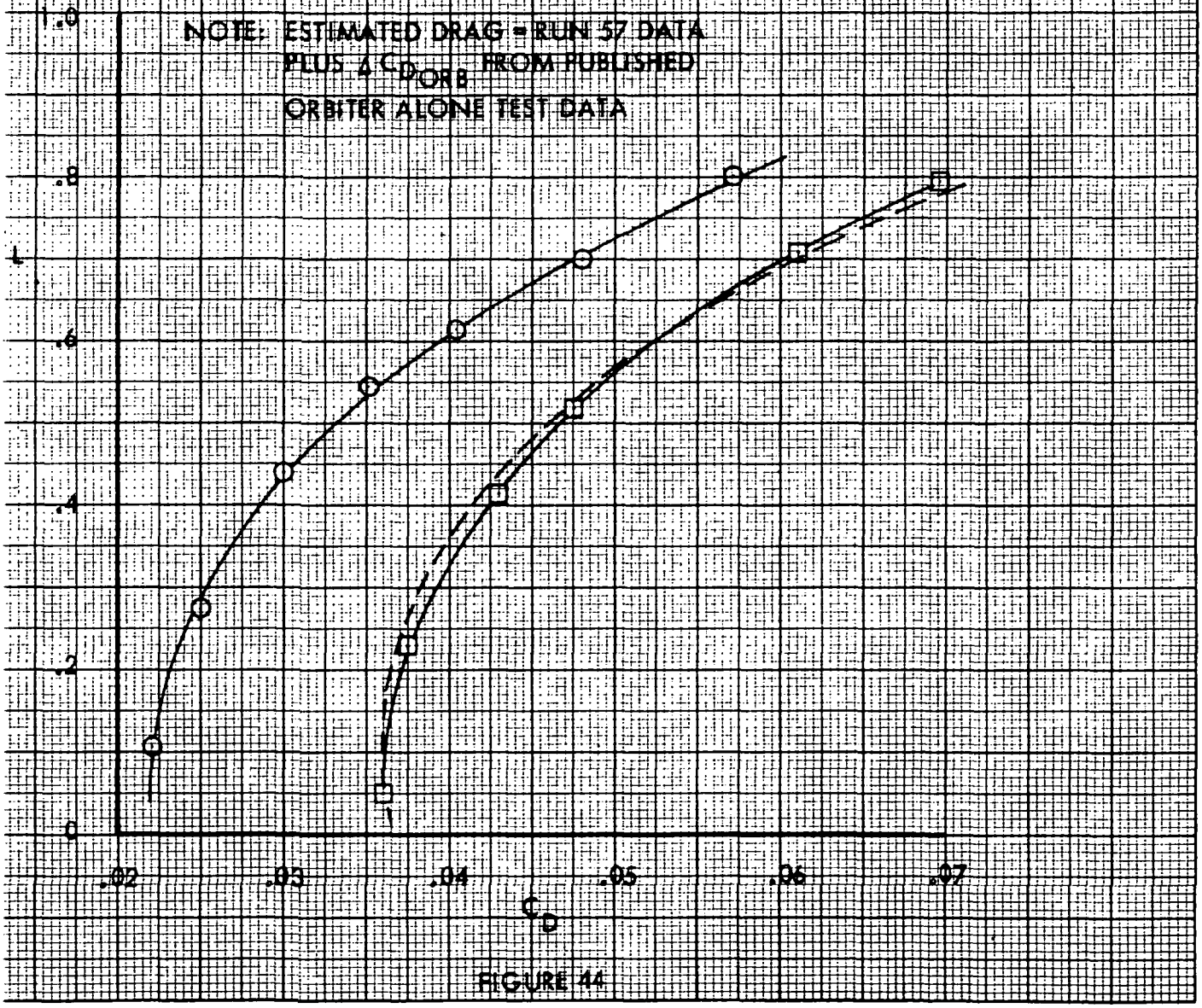

FIGURE 44

C-5/ORBITER PIGGYBACK

COMPARISON OF L/D FOR THE C-5 AND C-5/ORBITER PIGGYBACK

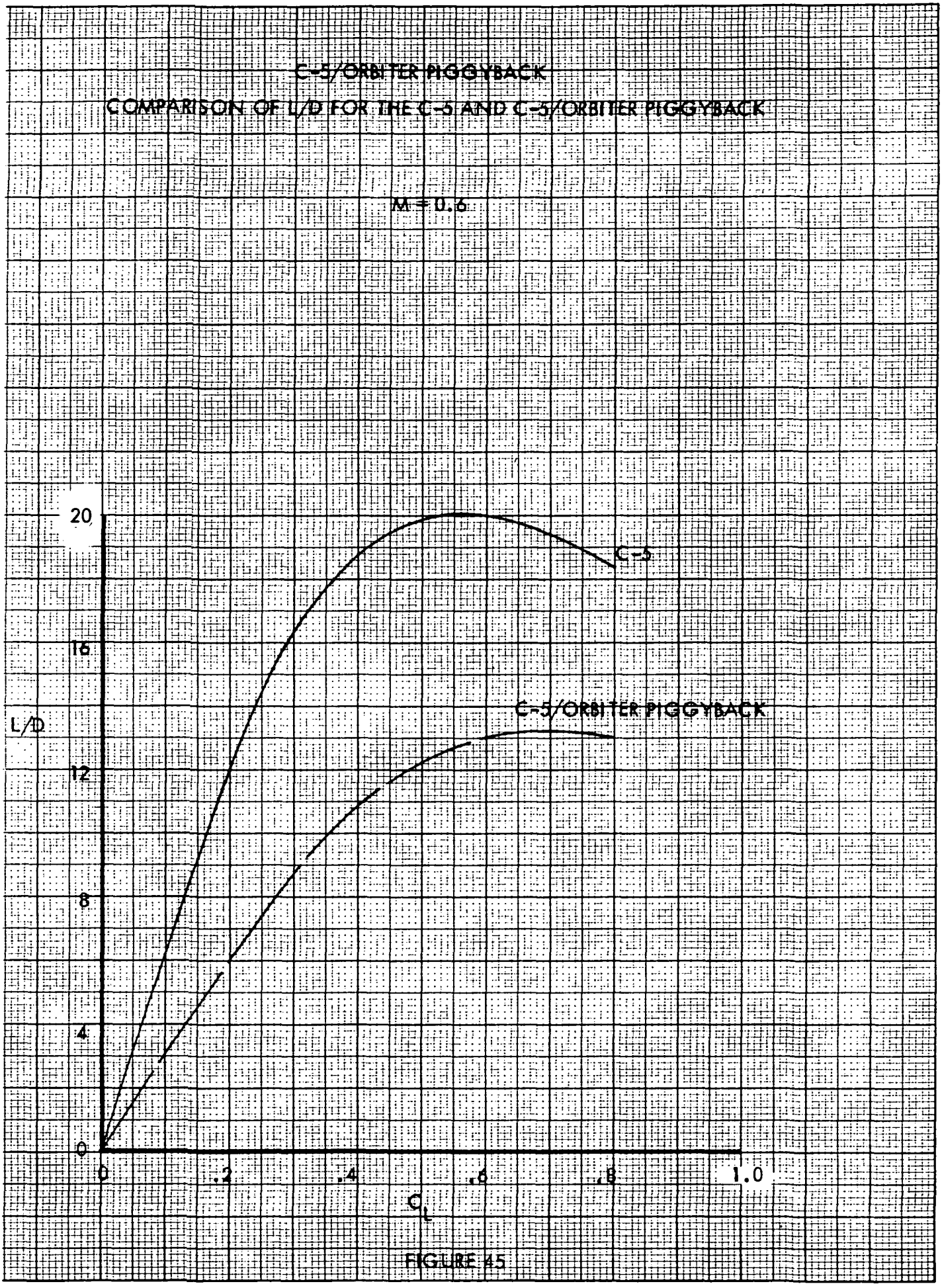

FIGURE 45

C-5/ORBITER PIGGYBACK

COMPARISON OF ESTIMATED AND WIND TUNNEL TEST DRAG POLARS
LANDING CONFIGURATION

FLAPS = 40°

TEST $R_N = 1.4 \times 10^6$/FT

○ RUN 95 - C-5

□ RUN 85 - C-5 PLUS ORBITER

— — — ESTIMATED C-5 PLUS ORBITER

NOTE: ESTIMATED DRAG = RUN 95 DATA PLUS $\Delta C_{D_{ORB}}$ FROM PUBLISHED ORBITER ALONE TEST RESULTS

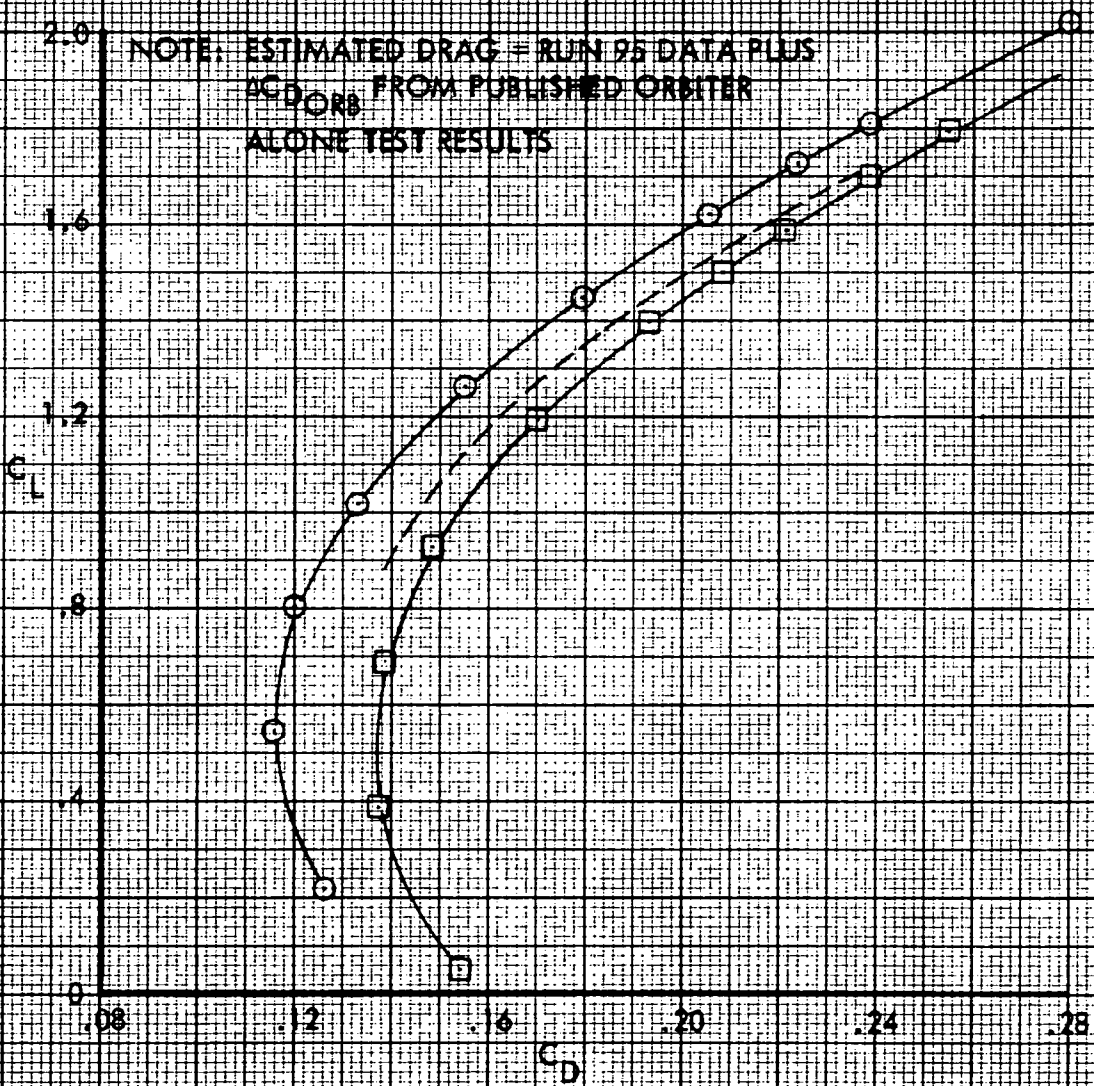

FIGURE 46

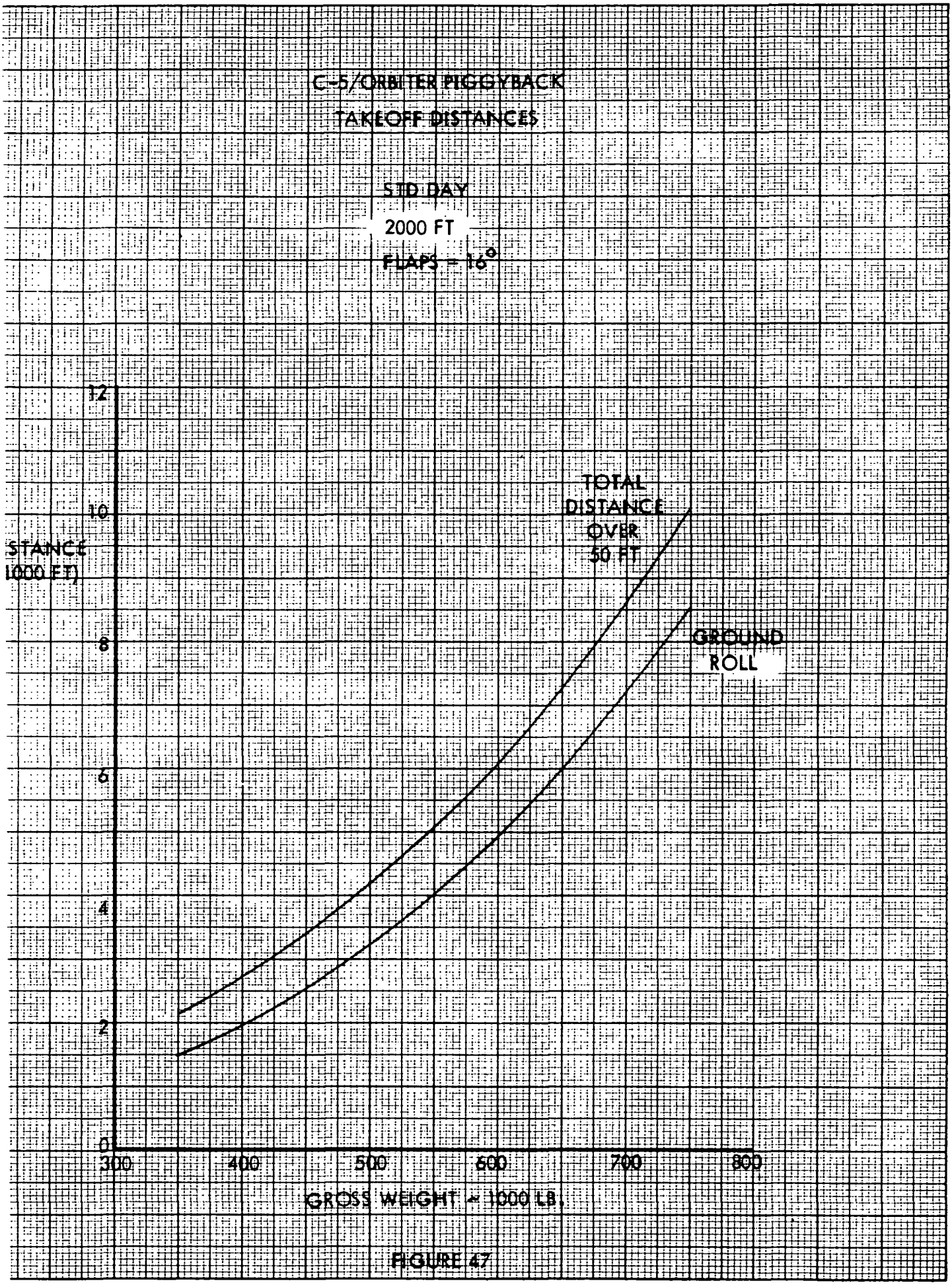
C-5/ORBITER PIGGYBACK
TAKEOFF DISTANCES
STD DAY
2000 FT
FLAPS = 16°
12
10
8
6
4
2
0
STANCE
1000 FT)
TOTAL
DISTANCE
OVER
50 FT
GROUND
ROLL
300
400
500
600
700
800
GROSS WEIGHT ~ 1000 LB.

FIGURE 47

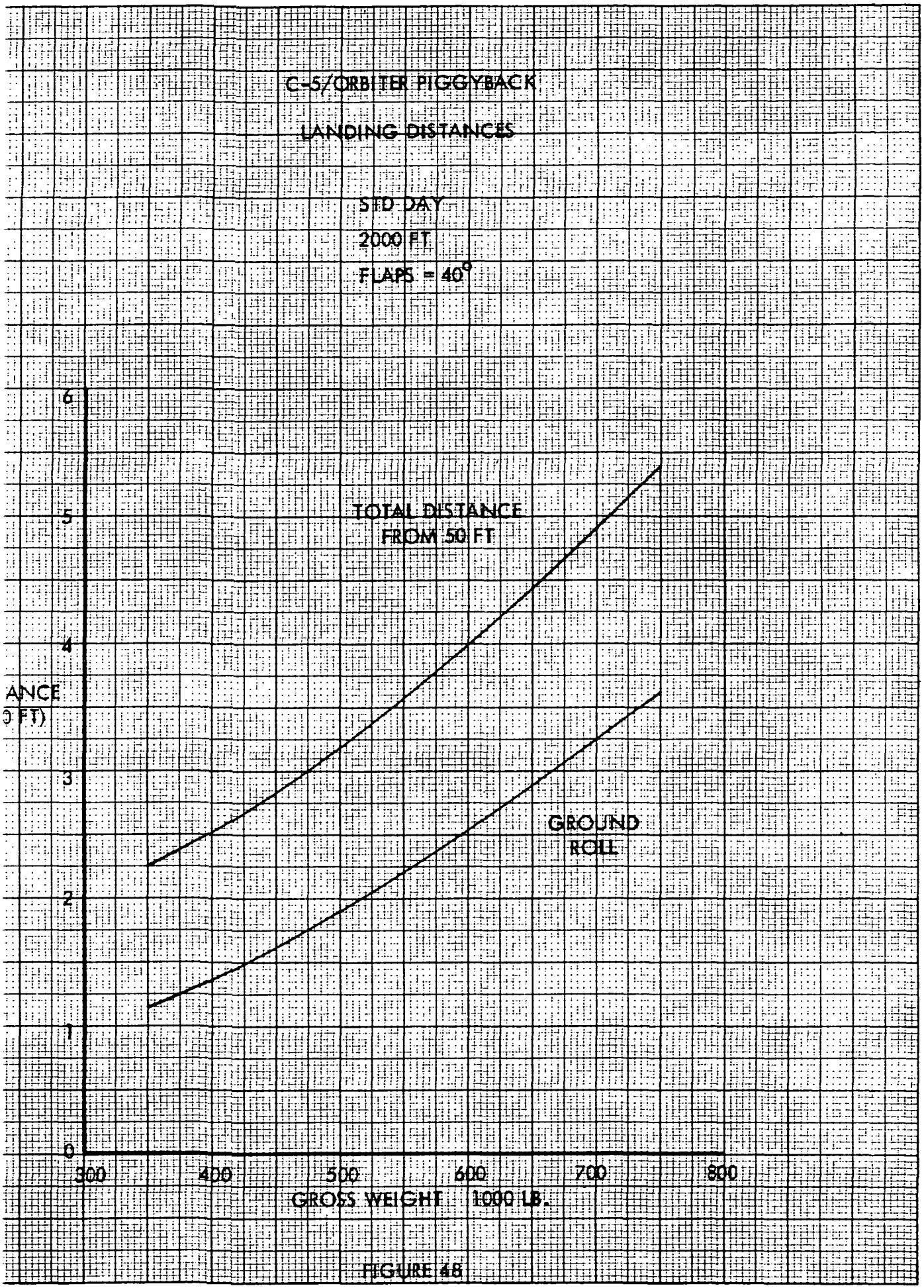
C-5/ORBITER PIGGYBACK
LANDING DISTANCES
STD DAY
2000 FT
FLAPS = 40°
TOTAL DISTANCE
FROM 50 FT
GROUND
ROLL
ANCE
0 FT)
0
1
2
3
4
5
6
300
400
500
600
700
800
GROSS WEIGHT 1000 LB.

FIGURE 46

C-5/ORBITER PIGGYBACK

ONE ENGINE INOPERATIVE CLIMB GRADIENT

STD DAY

2000 FT

FLAPS = 16°

GEAR UP

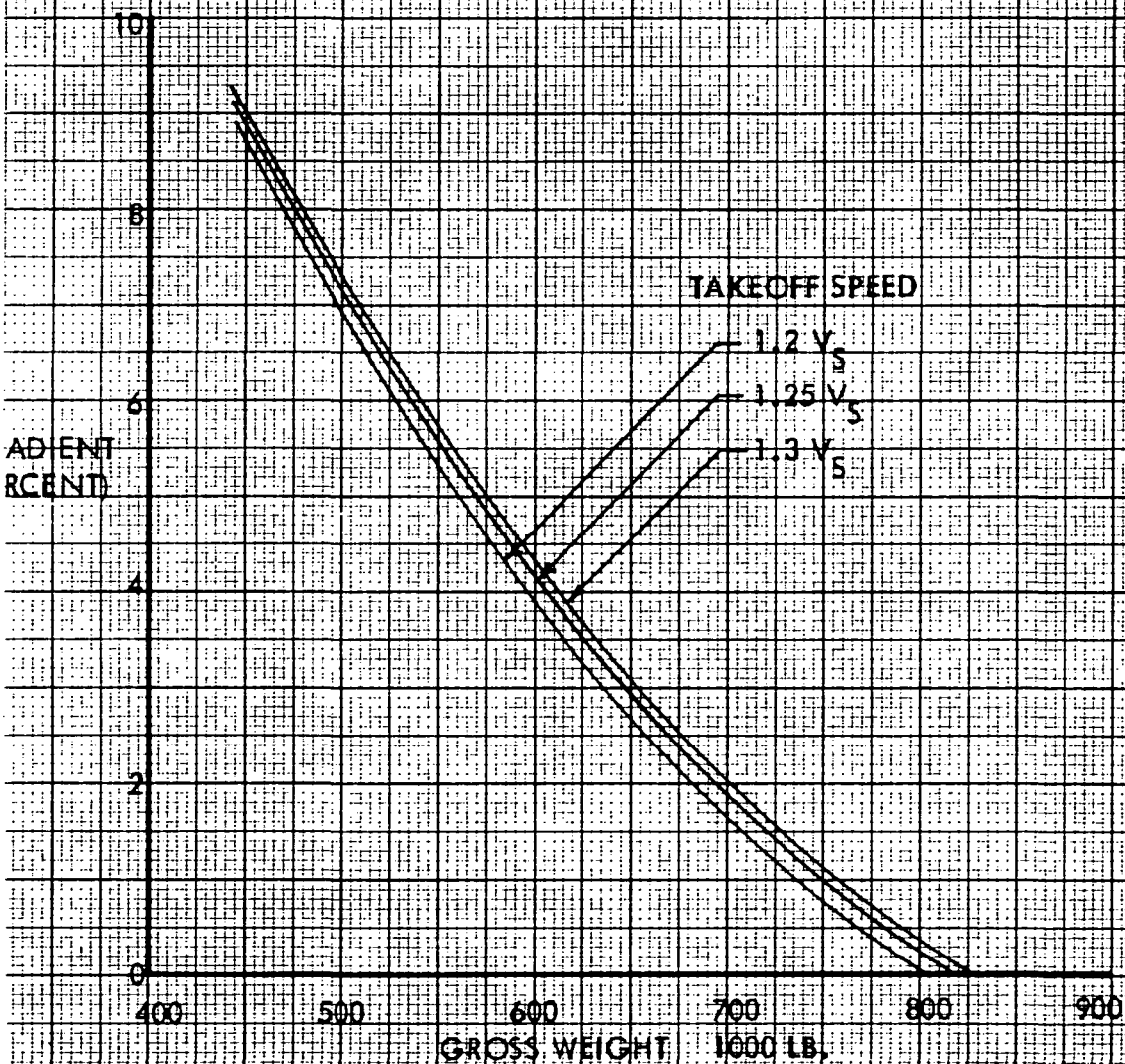

FIGURE 49

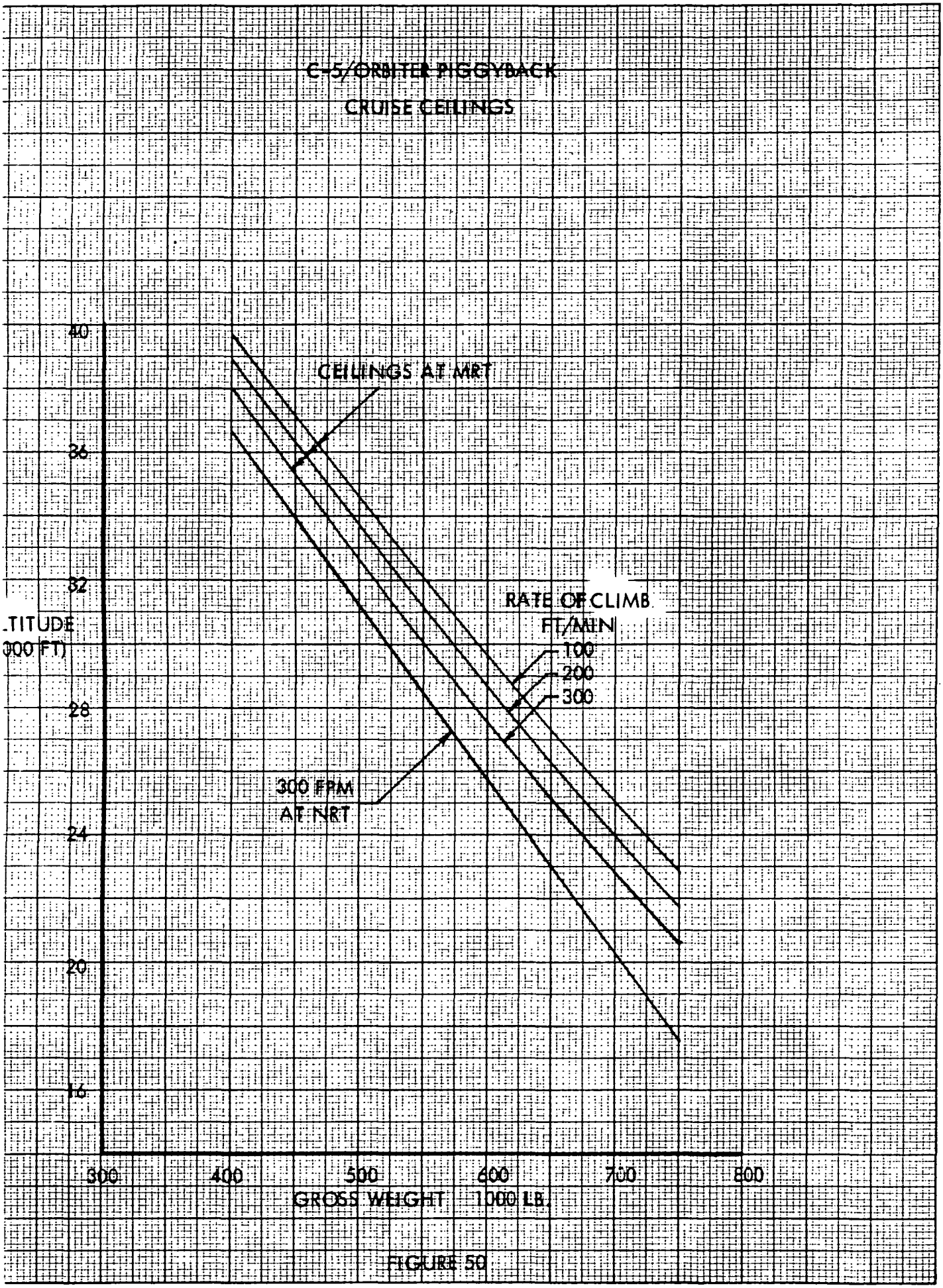
C-5/ORBITER PIGGYBACK
CRUISE CEILINGS
CEILINGS AT MRT
RATE OF CLIMB
FT/MIN
100
200
300
300 FPM
AT NRT
40
36
32
28
24
20
16
TITUDE
00 FT)
300
400
500
600
700
800
GROSS WEIGHT 1000 LB.

FIGURE 50

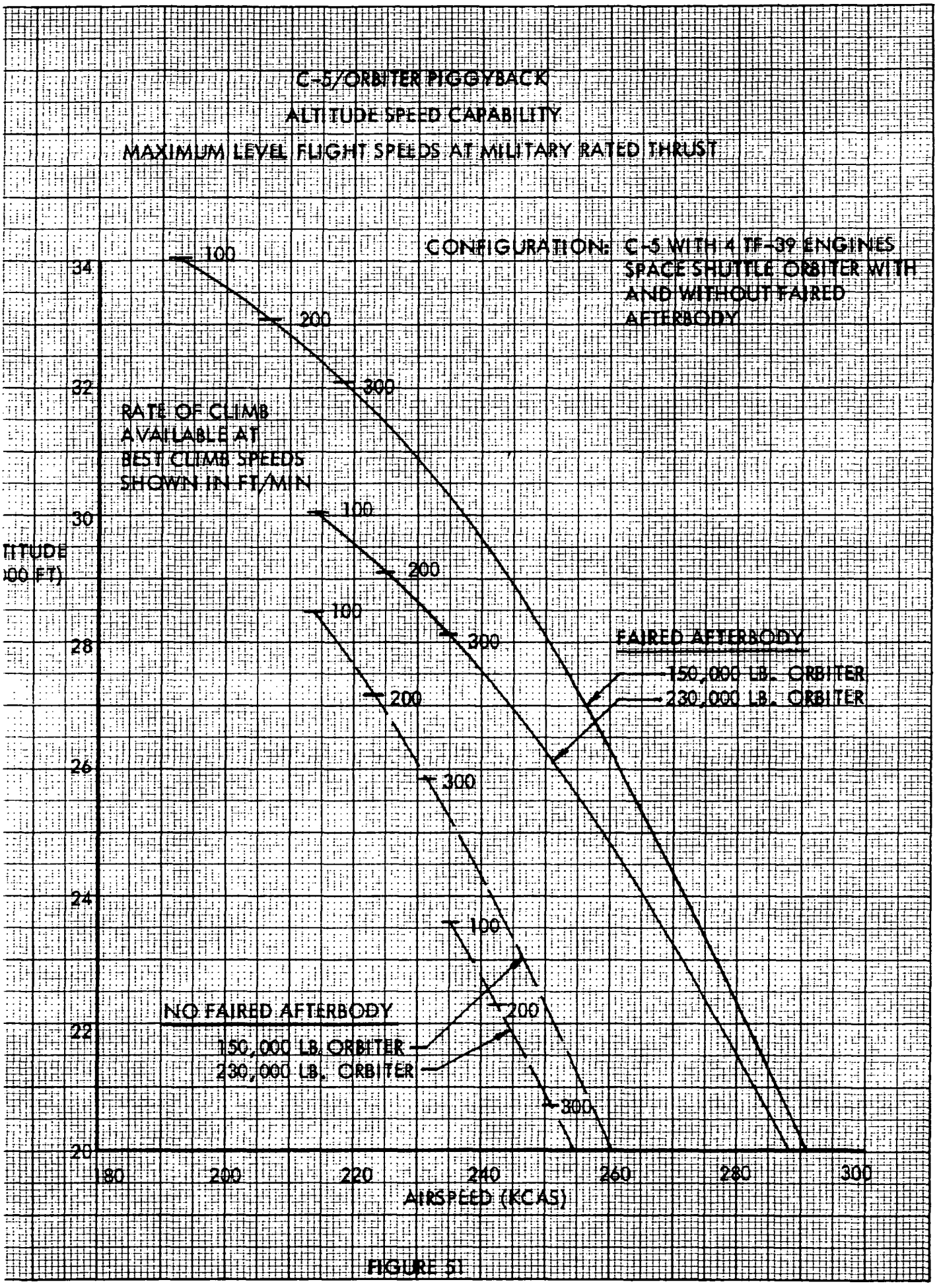
C-5/ORBITER PIGGYBACK
ALTITUDE SPEED CAPABILITY
MAXIMUM LEVEL FLIGHT SPEEDS AT MILITARY RATED THRUST
CONFIGURATION: C-5 WITH 4 TF-39 ENGINES
SPACE SHUTTLE ORBITER WITH
AND WITHOUT FAIRED
AFTERBODY
RATE OF CLIMB
AVAILABLE AT
BEST CLIMB SPEEDS
SHOWN IN FT/MIN
100
200
300
FAIRED AFTERBODY
150,000 LB. ORBITER
230,000 LB. ORBITER
NO FAIRED AFTERBODY
150,000 LB. ORBITER
230,000 LB. ORBITER
34
32
30
28
26
24
22
20
180
200
220
240
260
280
300
AIRSPEED (KCAS)

FIGURE 51

C-5/ORBITER PIGGYBACK

FERRY PERFORMANCE SUMMARY

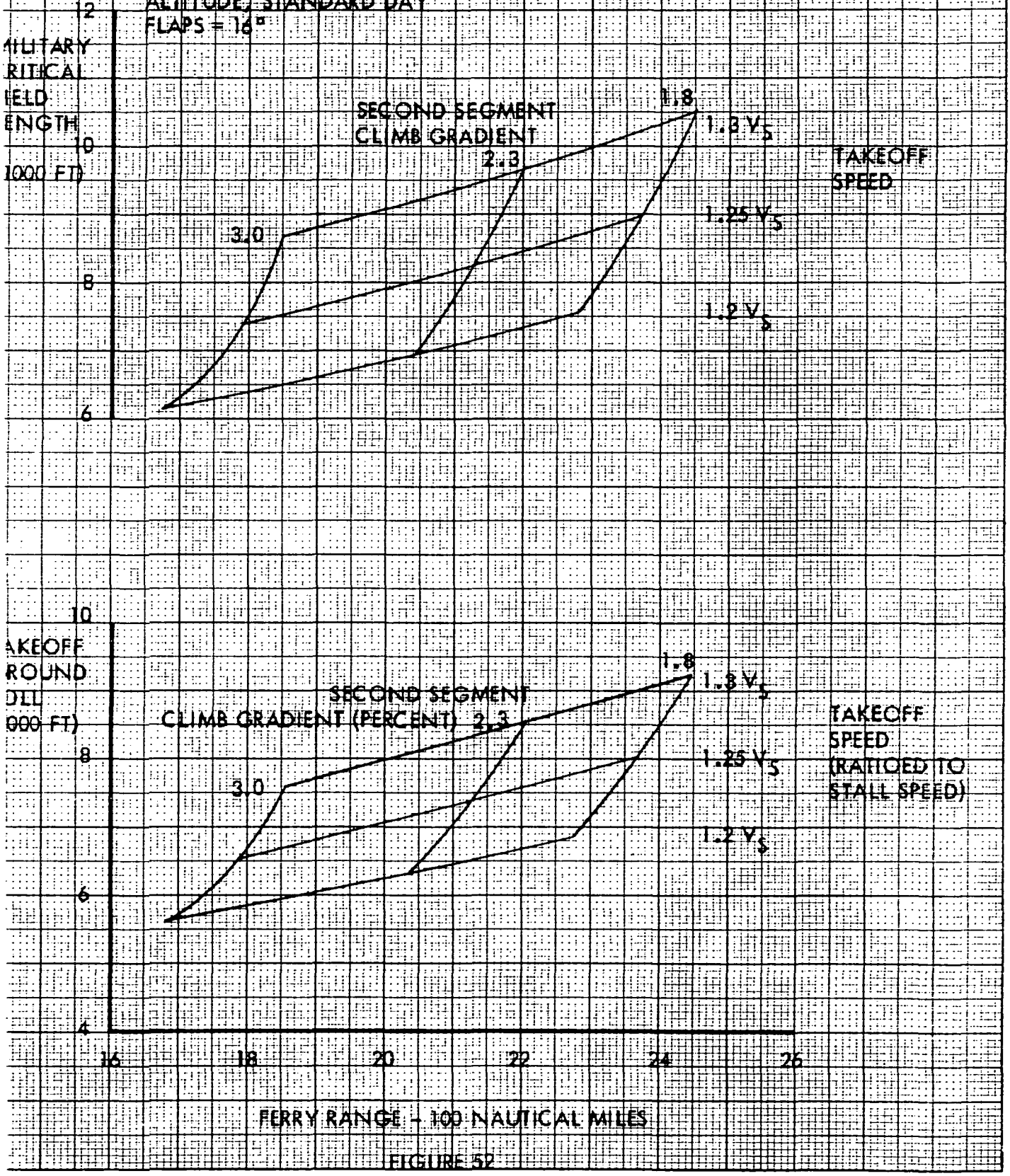

FIGURE 52

FLIGHT RESTRICTIONS

	A	B
LEVEL FLIGHT MAXIMUM SPEED, V_{HR}/M_H, KCAS	300/.775	280/.75
LIMIT SPEED, V_L/M_L, KCAS	360/.85	350/.8
SPEED FOR MAXIMUM GUST INTENSITY, V_G/M_H, KCAS	240/.775	210/.75
MANEUVER LOAD FACTOR, G	+2.0, -0.0	+2.0, -0.0
DESIGN SINK SPEED, F. P. S.	6.0	6.0
NO ABRUPT MANEUVERS	x	x
SIDE LOAD FACTOR DURING TURNS, G	.2	.2
WEIGHTS FOR STRUCTURAL DESIGN		
OPERATING WEIGHT, LB	334,900	336,310
MAXIMUM ZERO WING FUEL WEIGHT, LB	598,204 *	
MAXIMUM WING FUEL, LB	318,500	
MAXIMUM FUSELAGE FUEL, LB	11,300	13,525
MAXIMUM GROSS WEIGHT, LB	865,000	
MAXIMUM LANDING WEIGHT, LB	635,850	

* INCLUDES FUSELAGE FUEL

A = NO INCREASE IN VERTICAL STABILIZER AREA.

B = INCREASED VERTICAL STABILIZER AREA.

FIGURE 53

FLIGHT RESTRICTIONS

	A	SUPER GUPPY
LEVEL FLIGHT MAXIMUM SPEED, V_{HR}/M_H, KCAS	300/.775	219
LIMIT SPEED, V_L/M_L, KCAS	360/.85	219/.58
SPEED FOR MAXIMUM GUST INTENSITY, V_G/M_H, KCAS	240/.775	180-198
MANEUVER LOAD FACTOR, G	+2.0, -0.0	2.2 FLAPS UP 2.0 FLAPS DOWN
DESIGN SINK SPEED, F.P.S.	6.0	7.5
NO ABRUPT MANEUVERS	x	x
SIDE LOAD FACTOR DURING TURNS, G	.2	NO BRAKES
MAXIMUM GROSS WEIGHT, LB	865,000	162,000

FIGURE 54

APPENDIX A

WIND TUNNEL TEST DESCRIPTION AND PLOTTED DATA

CONTENTS

LIST OF FIGURES

LIST OF FIGURES (Continued)

I - MODEL DESCRIPTION

The C-5A Piggyback model is a combination of the Rockwell International 0.0405 Shuttle Orbiter model and the Lockheed-Georgia 0.0399-scale low speed C-5A model joined with suitable attach fittings.

The Orbiter model is fabricated from wood and metal and incorporates adjustable control surfaces. Provision was made for the installation of various afterbody fairings. Five afterbody fairing shapes were available for test. The basic Rockwell International fairing is denoted by a superscript 1. The original Lockheed-Georgia fairing, denoted by a superscript 2, was designed to minimize the afterbody drag. Fairings 3, 4, and 5 were fabricated by cutting away various portions of the fairing in an attempt to improve the flow at the C-5A tail.

The 0.0399-scale, low speed C-5A model is assembled from numerous components that allow the simulation of configurations encompassing the entire flight regime of the aircraft. The model is fabricated primarily from aluminum with some steel and plastic parts. All control surfaces are adjustable, and the landing gears and cargo doors may be positioned in increments from fully retracted to fully extended.

A symbol list of all the model components used in this test is presented in Section VI.

II - TEST FACILITY

The C-5A - Orbiter Piggyback combination tests were conducted in the Lockheed-California Company 8 X 12-Foot Low Speed Wind Tunnel. The tunnel is a conventional, low speed, single-return type with the test section vented to atmospheric pressure. Details of the facility are presented in Reference 1.

The model is supported in the upright position by a three-support fork. The fork is connected to an external, six-component, pyramidal-type balance located below the floor of the test section. The balance transmits loads from the model and support to an electrical readout system. Raw data are converted to punched cards using an IBM 1442 card reader punch. The raw data cards are input to the IBM 1131 Processor computer, which converts these data into coefficient form for output as tabulated data and provides the input for the Calcomp 565 plotter which produced the finished data plots presented in this appendix.

III - TEST CONDITIONS

All runs with flaps deflected were made at a dynamic pressure of 40 P.S.F. Flaps up runs were made at a dynamic pressure of 60 P.S.F. These dynamic pressures correspond to Mach Numbers of 0.165 and 0.201, and Reynolds Numbers of 1.436 X 10^6 and 1.758 X 10^6, respectively. Reynolds Numbers are based on the C-5A model M.A.C.

IV - DATA REDUCTION

Six-component force data were measured during all runs. The data were reduced to coefficient form and transferred to the stability axis system coincident at the reference moment center (F.S. 53.762, W.L. 10.578, BL 0.000). Corrections applied to the six-component data include tunnel wall corrections, blockage, buoyancy drag, and support tare and interference corrections.

The support tare and interference were obtained in a previous test of a similar model (Reference 2). The correction values applied to the longitudinal components data were taken from faired plots of the tare and interference corrections, whereas the values applied to the lateral component data were taken directly from the computed results.

The six-component data reduction constants are listed below.

Wing Area, square feet		9.878
Wing Span, inches		104. 997
Wing Mean Aerodynamic Chord, inches		14.817
Wing Mean Aerodynamic Chord Location	F.S.	53 .762
	W.L.	12.577
	B.L.	21.654
Front Trunnion Location	F.S.	53.742
	W.L	4.328
Moment Reference Center	F.S.	53.762
	W.L.	10.578

V - REFERENCES

1. "Wind Tunnel Computing Handbook," Lockheed California Company Report LALI, 15 June 1955.

2. "C-141: Investigation of the Low Speed Characteristics of the Production Airplane Configuration Using a 0.044 Scale Model in the Lockheed-California Company 8 X 12-Foot Wind Tunnel," Tests L-45-1, II, and III; Report No. ER 5071, June 1963.

VI - MODEL CONFIGURATION SYMBOLS

a^{10} — Aileron, Simple hinge, sealed. Deflection range $\pm 25^{\circ}$, denoted by subscripts. angles set with protractor. 07-C5A-0197-110

A — Orbiter, Shuttle - 0.0405 Scale Rockwell International Model. with/without aft fairing; capability of being located at 4 position on C-5A model, 3 angles of attack (ref. Orbiter FRL; $-1\ 1/2^{\circ}$, $+\ 1/2^{\circ}$, $+\ 2\ 1/2^{\circ}$)

Superscripts: Afterbody fairing shape and Orbiter location are denoted by number and letter superscripts, respectively. Lack of a number superscript indicates afterbody fairing removed.

1 — Rockwell International fairing

2 — Lockheed-Georgia fairing

3 — Lockheed-Georgia fairing modified to lower surface upsweep

4 — Lockheed-Georgia fairing modified to upper surface downsweep.

5 — Lockheed-Georgia fairing modified to shorter fairing with horizontal knife edge Orbiter c.g. locations in terms of C-5 Fuselage Stations

	Longitudinal Position	Vertical Position
A (BASE)	54.424"	Base
B	56.819"	Base
C	59.235"	Base
D	54.424"	Base + 2.395"
E	56.819"	Base + 2.395"
F	59.235"	Base + 2.395"

Subscripts: Orbiter incidence in degrees referenced to C-5A FRL is denoted by a subscript

(i.e. $A^{1A}_{1.5}$ - Orbiter with Rockwell International afterbody fairing located in the base position at 1.5° incidence)

B^{22}	Fuselage		07-C5A-0181-200
b^{16}	Bullet		07-C5A-0182-403
$D^{8\ MOD}$	Dorsal		07-C5A-0181-402A
e^{12}	Elevator	Inboard. Simple hinge, hinge line gap sealed. Deflection range -25° +15°; denoted by subscripts. Set with protractor.	07-C5A-0198-401
e^{13}	Elevator	Outboard. Simple hinge, hinge line gap sealed. Deflections range - 25° 15°, denoted by subscripts. Set with protractor.	07-C5A-0198-401
f^{37}	Flaps, T.E. Fowler.	Six sections/side, 0° and 40° (ldg.) to be tested.	07-C5A-0198-105
H^{8}	Horizontal Stabilizer.	Incidence settings capability. 0°, ± 4°, ± 6°, -8°, -12°; set with pin in push rod in vertical.	07-C5A-0198-401- -0195-400
$K^{24A}N^{20A}$	Pylon/Nacelles		07-C5A-0197-300
Q^{13}	Slats, Leading Edge.	14% C_W, 3 section/side. Inboard 2 section sealed to wing and pylon, outboard section 1.25% C_W T.E. gap and sealed to pylons. Deflection 20° inboard sections, 20° outboard; denoted by subscript "20".	07-C5A-0197-109

$r^{7}r^{8}$	Rudders, lower and upper, respectively. Simple hinge, hinge line gap sealed; deflections $\pm 30^{o}$.	07-C5A-0192-402
V^{9}	Vertical Stabilizer	07-C5A-0182-402
W^{11A}	Wing	07-C5A-0197-100
Z^{f6}	Flap Track Fairing	07-C5A-0197-106
Z^{g27}	Nose Landing Gear Fairing	07-C5A-0197-201
Z^{g23}	Main Landing Gear Fairing	07-C5A-0151-204
Z^{w27}	Wing - Fuselage Fillet - Alum. and Plastic; Composed of Z^{w26} fwd. fillet and Z^{w22} aft. fillet.	07-C5A-0197-200

$S^{1} = B^{22}W^{11A}A^{w27}K^{24A}N^{20A}Z^{f6}Z^{g27}Z^{g23}$

V^{1}	Center Vertical Fin Extension - Alum. plate, cut to match L.E - T.E vertical stabilizer sweep and tip chord of vertical (V^{9}), span 6", attached to top of horizontal bullet fairing.
h^{1}	Horizontal Stab. Fins. - end plates on tips of horizontal stabilizer 1" inbd. from horizontal tips, 4" chord, 8" span (or height).

VII - MODEL DIMENSIONAL DATA

		0.039916 Scale
Aileron, (a^{10})		
Area per side, square feet		0.188
Span, inches		10.651
Chord lengths, inches		
Inboard		2.978
Outboard		2.337
Mean (RMS, streamwise)		
Sweep of hinge line, degrees		20.417
Deflection limits, degrees		±25
Fuselage, (B^{22})		
Length, inches		110.487 (9.207')
Maximum frontal area, square inches		126.60
Equivalent maximum diameter, inches		12.69
Fuselage reference line	W.L.	7.983
Nose location	F.S.	6.387
Wetted area, square feet (imprints not removed)		25.223
Volume, Cu. Ft.		5.379
Bullet, (b^{16})		
Length, inches		21.44
Maximum frontal area, square inches		3.22
Equivalent diameter, inches		2.03
Wetted area, square feet (Exposed Only)		0.541

MODEL DIMENSIONAL DATA (CONT.)

Dorsal, ($D^{8\ mod.}$)	
Wetted area, square feet	0.129
Imprint area, square feet (On fuselage)	0.075
Elevator, Inboard (e^{12})	
Area per side, square feet	0.1434
Root chord, inches	3.227
Tip chord, inches	2.228
Mean chord length (RMS), inches	2.773
Span per side, inches	7.569
Hinge line, % horizontal chord	66.000
Deflections, degrees	$\pm$ 30.000
Elevator, Outboard (e^{13})	
Area per side, square feet	0.0624
Root chord, inches	2.228
Tip chord, inches	1.609
Mean chord length (RMS), inches	1.943
Span per side, inches	4.684
Hinge line, % horizontal chord	66.000
Deflections, degrees	$\pm$33.000
Trailing Edge Fowler Flaps, (f^{37})*	
Panel 1 (Inboard)	
Area per side, square feet	0.214

*All dimensions given in Wing Reference Plane.

MODEL DIMENSIONAL DATA (CONT.)

Trailing Edge Fowler Flaps, (Cont.)		
Span, inches		7.085
Sweep of leading edge, degrees		9.832
Chord lengths, inches		
Root		4.410
Tip		4.410
Average		4.410
Mean (RMS)		4.410
Chord locations, inches		
Root	W.S.	5.620
Tip	W.S.	12.705
Average	W.S.	9.163
Mean (RMS)	W.S.	9.163
Maximum deflection, degrees		40.000
Panel 2		
Area per side, square feet		0.173
Span, inches		5.718
Sweep of leading edge, degrees		9.832
Chord lengths, inches		
Root		4.410
Tip		4.410
Average		4.410
Mean (RMS)		4.410
Chord locations, inches		
Root	W.S.	13.344
Tip	W.S.	19.062
Average	W.S.	16.203

MODEL DIMENSIONAL DATA (CONT.)

Trailing Edge Fowler Flaps, (Cont.)		
Mean (RMS	W.S.	16.203
Maximum deflection, degrees		40 .000
Panel 3		
Area per side, square feet		0.125
Span, inches		4.845
Sweep of leading edge, degrees		12.364
Chord lengths, inches		
Root		3.804
Tip		3.804
Average		3.804
Mean (RMS)		3.804
Chord locations, inches		
Root	W.S.	19.701
Tip	W.S.	24.546
Average	W.S.	22.123
Mean (RMS)	W.S.	22.123
Maximum deflection		40 .000
Panel 4		
Area per side, square feet		0.094
Span, inches		4.497
Sweep of leading edge, degrees		17.033
Chord lengths, inches		
Root		3.133
Tip		3.133
Average		3.133
Mean (RMS)		3.133

MODEL DIMENSIONAL DATA (CONT.)

Trailing Edge Fowler Flaps (Cont.)

Chord locations, inches		
Root	W.S.	25.184
Tip	W.S.	29.681
Average	W.S.	27.433
Mean (RMS)	W.S.	27.433
Maximum deflection, degrees		40 .000
Panel 5		
Area per side, square feet		0.079
Span, inches		3.802
Sweep of leading edge, degrees		17.033
Chord lengths, inches		
Root		3.133
Tip		3.133
Average		3.133
Mean (RMS)		3.133
Chord locations, inches		
Root	W.S.	30.321
Tip	W.S.	34.135
Average	W.S.	32.222
Mean (RMS)	W.S.	32.222
Maximum deflection, degrees		40.000
Panel 6		
Area per side, square feet		0.082
Span, inches		3.938
Sweep of leading edge, degrees		17.033

MODEL DIMENSIONAL DATA (CONT.)

Trailing Edge Fowler Flaps (Cont.)

Chord lengths, inches		
Root		3.133
Tip		3.133
Average		3.133
Mean (RMS)		3.133
Chord locations, inches		
Root	W.S.	34.773
Tip	W.S.	38.712
Average	W.S.	36.742
Mean (RMS)	W.S.	36.742
Maximum deflection, degrees		40.000

Horizontal Stabilizer, (H^8)

Airfoil Section NACA 0010.5-0.833-0.40/1.432 (modified)		
Area - projected square feet		1.539
- wetted, square feet (Exposed only)		2.910
Span		32.397
Chord lengths - MAC, inches		7.322
Root, inches		9.985
Tip, inches		3.695
Aspect ratio		4.736
Taper ratio		0.370
Sweep of 25% chord line, degrees		24.583
25% MAC Location	F.S.	115.533

MODEL DIMENSIONAL DATA (CONT.)

Horizontal Stabilizer, (Cont.)		
	B.L.	6.858
Volume coefficient		0.629
Tail length, inches		60.028
Pylon, (K^{24A})		
Sweep of L.E., degrees		71 .504
Chord length, inches		13.073
Taper ratio		0.876
Airfoil section NACA 0008-1.100-0.335/1.575 (modified)		
Wing intersection, % wing chord		1.4
Toe-in, degrees		1.0
Wing intersection, inboard	B.L.	19.122
Wing intersection, outboard	B.L.	29.781
Nacelle, (N^{20A})		
Length, inches		9.228
Maximum diameter, inches		4.091
Duct diameter, inches		3.409
Fineness ratio		2.256
Area, square feet		
Maximum frontal area		0.091
Inlet area		0.075
Side area		0.249
Toe-in angle, degrees		1.0
Incidence, degrees		2.0

MODEL DIMENSIONAL DATA (CONT.)

Nacelle (Cont.)

Inlet location		
Inboard nacelle	F.S.	41.970
	W.L.	8.864
	B.L.	18.999
Outboard nacelle	F.S.	47.490
	W.L.	7.891
	B.L.	29.658

Leading Edge Slat, (Q^{13})

Section I (outboard) 1-1/4% C_w gap		
Area, square feet		0.191
Span, inches		19.556
Chord length - root, inches		1.698
tip, inches		1.135
average, inches		1.417
Chord location - root	B.L.	29.291
tip	B.L.	48.788
Angle from stowed position, degrees		22.0
Section II (mid section), sealed		
Area, square feet		0.079
Span, inches		6.336
Chord length - root, inches		1.881
tip, inches		1.698
average, inches		1.790

MODEL DIMENSIONAL DATA (CONT.)

Leading Edge Slat (Cont.)		
Chord location - root	B.L.	22.974
tip	B.L.	29.291
Angle from stowed position, degrees		20.0
Section III (inboard), sealed		
Area, square feet		0.261
Span		16.377
Chord length - root, inches		2.714
tip, inches		1.881
average, inches		2.298
Chord location - root	B.L.	6.646
tip	B.L.	22.974
Angle from stowed position, degrees		20.0

Rudder, (r^7, r^8)		r^8 (Upper)	r^7 (Lower)
Area, square feet		0.161	0.203
Location			
Lower end	W.L.	22.924	15.793
Upper end	W.L.	29.119	22.924
Hinge line, percent vertical chord		71	71
Span, inches		6.195	7.133
Deflection limits, degrees		±30	±30
Root chord, inches		3.097	4.278
Tip chord, inches		3.585	3.907

MODEL DIMENSIONAL DATA (CONT.)

Rudder, (Cont.)			
Mean chord length (RMS), inches		3.750	4.097
Mean chord location	W.L.	25.949	19.272
Percent of vertical tail		10.5	13.1
Spoiler, (a^{22})*			
Panel 1 (Inboard Section)			
Area per side, square feet			0.0514
Span, inches			3.606
Sweep of hinge line, degrees			9.832
Chord lengths, inches			
Root			2.206
Tip			2.026
Average			
Mean (RMS)			
Chord locations, inches			
Root		W.S.	5.550
Tip		W.S.	9.157
Average		W.S.	
Mean (RMS)		W.S.	
Maximum deflection, degrees			60.000
Panel 2			
Area per side, square feet			0.0508
Span, inches			3.610
Sweep of hinge line, degrees			9.832
Chord lengths, inches			
Root			2.026

*All dimensions given in wing reference plane.

MODEL DIMENSIONAL DATA (CONT.)

Spoiler, (Cont.)		
Tip		2.026
Average		2.026
Mean (RMS)		2.026
Chord locations, inches		
Root	W.S.	9.169
Tip	W.S.	12.779
Average	W.S.	
Mean (RMS)	W.S.	
Maximum deflection, degrees		60.000
Panel 3		
Area per side, square feet		0.0412
Span, inches		2.927
Sweep of hinge line, degrees		9.832
Chord lengths, inches		
Root		2.026
Tip		2.026
Average		2.026
Mean (RMS)		2.026
Chord locations, inches		
Root	W.S.	13.270
Tip	W.S.	16.197
Average	W.S.	
Mean (RMS)	W.S.	
Maximum deflection, degrees		60.000
Panel 4		
Area per side, square feet		0.0412
Span, inches		2.927
Sweep of hinge line, degrees		9.832

MODEL DIMENSIONAL DATA (CONT.)

Spoiler (Cont.)

Chord lengths, inches		
Root		2.026
Tip		2.026
Average		2.026
Mean (RMS)		2.026
Chord locations, inches		
Root	W.S.	16.209
Tip	W.S.	19.136
Average	W.S.	
Mean (RMS)	W.S.	
Maximum deflection, degrees		60.000

Panel 5

Area per side, square feet		0.0272
Span, inches		2.490
Sweep of hinge line, degrees		12.347
Distance hinge line forward of leading edge, inches		0.336
Chord lengths, inches		
Root		1.910
Tip		1.910
Average		1.910
Reference**		2.247

**Reference chord is defined as twice the distance from the hinge line to spoiler t.e. minus the average chord.

MODEL DIMENSIONAL DATA (CONT.)

Spoiler (Cont.)

Chord locations, inches		
Root	W.S.	19.627
Tip	W.S.	22.117
Average	W.S.	
Reference	W.S.	
Maximum deflection, degrees		60.000
Panel 6		
Area per side, square feet		0.0272
Span, inches		2.490
Sweep of hinge line, degrees		12.347
Distance hinge line forward of leading edge, inches		0.336
Chord lengths, inches		
Root		1.910
Tip		1.910
Average		1.910
References**		2.247
Chord locations, inches		
Root	W.S.	22.129
Tip	W.S.	24.620
Average	W.S.	
Reference	W.S.	
Maximum deflection, degrees		60.000

**Reference chord is defined as twice the distance from the hinge line to spoiler t.e. minus the average chord.

MODEL DIMENSIONAL DATA (CONT.)

Spoiler (Cont.)

Panel 7

Area per side, square feet		0.0399
Span, inches		4.645
Distance hinge line forward of leading edge, inches		0.260
Sweep of hinge line, degrees		17.033
Chord lengths, inches		
Root		1.236
Tip		1.236
Average		1.236
Reference**		1.757
Chord locations, inches		
Root	W.S.	25.111
Tip	W.S.	29.756
Average	W.S.	
Reference	W.S.	
Maximum deflection, degrees		60.000

Panel 8

Area per side, square feet		0.0340
Span, inches		3.962
Sweep of hinge line, degrees		17.033
Distance hinge line forward of leading edge, inches		0.260
Chord lengths, inches		
Root		1.236
Tip		1.236
Average		1.236
Reference**		1.757

**Reference chord is defined as twice the distance from the hinge line to spoiler t.e. minus the average chord.

MODEL DIMENSIONAL DATA (CONT.)

Spoiler (Cont.)

Chord locations, inches		
Root	W.S.	30.247
Tip	W.S.	34.209
Average	W.S.	
Reference	W.S.	
Maximum deflection, degrees		60.000
Panel 9		
Area per side, square feet		0.0336
Span, inches		4.086
Sweep of hinge line, degrees		17.033
Distance hinge line forward of leading edge, inches		0.247
Chord lengths, inches		
Root		1.184
Tip		1.184
Average		1.184
Reference**		1.679
Chord locations, inches		
Root	W.S.	34.700
Tip	W.S.	38.785
Average	W.S.	
Reference	W.S.	
Maximum deflection, degrees		60.000

**Reference chord is defined as twice the distance from the hinge line to spoiler t.e. minus the average chord.

MODEL DIMENSIONAL DATA (CONT.)

Vortex Generator, (U^2)	
Height, inches	
Superscript A	0.08
Superscript B	0.10
Superscript C	0.12
Width, inches	
Superscript A	0.16
Superscript B	0.20
Superscript C	0.24
Angle to freestream, degrees	15.00
Chordwise location (centerline of generator), % of t.e. flap	15.00
Spanwise location, inches from flap tip chord	
Subscript 1	0.18
Subscript 2	0.23
Subscript 3	0.28
Subscript 4	0.33
Subscript 5	0.38
Vertical Stabilizer, (V^9)	
Airfoil section NACA 0013-1.1-0.40/1.575 (modified)	
Areas (theoretical), square feet	
Projected	1.531
Wetted (exposed only)	2.848
Span, inches	16.535
Chord lengths, MAC, inches	13.390
Root, inches	14.817
Tip, inches	11.853
Aspect ratio	1.240

MODEL DIMENSIONAL DATA (CONT.)

Vertical Stabilizer (Cont.)			
Taper ratio		0.800	
Sweep of 25% chord line, degrees		34.931	
25% MAC location	F.S.	107.992	
	W.L.	23.388	
Volume coefficient		0.079	
Tail length, inches		53.246	
Wing, (W^{11A}) (6204.601 ft^2 Full Scale)			
Area, square feet			Data Reduction
Planform, theoretical		9.8857	9.878
Planform, exposed (Outboard of B.L.)		8.4930	
Wetted, exposed (Outboard of B.L.)		16.504	
Volume, Cu. Ft.			0.770
Span, inches	(8.749')	104.997	104.997
MAC chord length, inches		14.826	14.817
Location of 0.25 chord MAC	F.S.	53.765	
	W.L.	12.557	
	B.L.	21.658	
Aspect ratio		7.744	
Taper ratio, theoretical		0.371	
Taper ratio, exposed		0.401	
Dihedral (0.25 chord), degrees		3.500	
Sweep angle, degrees			
Panel I (Inboard)			
Leading edge		28.449	
0.25 chord		24.268	
Trailing edge		10.046	

MODEL DIMENSIONAL DATA (CONT.)

Wing (Cont.)		
Panel 2		
Leading edge		28.449
0.25 chord		24.803
Trailing edge		12.581
Panel 3		
Leading edge		27.382
0.25 chord		23.954
Trailing edge		12.581
Panel 4		
Leading edge		27.382
0.25 chord		25.001
Trailing edge		17.298
Chord length, inches		
Root		21.806
Break station, inboard		14.826
Break Station, Mid		13.606
Break Station, Outboard		13.018
Tip		7.332
Chord location, inches		
Root	B.L.	0
Break Station, Inboard	B.L.	19.144
Break Station, Mid	B.L.	22.973
Break Station, Outboard	B.L.	24.970
Tip	B.L.	52.498
Geometric twist, degrees		
Root		0
Break Station, Inboard		1.132
Break Station, Mid		1.500
Break Station, Outboard		1.576

MODEL DIMENSIONAL DATA (CONT.)

Wing (Cont.)			
Tip		3.500	
Flap Track Fairing, Z^{f6}			
Centerline locations	W.S.		
	W.S.		
	W.S.		
	W.S.		
	W.S.		
	W.S.		
	W.S.		
Nose Landing Gear Fairing (Z^{G27})			
Maximum length, inches		11.30	
Maximum frontal area, square inches		6.06	
Wetted area, square feet		0.6311	
Imprint area on fuselage, square feet		0.5886	
Main Landing Gear Fairing, (Z^{G28})			(Z^{G23})
Maximum length, inches		33.290	35.36
Maximum frontal area, square feet		0.125	0.135
Wetted area, square feet		4.364	4.366
Imprint area on fuselage, square feet		3.513	
Maximum width, inches		14.078	14.18
Wing - Fuselage Fillet, (Z^{W27})			
Maximum length		41.71	
Wetted area		3.638	
Imprint area of fuselage and fillet on Wing		3.582	
Side area		1.10	

MODEL DIMENSIONAL DATA (CONT.)

Wing - Fuselage Fillet (Cont.)

Imprint area of wing and fillet on fuselage		3.013
Location:		
Most forward point	F.S.	32.13
Most aft point	F.S.	73.84

Main Landing Gear Outer Door (FWD), (d^{m3})

Length, inches	6.63
Reference area, square feet	0.1932
Span, inches	4.19
Deflections, % Open	0,10,25,50, 75,100

Main Landing Gear Outer Door (AFT), (d^{m4})

Length, inches	6.63
Reference area, square feet	0.1932
Span, inches	4.19
Deflections, % Open	0,10,25,50, 75,100

Main Landing Gear Inner Door (FWD), (d^{m5})

Length, inches	4.23
Reference area, square feet	0.0311
Span, inches	1.06
Deflections, degrees	0,3,6,29,75,95

Main Landing Gear Inner Door (AFT), (d^{m6})

Length, inches	4.23
Reference area, square feet	0.0311
Span, inches	1.06
Deflections, degrees	0,3,6,29,75,95

MODEL DIMENSIONAL DATA (CONT.)

Nose Landing Gear Inner Door, (d^{n3})

Length, inches	5.35
Reference area, square feet	0.0884
Span, inches	2.37
Deflections, % Open	0,10,25,50,75,100

Nose Landing Gear Outer Door, (d^{n4})

Length, inches	4.18
Reference area, square feet	0.0371
Span, inches	1.28
Deflections, % Open	0,10,25,50,75,100

Ref. Moment Center:

F.S.	53.762
W.L.	10.578
B.L.	0.000

VIII - RUN SCHEDULE

The following three pages present the run schedule for the wind tunnel test program.

$S^1 - B^{22}\ W^{11A}\ Z^{W27}\ N^{20A}\ Z^{f6}\ Z^{G27}\ Z^{G23}$

TEST NO.
LOCATION

RUN NO.	CONFIGURATION														TYPE RUN	q	REMARKS	PLOTTED FIG. NO.
	ASSY	AIL	L. E. SLATS	T. E. FLAP	ORB ITER	DOR SAL	BUL LET	VERT	HOR.	ELEV.	RUD DER	SPOI LER	VERT EXT	TIP FINS				
26	S^1	a^{10}	Q^{13}	f^{37}	$A^{A}_{-1.5}$	D^8	b^{16}	V^9	H^8	$e^{12,13}$	$r^{7,8}$				Pitch	60		
27	↑	↑	↑	↑	↓	↓	↓	↓	↓	↓	↓				Yaw	↓		A13, A27
31					$A^{2A}_{-1.5}$										Pitch			A5
32					↓										Yaw			A13, A27
33					$A^{2A}_{0.5}$										Pitch			A5
34					↓										Yaw			A26
35					$A^{2D}_{0.5}$										Pitch			A2
36					↓	↓	↓	↓	↓	↓	↓				Yaw			A26
39															Pitch			A2
40					↓										Yaw			
43					$A^{2F}_{0.5}$										Pitch			A2
44					$A^{2F}_{0.5}$										Yaw			A25
47						D^8	b^{16}	V^9	H^8	$e^{12,13}$	$r^{7,8}$				Pitch			A2
48					↓	↓	↓	↓	↓	↓	↓				Yaw			A21, A24, A25
49					$A^{2C}_{0.5}$										Pitch			A6
50					↓										Yaw			A24
53					$A^{1C}_{0.5}$										Pitch			A6
54					↓										Yaw			A24
55					$A^{1F}_{0.5}$										Pitch			A6
56					↓										Yaw			A24
57															Pitch			A1, A7, A8
58											↓				Yaw			A12, A13, A26
59									↓		$r^{7,8}_{10}$				Yaw			A12
60									H^8_{-4}		$r^{7,8}$				Pitch			A1
61						↓	↓	↓	H^8_{+4}	↓	↓				Pitch			A1
63															Pitch			A1
64															Yaw	↓		A12
65	S^1	a^{10}	Q^{13}	f^{37}		D^8	b^{16}	V^9	H^8	$e^{12,13}$	$r^{7,8}$	$^{22}s^{60}$			Pitch	60		A7

$S^1 - B^{22}.W^{11A}\ Z^{W27}\ N^{20A}\ Z^{f6}\ Z^{G27}\ Z^{G23}$

TEST NO.
LOCATION

RUN NO.	CONFIGURATION															TYPE RUN	q	REMARKS	PLOTTED FIG. NO.
	ASSY	AIL	L. E. SLATS	T. E FLAP	ORB ITER	DOR SAL	BUL LET	VERT	HOR.	ELEV	RUD DER	SPOI LER	VERT EXT	TIP FINS					
66	S^1	a^{10}	Q^{13}	f^{37}	$A^{5F}_{0.5}$	D^8	b^{16}	V^9	H^8	$e^{12,13}$	$r^{7,8}$					Pitch	60		
67																Yaw			A21
68					$A^{5F}_{0.5}$											Pitch			A5
69																Yaw			A20, A21
70					$A^{5F}_{-1.5}$											Pitch			A5, A8
71																Yaw			A21
72													v^1			Pitch			A8,A9,A11
73																Yaw			A20
74					$A^{5F}_{0.5}$											Pitch			A7,A9,A10
75																Yaw			
76					$A^{5A}_{0.5}$											Pitch			A11
77																Yaw			A20
78					$A^{5F}_{0.5}$											Pitch			A10
79																Yaw			A15
80						D^8	b^{16}	V^9	H^8_{+4}	$e^{12,13}$	$r^{7,8}$		v^1			Pitch			A10
81									H^8_{-4}							Pitch			A10
82									H^8		$r^{7,8}_{+10}$					Yaw			A19
83											$r^{7,8}$	$^{22}s60$				Pitch			A7
84			Q^{13}_{20}	f^{37}_{40}												Yaw	60		A15,A19,A20
85																Pitch	40		
86																Yaw			A17
87																Pitch			
88																Yaw			
89						D^8	b^{16}	V^9	H^8	$e^{12,13}$	$r^{7,8}$		v^1	h^1		Yaw			A17
90																Yaw			A17
91					$A^{5F}_{0.5}$											Yaw			A17
92																Yaw			
93	S^1	a^{10}	Q^{13}_{20}	f^{37}_{40}		D^8	b^{16}	V^9	H^8	$e^{12,13}$	$r^{7,8}$			h^1		Yaw			

$S^1 - B^{22}\ W^{11A}\ Z^{W27}\ N^{20A}\ Z^{f6}\ Z^{G27}\ Z^{G23}$

TEST NO.
LOCATION

RUN NO.	CONFIGURATION															TYPE RUN	q	REMARKS	PLOTTED FIG. NO.
	ASSY	AIL	L. E. SLATS	T. E. FLAP	ORBITER	DORSAL	BULLET	VERT	HOR.	ELEV	RUDDER	SPOILER	VERT EXT	TIP FINS					
94	S^1	a^{10}	Q^{13}_{20}	f^{37}_{40}		D^8	b^{16}	V^9	H^8	$e^{12,13}$	$r^{7,8}$		v^1	h^1		Yaw	40		
95																Pitch			A28
96																Yaw			A22
97																Pitch			A28
98																Pitch			A28
99																Yaw	40		A22
100			Q^{13}	f^{37}		D^8	b^{16}	V^9	H^8	$e^{12,13}$	$r^{7,8}$		v^1			Pitch	60		
101																Yaw			
102	S^1	a^{10}	Q^{13}	f^{37}	$A^{5F}_{0.5}$	D^8	b^{16}	V^9	H^8	$e^{12,13}$	$r^{7,8}$		v^1	h^1		Yaw	60		A31

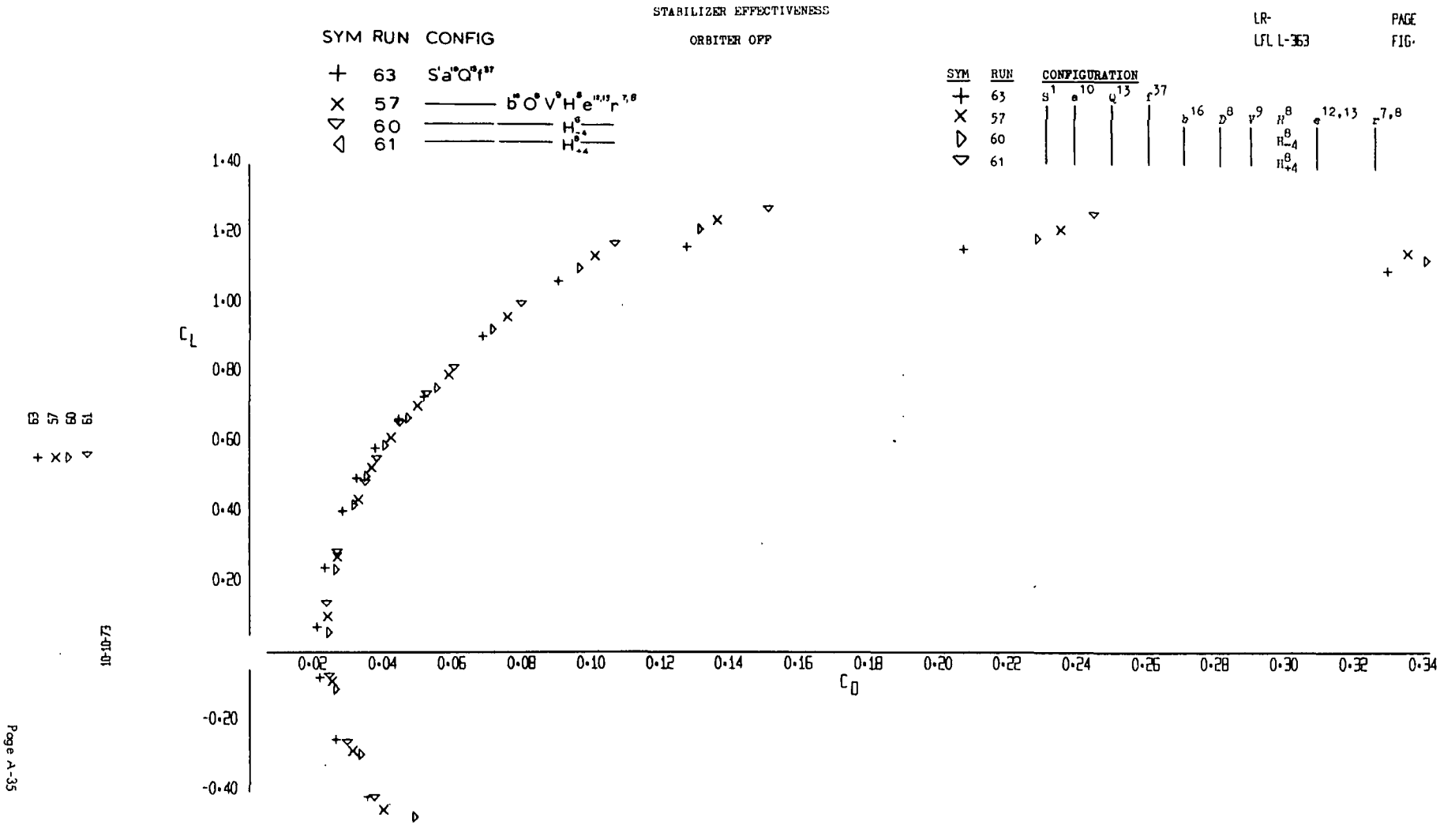

FIGURE 1 (SHEET 1)

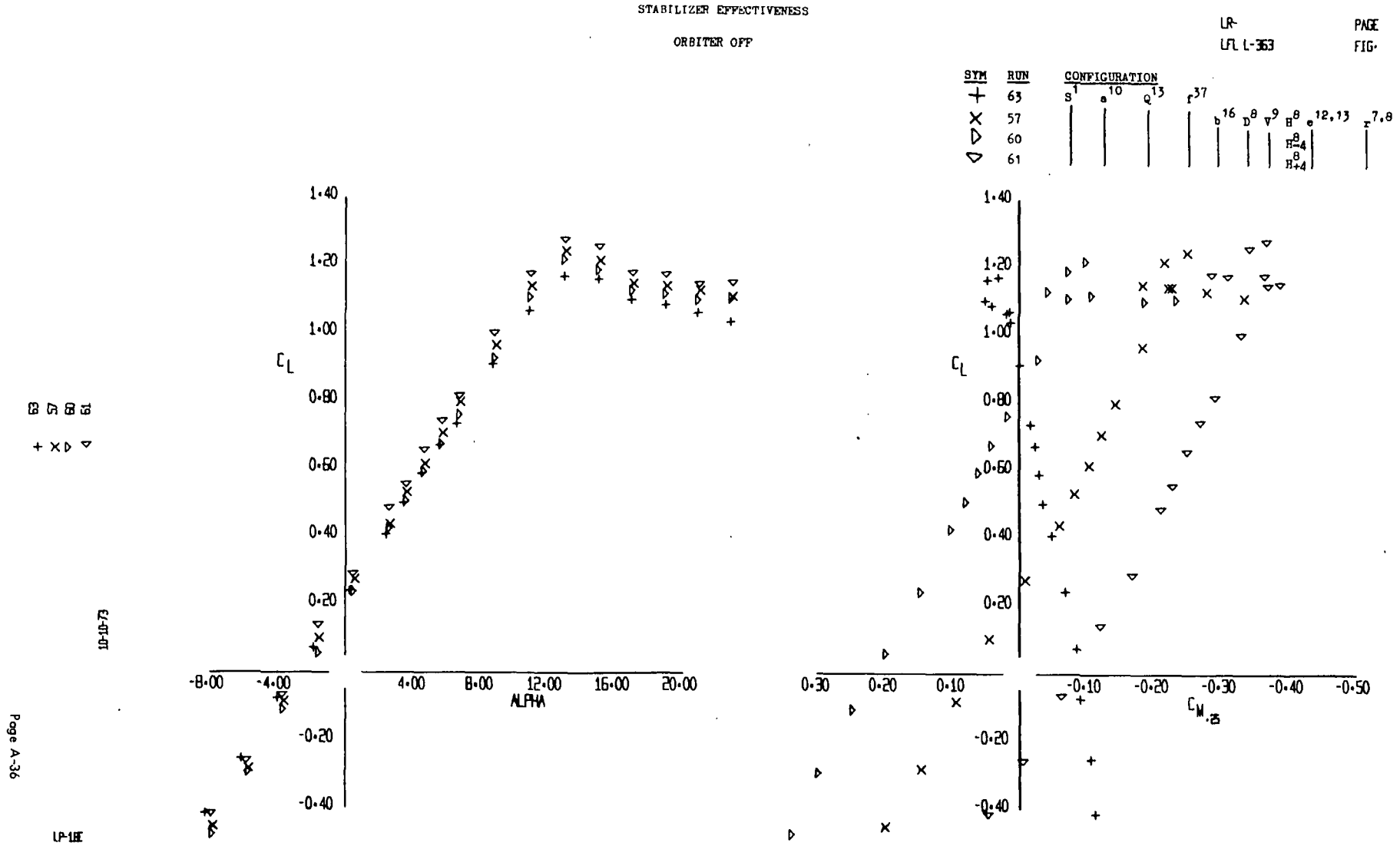

FIGURE 1 (SHEET 2)

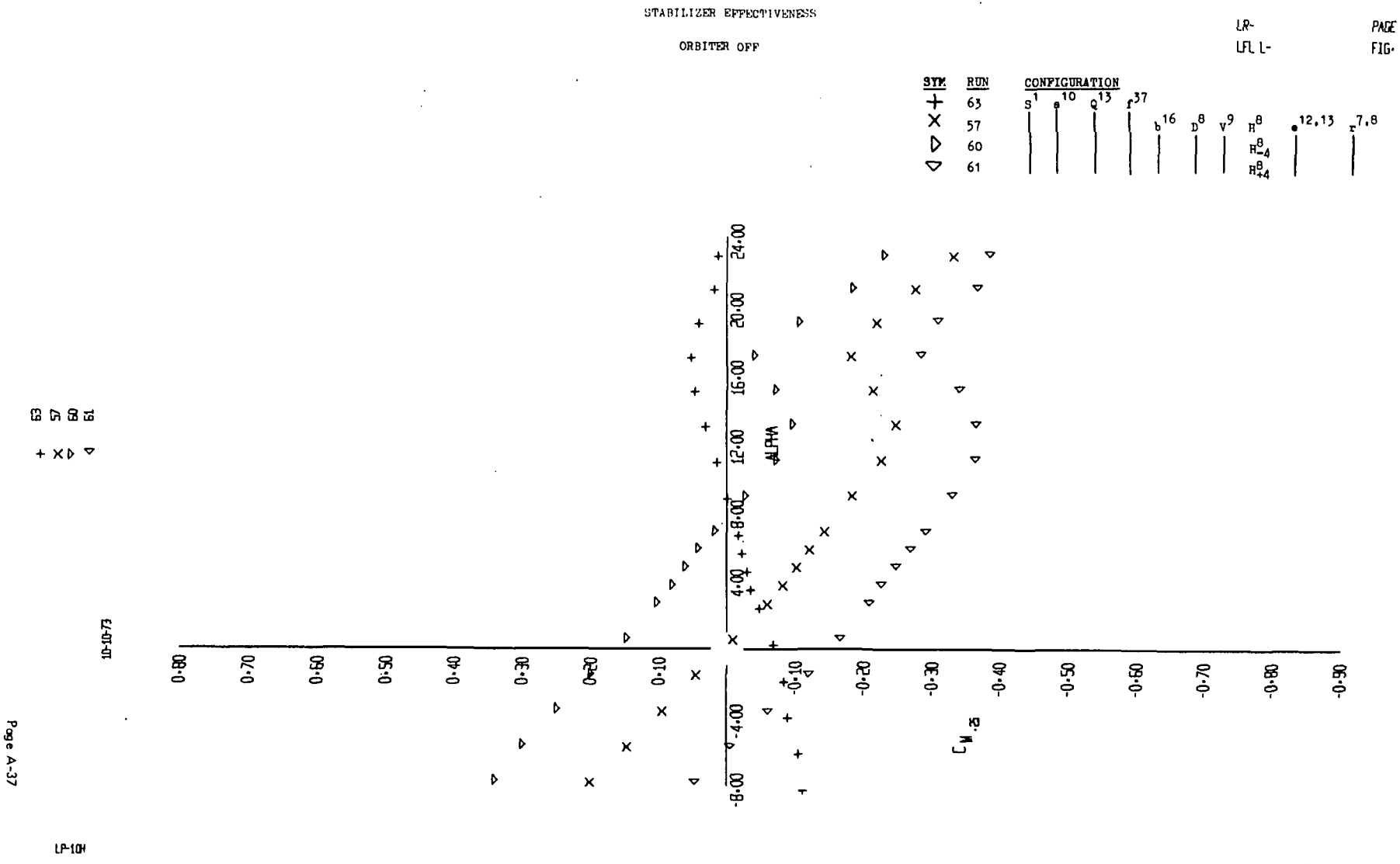

FIGURE 1 (SHEET 3)

STABILIZER EFFECTIVENESS

ORBITER OFF

LR-

LFL L-353

PAGE

FIG.

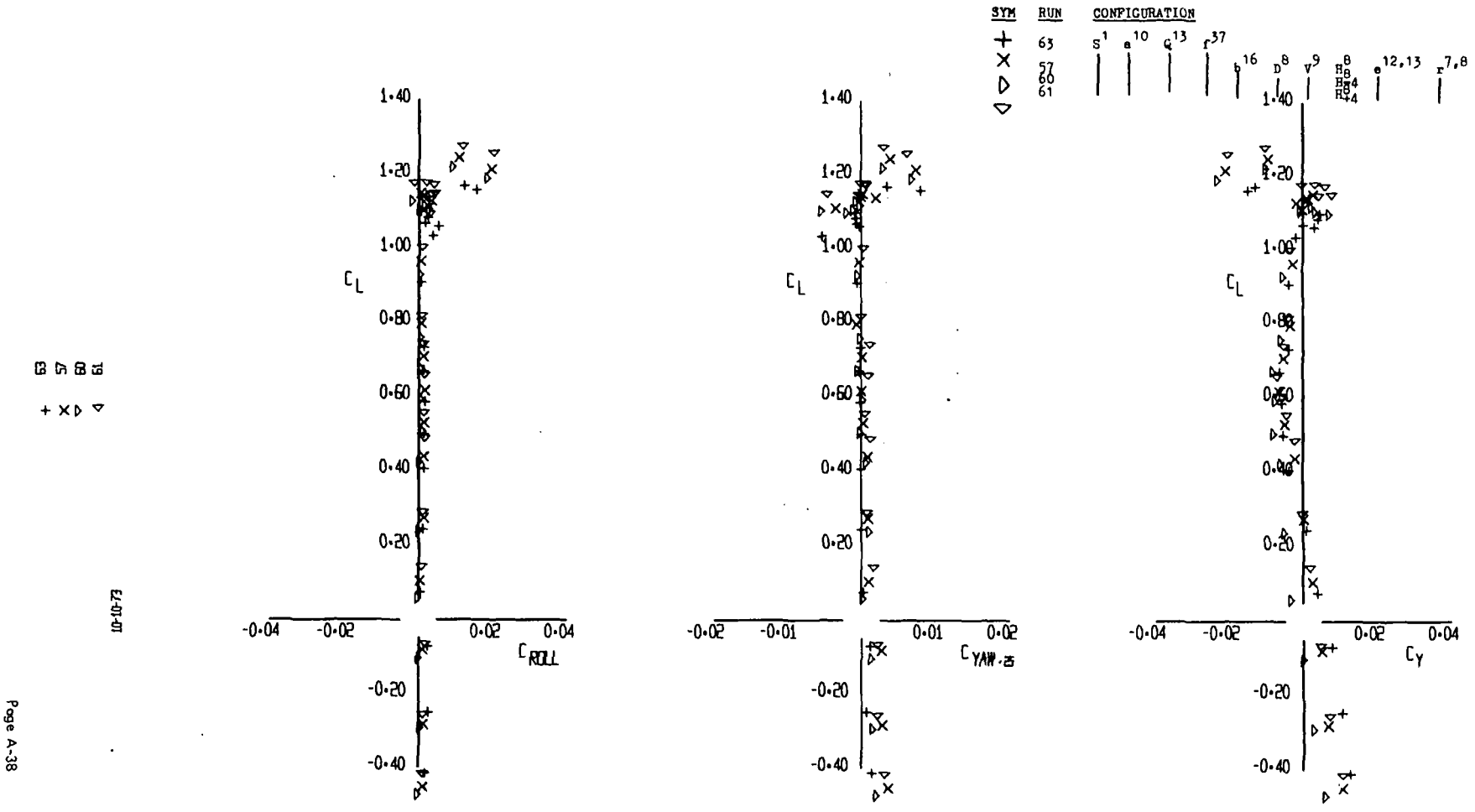

FIGURE 1 (SHEET 4)

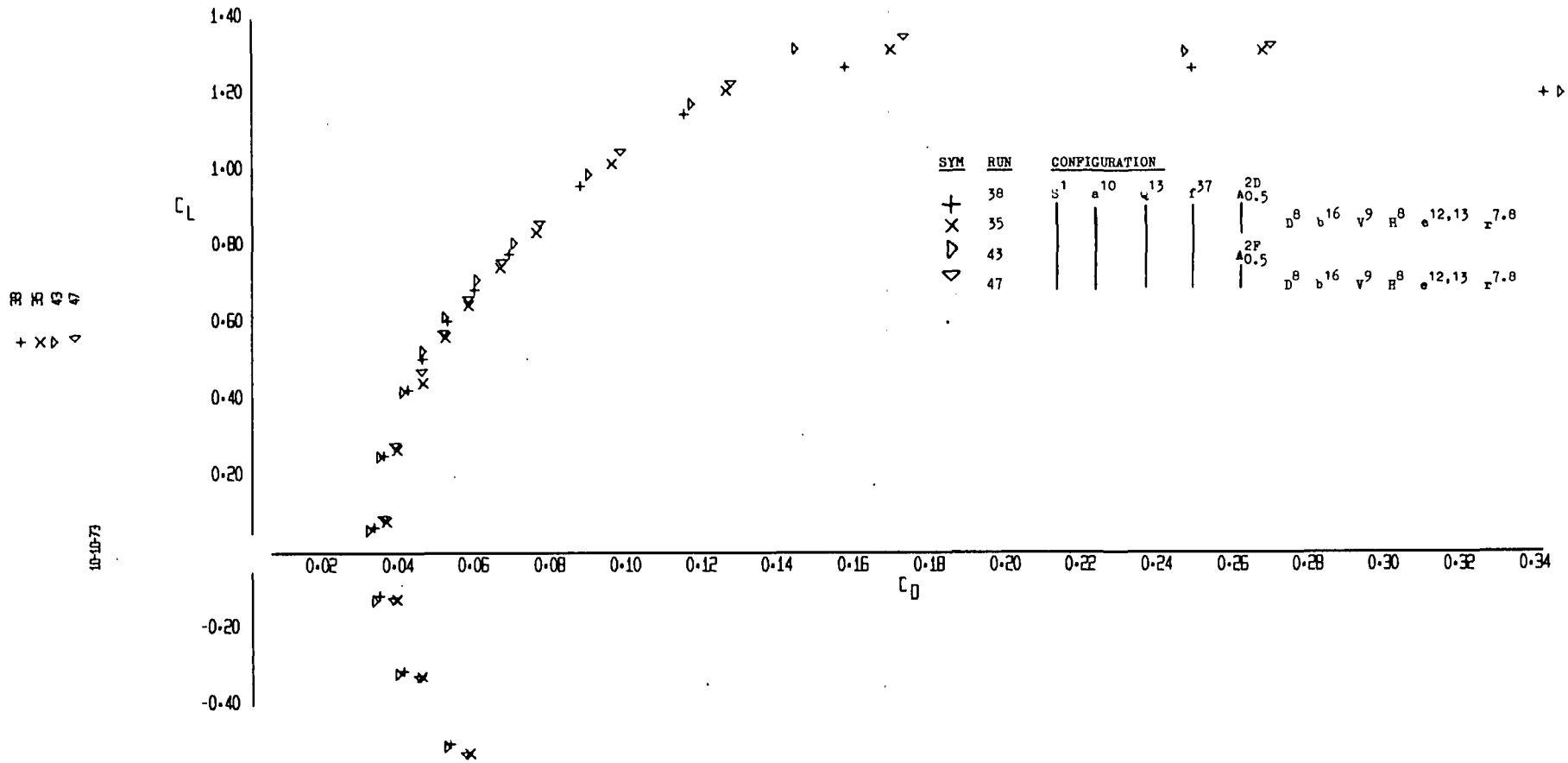

FIGURE 2 (SHEET 1)

EFFECT OF ORBITER POSITION

TAIL ON AND TAIL OFF

LR-
LFL L-363

PAGE
FIG.

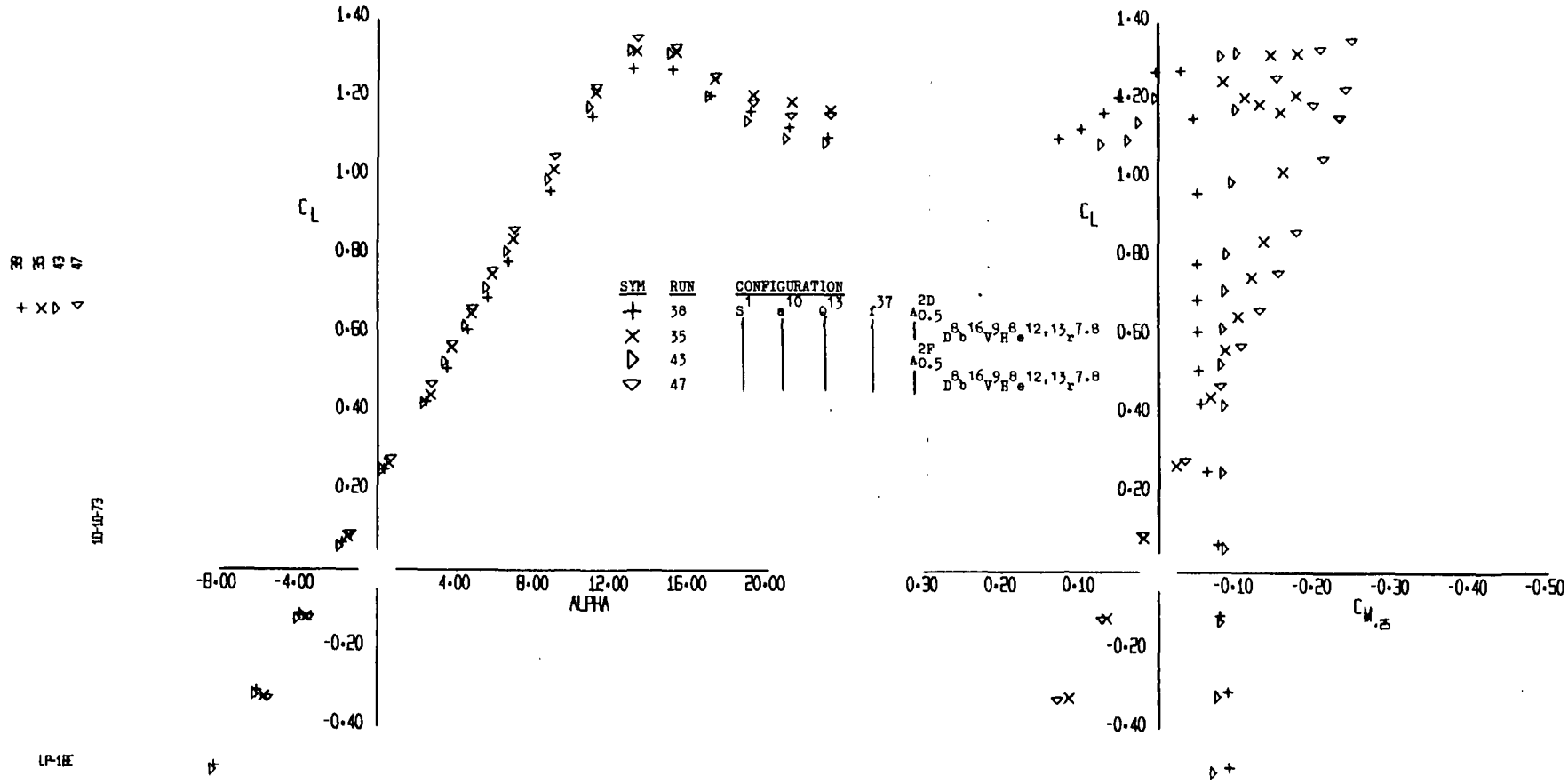

FIGURE 2 (SHEET 2)

EFFECT OF ORBITER POSITION

TAIL ON AND TAIL OFF

LR-

LFL L-

PAGE

FIG.

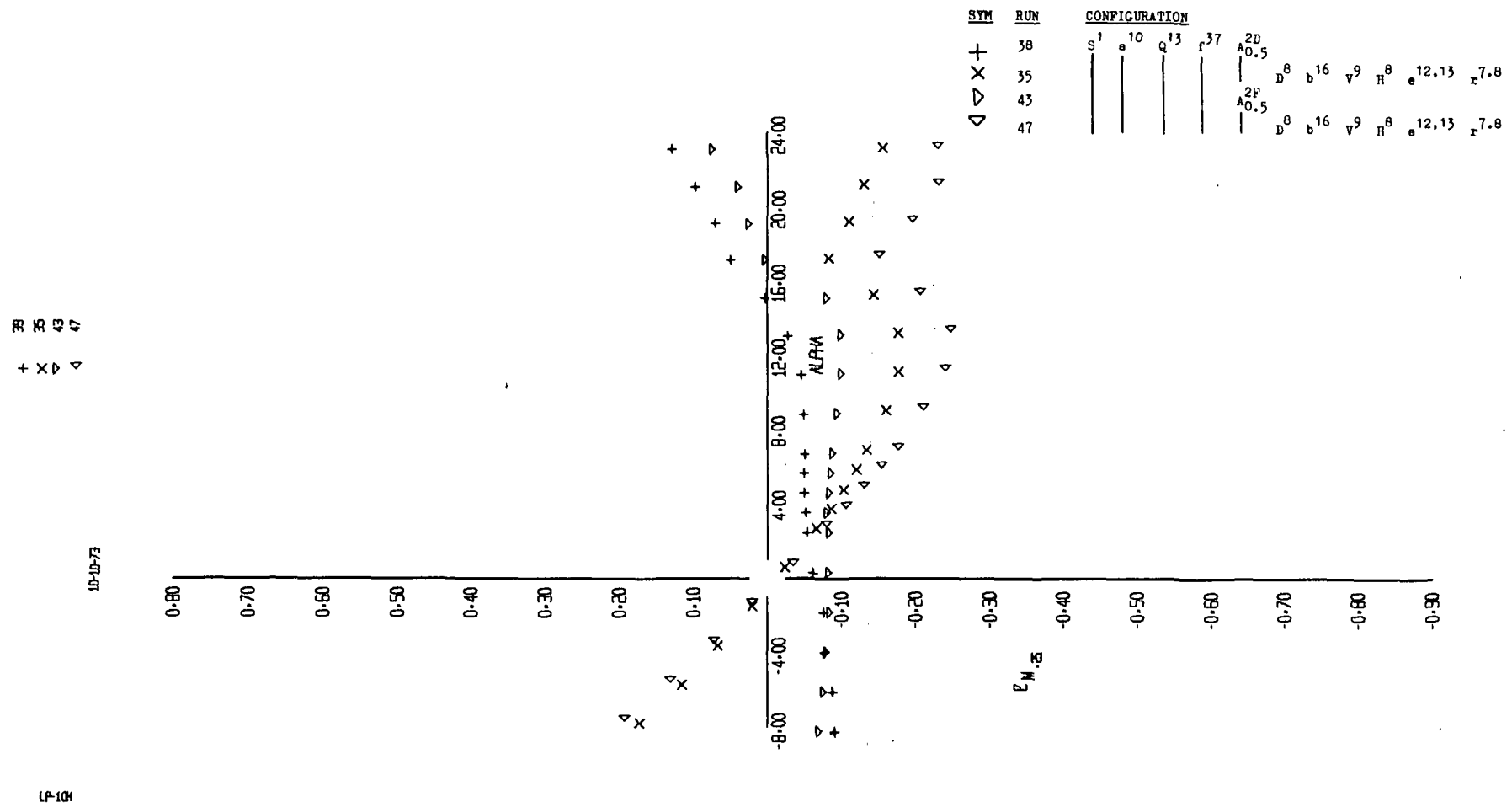

FIGURE 2 (SHEET 3)

LP-10H

EFFECT OF ORBITER POSITION

TAIL ON AND TAIL OFF

LR-

PAGE

LFL L-363

FIG.

SYM	RUN	CONFIGURATION
+	38	S^{1} a^{10} Q^{15} f^{37} $A^{2D}_{0.5}$ D^{8} b^{16} V^{9} H^{8} $e^{12,13}$ $r^{7.8}$
×	35	
▷	43	$A^{2F}_{0.5}$ D^{8} b^{16} V^{9} H^{8} $e^{12,13}$ $r^{7.8}$
◁	47	

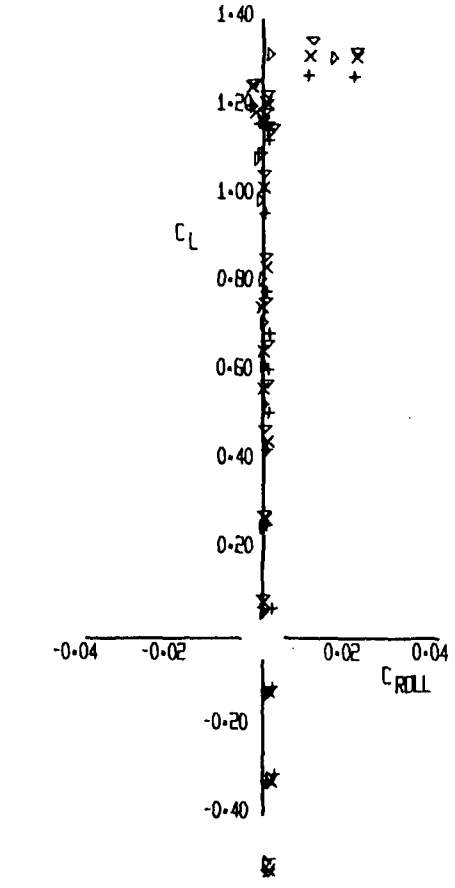

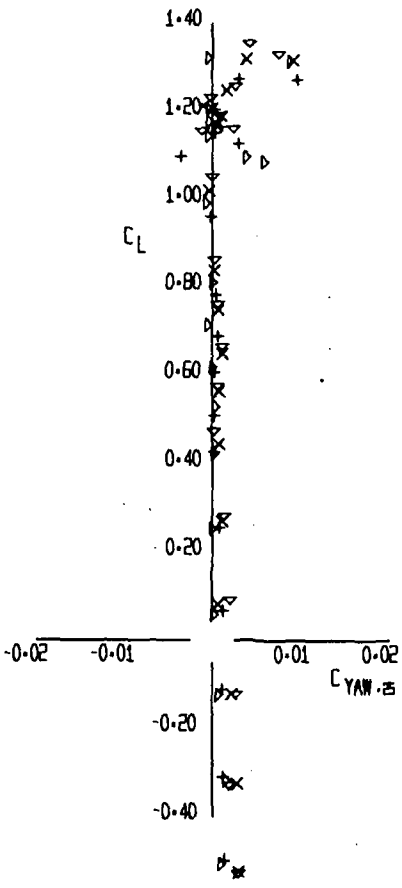

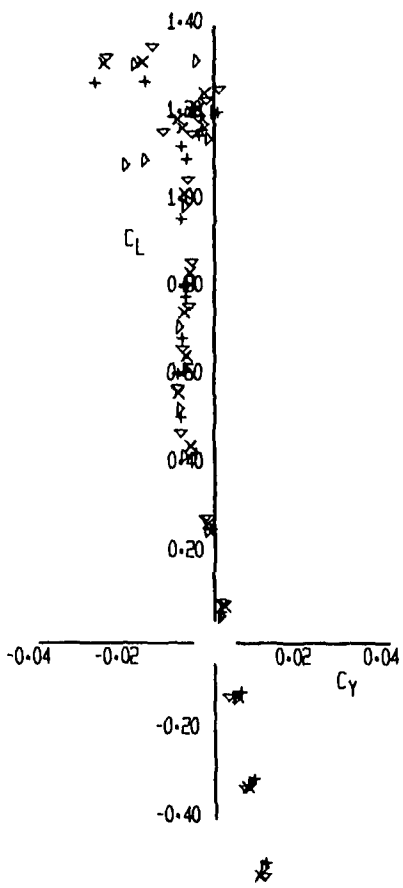

FIGURE 2 (SHEET 4)

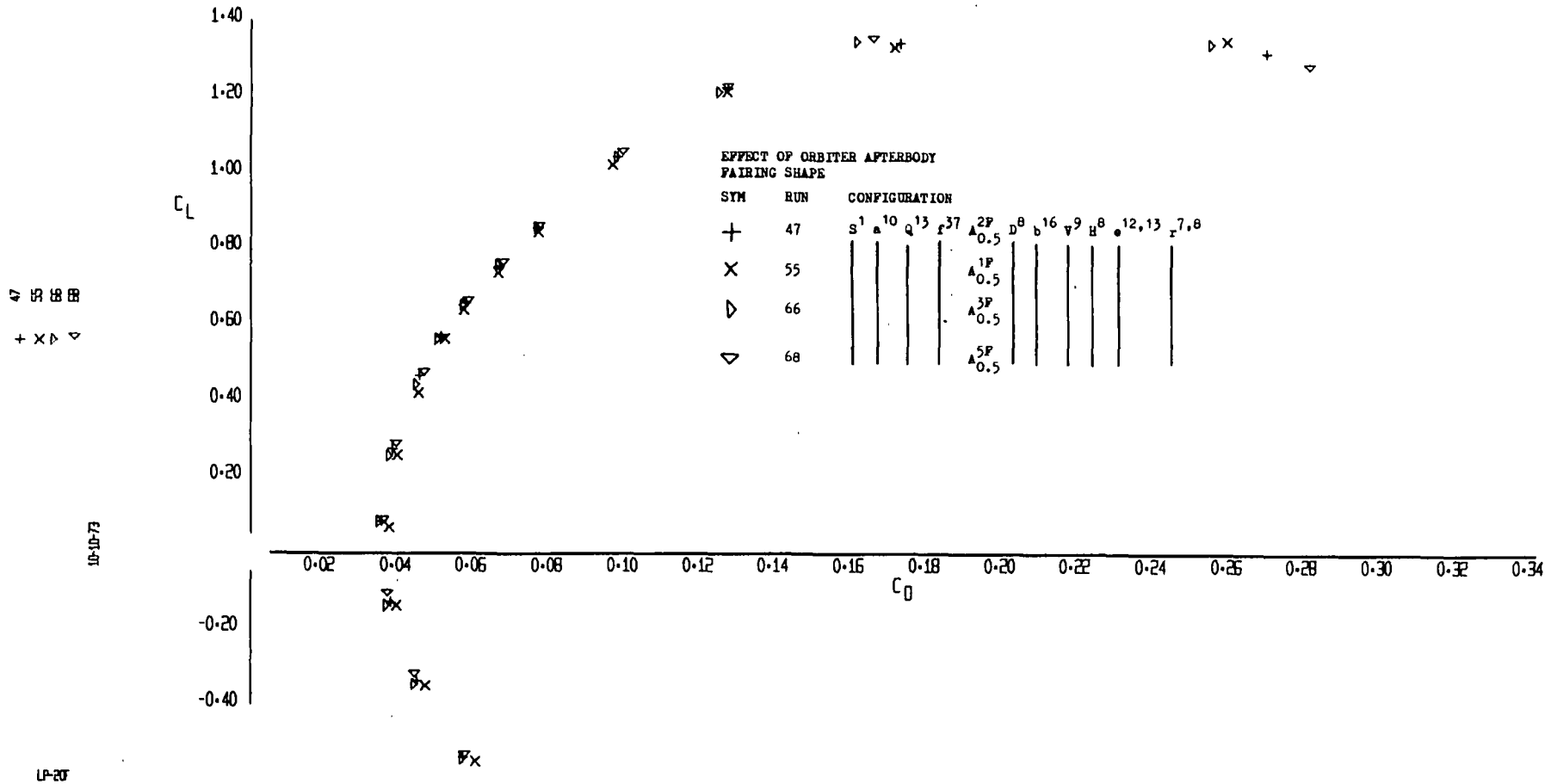

FIGURE 3 (SHEET 1)

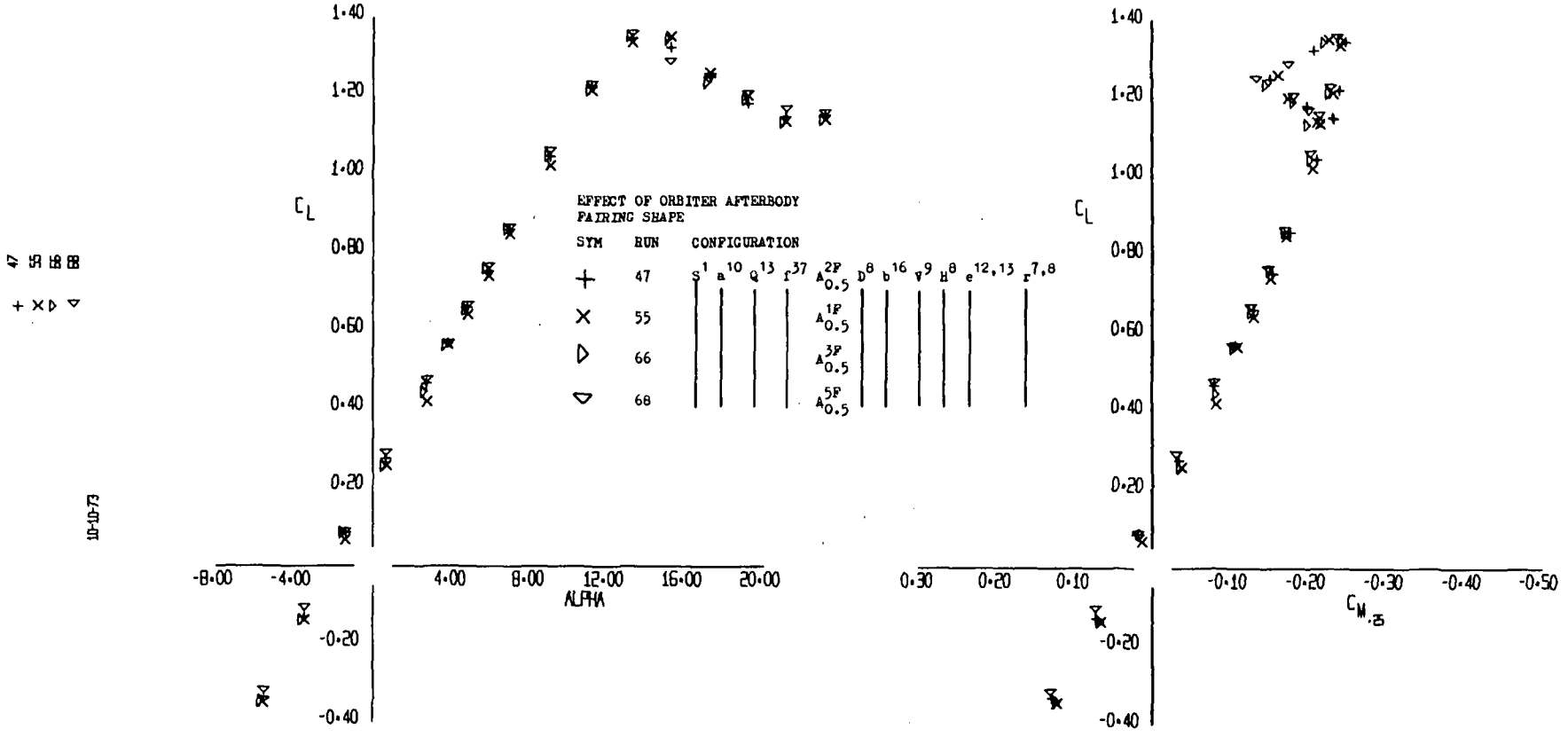

FIGURE 3 (SHEET 2)

FIGURE 3 (SHEET 3)

EFFECT OF ORBITER AFTERBODY

FAIRING SHAPE

SYM	RUN	CONFIGURATION
+	47	S^{1} a^{10} c^{13} f^{37} $A_{0.5}^{2F_{5P}}$ D^{8} b^{16} v^{9} H^{8} $e^{12,13}$ $r^{7,8}$
×	55	$A_{0.5}^{1P}$
▷	66	$A_{0.5}^{3F_{5P}}$
◁	68	$A_{0.5}^{5P}$

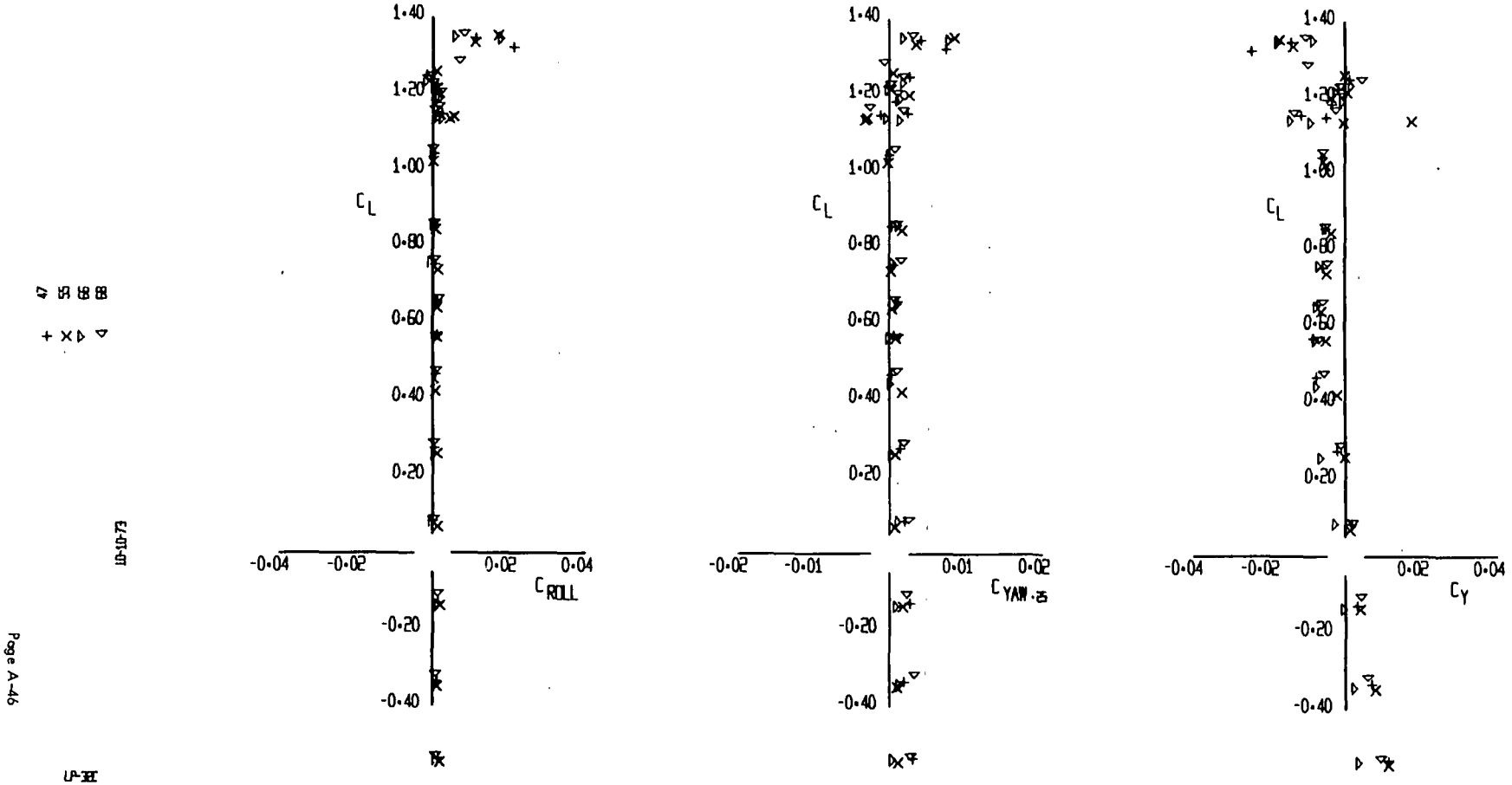

FIGURE 3 (SHEET 4)

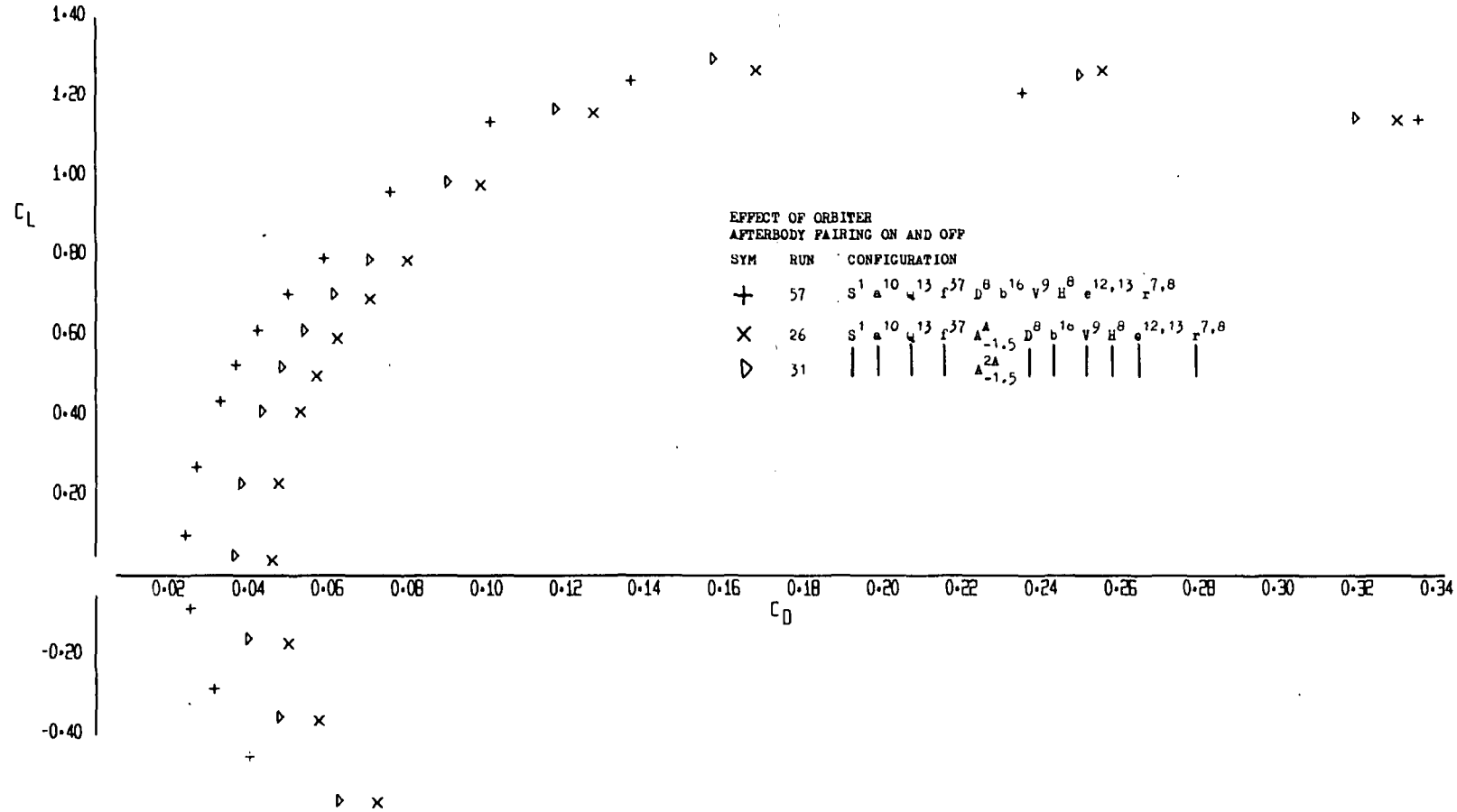

FIGURE 4 (SHEET 1)

EFFECT OF ORBITER AFTERBODY FAIRING ON AND OFF

LR-
LFL L-363

PAGE
FIG.

SYM	RUN	CONFIGURATION
+	57	S^{1} a^{10} Q^{13} f^{37} D^{8} b^{16} V^{9} H^{8} $e^{12,13}$ $r^{7,8}$
×	26	S^{1} a^{10} Q^{13} f^{37} A^{2}_{A} 1.5 D^{8} b^{16} V^{9} H^{8} $e^{12,13}$ $r^{7,8}$
▷	31	A^{2}_{A} -2.5

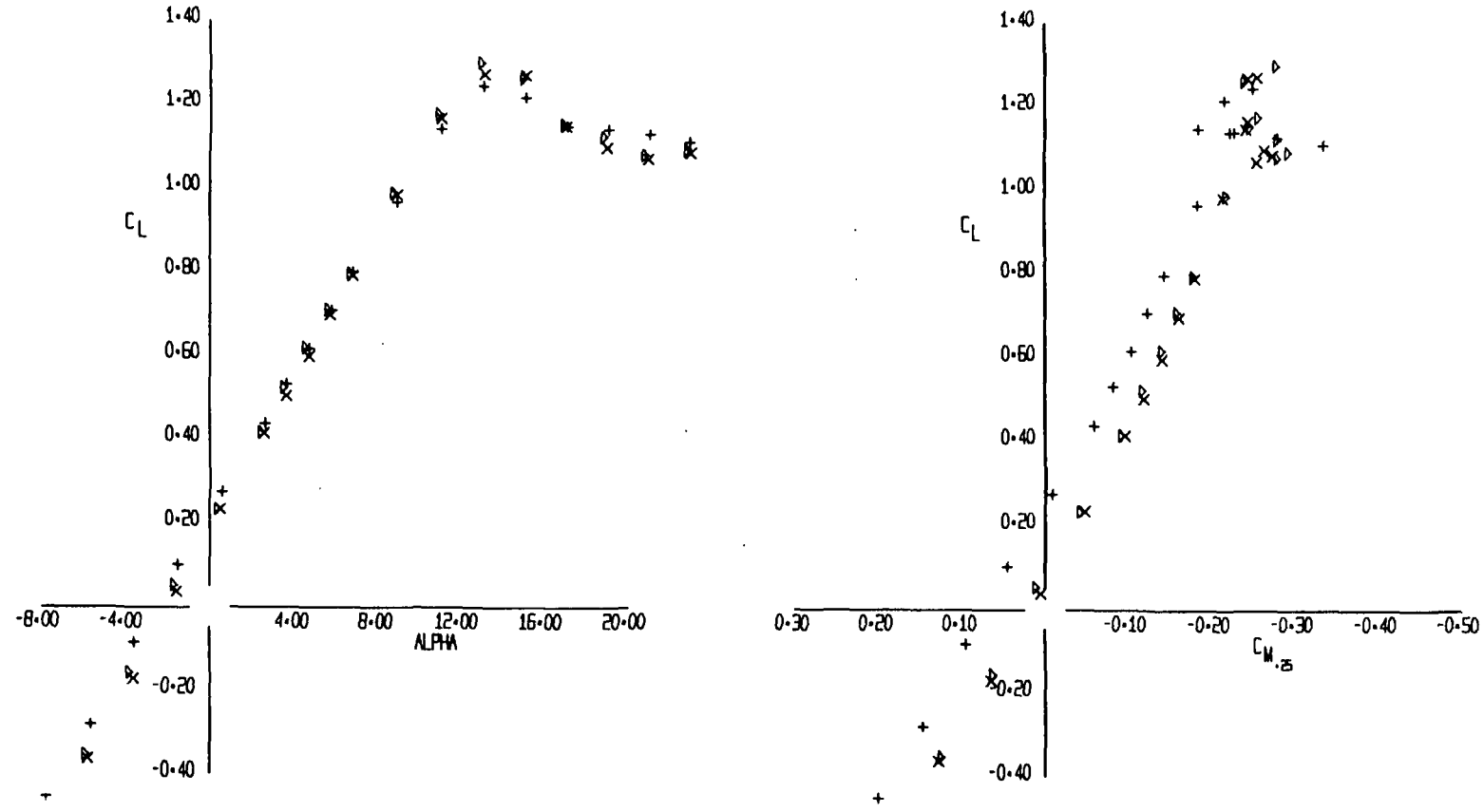

57 26 31
+ × ▷

10-11-73

LP-18E

Page A-48

FIGURE 4 (SHEET 2)

EFFECT OF ORBITER

AFTERBODY FAIRING ON AND OFF

LR-

LFL L-

PAGE

FIG.

SYM	RUN	CONFIGURATION
+	57	S^{1} a^{10} Q^{13} f^{37} D^{8} b^{16} V^{9} H^{8} $e^{12,13}$ $r^{7,8}$
×	26	S^{1} a^{10} Q^{13} f^{37} $A^{A}_{-1.5}$ D^{8} b^{16} V^{9} H^{8} $e^{12,13}$ $r^{7,8}$
▷	31	$A^{2A}_{-1.5}$

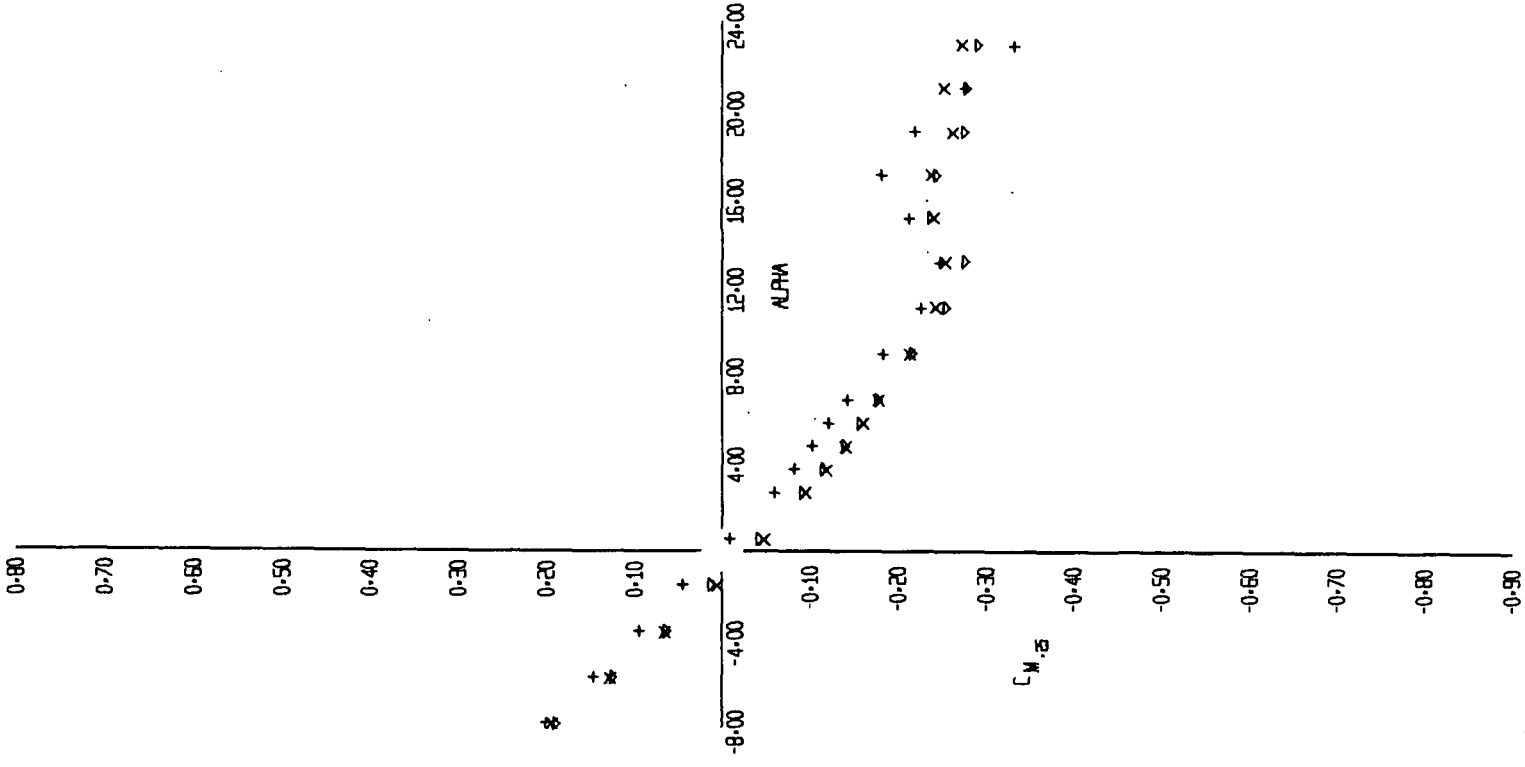

10-11-73

LP-10H

Page A-49

FIGURE 4 (SHEET 3)

EFFECT OF ORBITER
AFTERBODY FAIRING ON AND OFF

SYM	RUN	CONFIGURATION
+	57	S^{1} a^{10} Q^{13} f^{37} D^{8} b^{16} V^{9} H^{8} $e^{12,13}$ $r^{7,8}$
×	26	S^{1} a^{10} Q^{13} f^{37} $\Delta^{\Delta}_{1.5}$ D^{8} b^{16} V^{9} H^{8} $e^{12,13}$ $r^{7,8}$
▷	31	$\Delta^{2\Delta}_{1.5}$

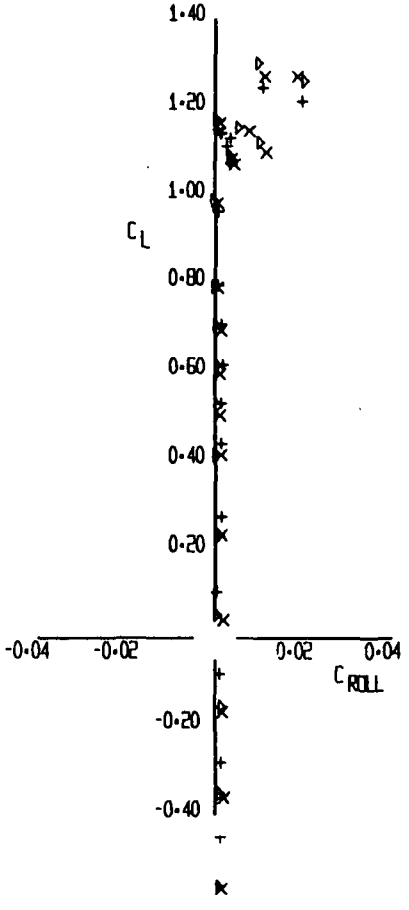

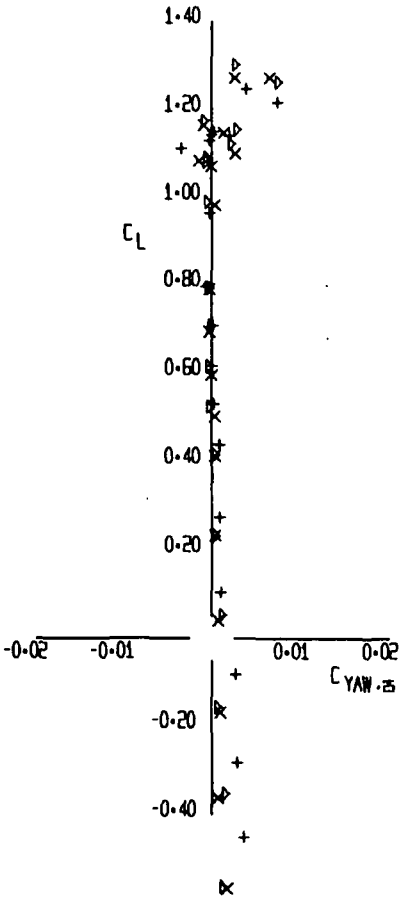

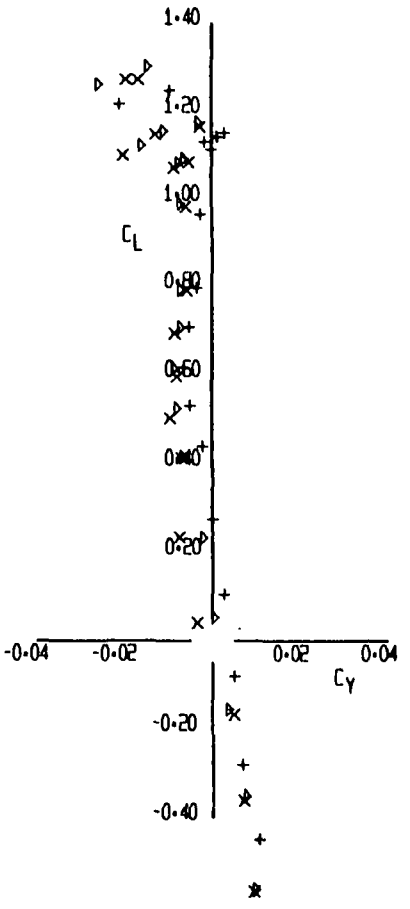

FIGURE 4 (SHEET 4)

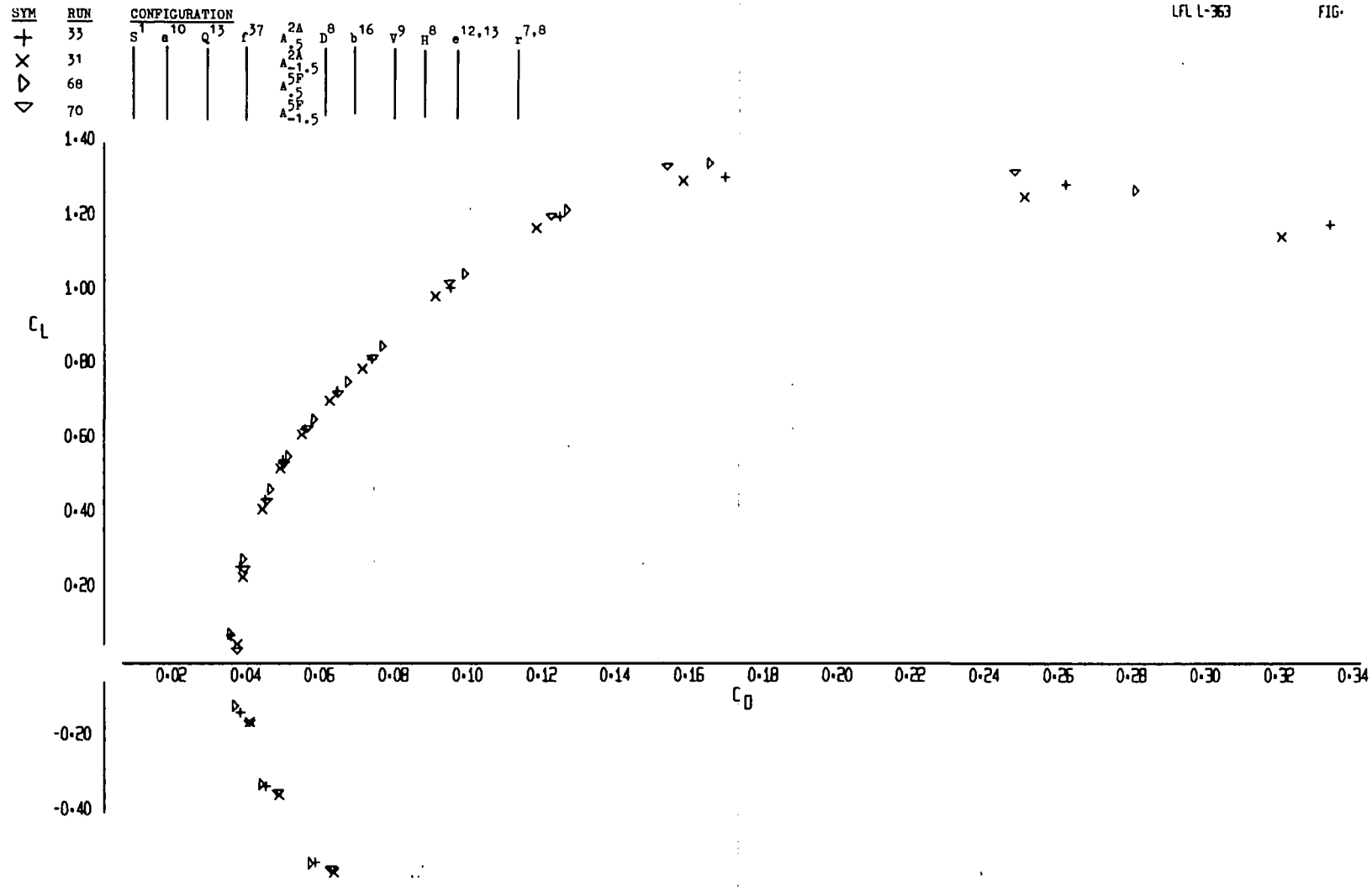

FIGURE 5 (SHEET 1)

SYM	RUN	CONFIGURATION
+	33	S[1] a[10] Q[13] f[37] A[2A .5] D[8] b[16] V[9] H[8] e[12,13] r[7,8]
×	31	A[2A -1.5 5F]
▷	68	A[.5]
◁	70	A[.5F -1.5]

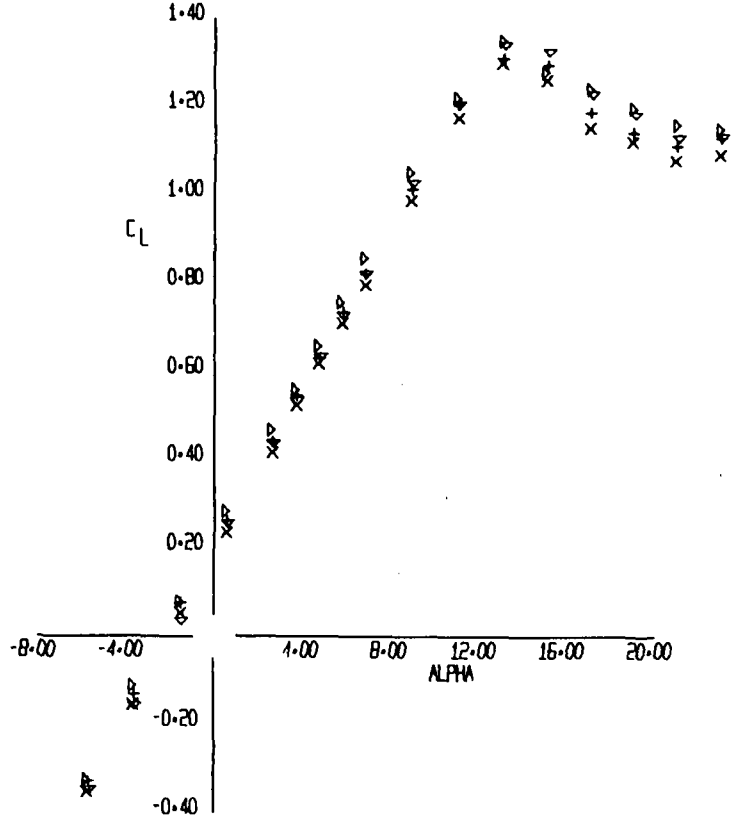

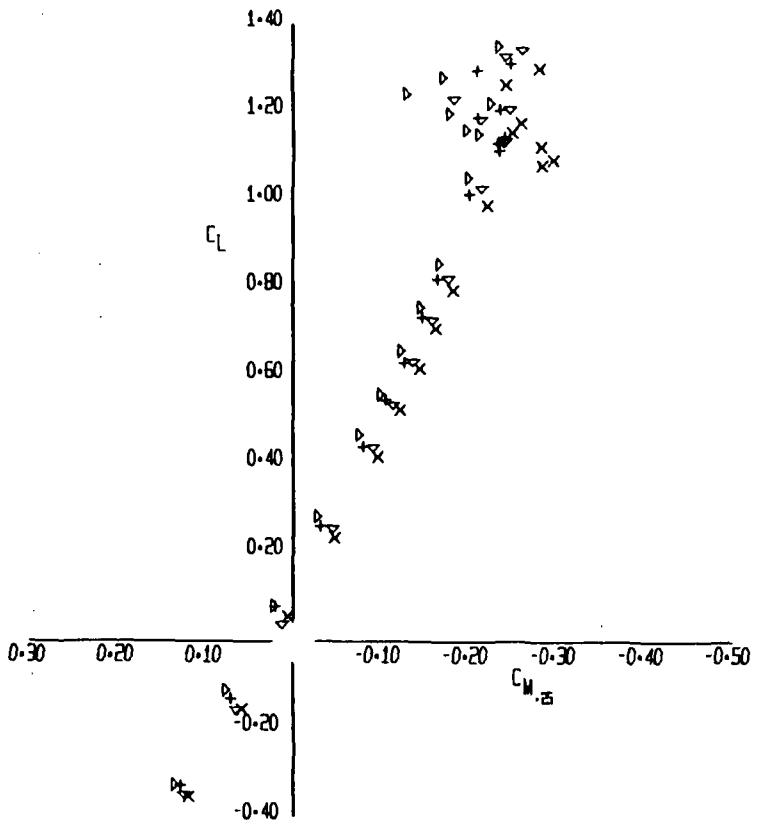

FIGURE 5 (SHEET 2)

EFFECT OF ORBITER INCIDENCE ANGLE

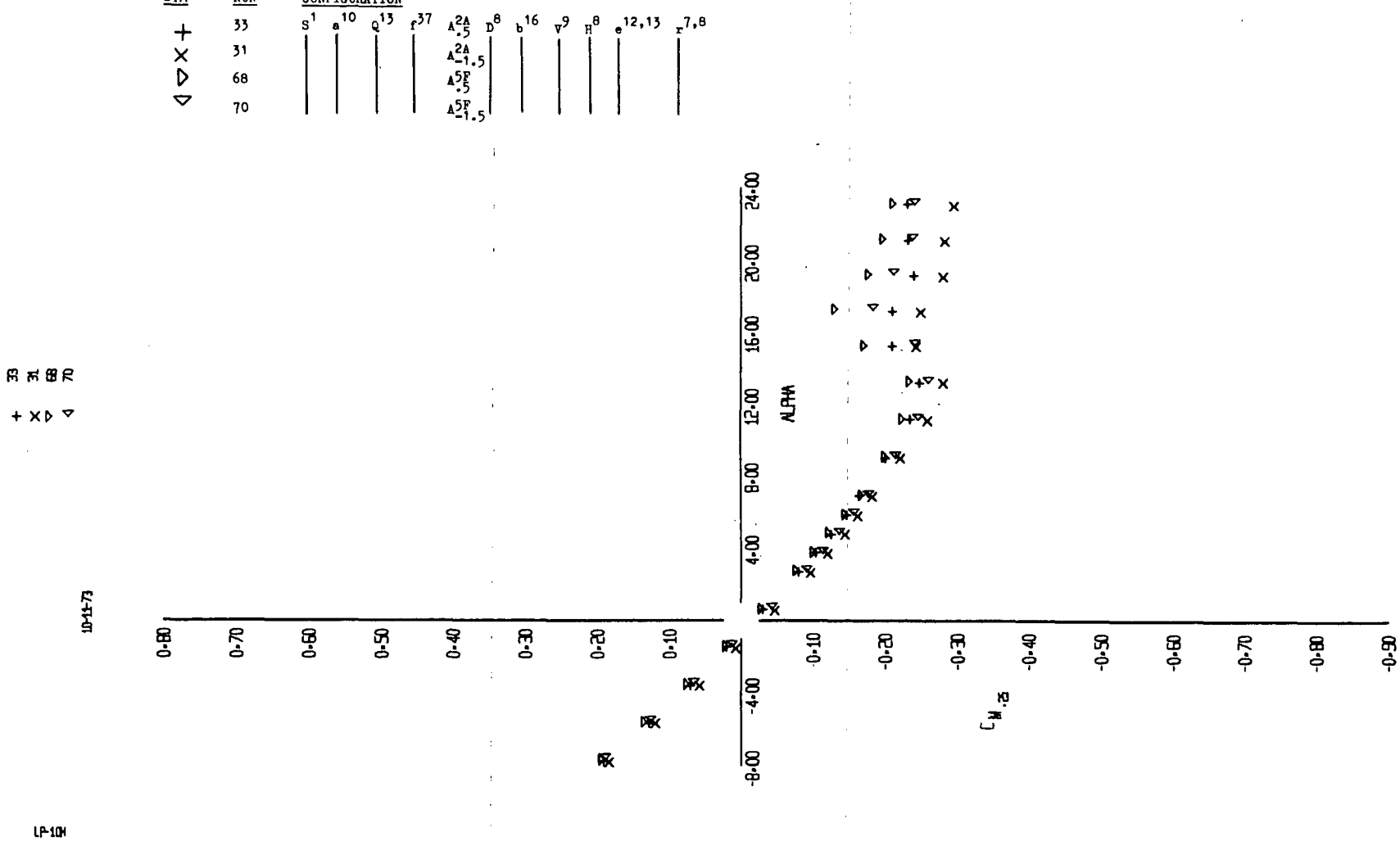

FIGURE 5 (SHEET 3)

EFFECT OF ORBITER INCIDENCE ANGLE

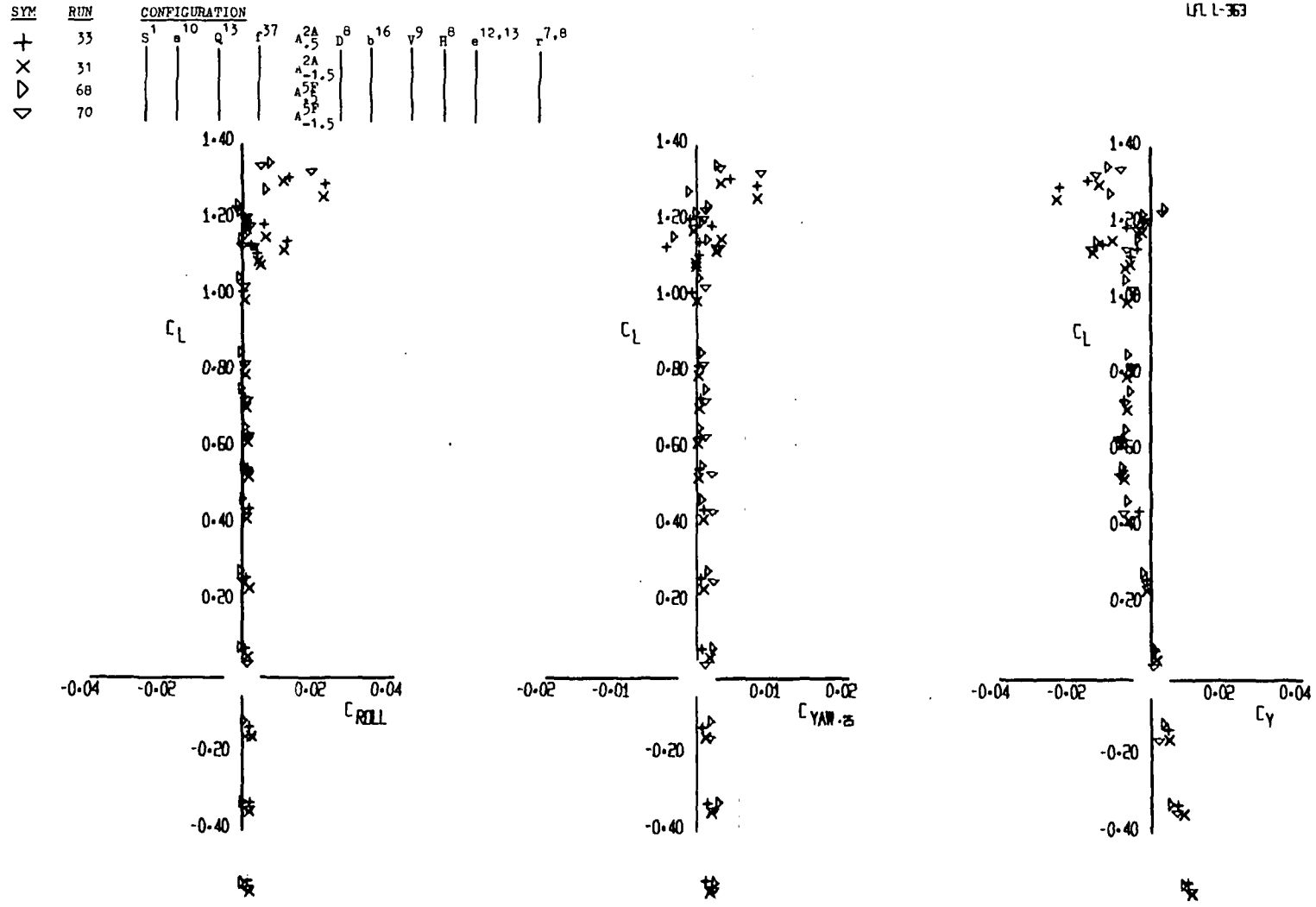

FIGURE 5 (SHEET 4)

EFFECT OF ORBITER POSITION AND AFTERBODY FAIRING SHAPE

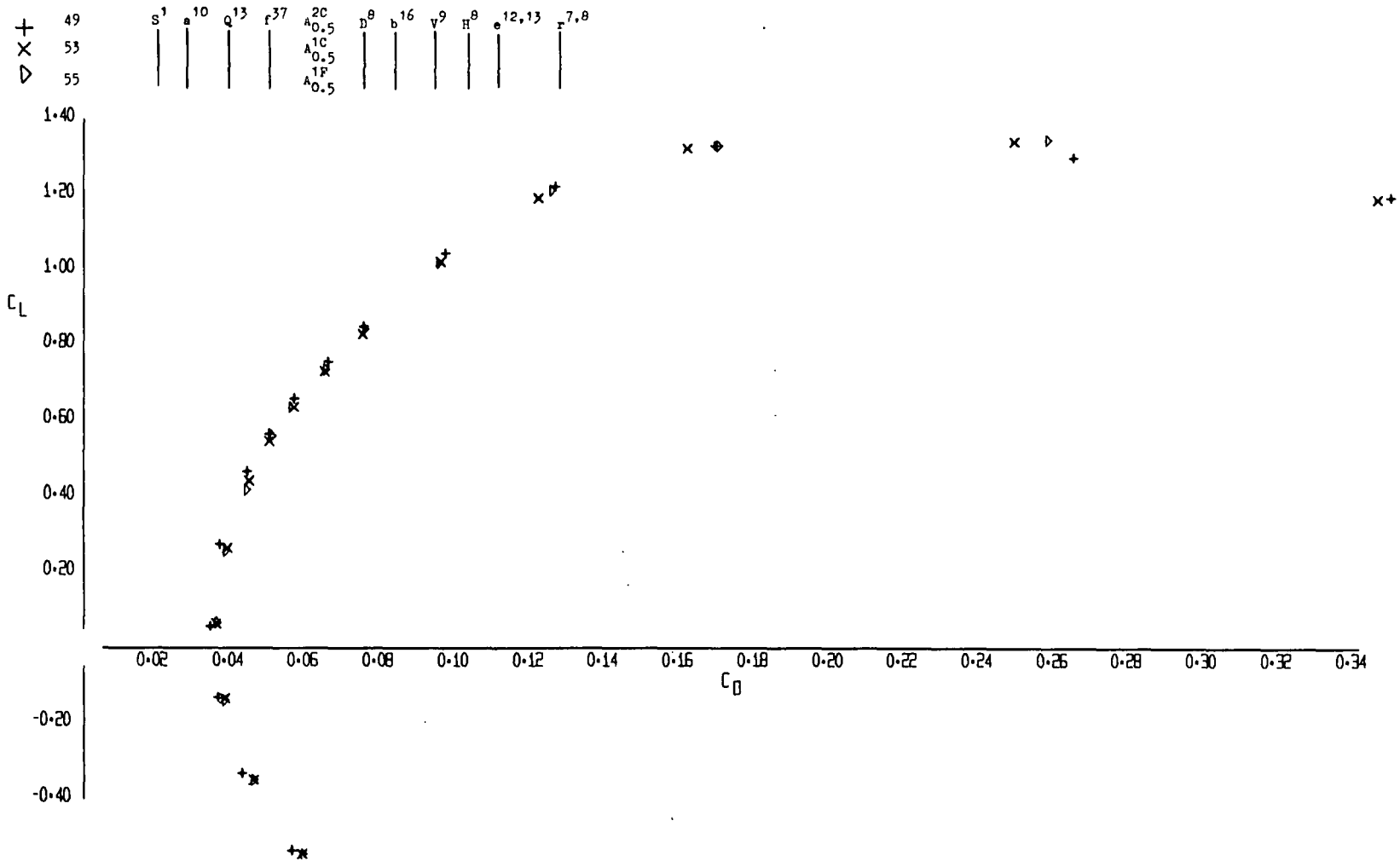

FIGURE 6 (SHEET 1)

EFFECT OF ORBITER POSITION AND AFTERBODY FAIRING SHAPE

SYM	RUN
+	49
×	53
▷	55

CONFIGURATION

S^{1} a^{10} Q^{13} f^{37} $A^{2C}_{O.5}$ D^{8} b^{16} V^{9} H^{8} $e^{12,13}$ $r^{7,8}$

$A^{1C}_{O.5}$

$A^{1F}_{O.5}$

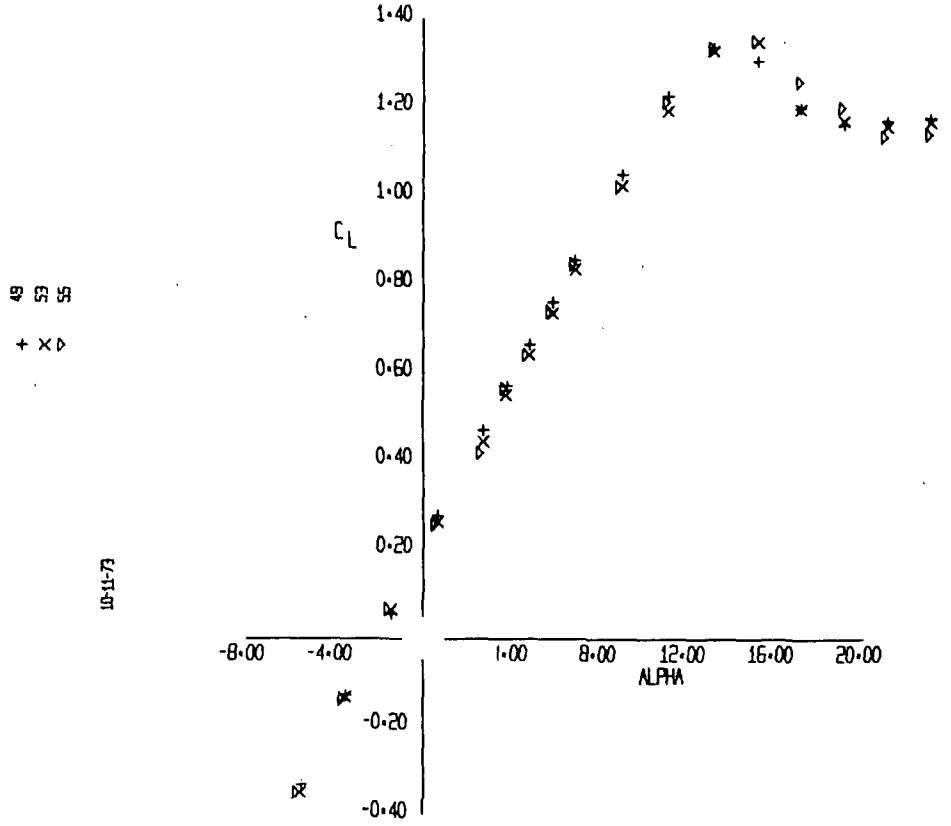

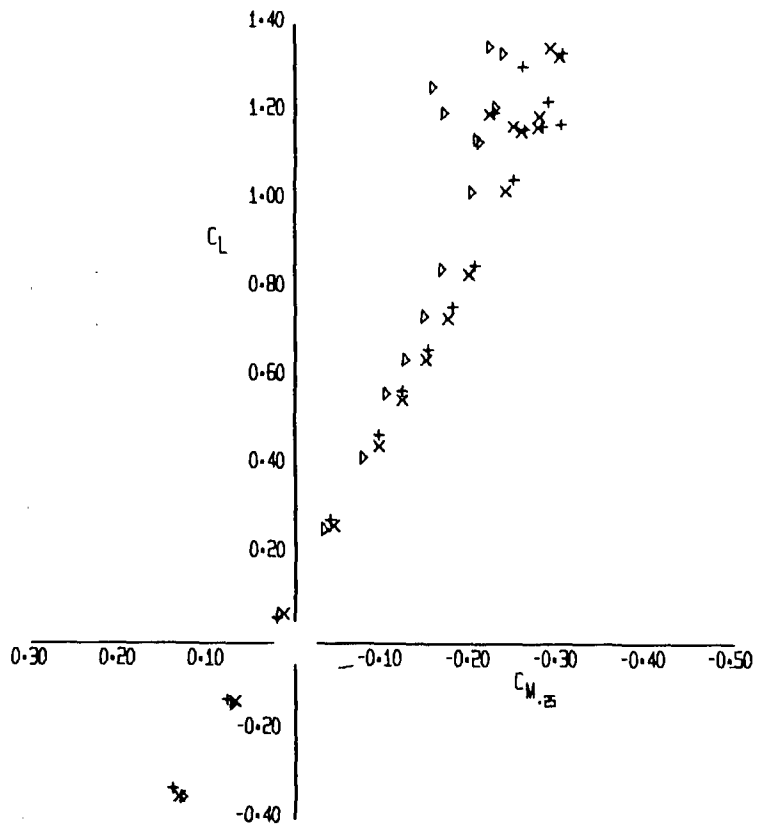

49 53 55

10-11-73

LP-1BE

FIGURE 6 (SHEET 2)

EFFECT OF ORBITER POSITION AND AFTERBODY FAIRING SHAPE

SYM	RUN	CONFIGURATION
+	49	S^{1} a^{10} Q^{13} f^{37} $A^{2C}_{0.5}$ D^{8} b^{16} V^{9} H^{8} $e^{12,13}$ $r^{7,8}$
×	53	$A^{1C}_{0.5}$
▷	55	$A^{1F}_{0.5}$

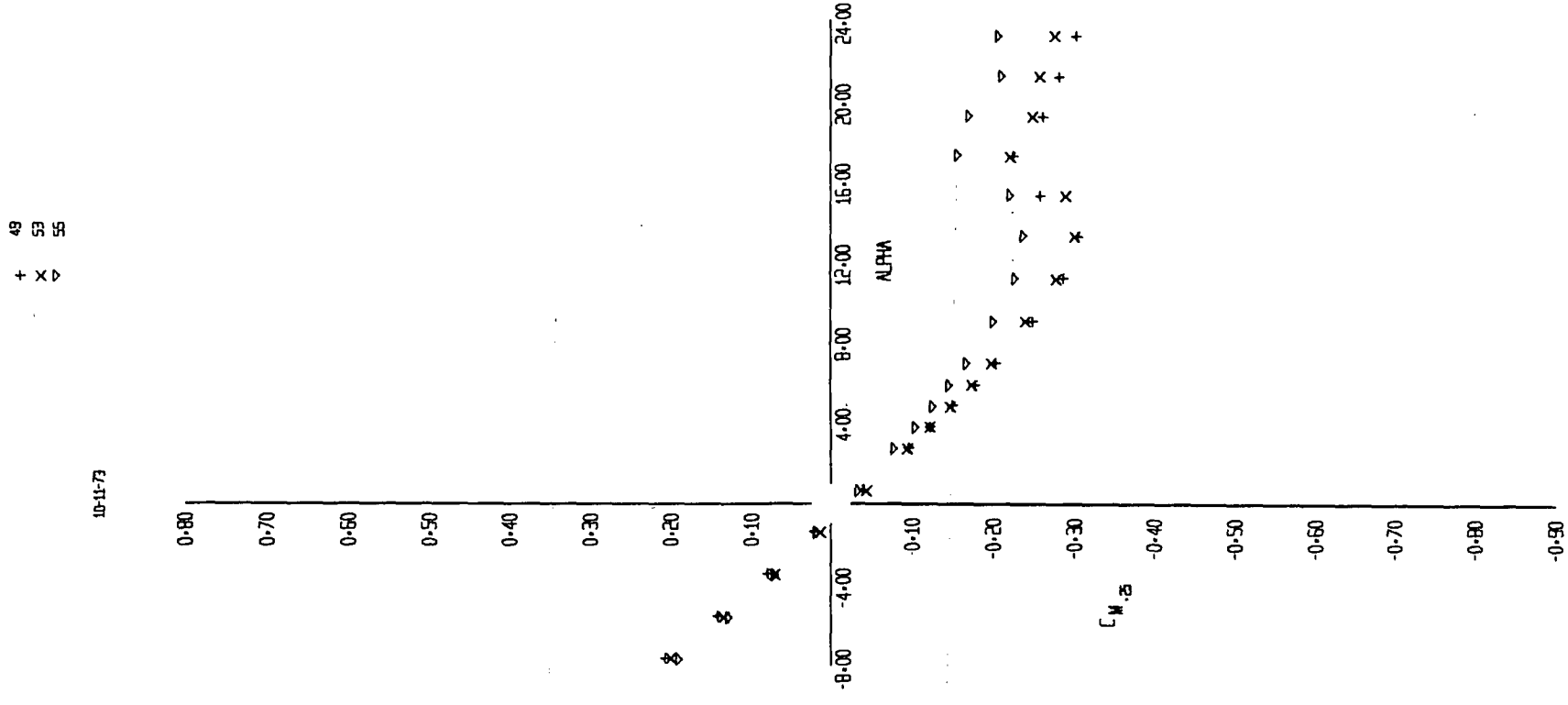

FIGURE 6 (SHEET 3)

SYM	RUN	CONFIGURATION
+	49	S^{1} e^{10} Q^{13} f^{37} $A^{2C}_{0.5}$ D^{8} b^{16} V^{9} H^{8} $e^{12,13}$ $r^{7,8}$
×	53	$A^{1C}_{0.5}$
▷	55	$A^{1F}_{0.5}$

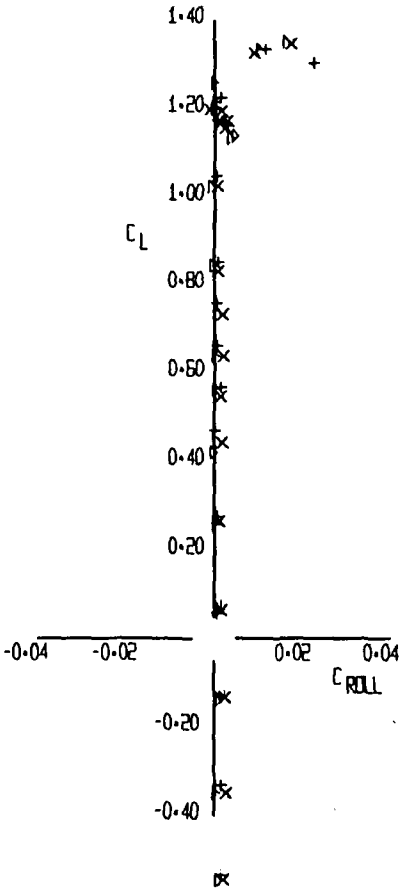

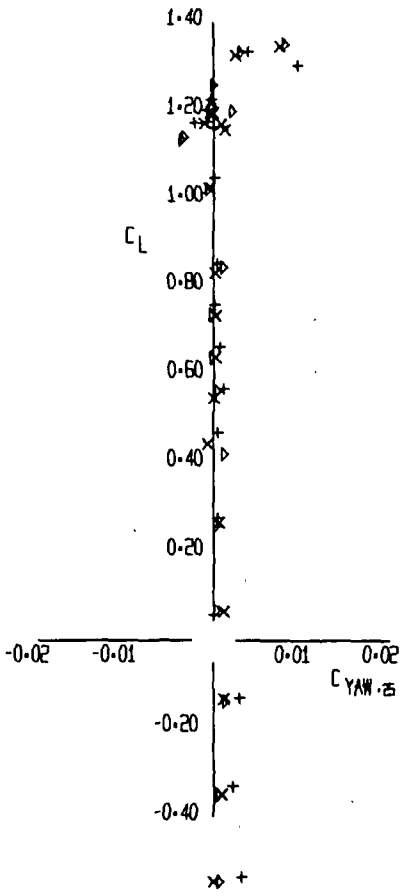

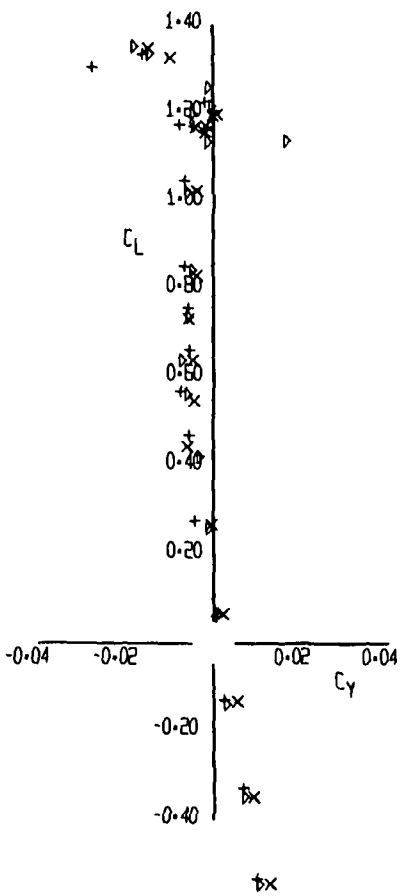

FIGURE 6 (SHEET 4)

SPOILER EFFECTIVENESS, ORBITER ON AND OFF

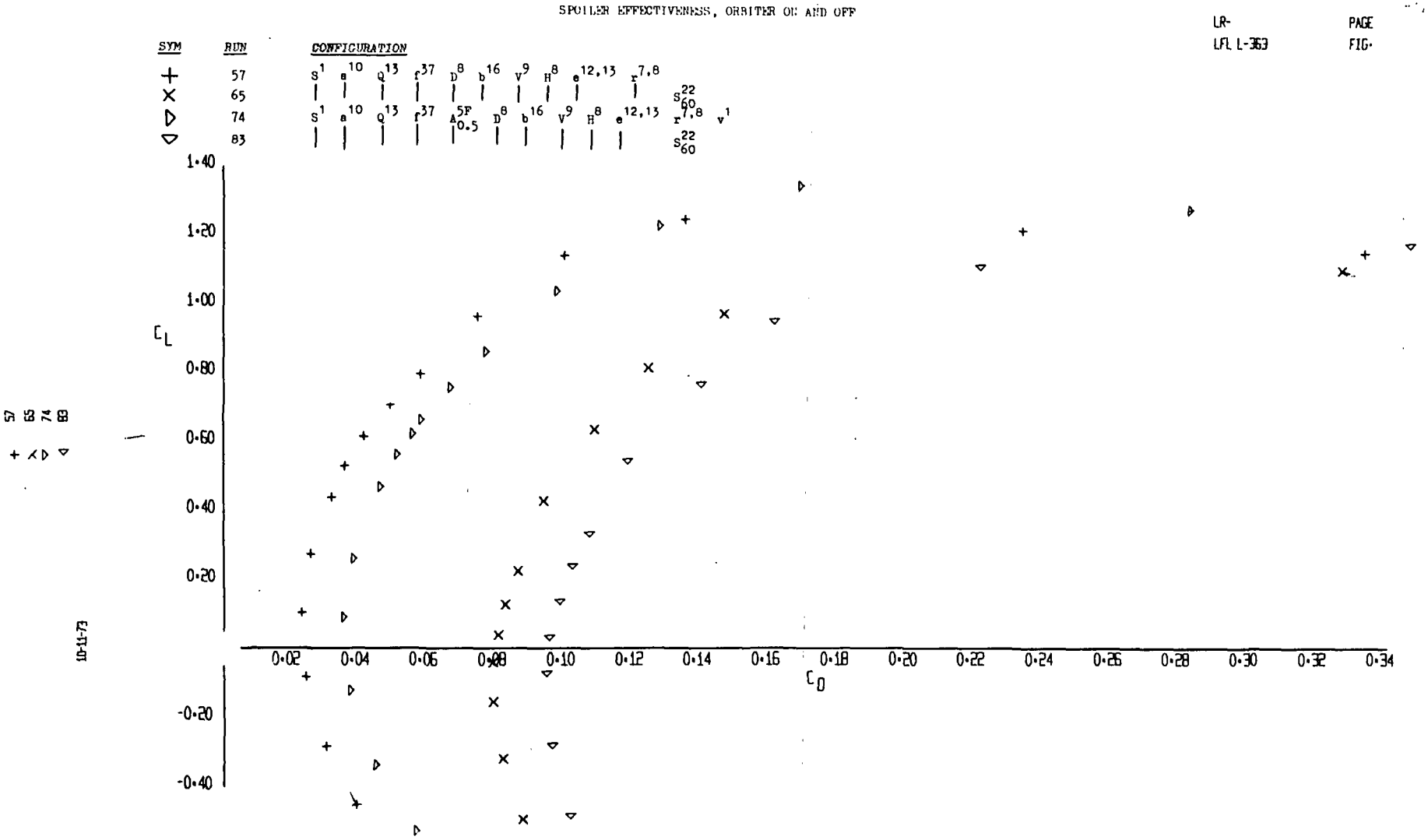

FIGURE 7 (SHEET 1)

SPOILER EFFECTIVENESS, ORBITER ON AND OFF

SYM	RUN	CONFIGURATION
+	57	S^{1} a^{10} Q^{13} f^{37} D^{8} b^{16} V^{9} H^{8} $e^{12,13}$ $r^{7,8}$ S^{22}_{60}
×	65	
▷	74	S^{1} a^{10} Q^{13} f^{37} $A^{5F}_{0.5}$ D^{8} b^{16} V^{9} H^{8} $e^{12,13}$ $r^{7,8}$ v^{1} S^{22}_{60}
◁	83	

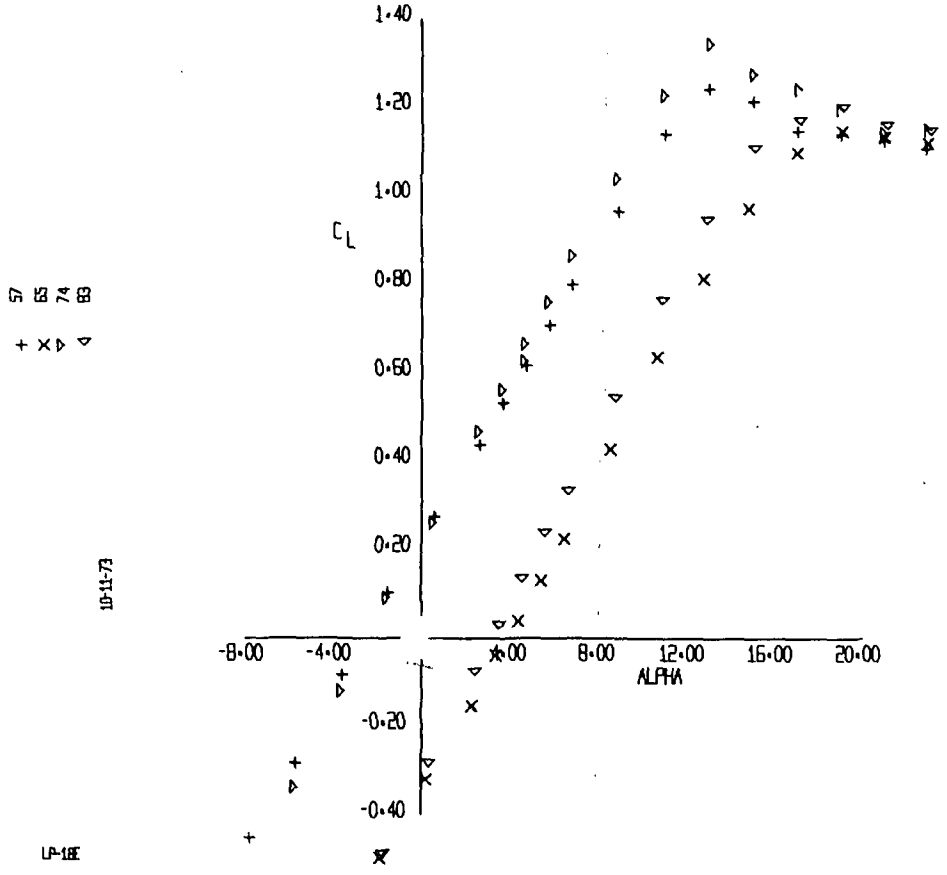

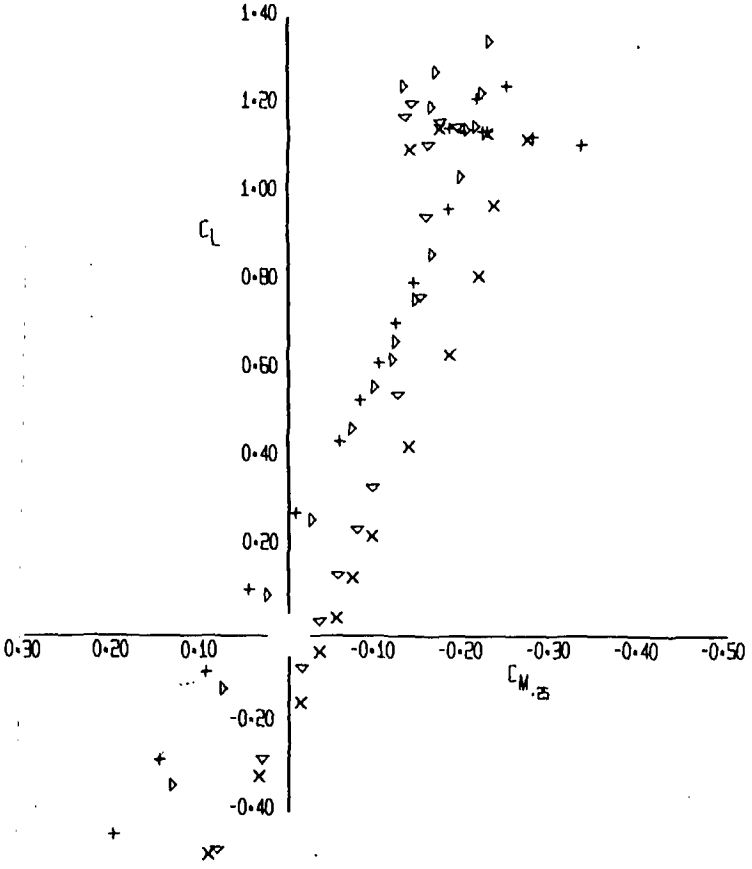

FIGURE 7 (SHEET 2)

SPOILER EFFECTIVENESS, ORBITER ON AND OFF

LR-
LFL L-

PAGE
FIG.

SYM	RUN	CONFIGURATION
+	57	S^{1} a^{10} Q^{13} f^{37} D^{8} b^{16} V^{9} H^{8} $e^{12,13}$ $r^{7,8}$ S^{22}_{60}
×	65	
▷	74	S^{1} a^{10} Q^{13} f^{37} $A^{5F}_{0.5}$ D^{8} b^{16} V^{9} H^{8} $e^{12,13}$ $r^{7,8}$ S^{22}_{60} v^{1}
◁	83	

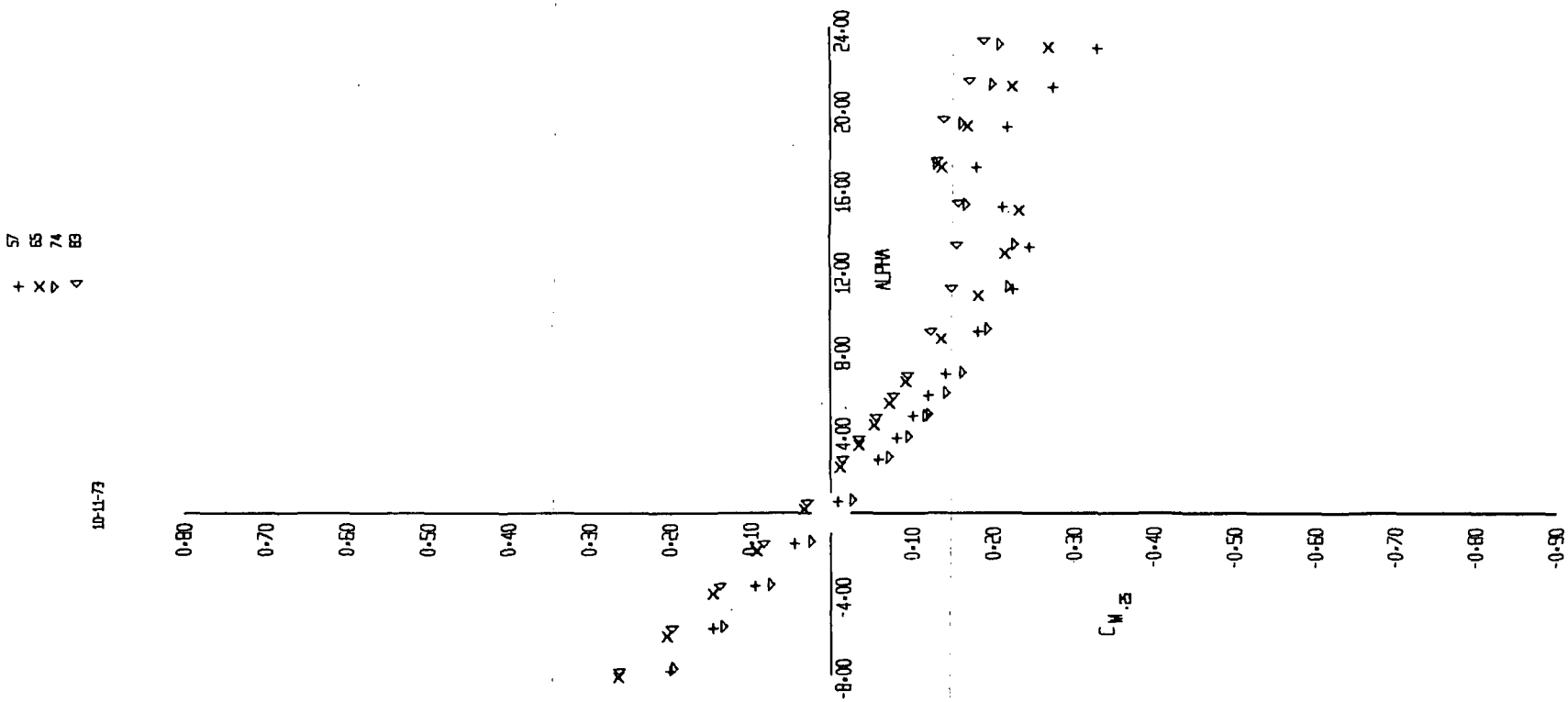

FIGURE 7 (SHEET 3)

LA-10H

SPOILER EFFECTIVENESS, ORBITER OR AND OFF

SYM	RUN	CONFIGURATION
+	57	S^{1} a^{10} Q^{13} f^{37} D^{8} b^{16} V^{9} H^{8} $e^{12,13}$ $r^{7,8}$ S_{60}^{22}
×	65	
▷	74	S^{1} a^{10} Q^{13} f^{37} $A_{0.5}^{5F}$ D^{8} b^{16} V^{9} H^{8} $e^{12,13}$ $r^{7,8}$ v^{1} S_{60}^{22}
◁	83	

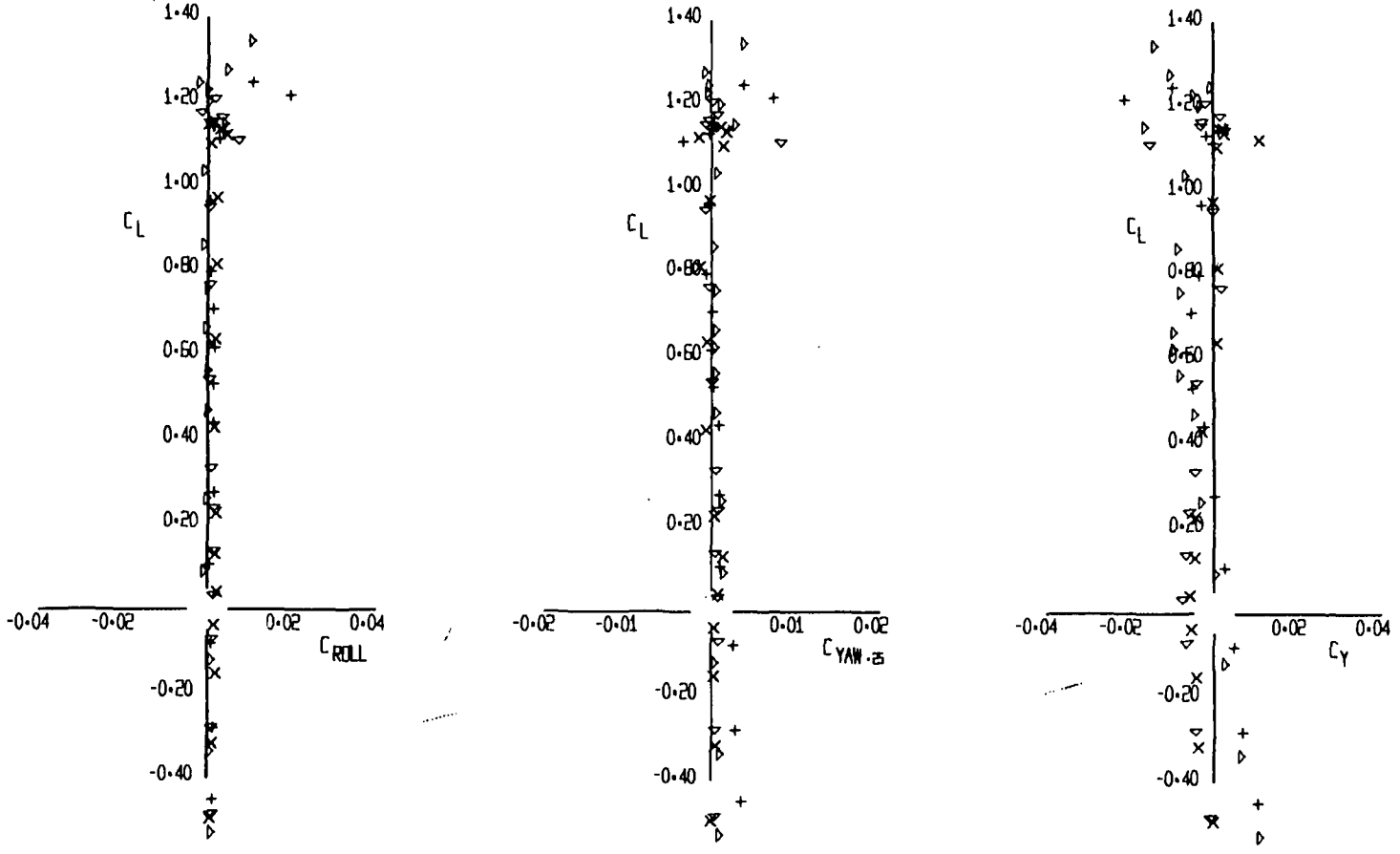

FIGURE 7 (SHEET 4)

EFFECT OF CENTER VERTICAL STABILIZER EXTENSION

LR-
LFL L-363

PAGE
FIG.

SYM	RUN	CONFIGURATION
+	57	S^{1} a^{10} Q^{13} f^{37} D^{8} b^{16} V^{9} H^{8} $e^{12,13}$ $r^{7,8}$
×	70	S^{1} a^{10} Q^{13} f^{37} $A^{5F}_{\sim 2.5}$ D^{8} b^{16} V^{9} H^{8} $e^{12,13}$ $r^{7,8}$
▷	72	v^{1}

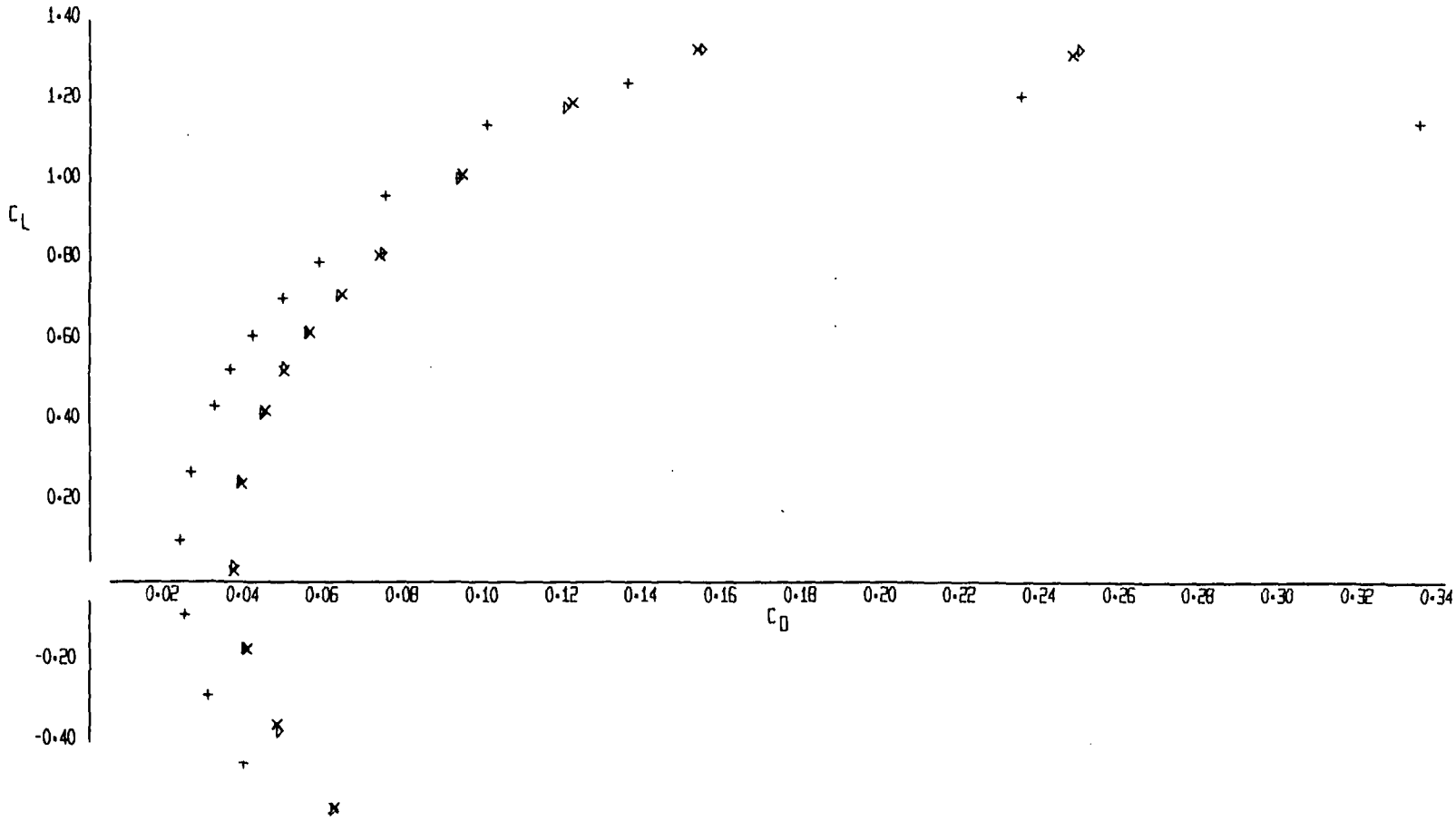

57 70 72
+ × ▷

10-12-73

Page A-63

LP-20F

FIGURE 8 (SHEET 1)

EFFECT OF CENTER VERTICAL STABILIZER EXTENSION

LR-
LFL L-363

PAGE
FIG.

SYM	RUN	CONFIGURATION
+	57	S^{1} a^{10} Q^{13} f^{37} D^{8} b^{16} V^{9} H^{8} $e^{12,13}$ $r^{7,8}$
×	70	S^{1} a^{10} Q^{13} f^{37} $\Delta_{5F}^{-1.5}$ D^{8} b^{16} V^{9} H^{8} $e^{12,13}$ $r^{7,8}$
▷	72	v^{1}

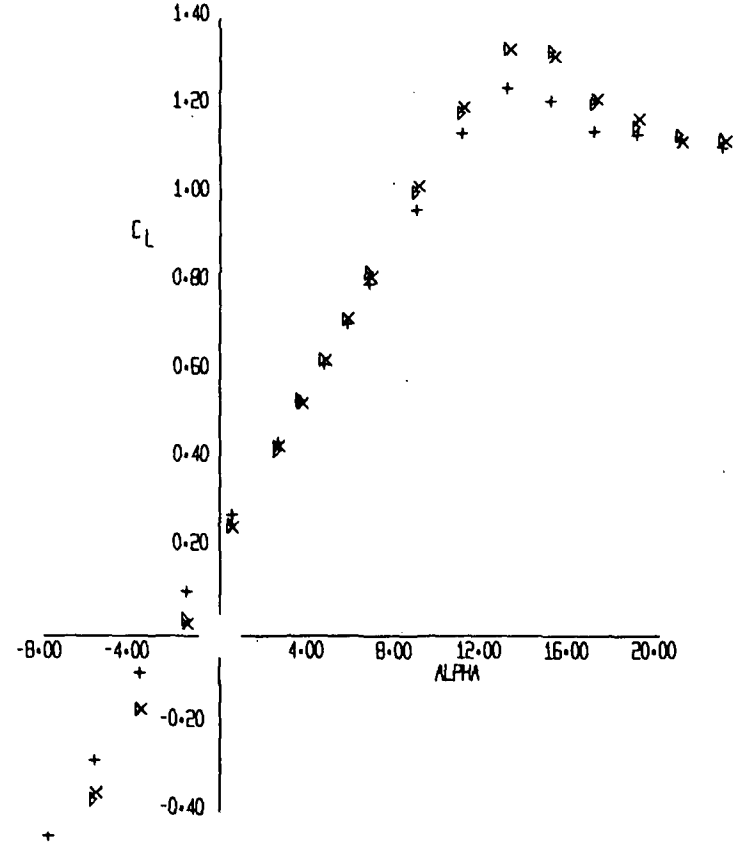

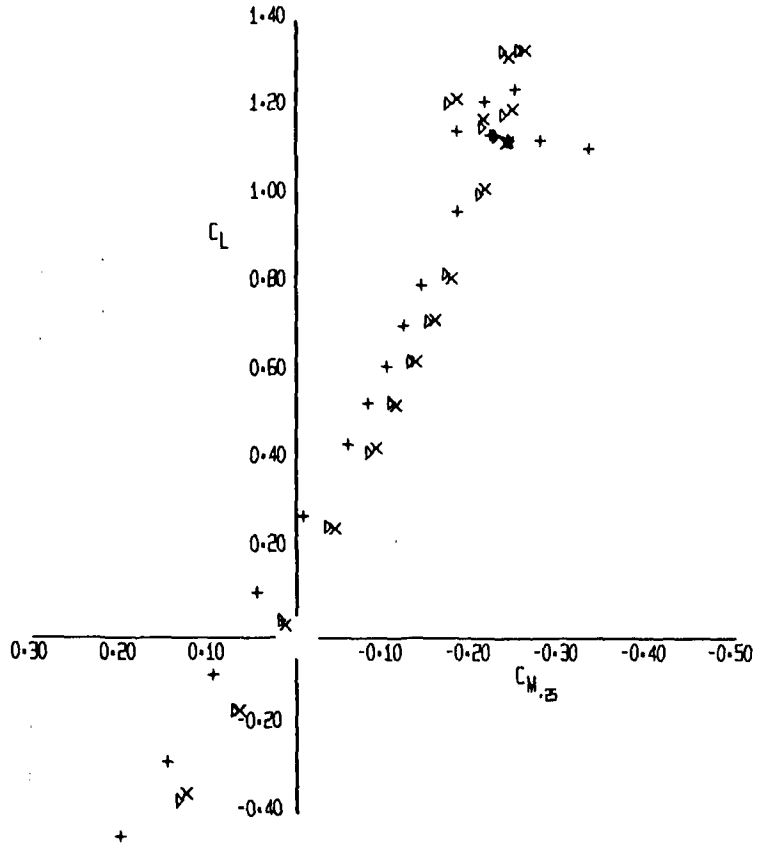

57 70 72
+ × ▷

10-12-73

LP-18E

FIGURE 8 (SHEET 2)

EFFECT OF CENTER VERTICAL STABILIZER EXTENSION

SYM	RUN	CONFIGURATION
+	57	$S^{1}\ a^{10}\ Q^{13}\ f^{37}\ D^{8}\ b^{16}\ v^{9}\ H^{8}\ e^{12,13}\ r^{7,8}$
×	70	$S^{1}\ a^{10}\ Q^{13}\ f^{37}\ A^{5F}_{-1.5}\ D^{8}\ b^{16}\ v^{9}\ H^{8}\ e^{12,13}\ r^{7,8}$
▷	72	v^{1}

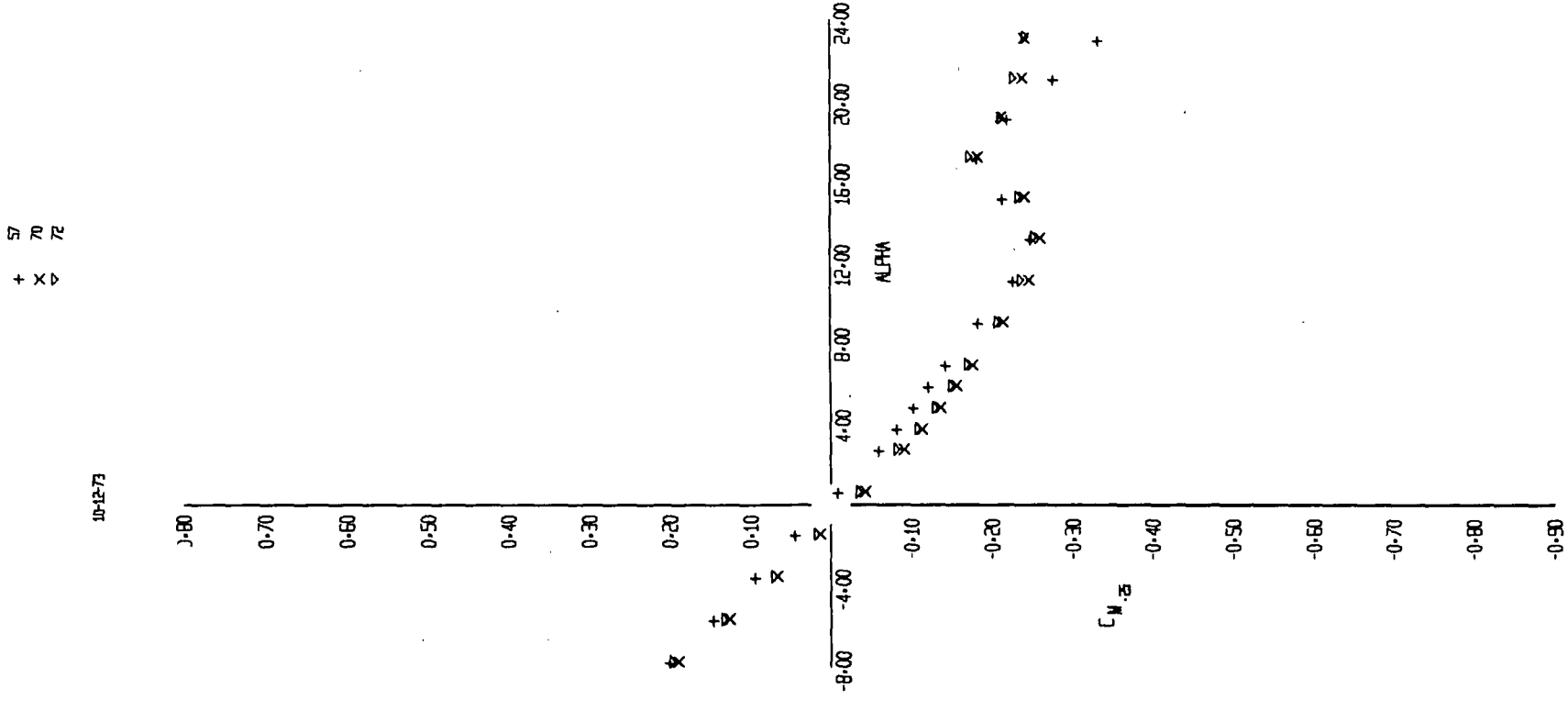

FIGURE 8 (SHEET 3)

EFFECT OF CENTER VERTICAL STABILIZER EXTENSION

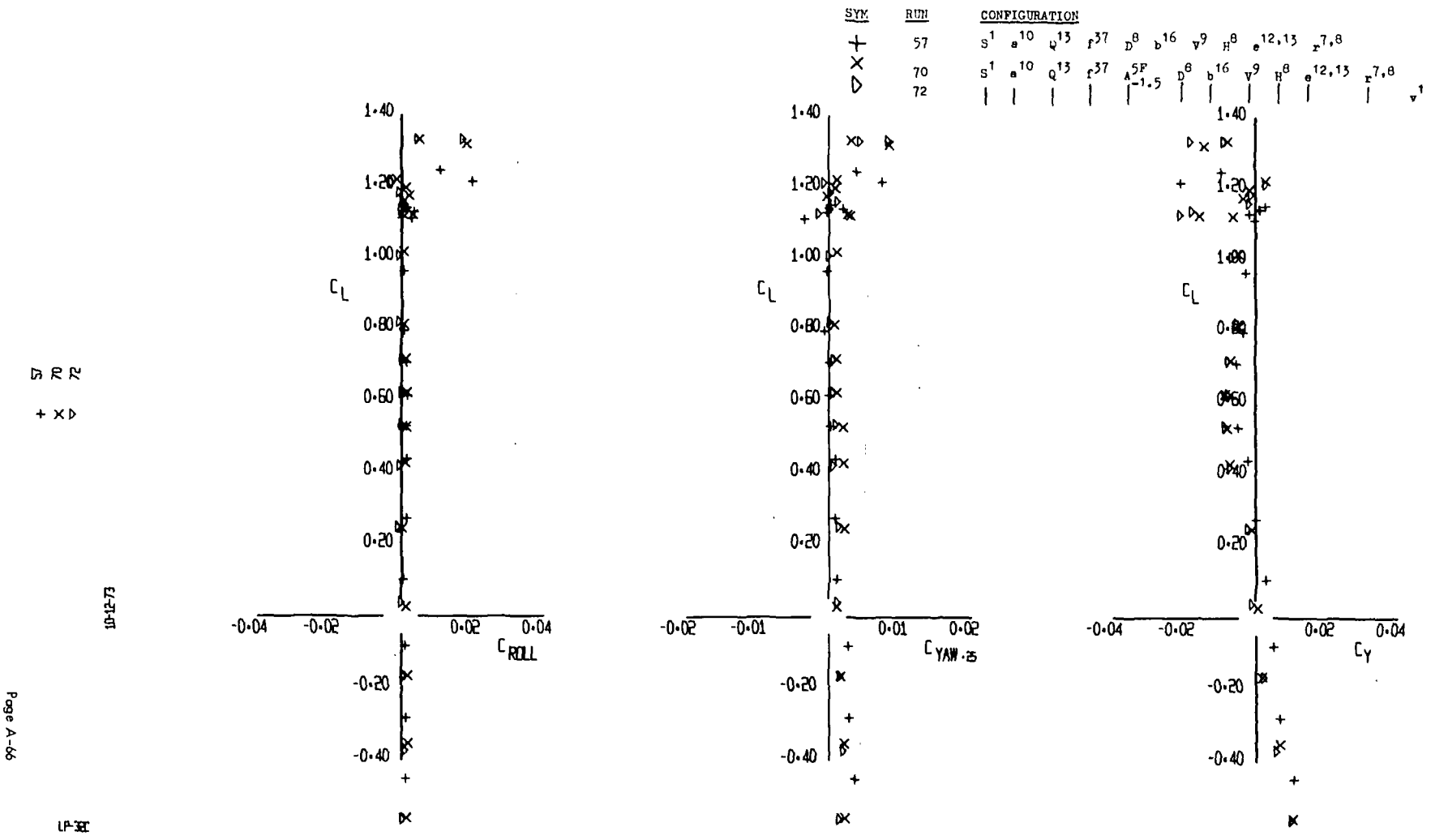

FIGURE 8 (SHEET 4)

EFFECT OF ORBITER INCIDENCE

SYM	RUN	CONFIGURATION
+	74	S^{1} a^{10} Q^{13} f^{37} $A^{5F}_{0.5}$ D^{8} b^{16} V^{9} H^{8} $e^{12,13}$ $r^{7,8}$
×	72	$A^{5F}_{21.5}$

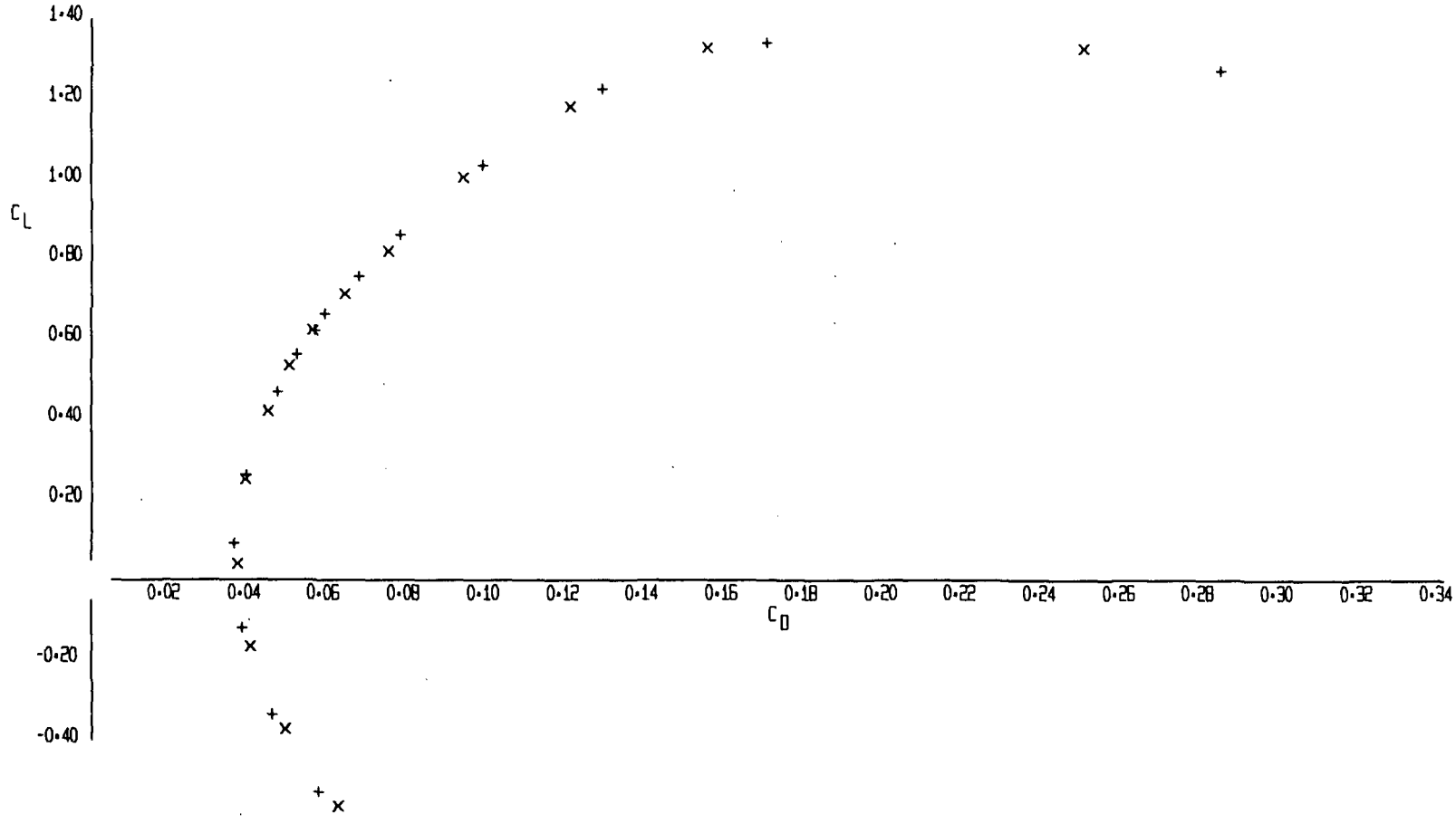

74
72

10-12-73

Page A-67

LR-20F

FIGURE 9 (SHEET 1)

EFFECT OF ORBITER INCIDENCE

SYM	RUN	CONFIGURATION
+	74	S^{1} a^{10} Q^{13} f^{37} $A^{5F}_{0.5}$ D^{8} b^{16} V^{9} H^{8} $e^{12,13}$ $r^{7,8}$ v^{1}
×	72	$A^{5F}_{-1.5}$

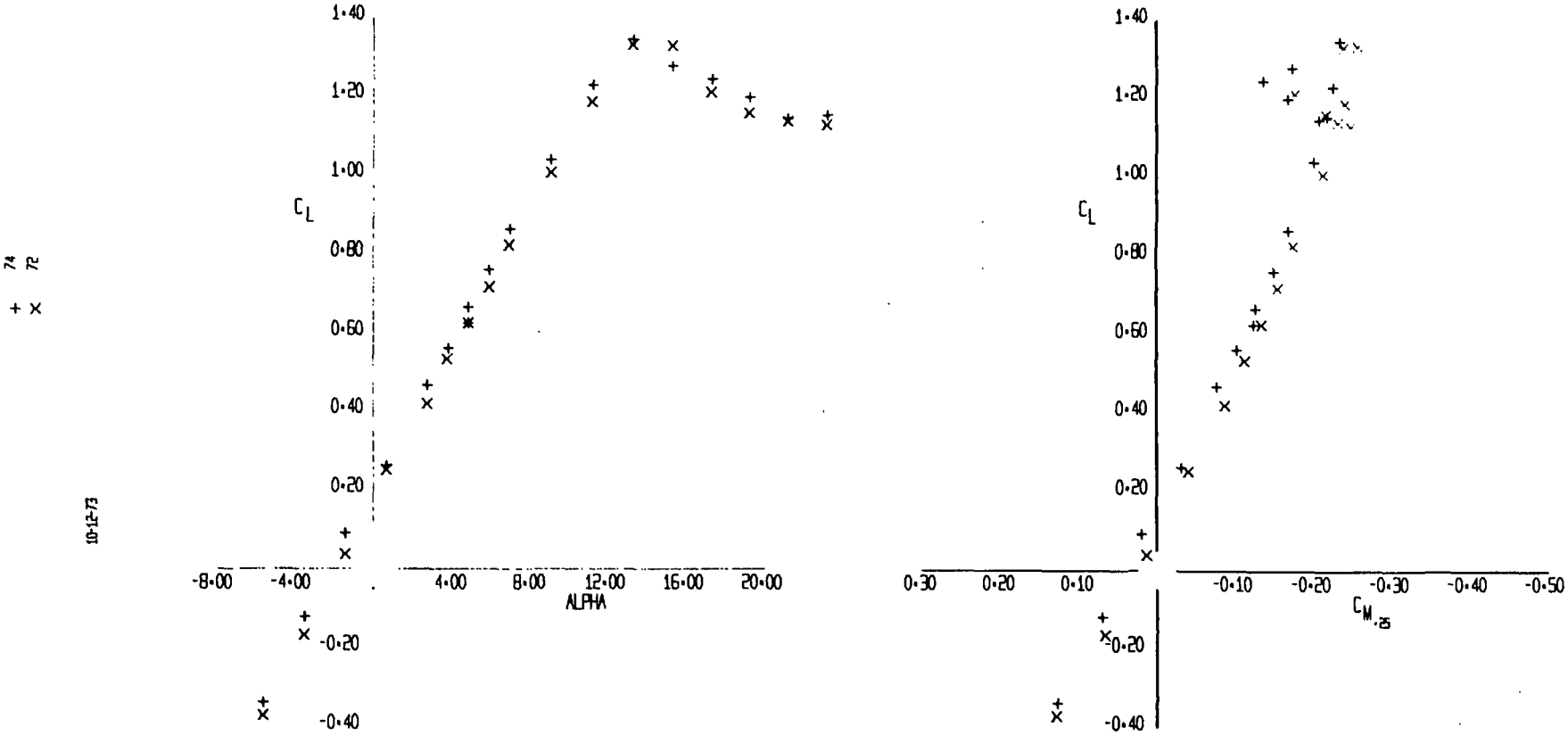

74 72

10-12-73

Page A-68

LR-18E

FIGURE 9 (SHEET 2)

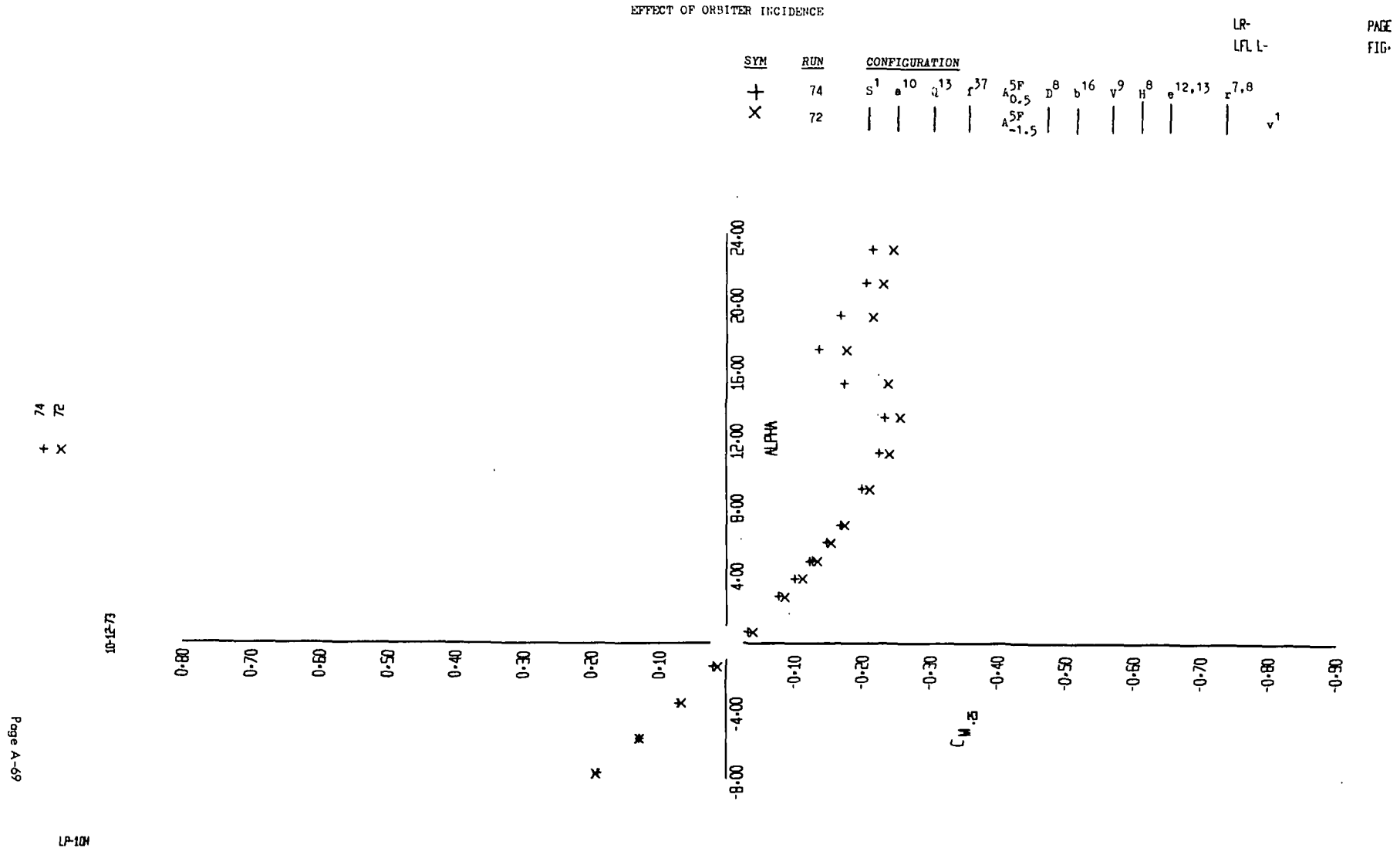

FIGURE 9 (SHEET 3)

EFFECT OF ORBITER INCIDENCE

LR-
LFL L-363

PAGE
FIG.

SYM	RUN	CONFIGURATION
+	74	S^{1} ϵ^{10} ζ^{13} f^{37} $A^{5F}_{0.5}$ D^{8} b^{16} V^{9} H^{8} $e^{12,13}$ $r^{7,8}$
×	72	$A^{5F}_{-1.5}$ v^{1}

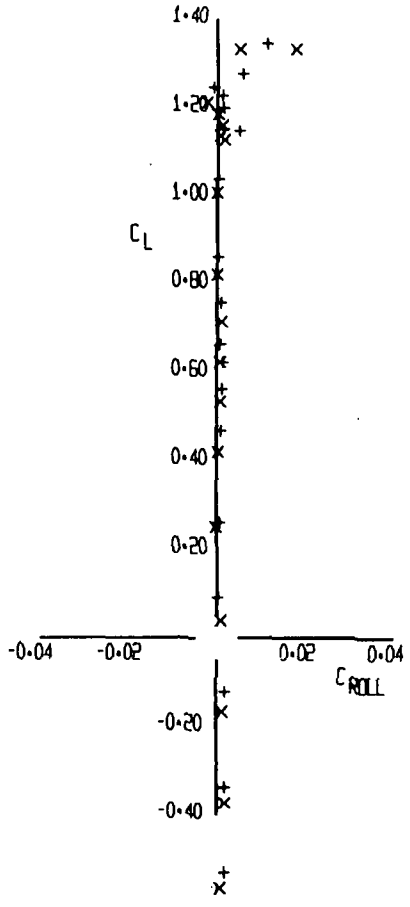

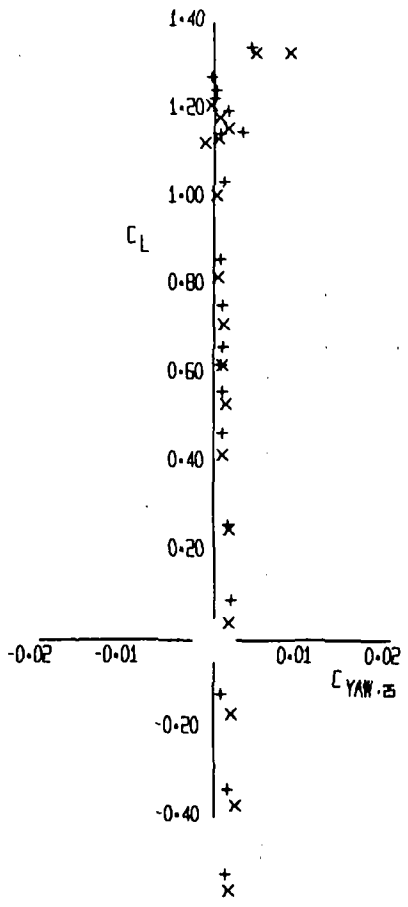

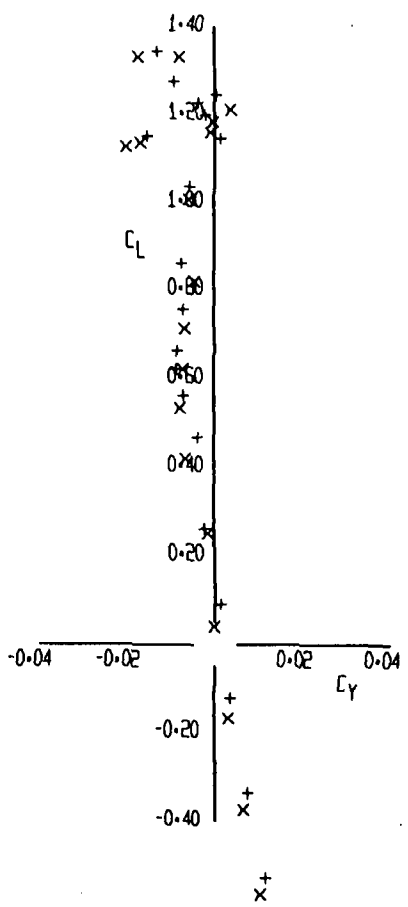

74
72

10-12-73

LP-38E

Page A-70

FIGURE 9 (SHEET 4)

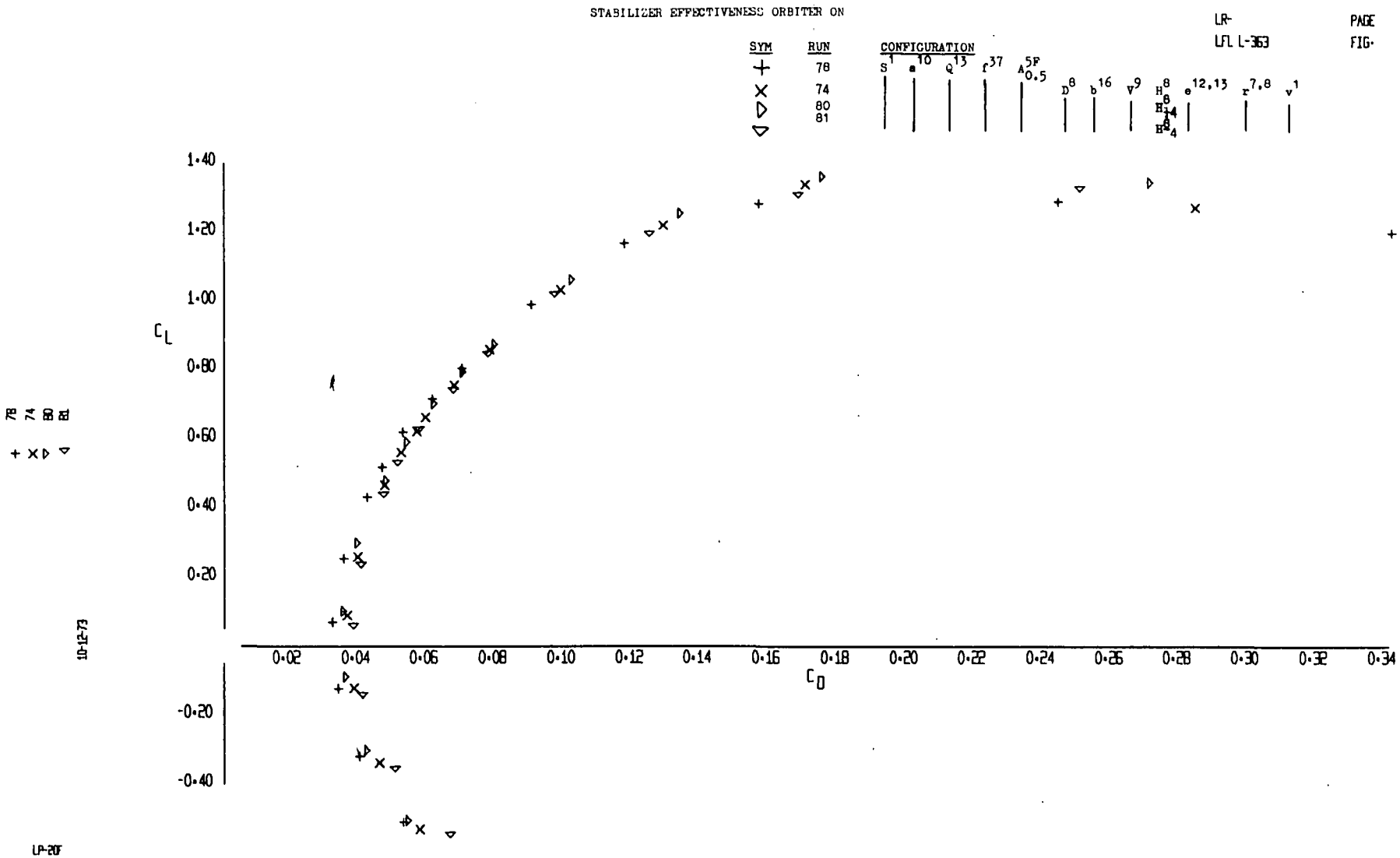

FIGURE 10 (SHEET 1)

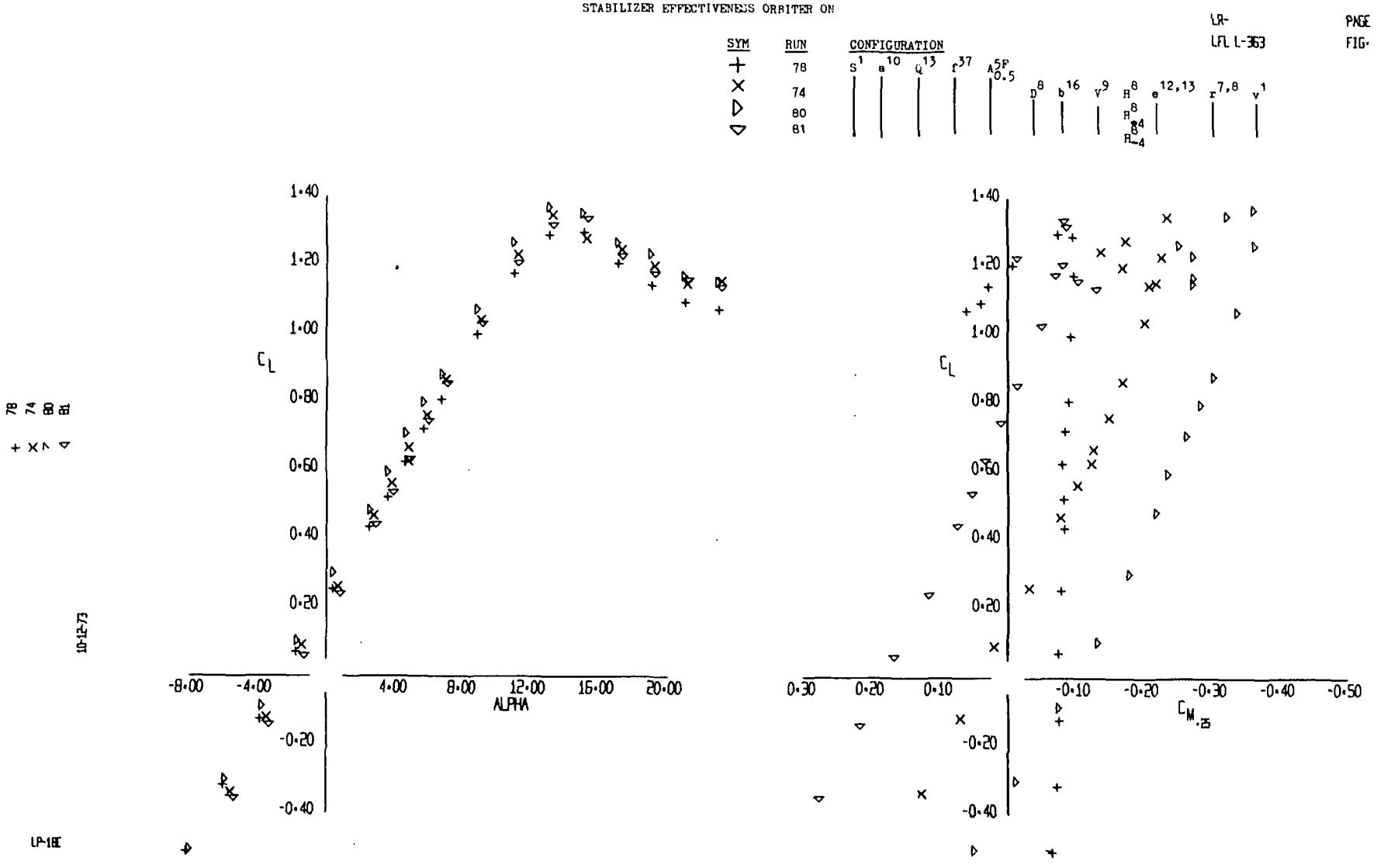

FIGURE 10 (SHEET 2)

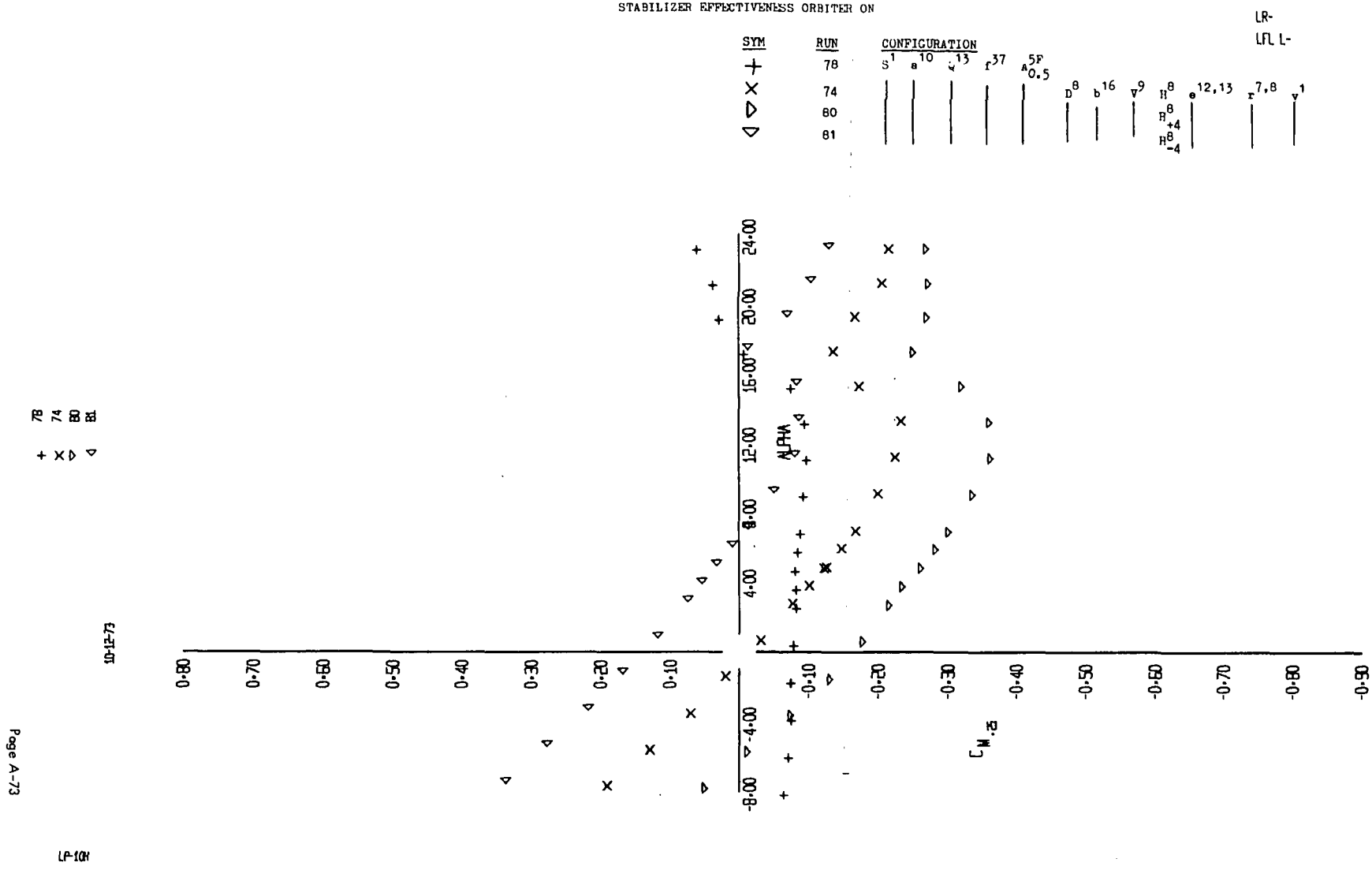

FIGURE 10 (SHEET 3)

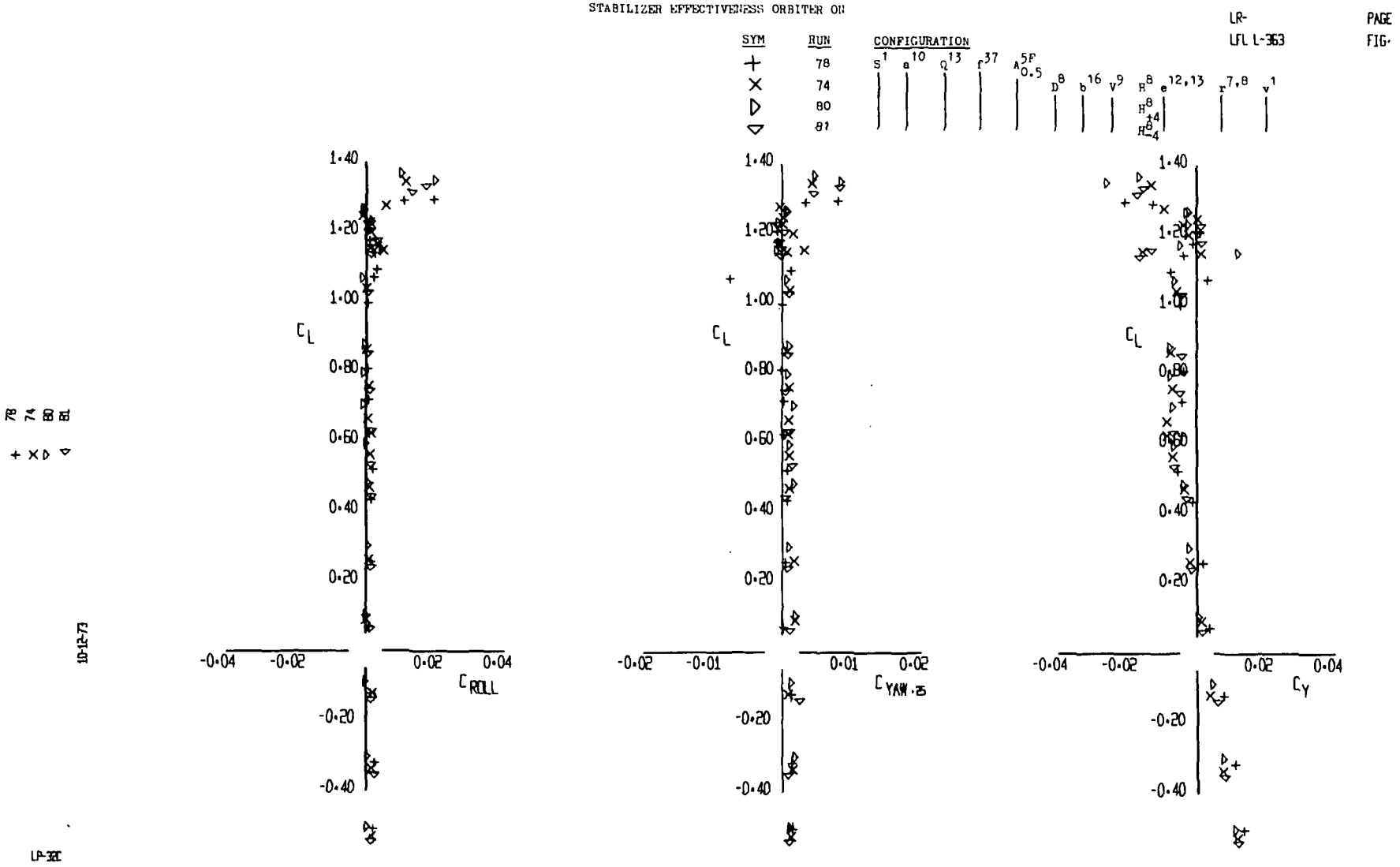

FIGURE 10 (SHEET 4)

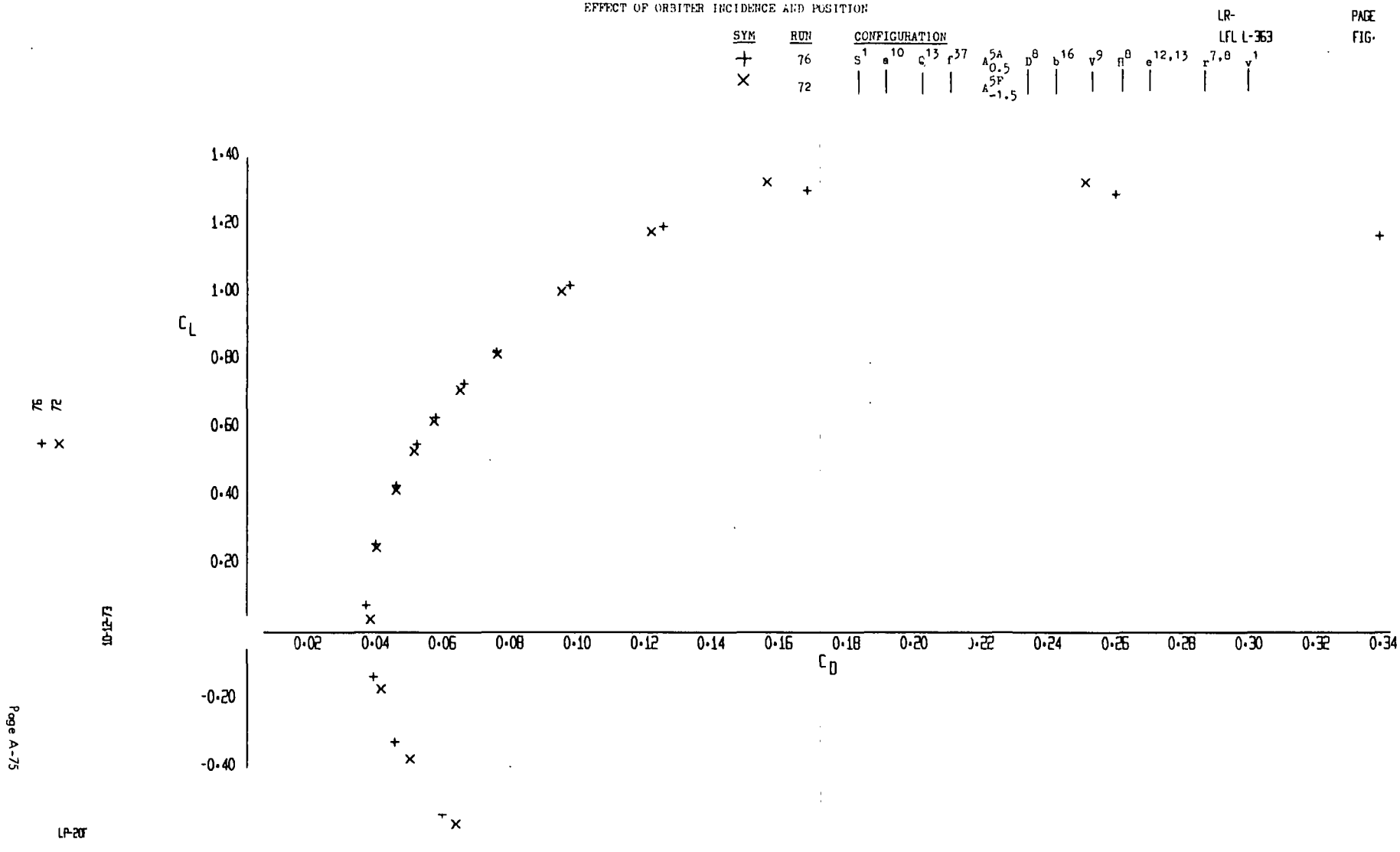

FIGURE 11 (SHEET 1)

SYM	RUN	CONFIGURATION
+	76	S^{1} a^{10} Q^{13} f^{37} $A^{5A}_{0.5}$ $A^{5F}_{-1.5}$ D^{8} b^{16} V^{9} H^{8} $e^{12,13}$ $r^{7,8}$ v^{1}
×	72	

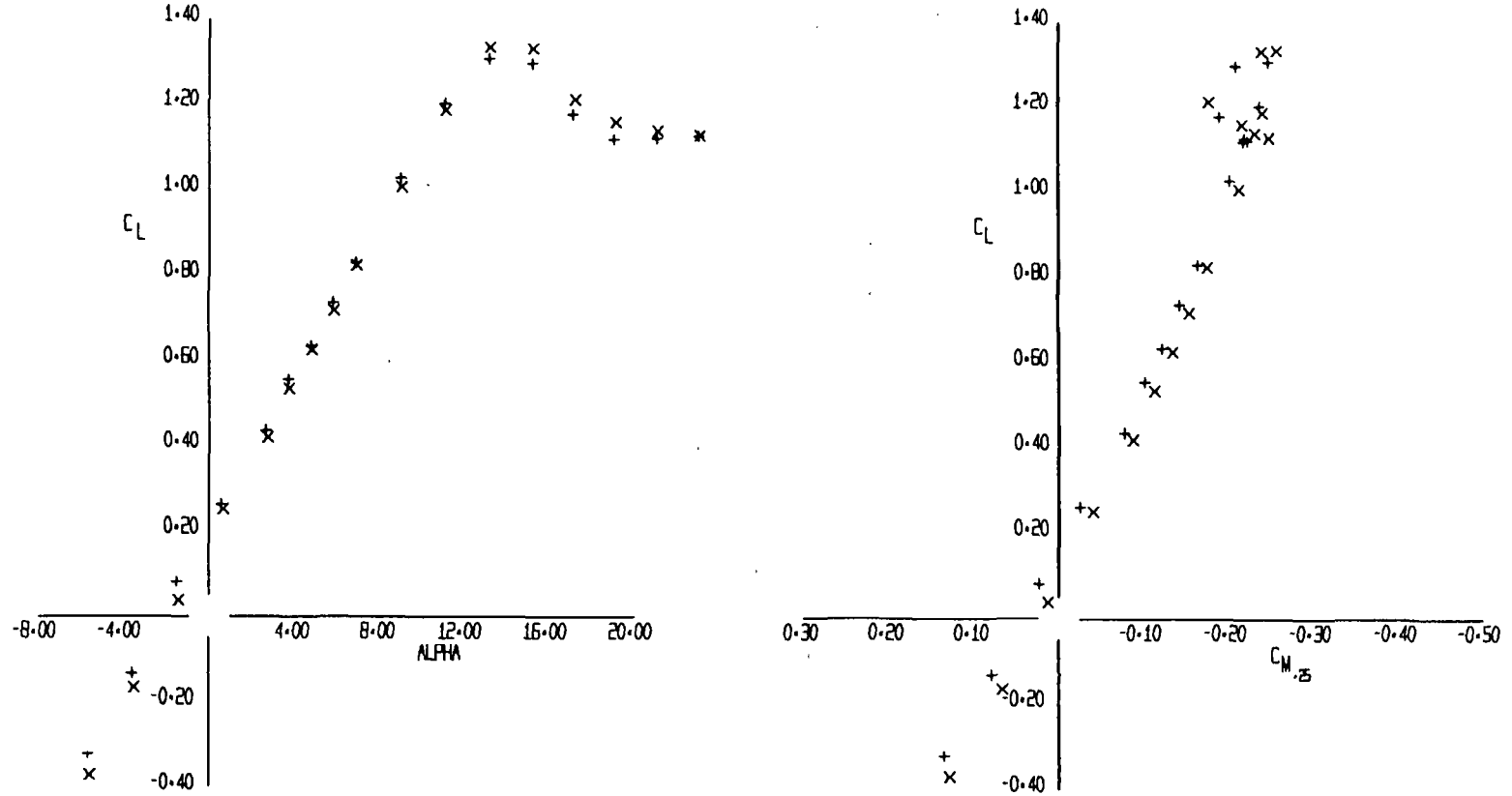

76 72

10-12-73

Page A-76

LP-18E

FIGURE 11 (SHEET 2)

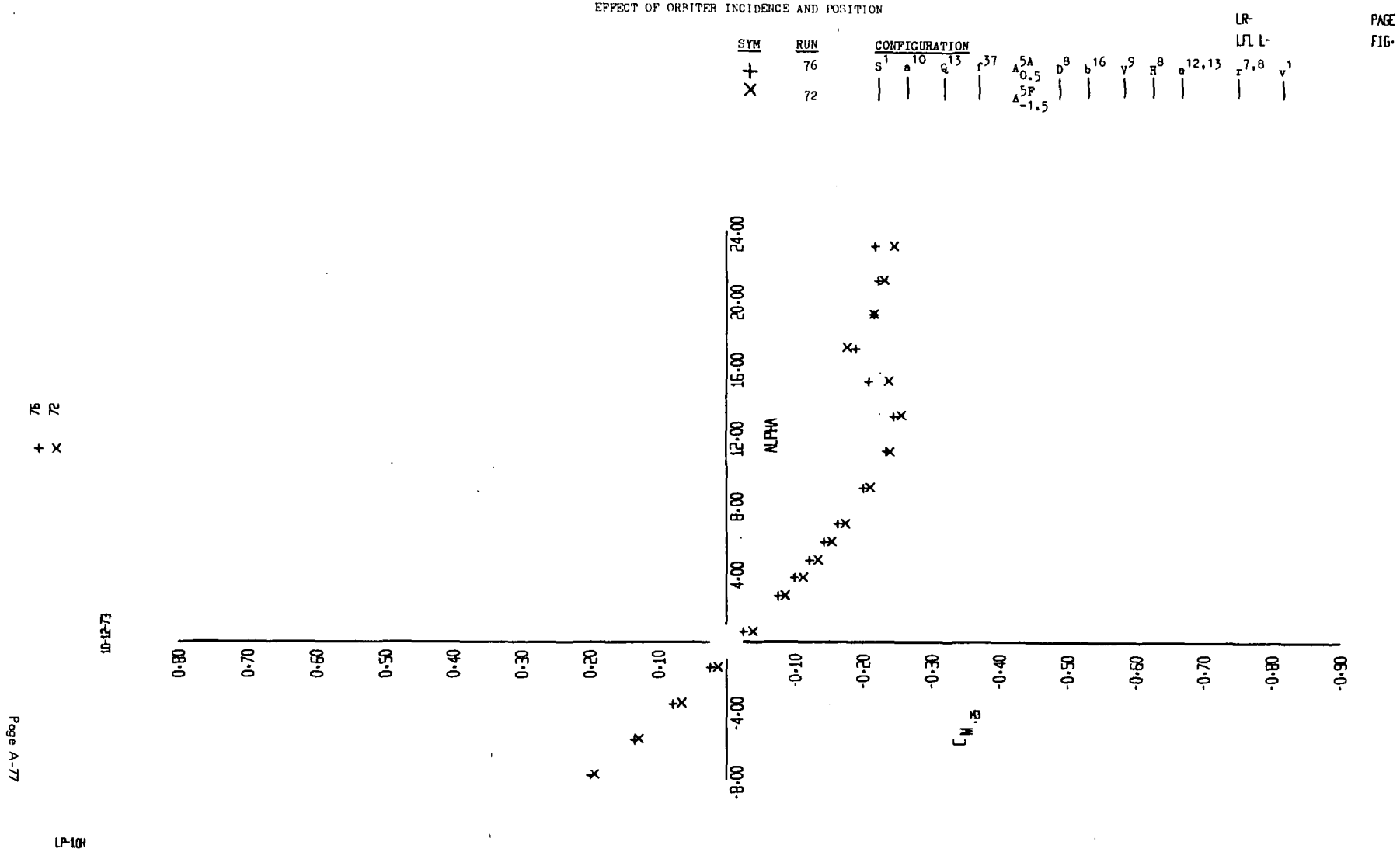

FIGURE 11 (SHEET 3)

EFFECT OF ORBITER INCIDENCE AND POSITION

LR-
LFL L-363

PAGE
FIG.

SYM	RUN	CONFIGURATION
+	76	S^{1} a^{10} Q^{13} f^{37} $A^{5A}_{0.5}$ $A^{5F}_{-1.5}$ D^{8} b^{16} V^{9} H^{8} $e^{12,13}$ $r^{7,8}$ v^{1}
×	72	

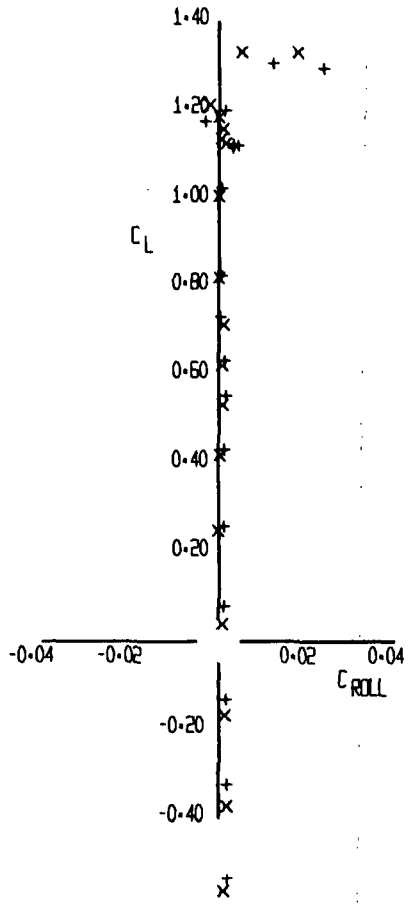

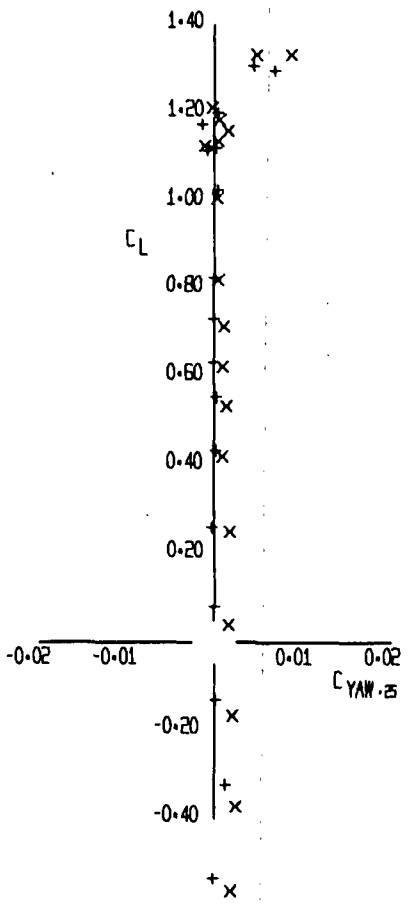

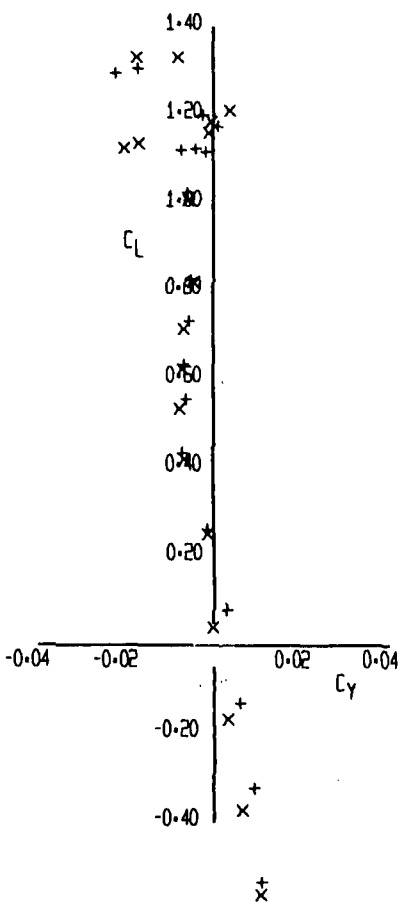

FIGURE 11 (SHEET 4)

76 72
+ ×

10-12-73

Page A-78

LR-361

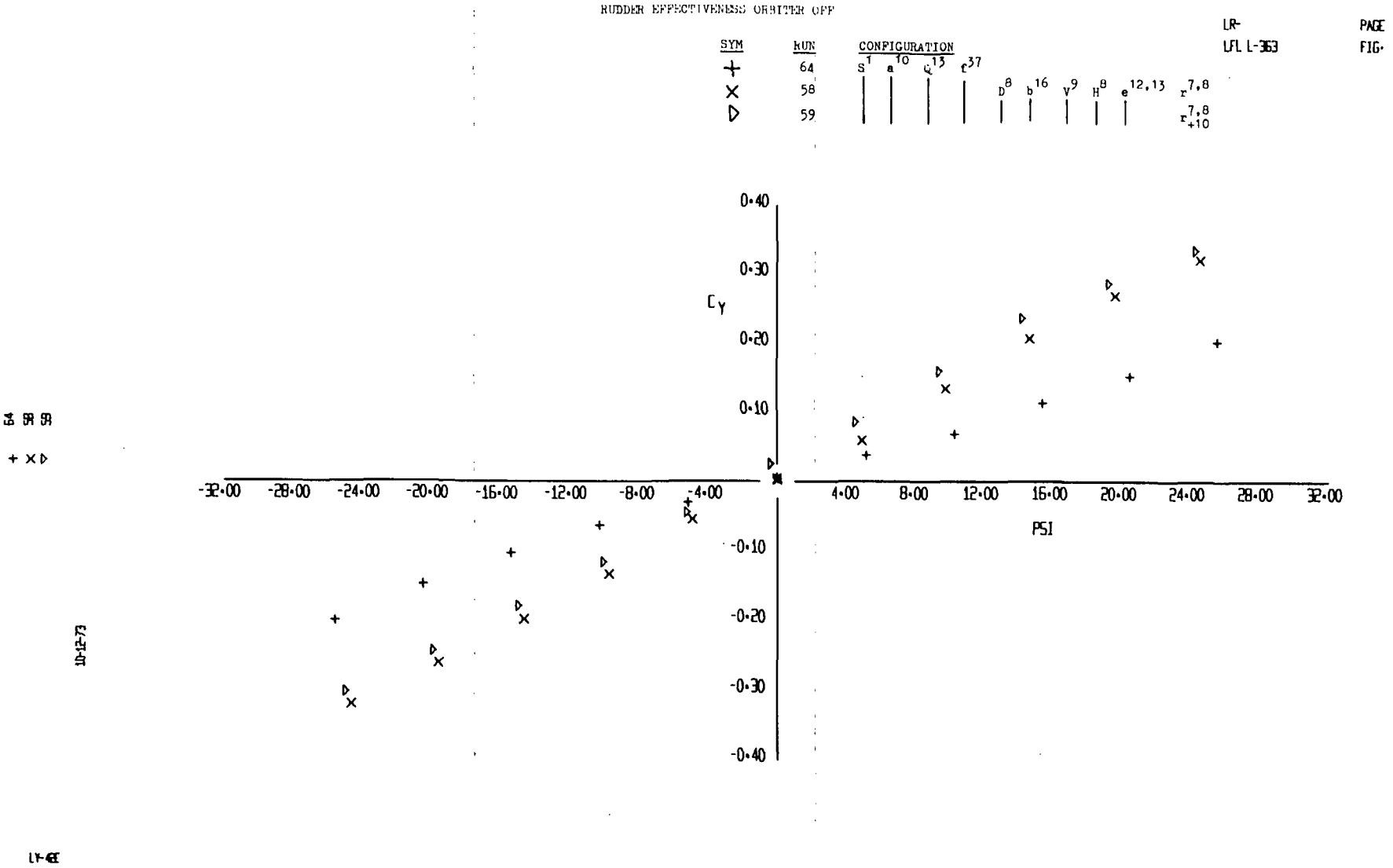

FIGURE 12 (SHEET 1)

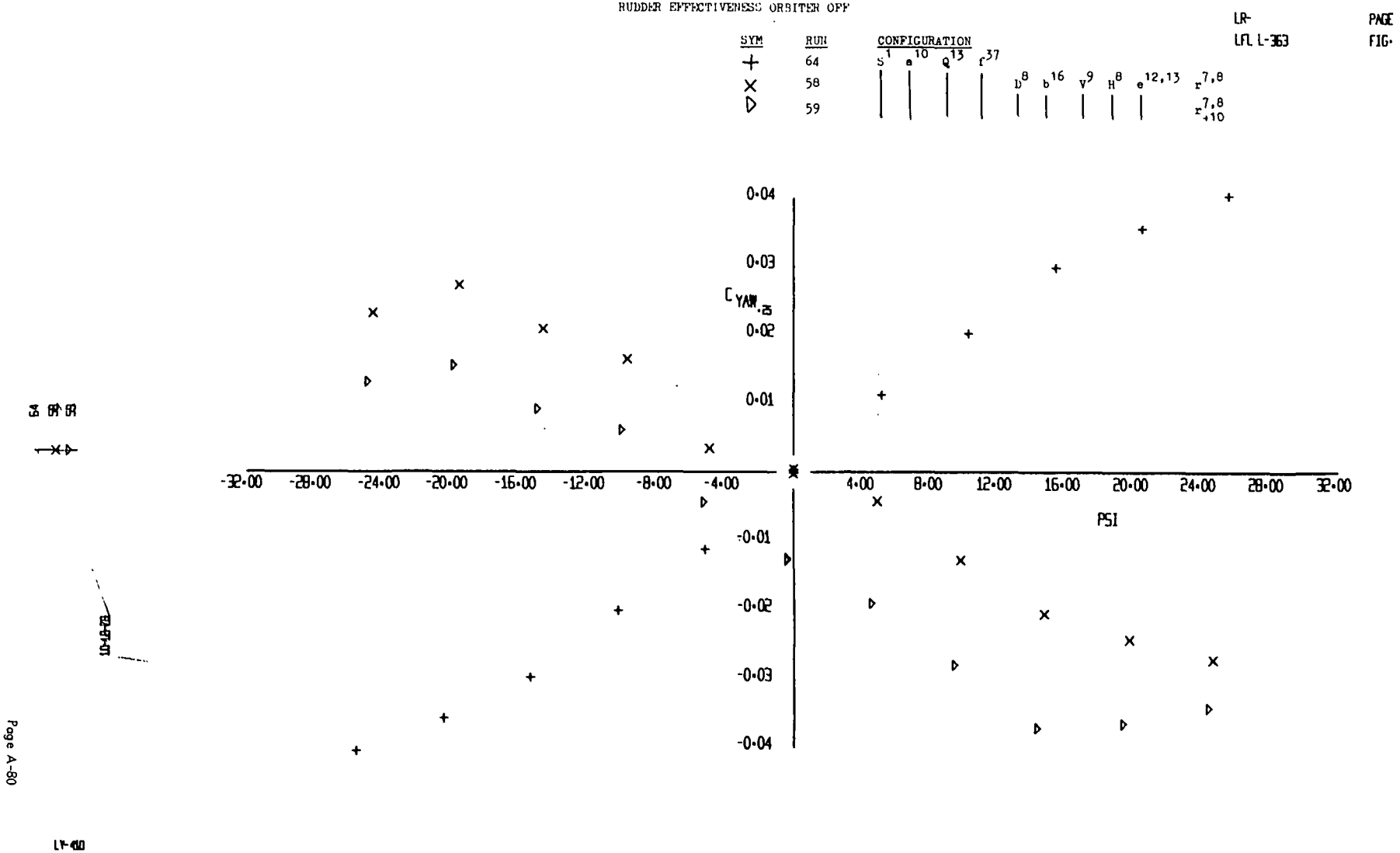

FIGURE 12 (SHEET 2)

RUDDER EFFECTIVENESS ORBITER OFF

SYM	RUN	CONFIGURATION
+	64	S^{1} a^{10} c^{13} f^{37} D^{8} b^{16} V^{9} H^{8} $e^{12,13}$ $r^{7,8}$
×	58	
▷	59	$r^{7,8}_{+10}$

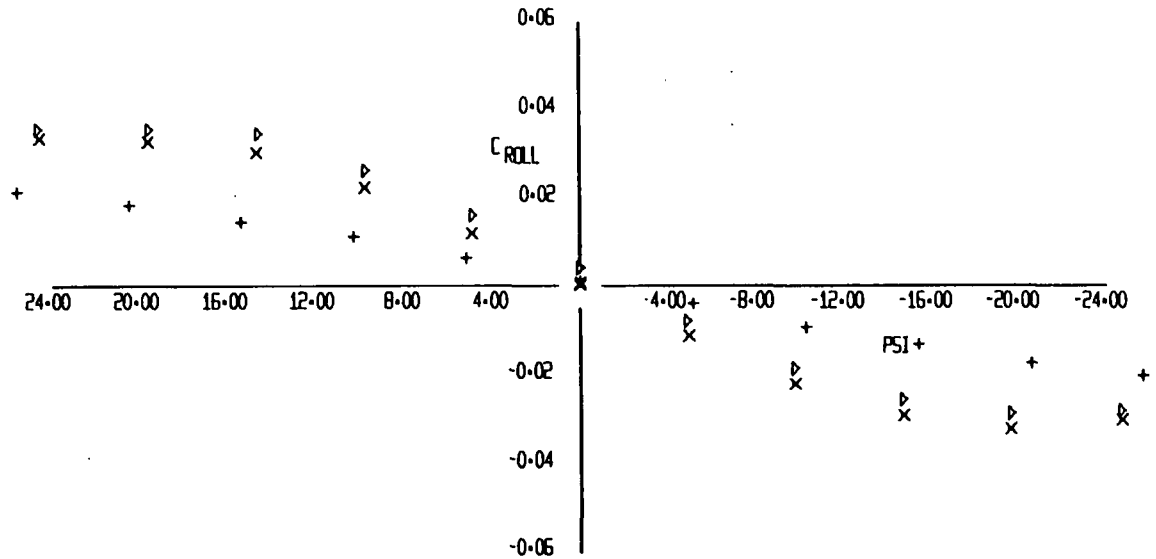

FIGURE 12 (SHEET 3)

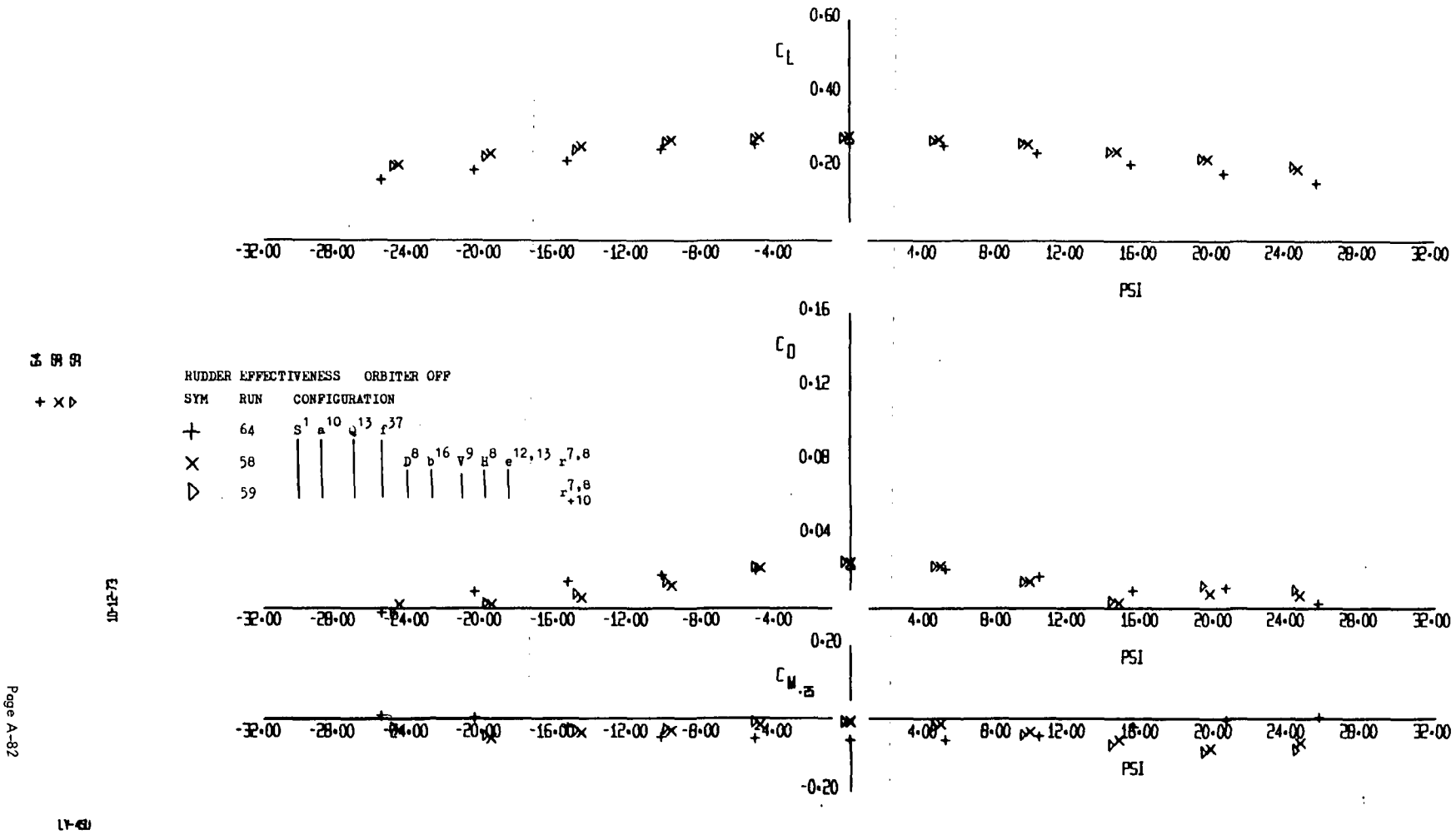

FIGURE 12 (SHEET 4)

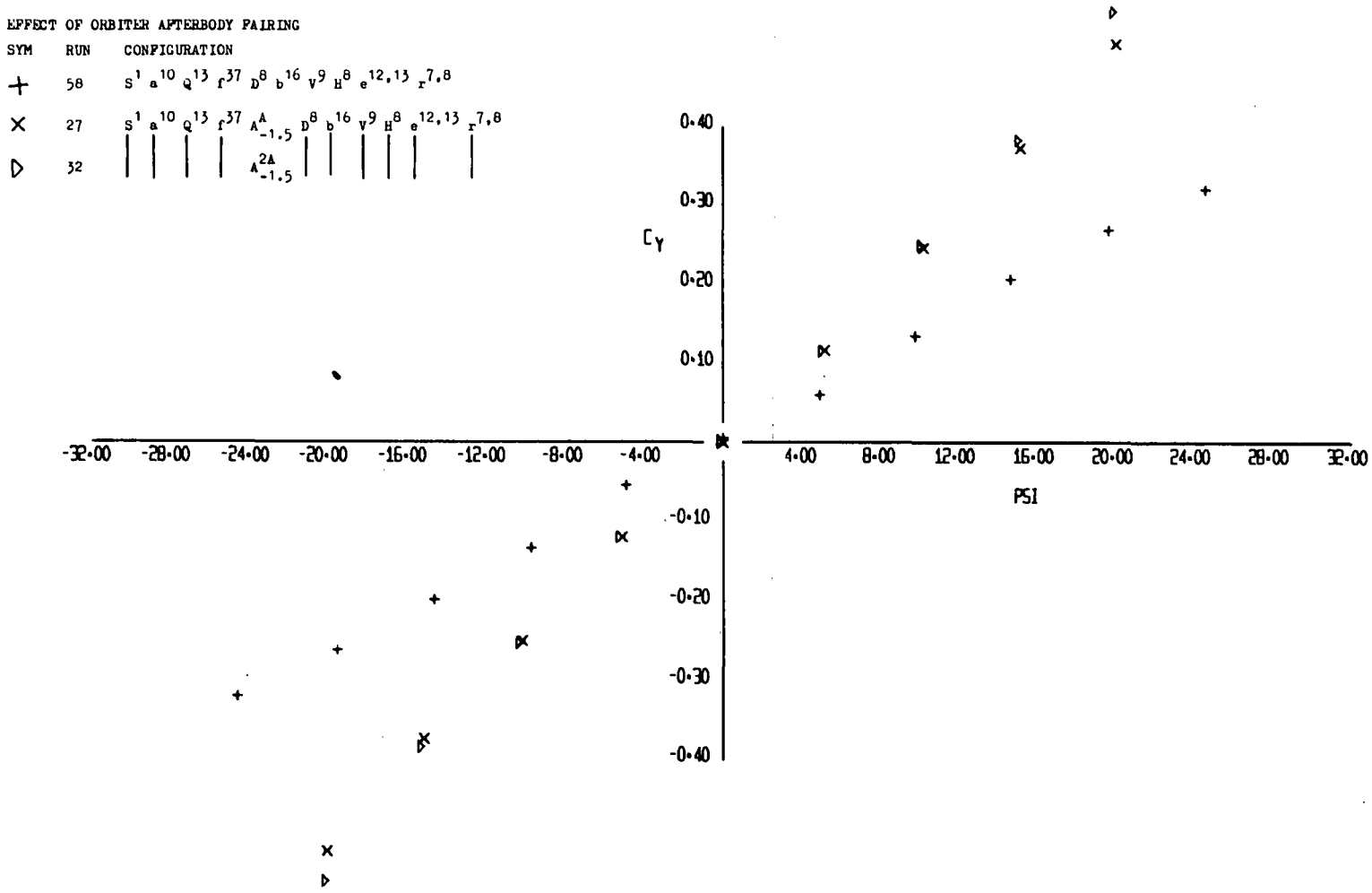

FIGURE 13 (SHEET 1)

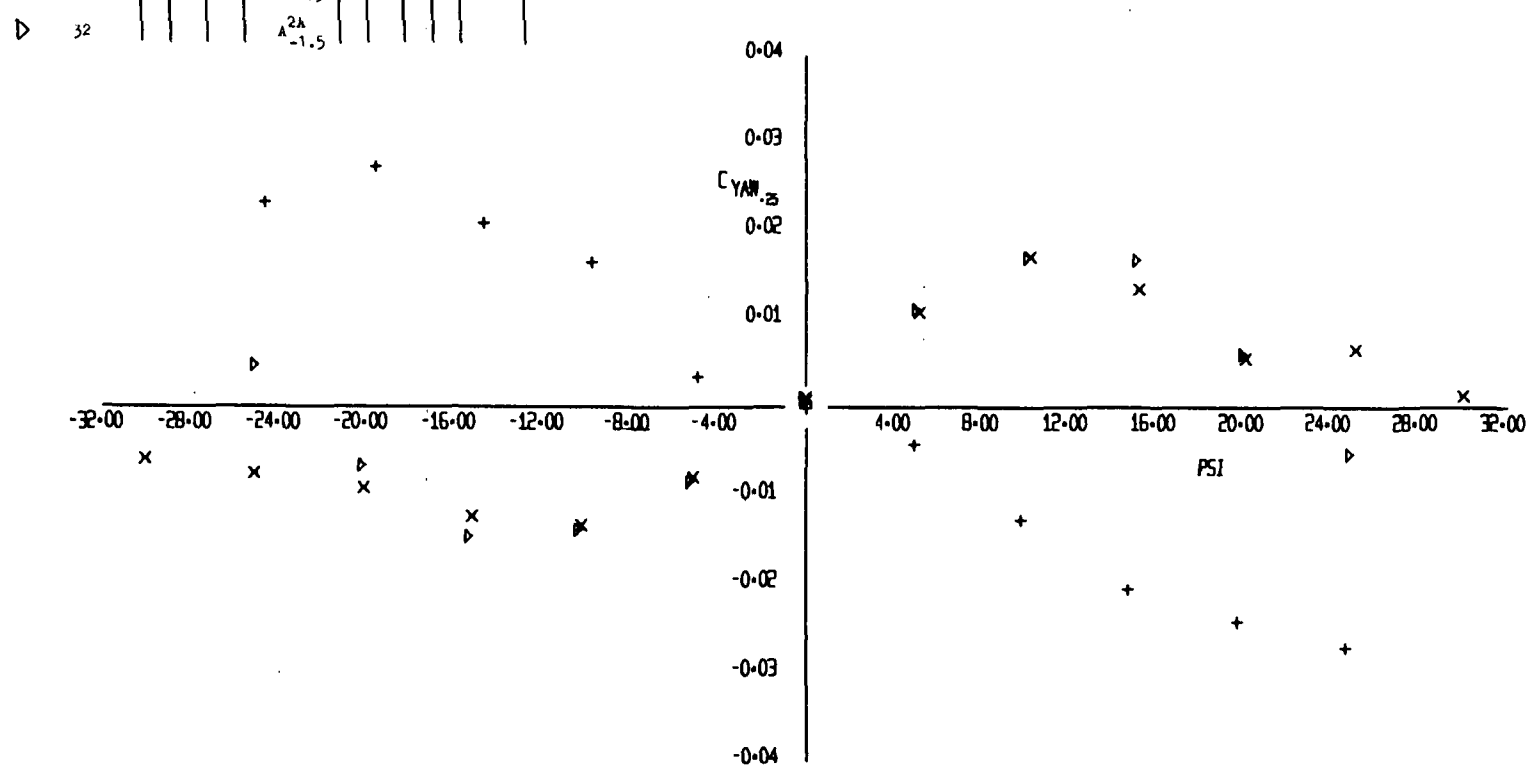

FIGURE 13 (SHEET 2)

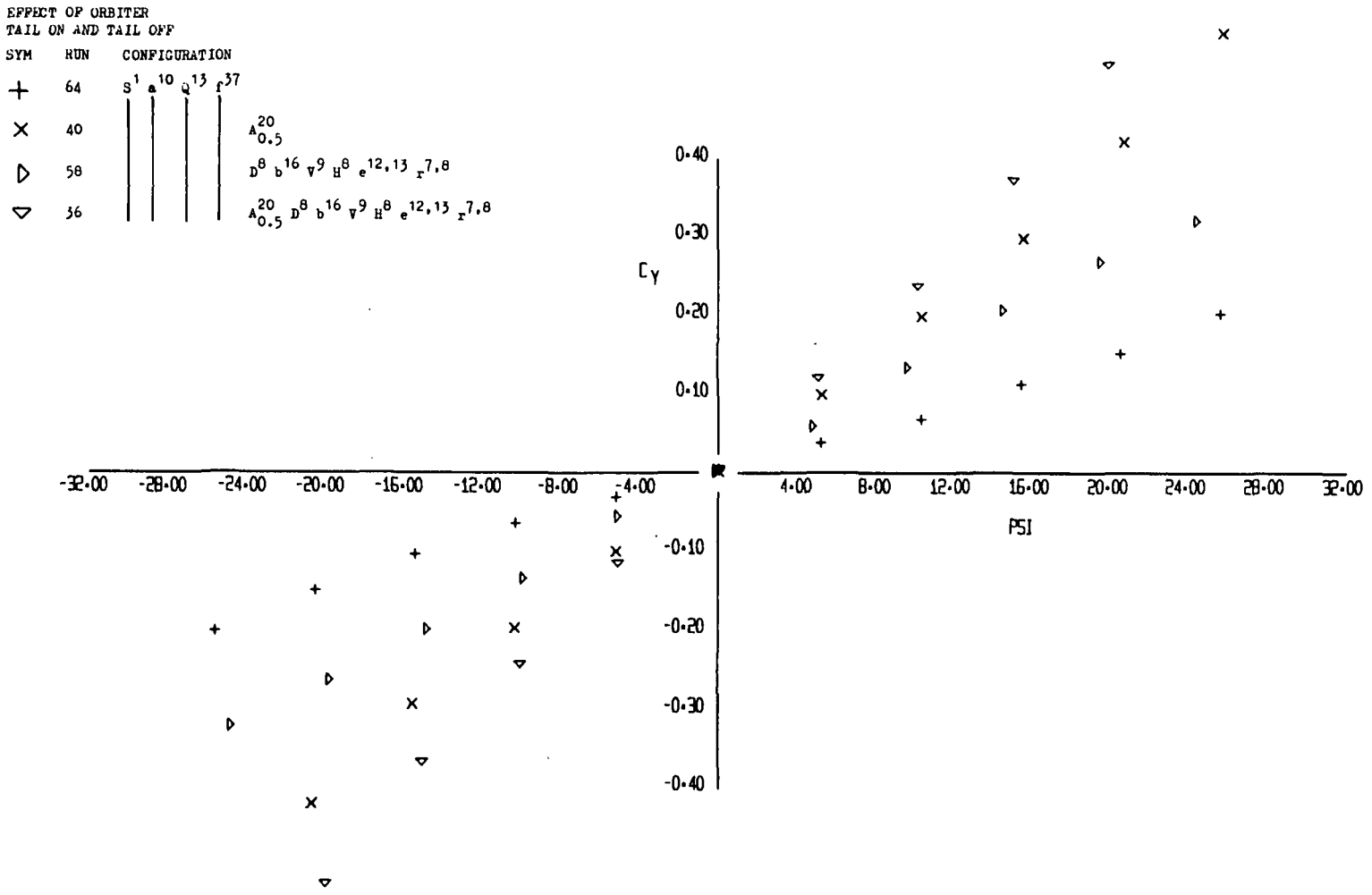

FIGURE 14 (SHEET 1)

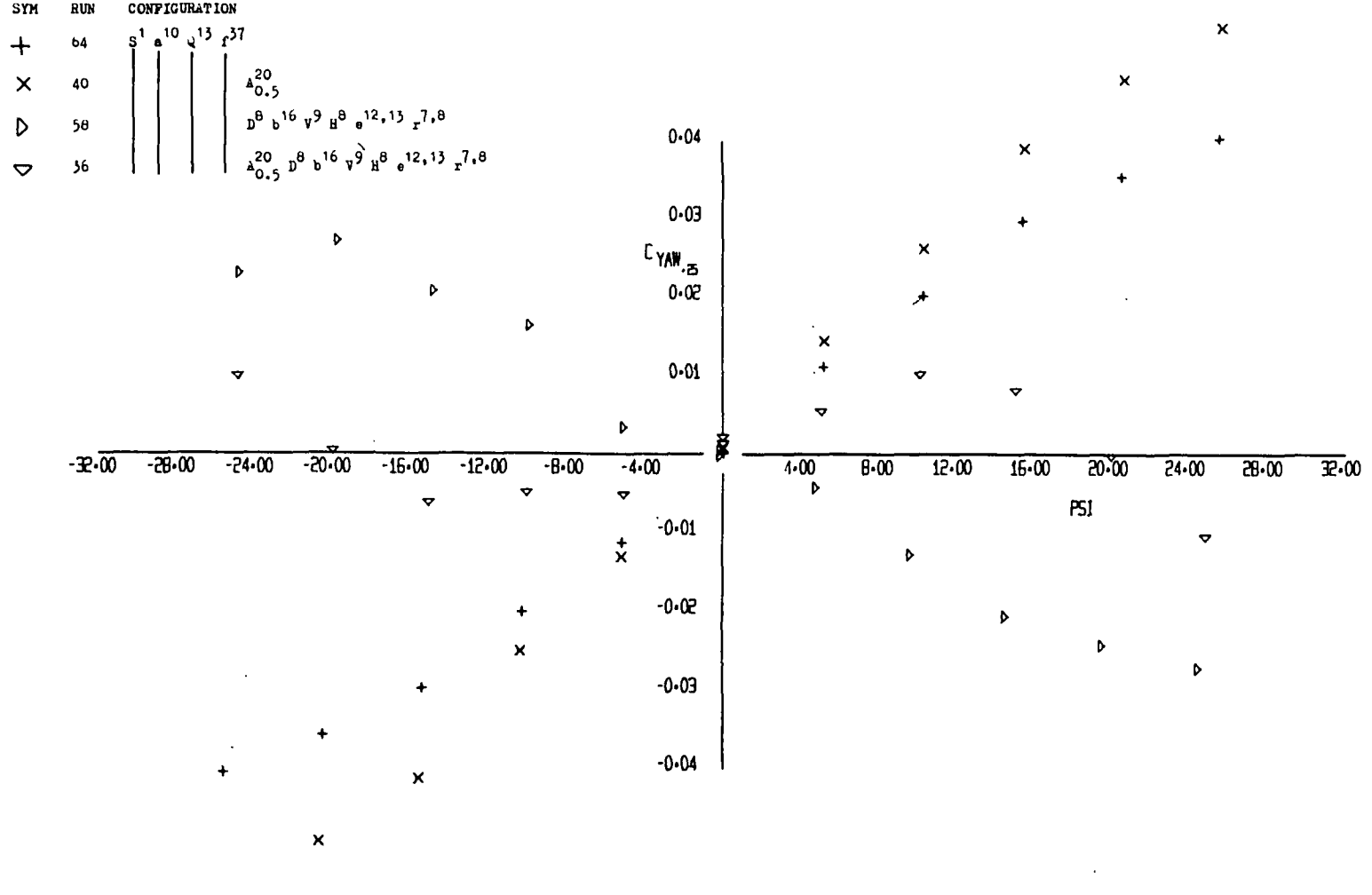

FIGURE 14 (SHEET 2)

EFFECT OF ORBITER
TAIL ON AND TAIL OFF

SYM	RUN	CONFIGURATION
+	64	$S^{1}\ a^{10}\ \_^{13}\ f^{37}$
×	40	$A^{20}_{0.5}$
▷	58	$D^{8}\ b^{16}\ v^{9}\ H^{8}\ e^{12,13}\ r^{7,8}$
▽	36	$A^{20}_{0.5}\ D^{8}\ b^{16}\ v^{9}\ H^{8}\ e^{12,13}\ r^{7,8}$

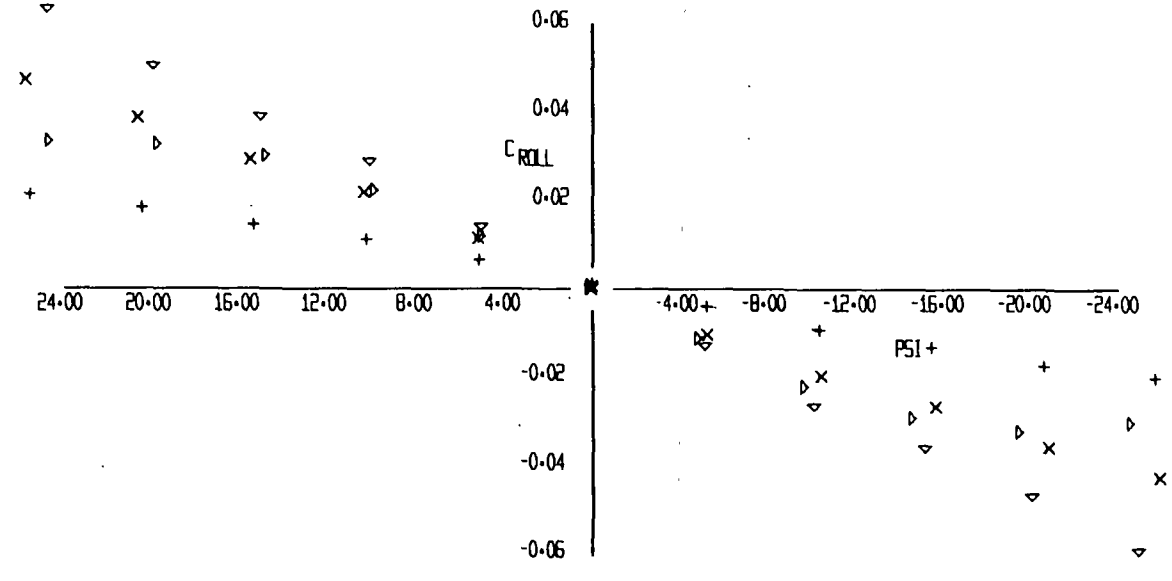

10-12-73

Page A-87

LF-408

FIGURE 14 (SHEET 3)

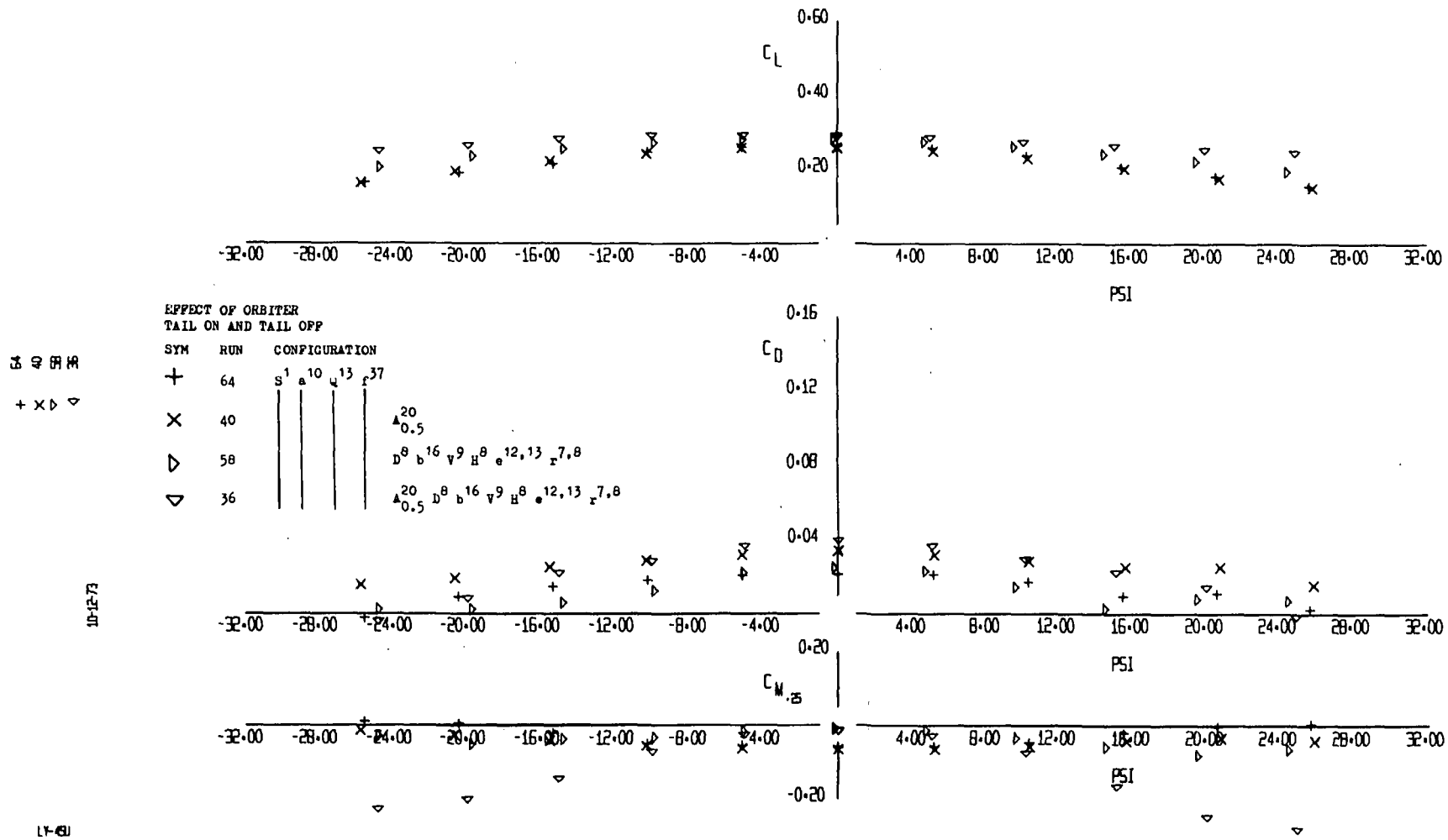

FIGURE 14 (SHEET 4)

EFFECT OF ORBITER
TAIL ON AND TAIL OFF

SYM	RUN	CONFIGURATION
+	64	$S^{1}\ a^{10}\ Q^{13}\ f^{37}$
×	40	$A^{20}_{0.5}$
▷	58	$D^{8}\ b^{16}\ v^{9}\ H^{8}\ e^{12,13}\ r^{7,8}$
▽	36	$A^{20}_{0.5}\ D^{8}\ b^{16}\ v^{9}\ H^{8}\ e^{12,13}\ r^{7,8}$

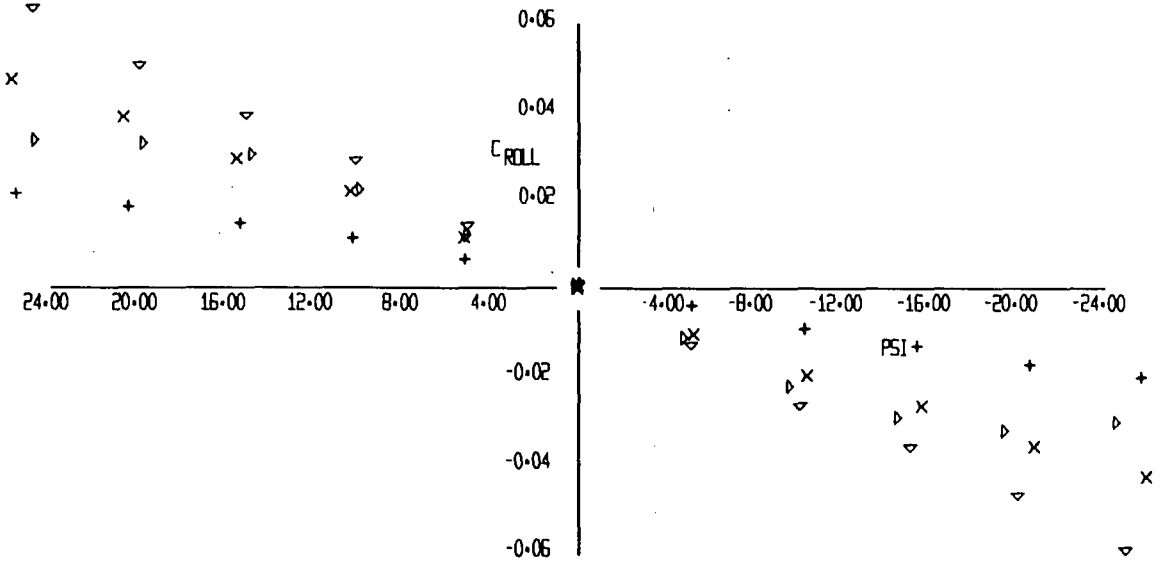

FIGURE 14 (SHEET 5)

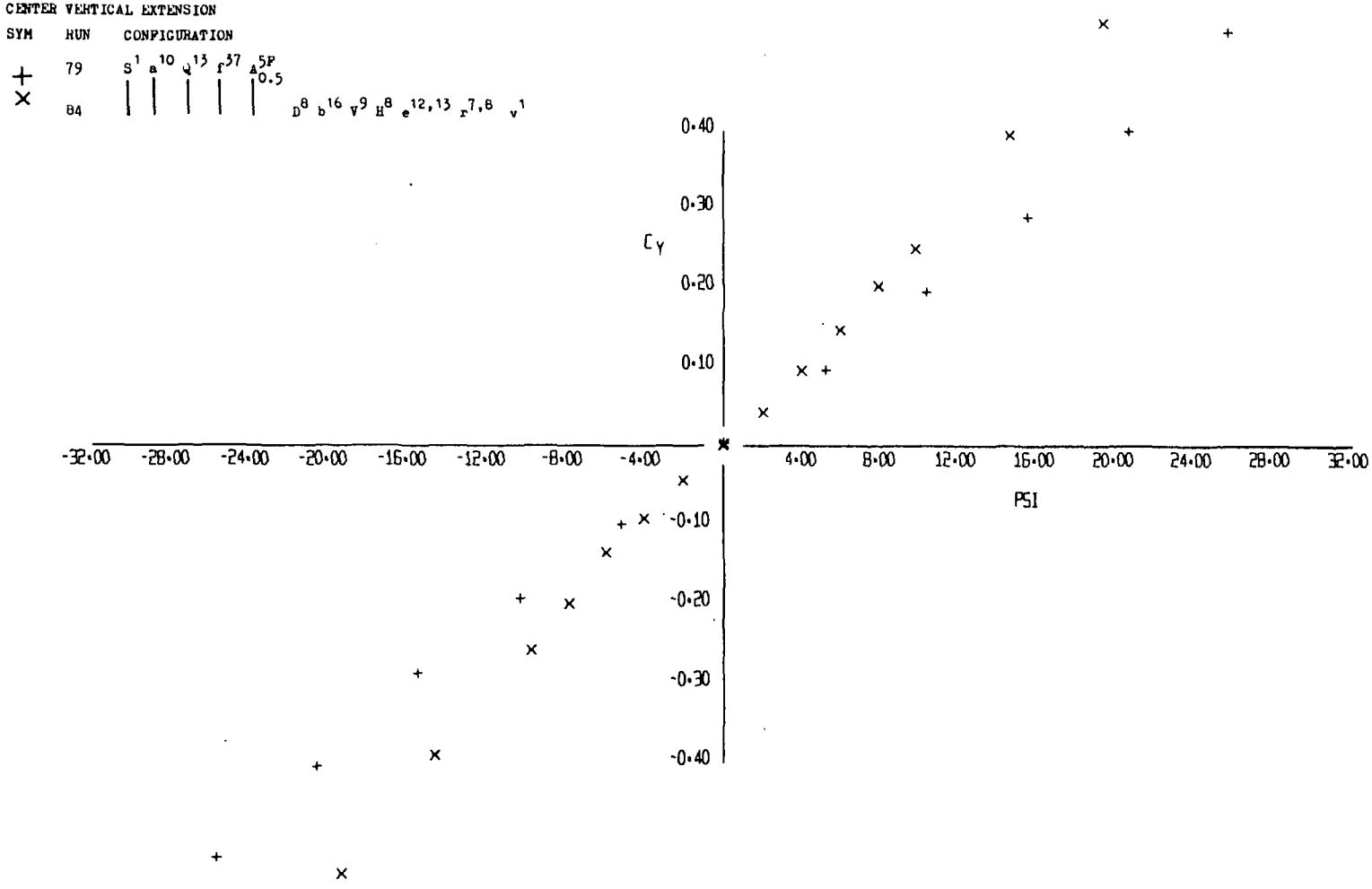

FIGURE 15 (SHEET 1)

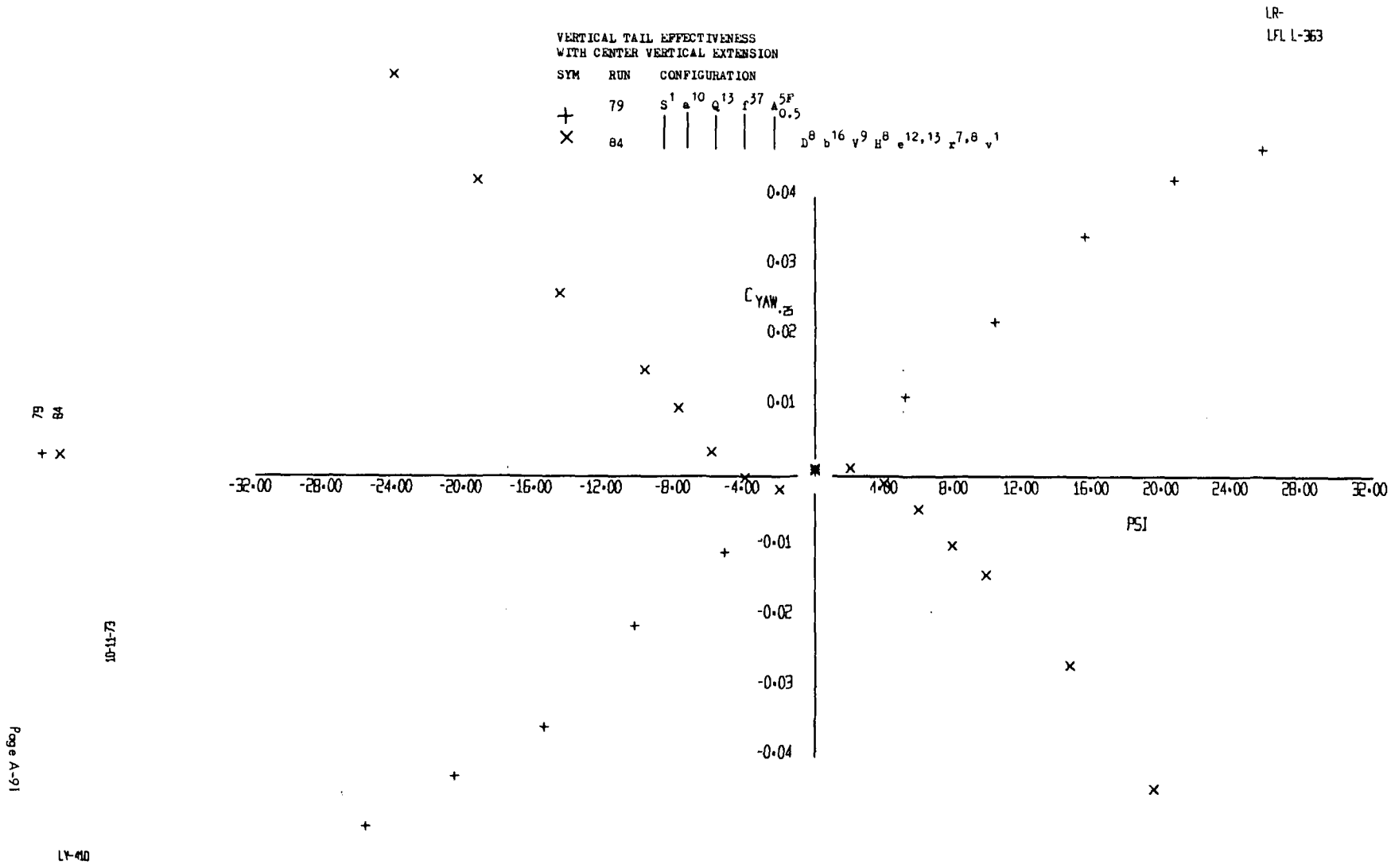

FIGURE 15 (SHEET 2)

VERTICAL TAIL EFFECTIVENESS WITH
CENTER VERTICAL EXTENSION

SYM	RUN	CONFIGURATION
+	79	$S^{1}\ a^{10}\ q^{13}\ f^{37}\ A^{5F}_{0.5}$
×	84	$D^{8}\ b^{16}\ v^{9}\ H^{8}\ e^{12,13}\ r^{7,8}\ v^{1}$

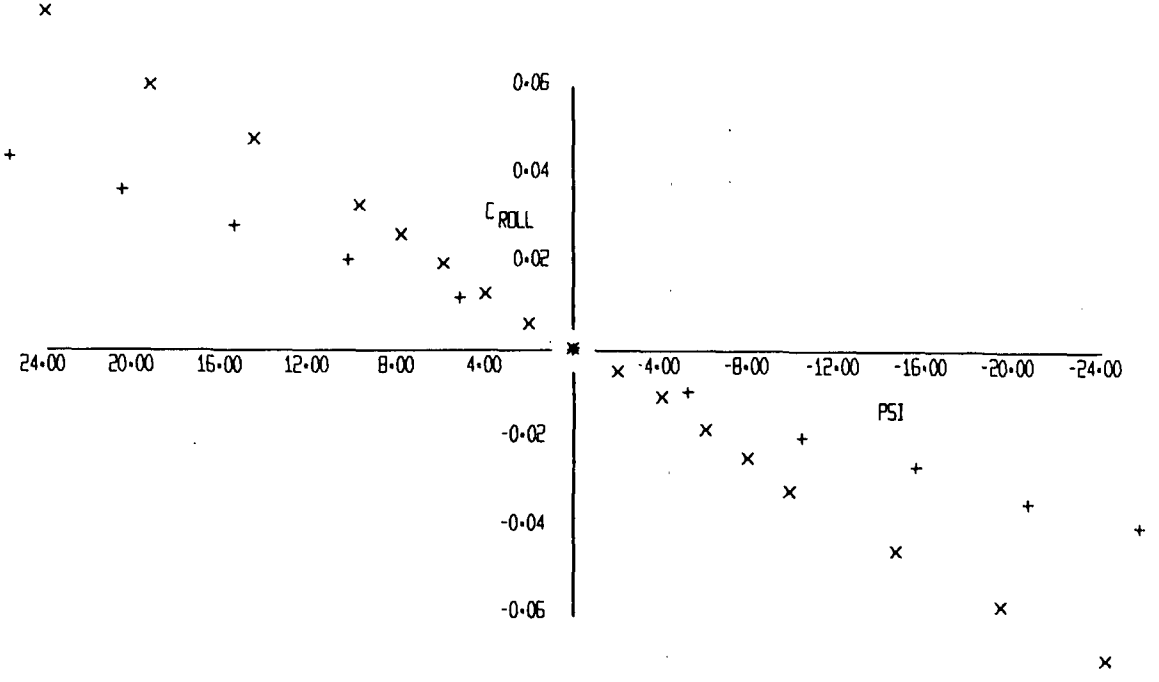

79 84

10-11-73

Page A-92

LY-40B

FIGURE 15 (SHEET 3)

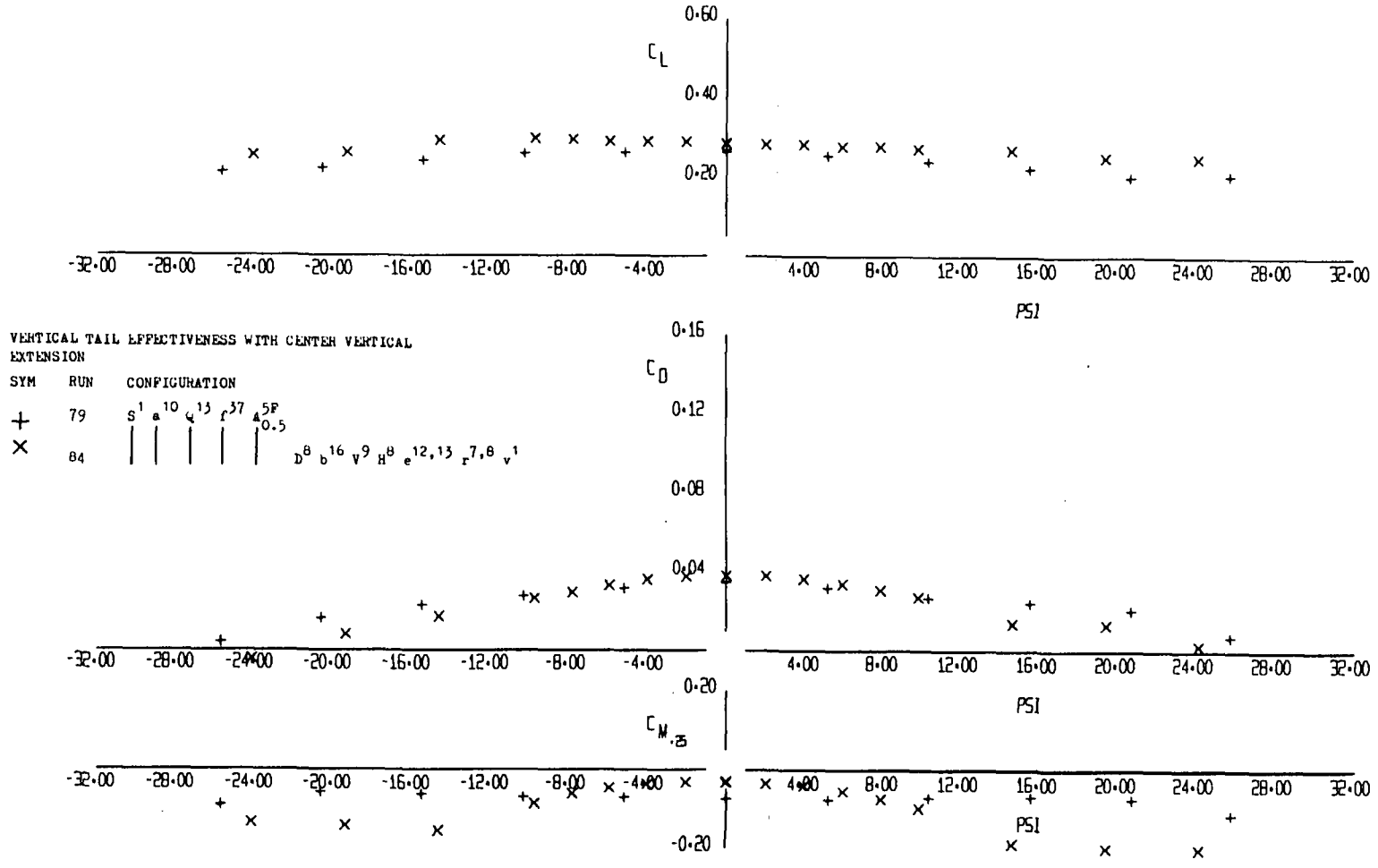

FIGURE 15 (SHEET 4)

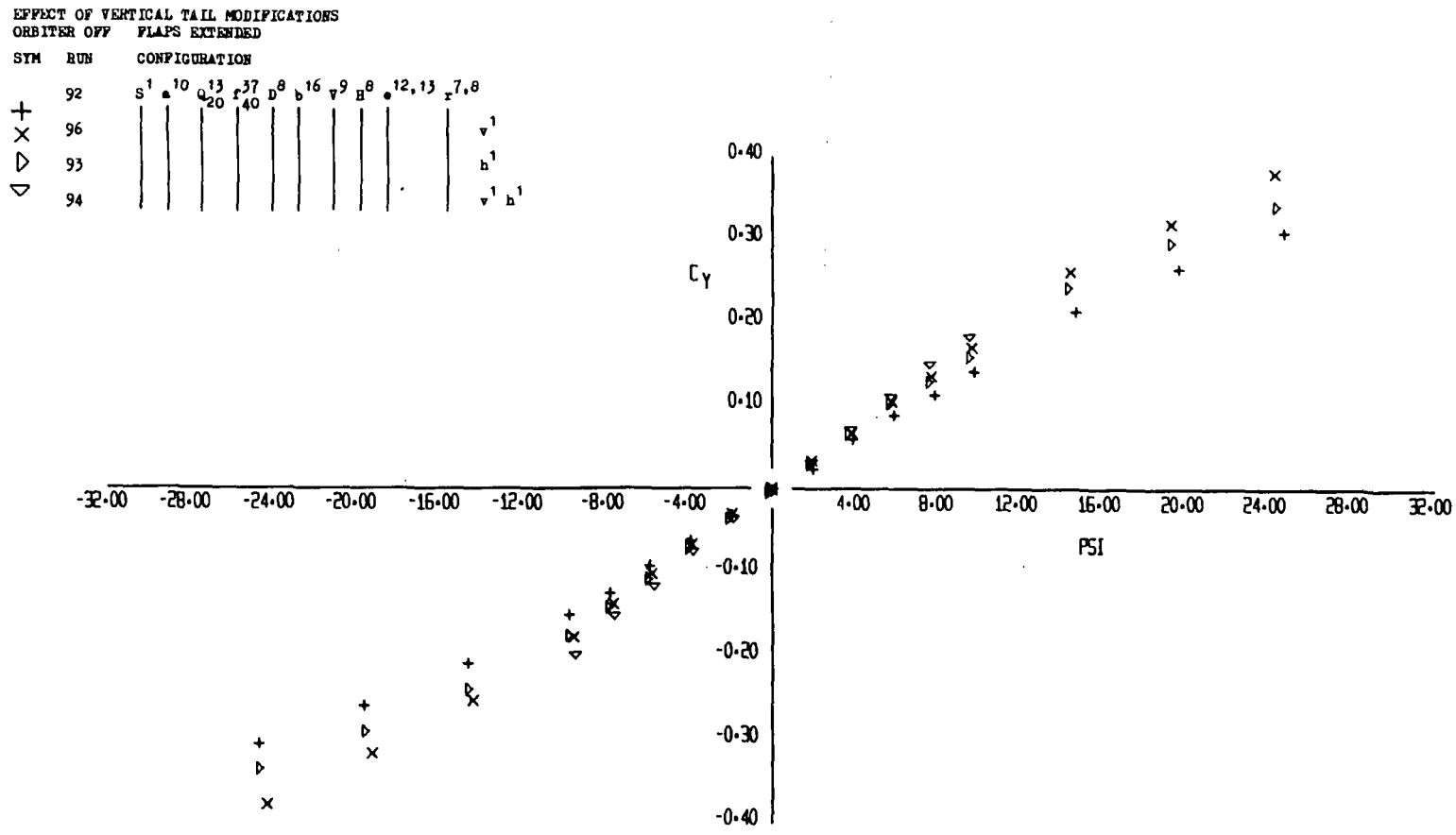

FIGURE 16 (SHEET 1)

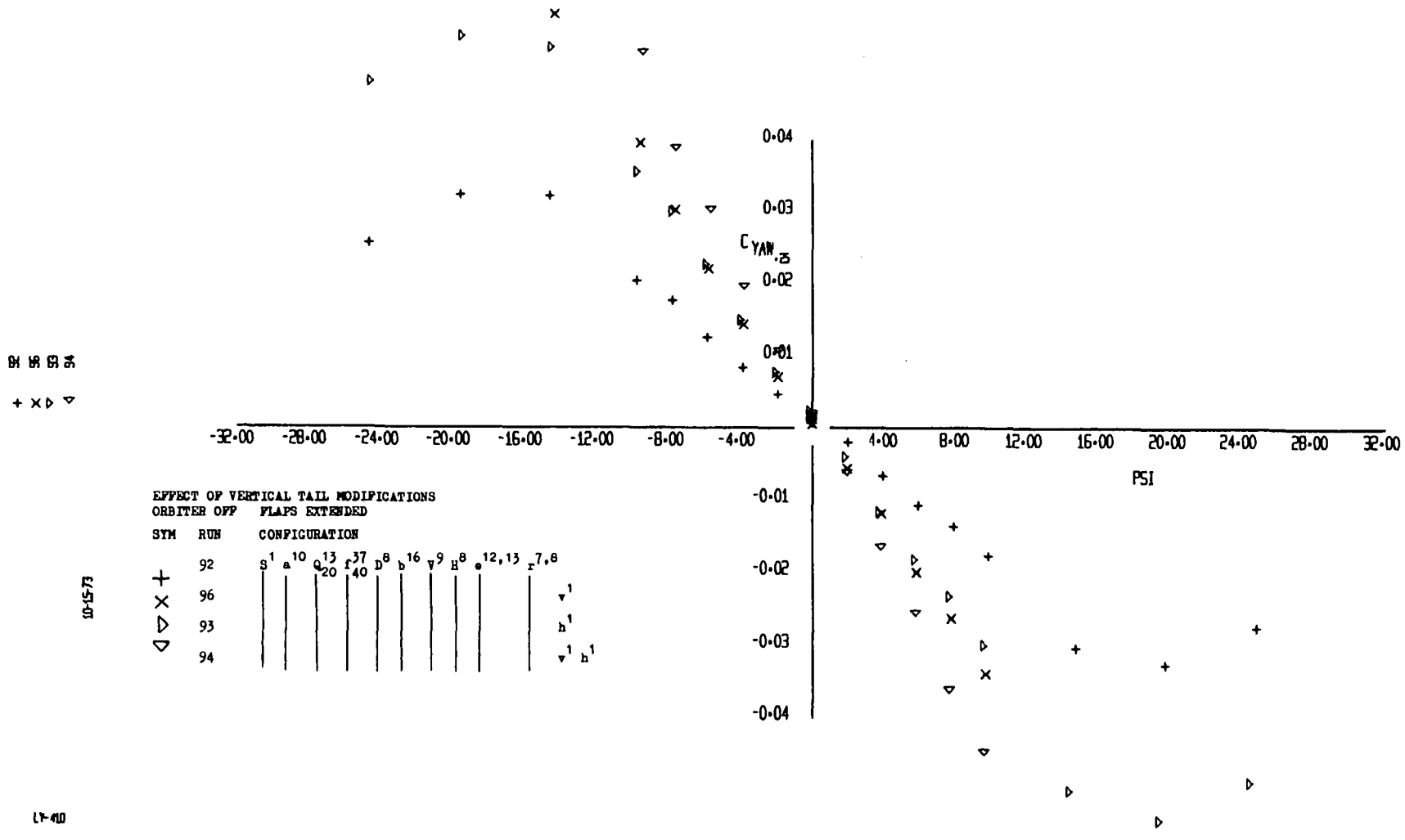

FIGURE 16 (SHEET 2)

EFFECT OF VERTICAL TAIL MODIFICATIONS
ORBITER OFF FLAPS EXTENDED

SYM	RUN	CONFIGURATION
+	92	S^{1} a^{10} Q_{20}^{13} f_{40}^{37} D^{8} b^{16} V^{9} H^{8} $e^{12,13}$ $r^{7,8}$
×	96	v^{1}
▷	93	h^{1}
◁	94	v^{1} h^{1}

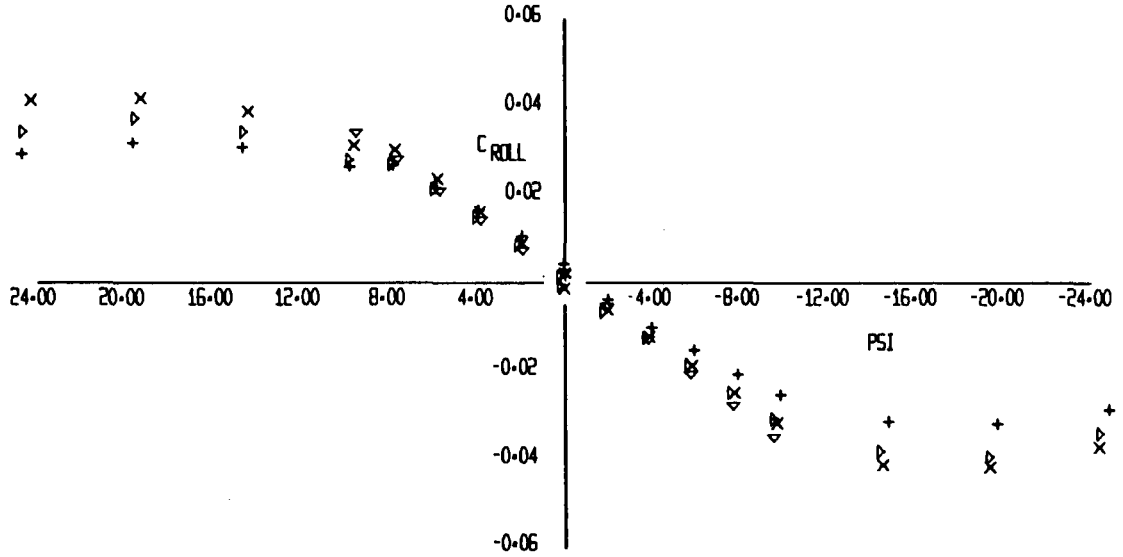

10-15-73

FIGURE 16 (SHEET 3)

FIGURE 16 (SHEET 4)

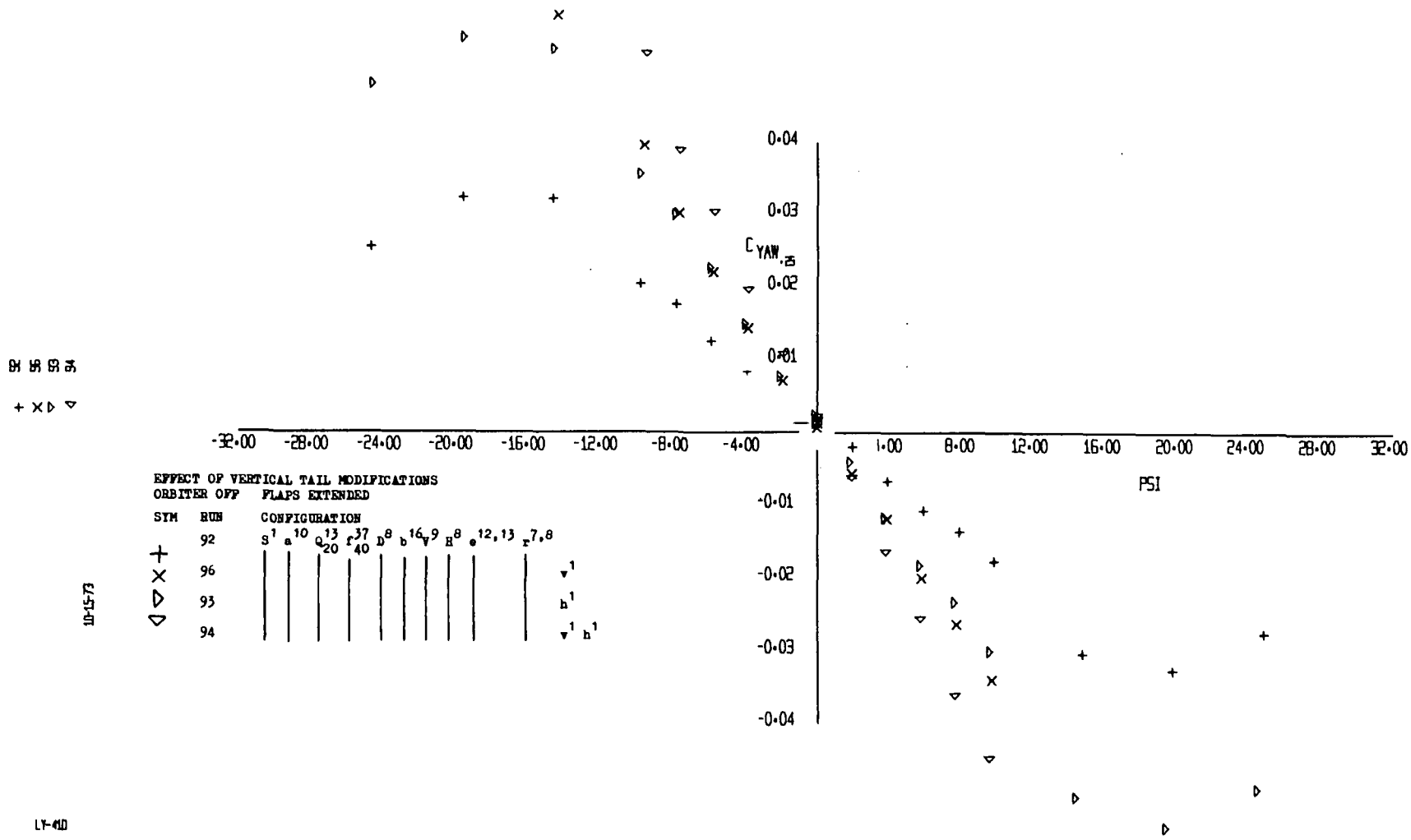

FIGURE 16 (SHEET 5)

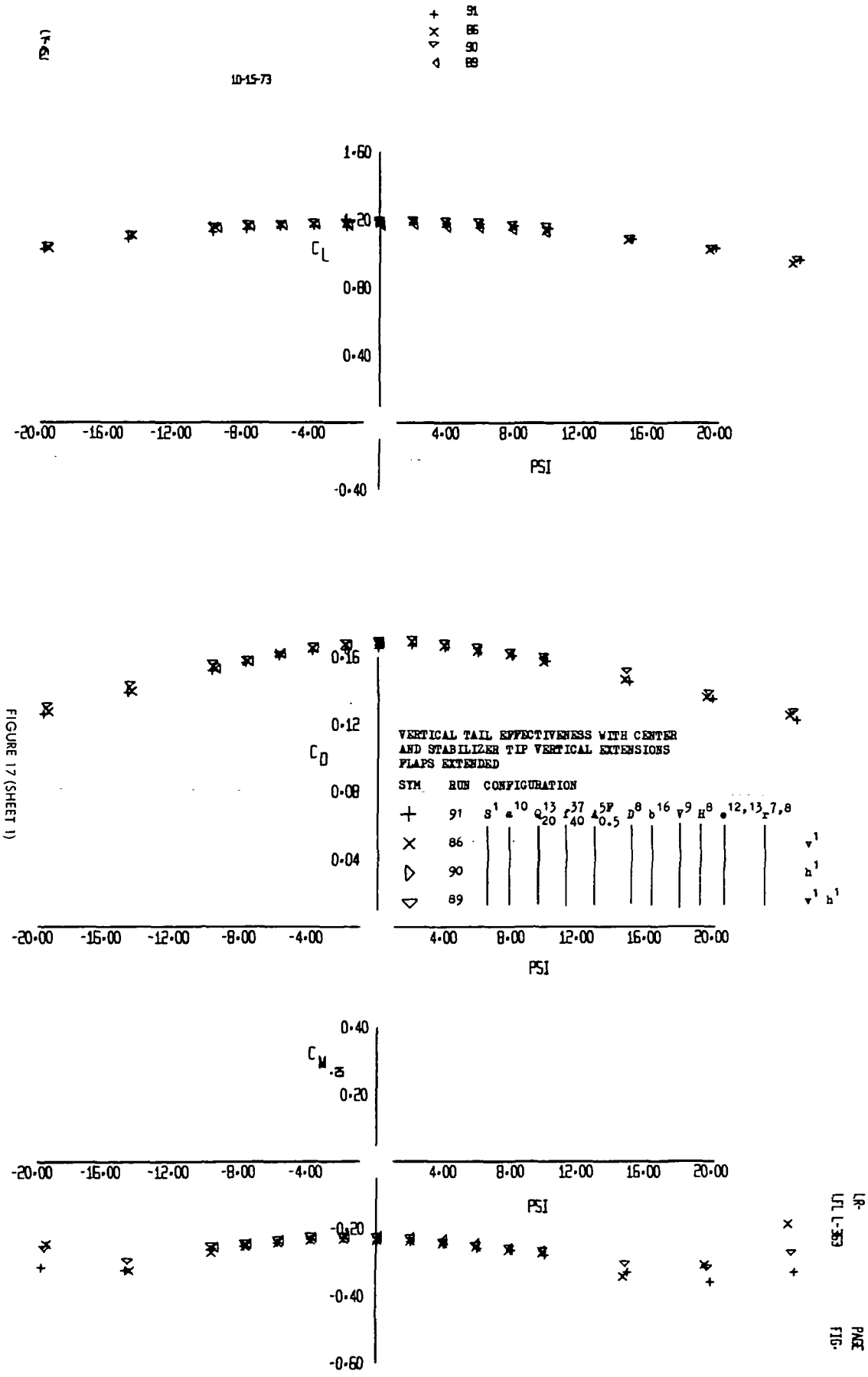

FIGURE 17 (SHEET 1)

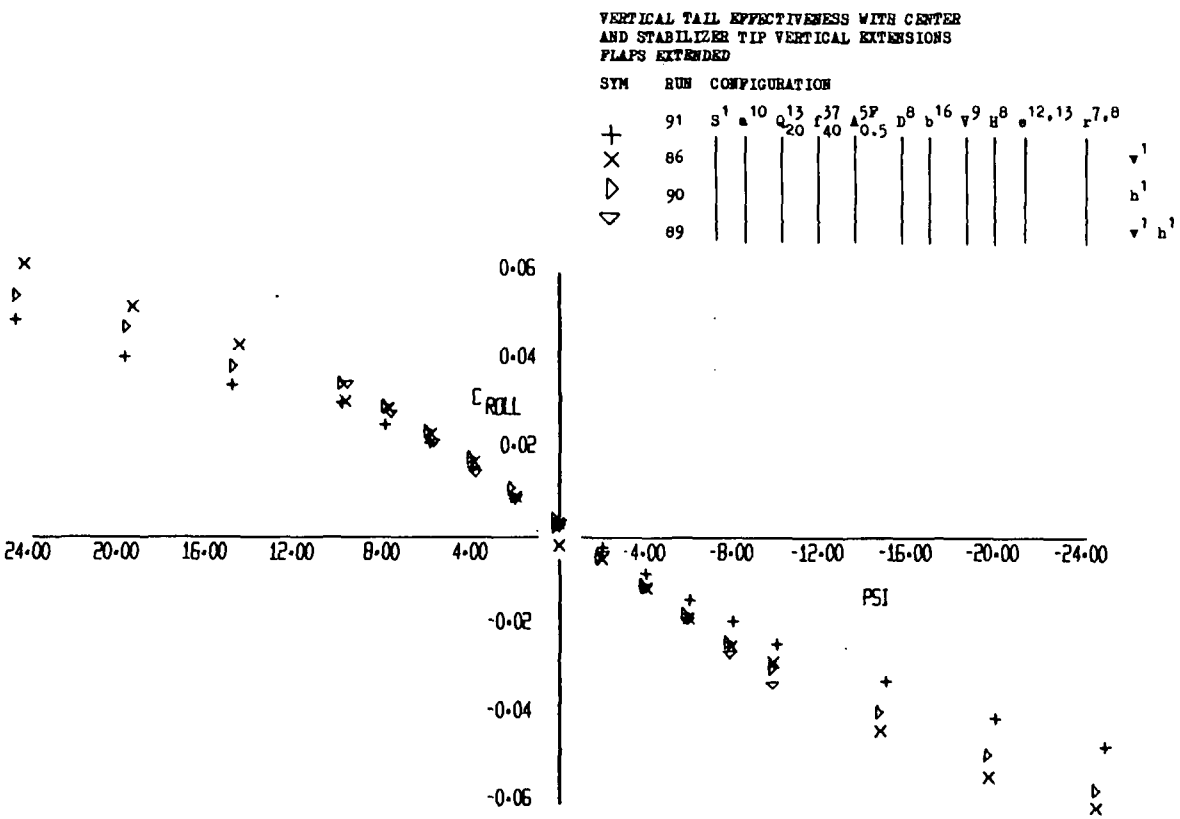

FIGURE 17 (SHEET 2)

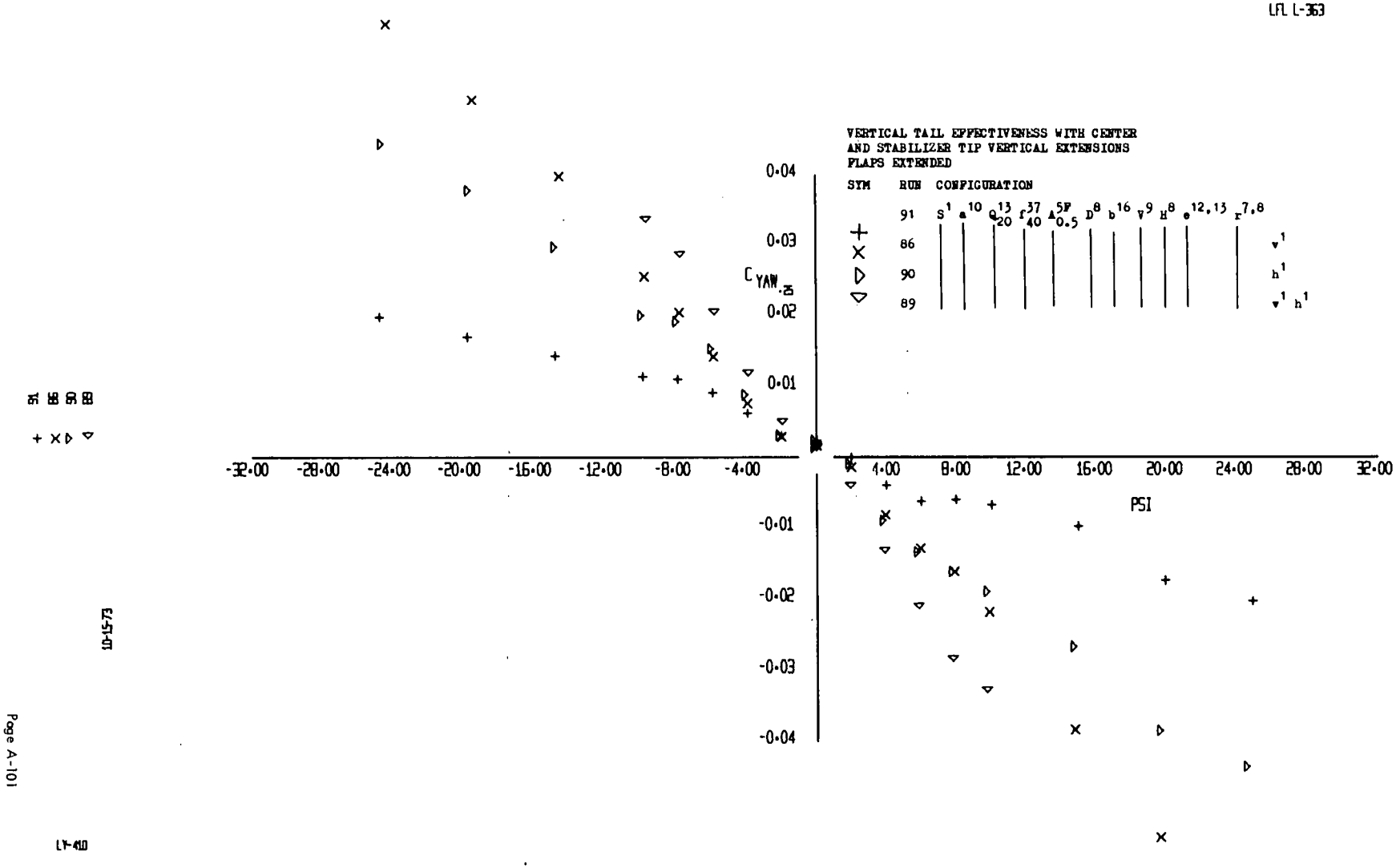

FIGURE 17 (SHEET 3)

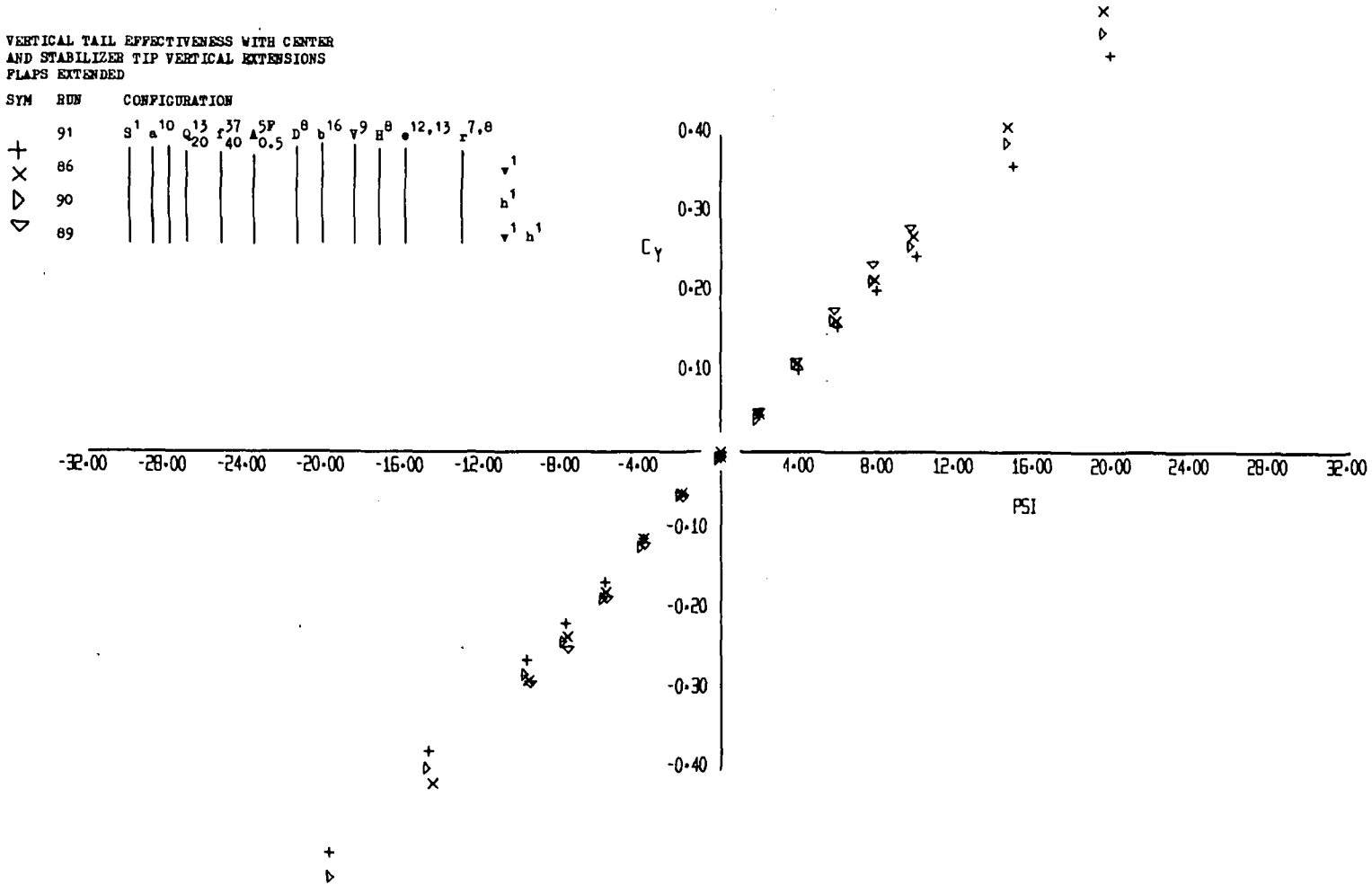

FIGURE 17 (SHEET 4)

FIGURE 18 (SHEET 1)

EFFECT OF ORBITER
FLAPS EXTENDED
TAIL ON AND TAIL OFF

SYM	RUN	CONFIGURATION
+	88	S^{1} a^{10} q^{13} P^{37} A^{5P} $_{20}$ $_{40}$ $_{0.5}$ D^{8} b^{16} v^{9} H^{8} $e^{12,13}$ $r^{7,8}$
×	91	

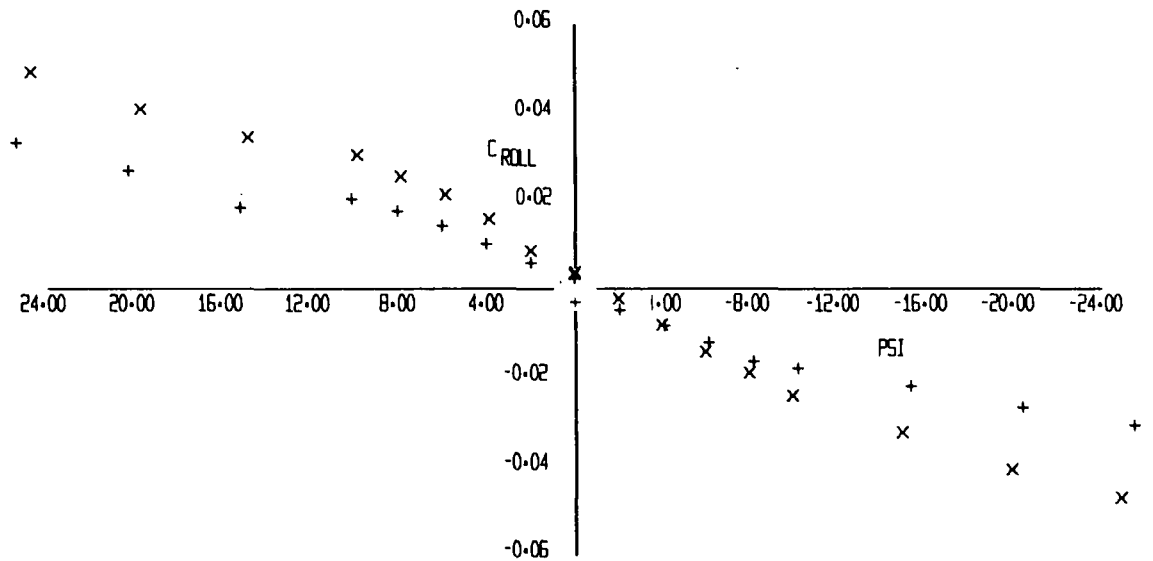

88 91

10-15-73

Page A-104

LF-408

FIGURE 18 (SHEET 2)

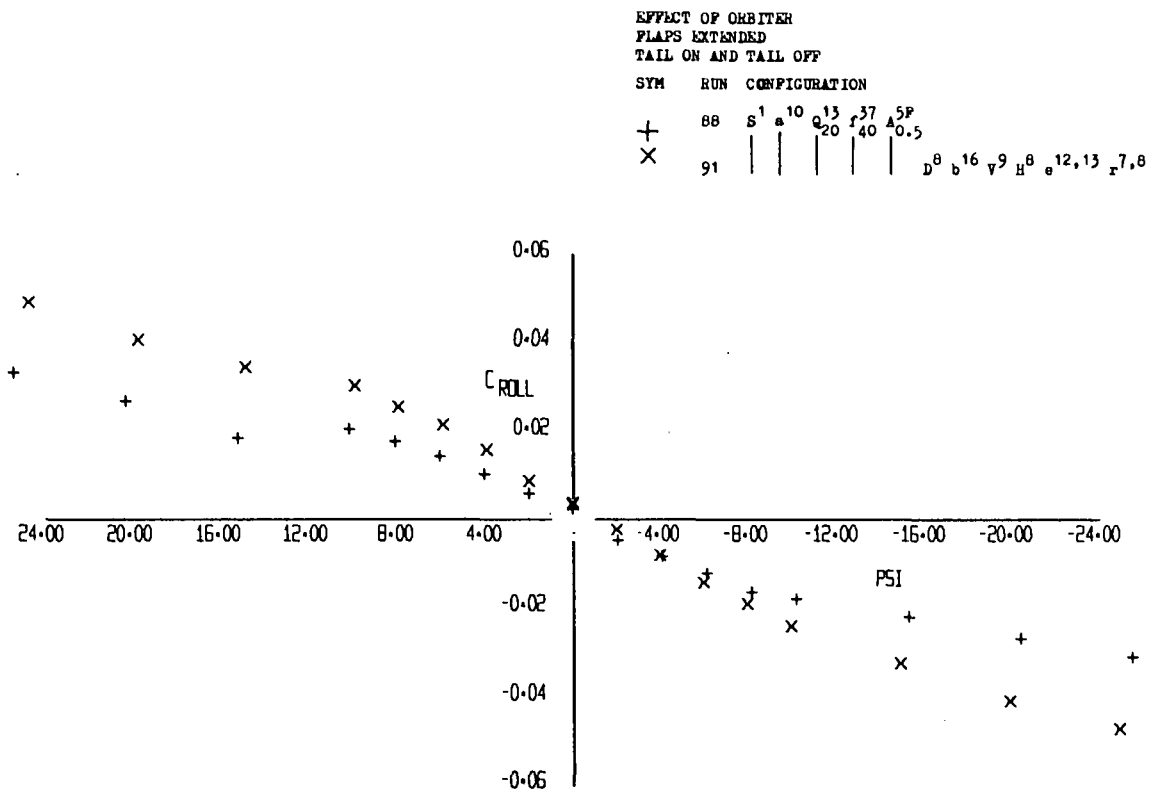

FIGURE 18 (SHEET 3)

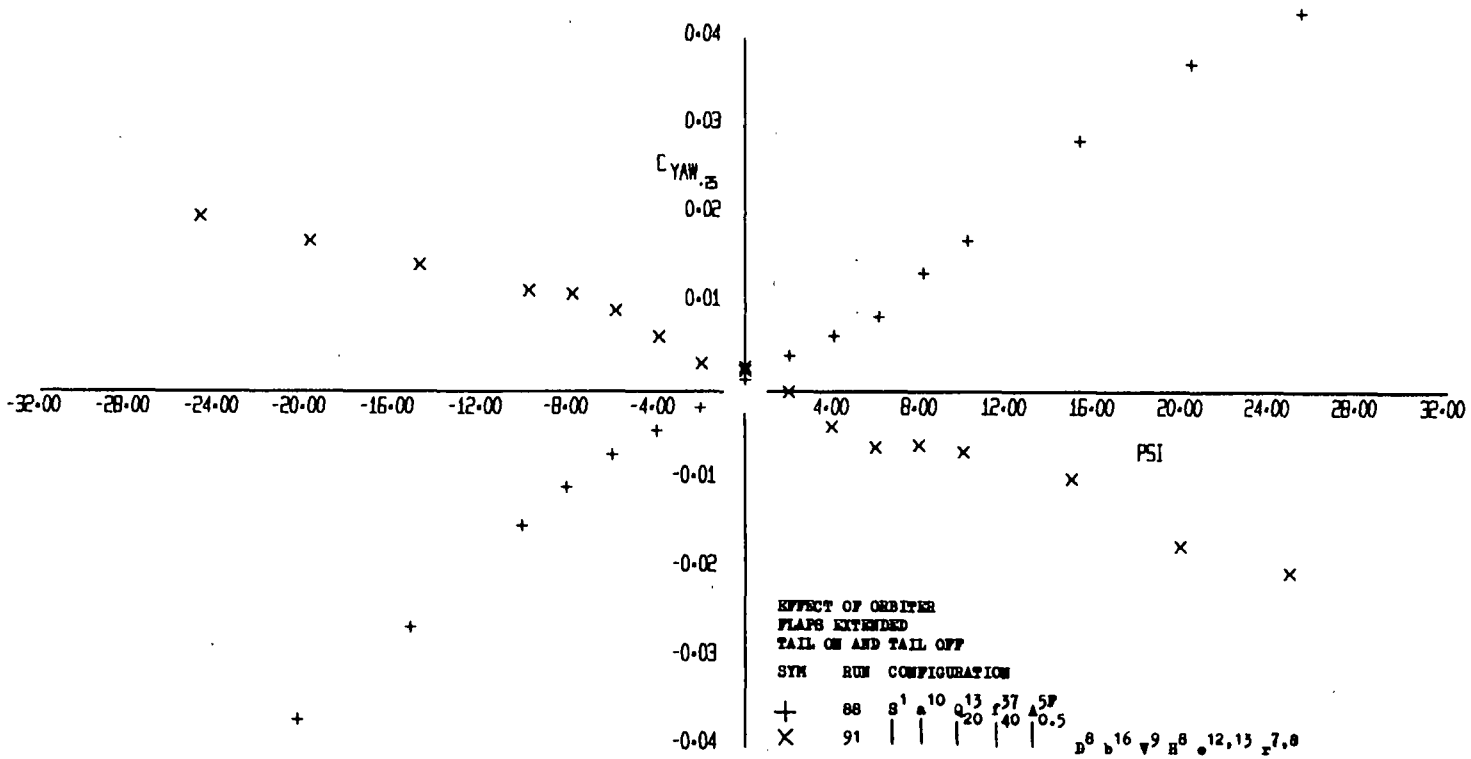

FIGURE 18 (SHEET 4)

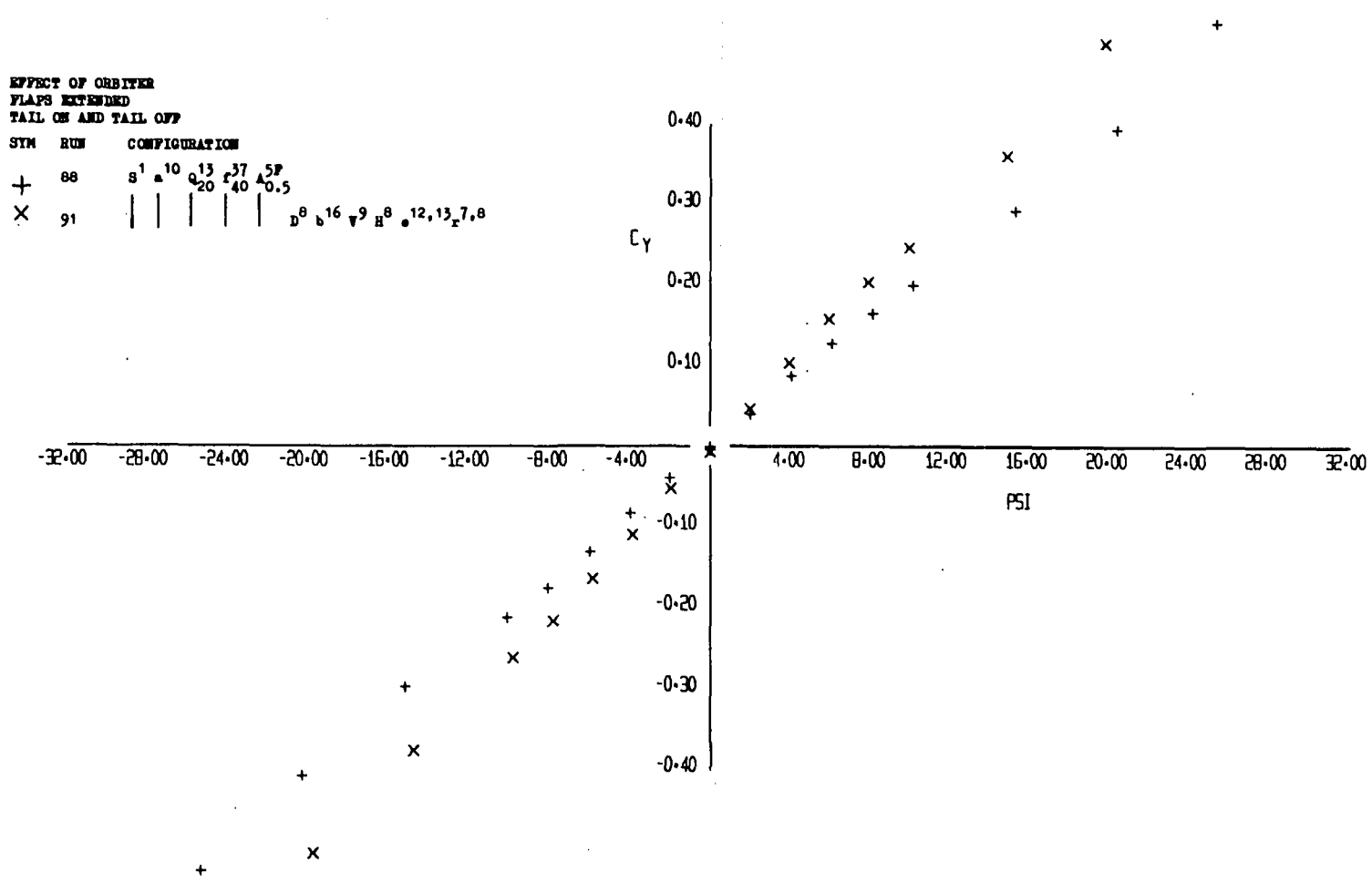

FIGURE 18 (SHEET 5)

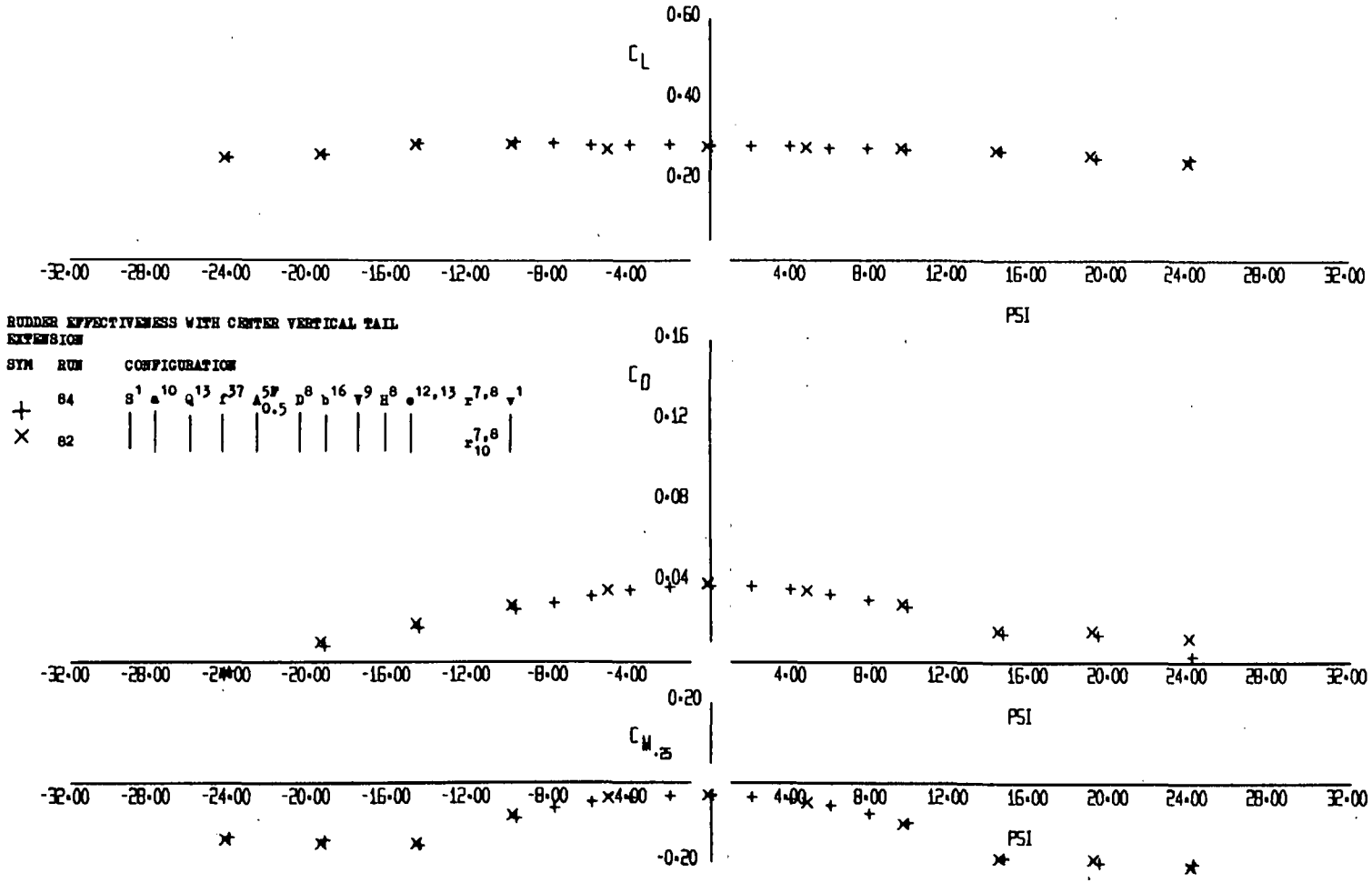

FIGURE 19 (SHEET 1)

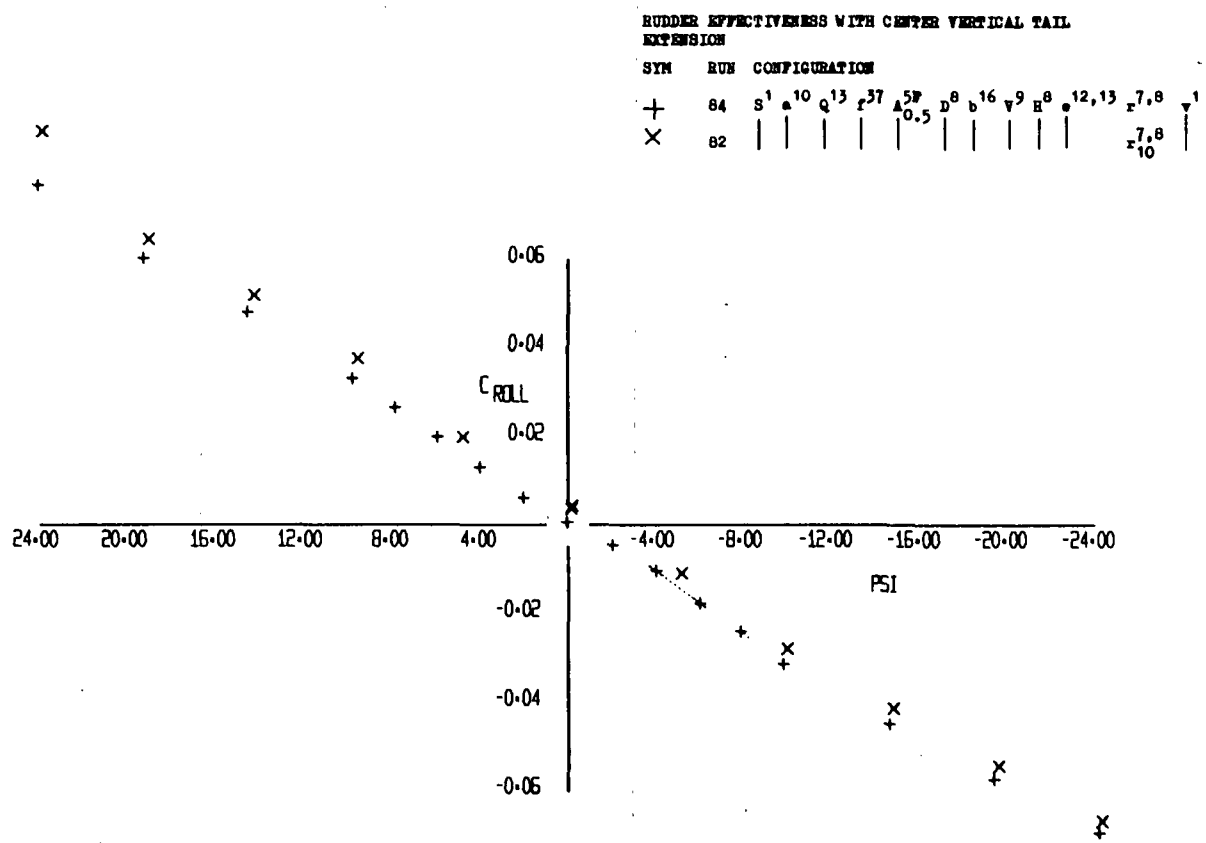

FIGURE 19 (SHEET 2)

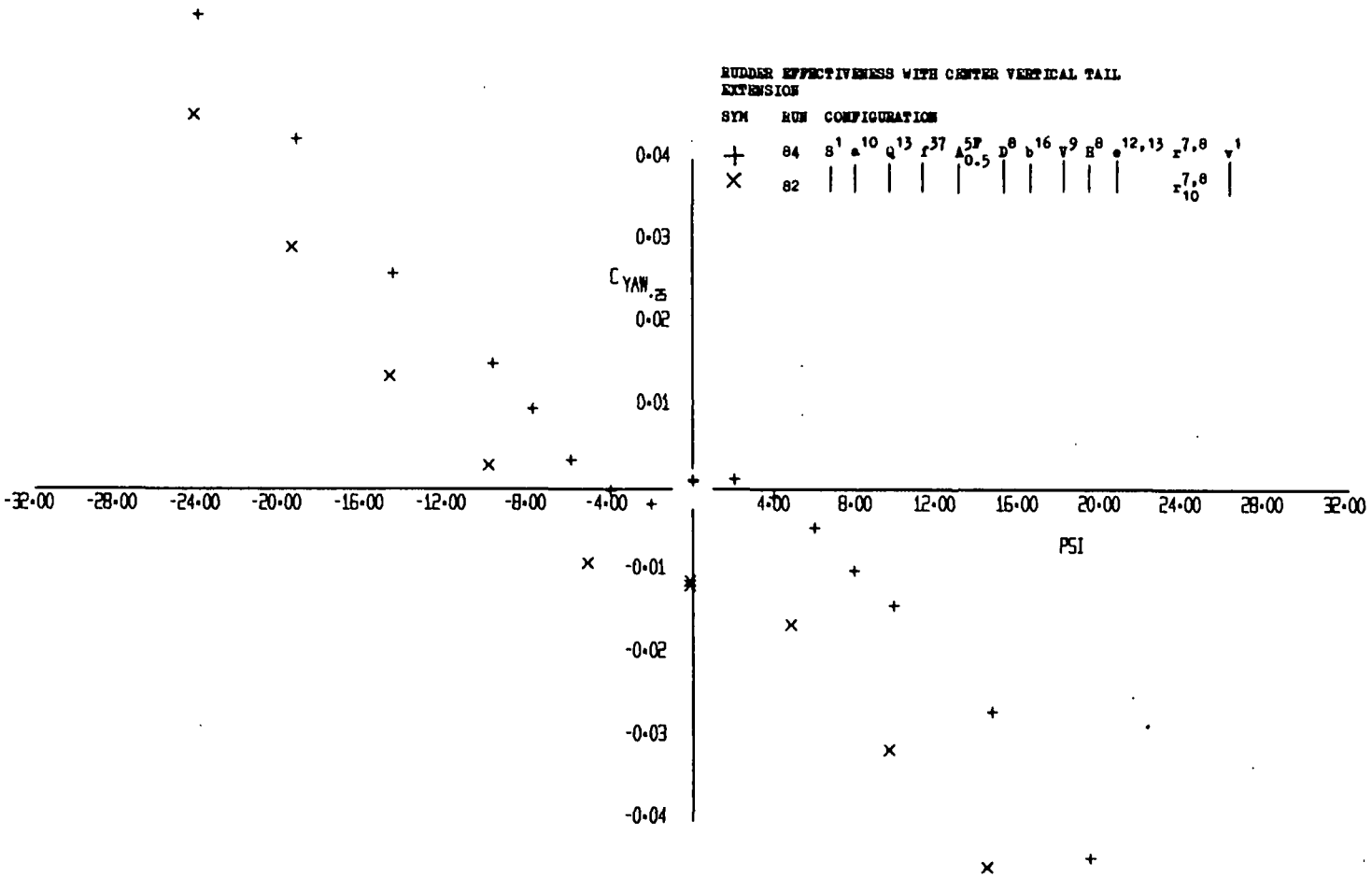

FIGURE 19 (SHEET 3)

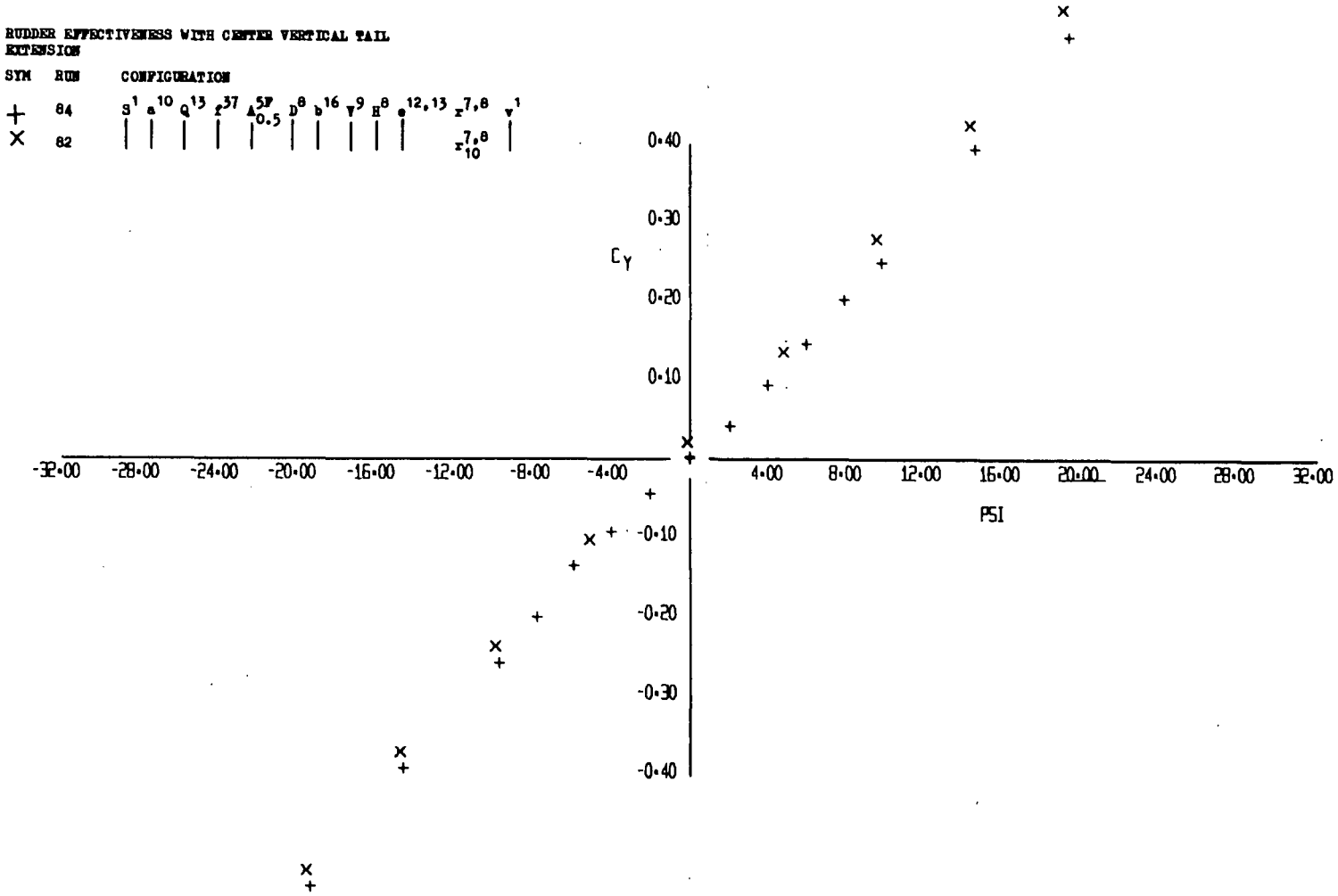

FIGURE 19 (SHEET 4)

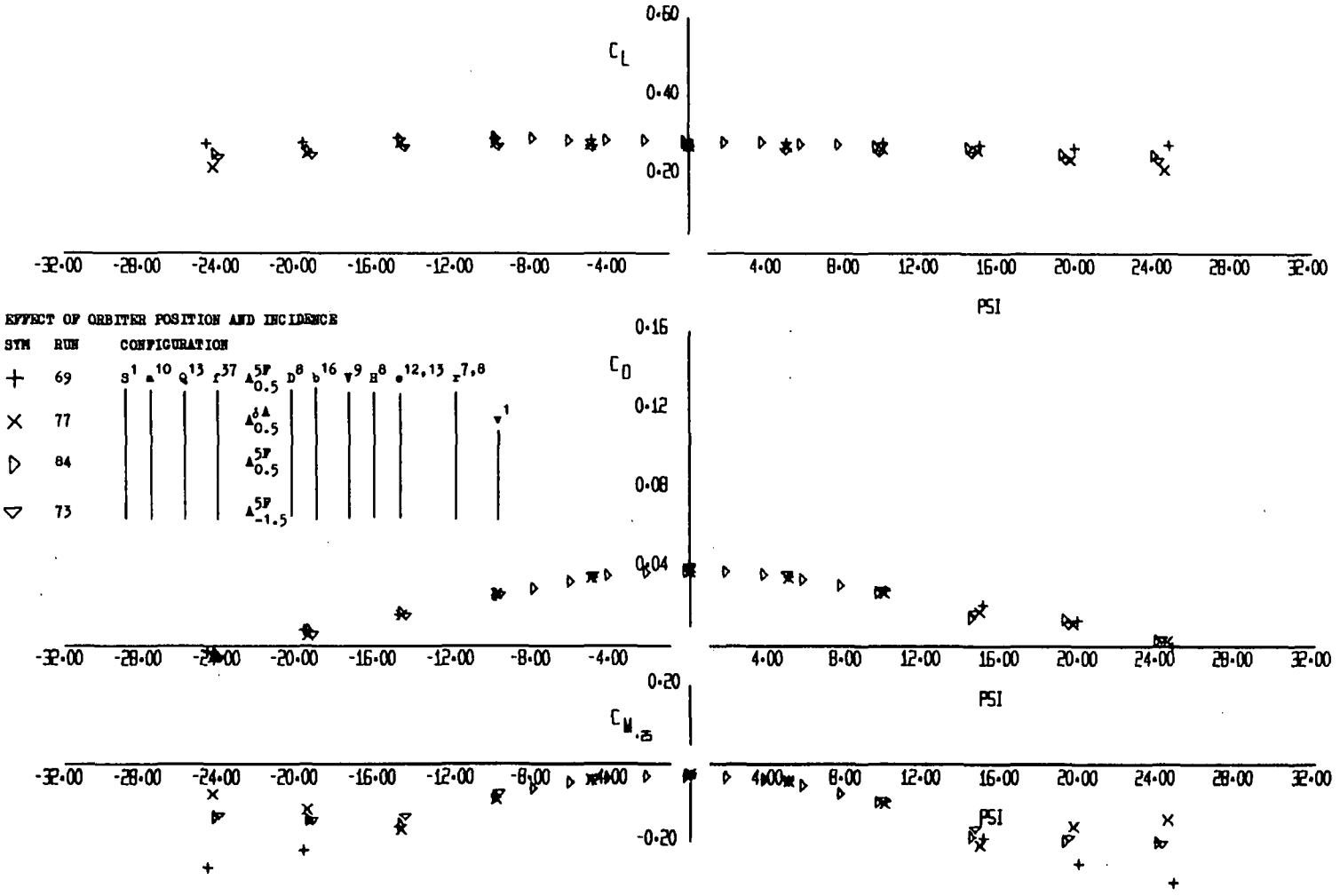

FIGURE 20 (SHEET 1)

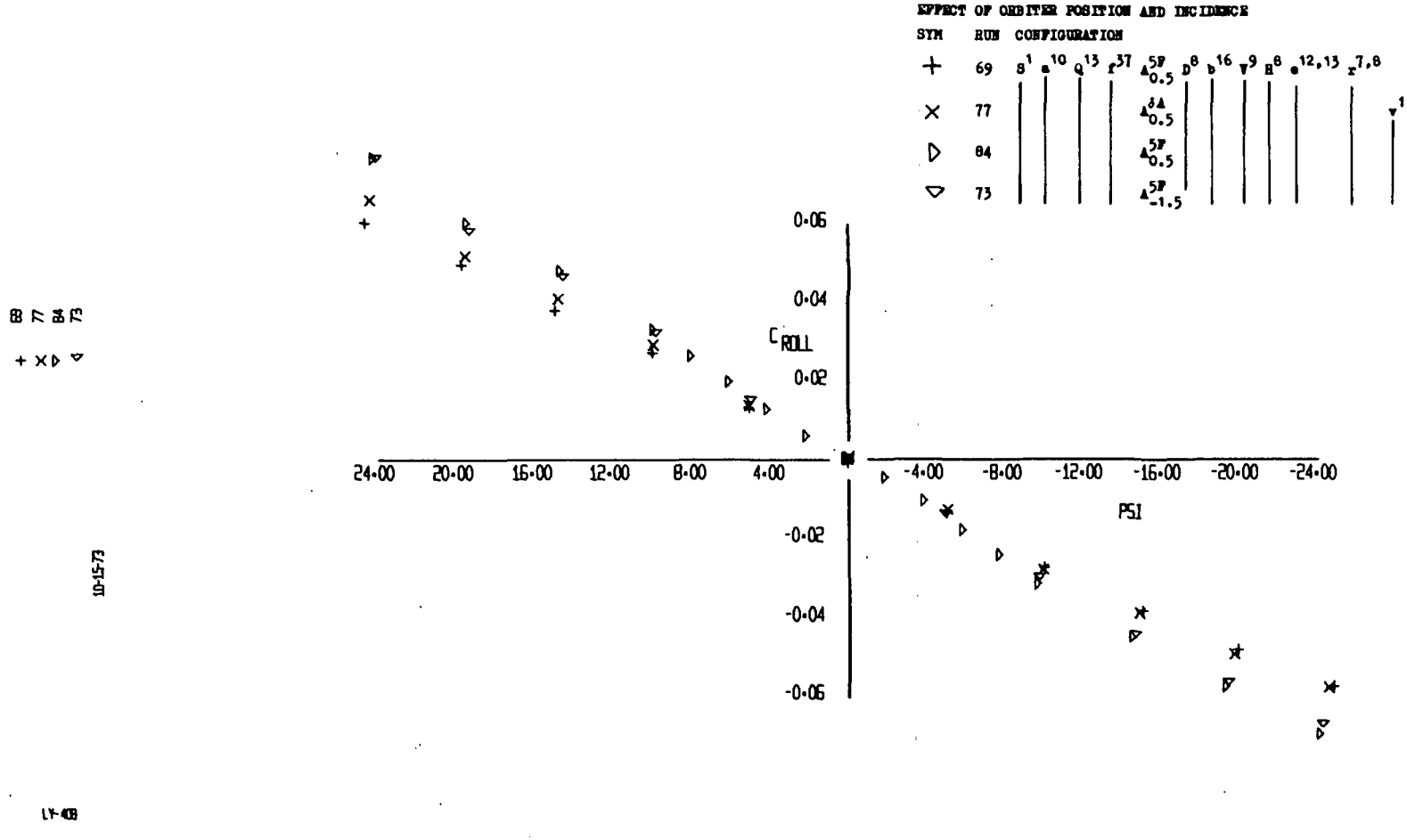

FIGURE 20 (SHEET 2)

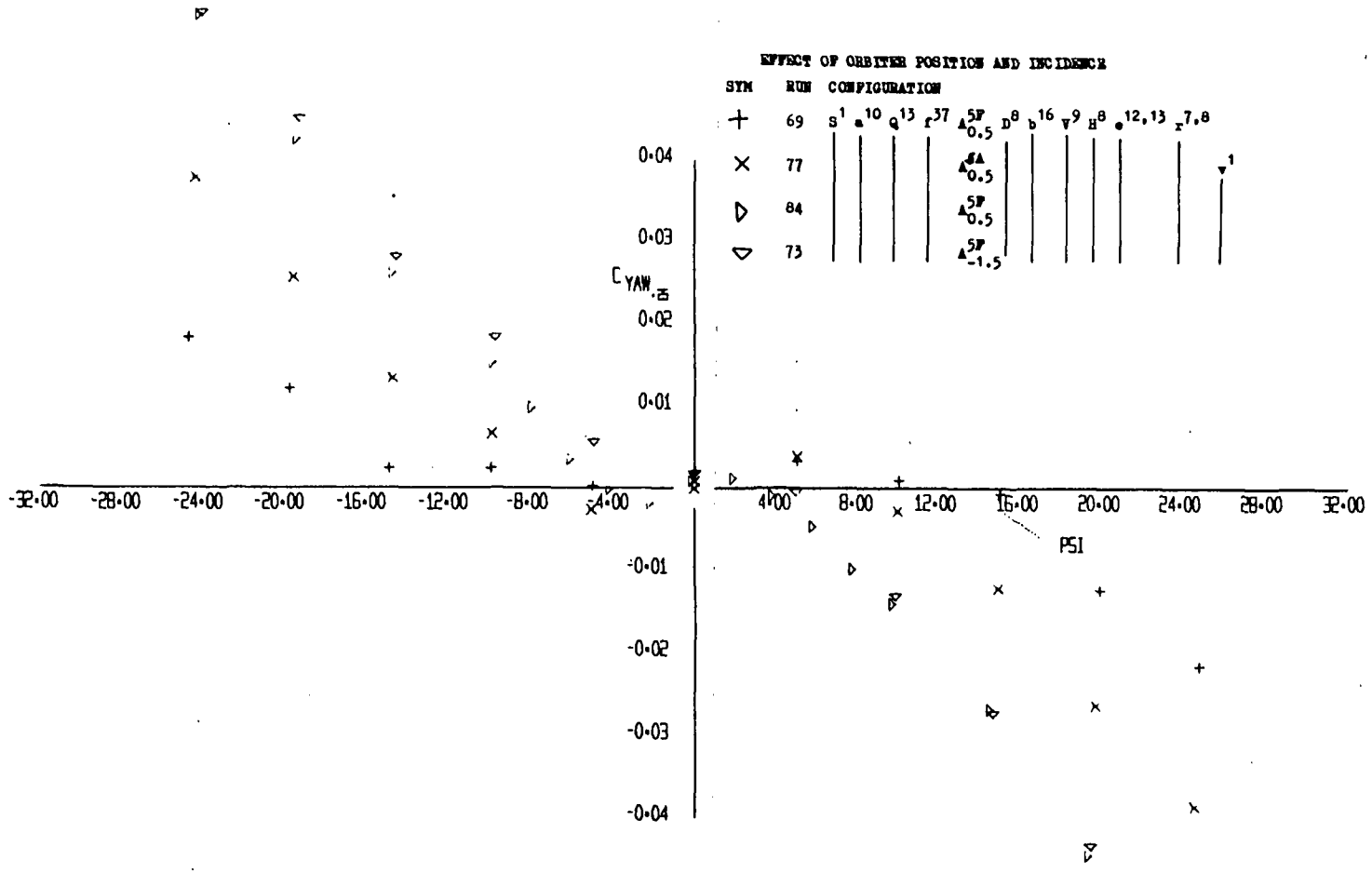

FIGURE 20 (SHEET 3)

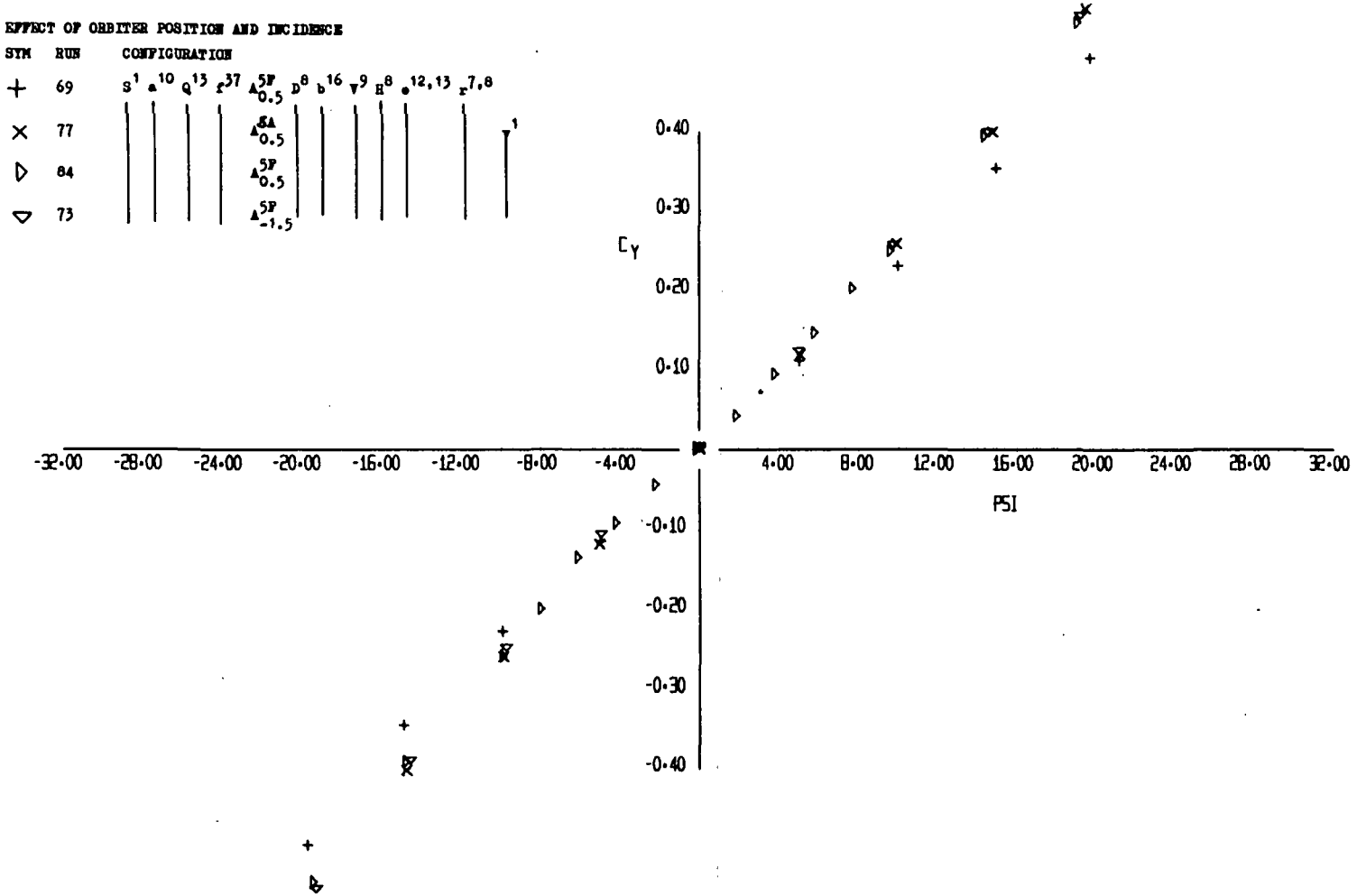

FIGURE 20 (SHEET 4)

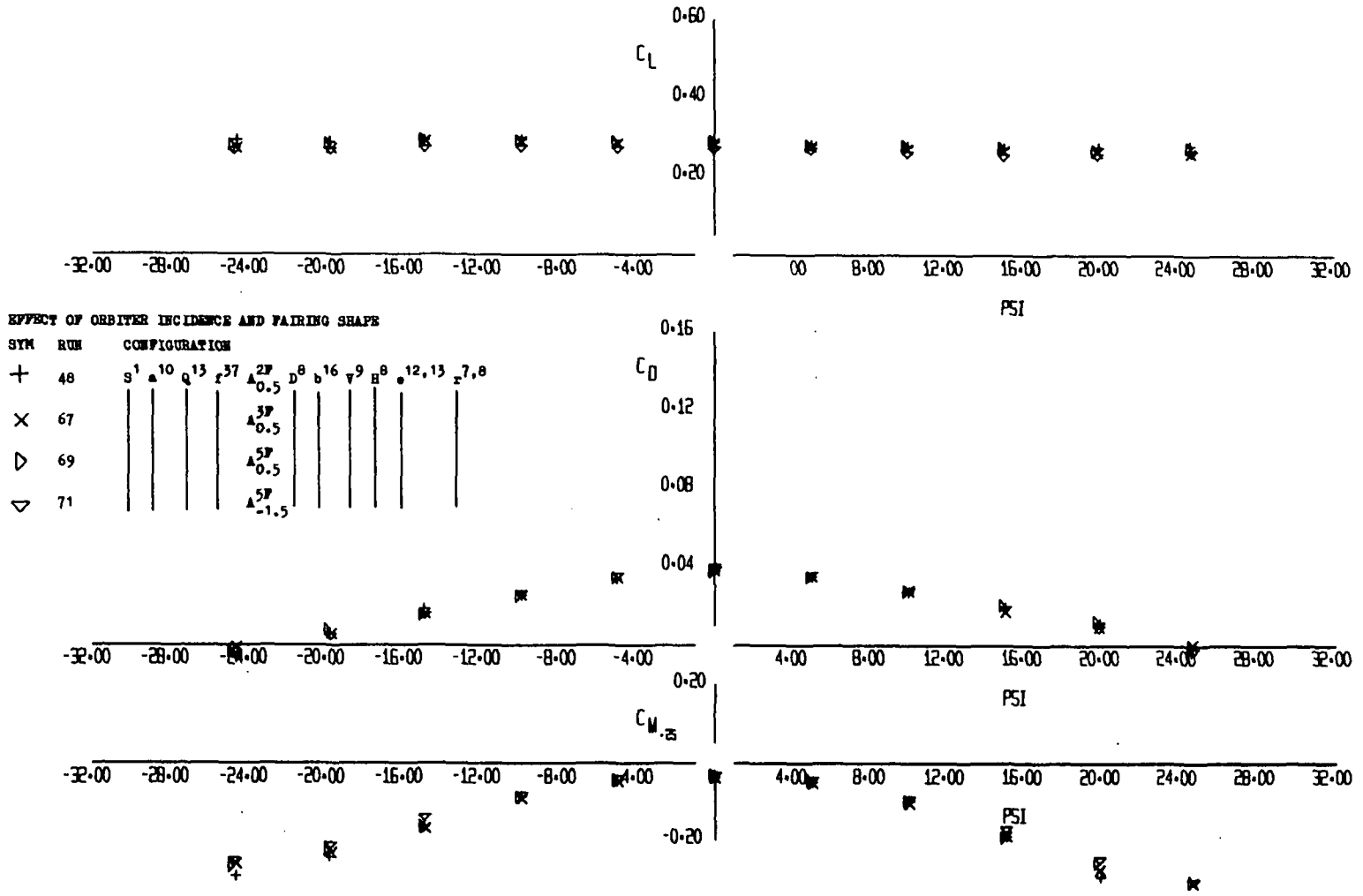

FIGURE 21 (SHEET 1)

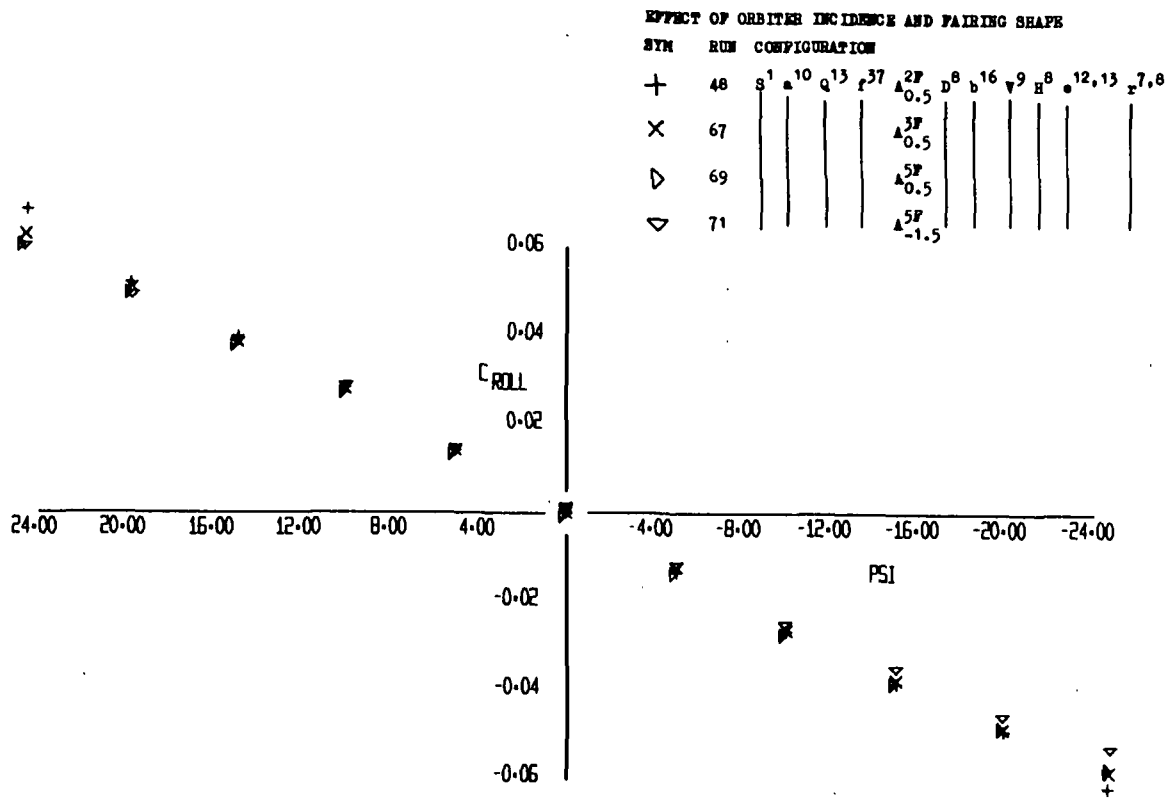

FIGURE 21 (SHEET 2)

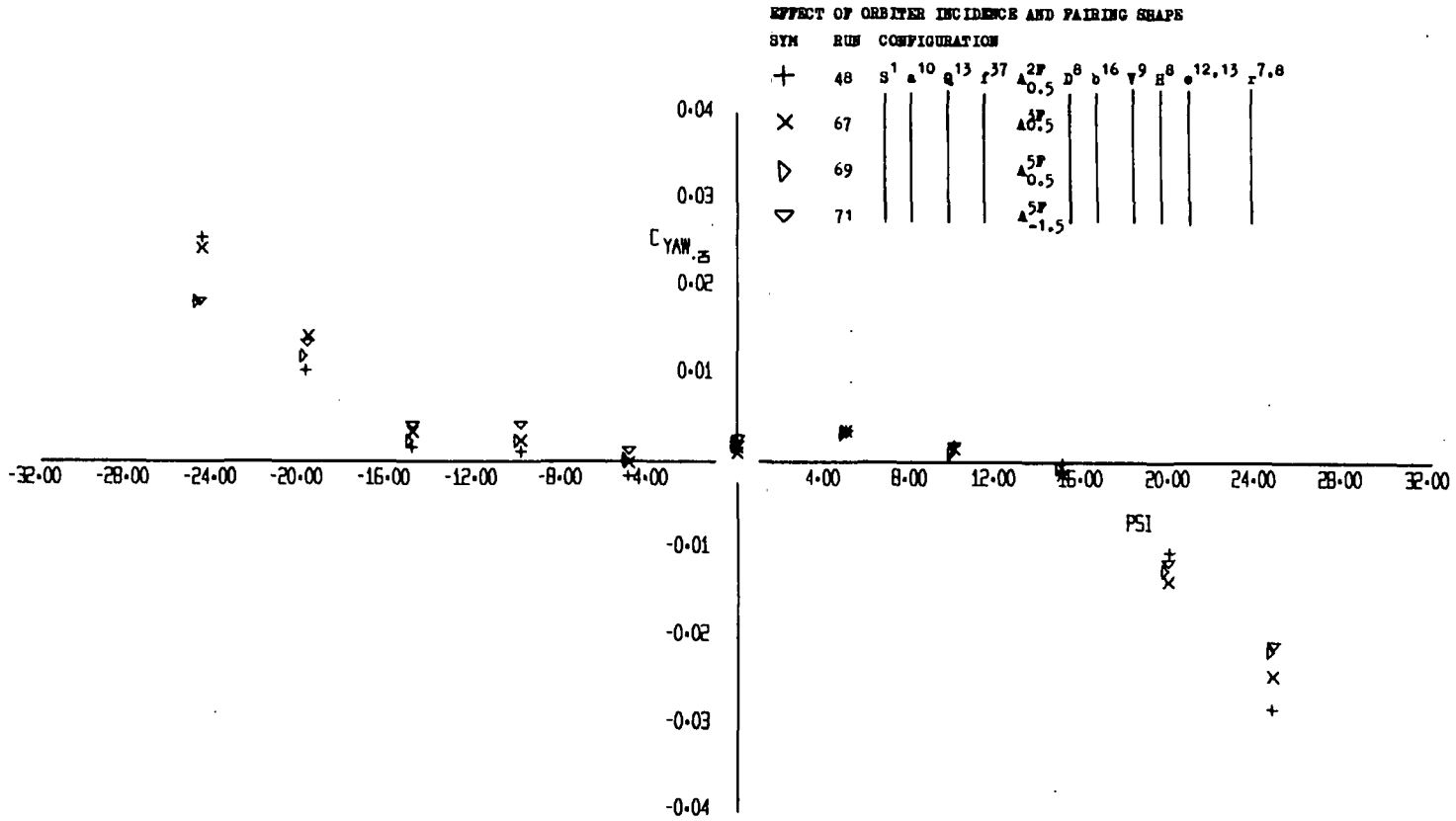

FIGURE 21 (SHEET 3)

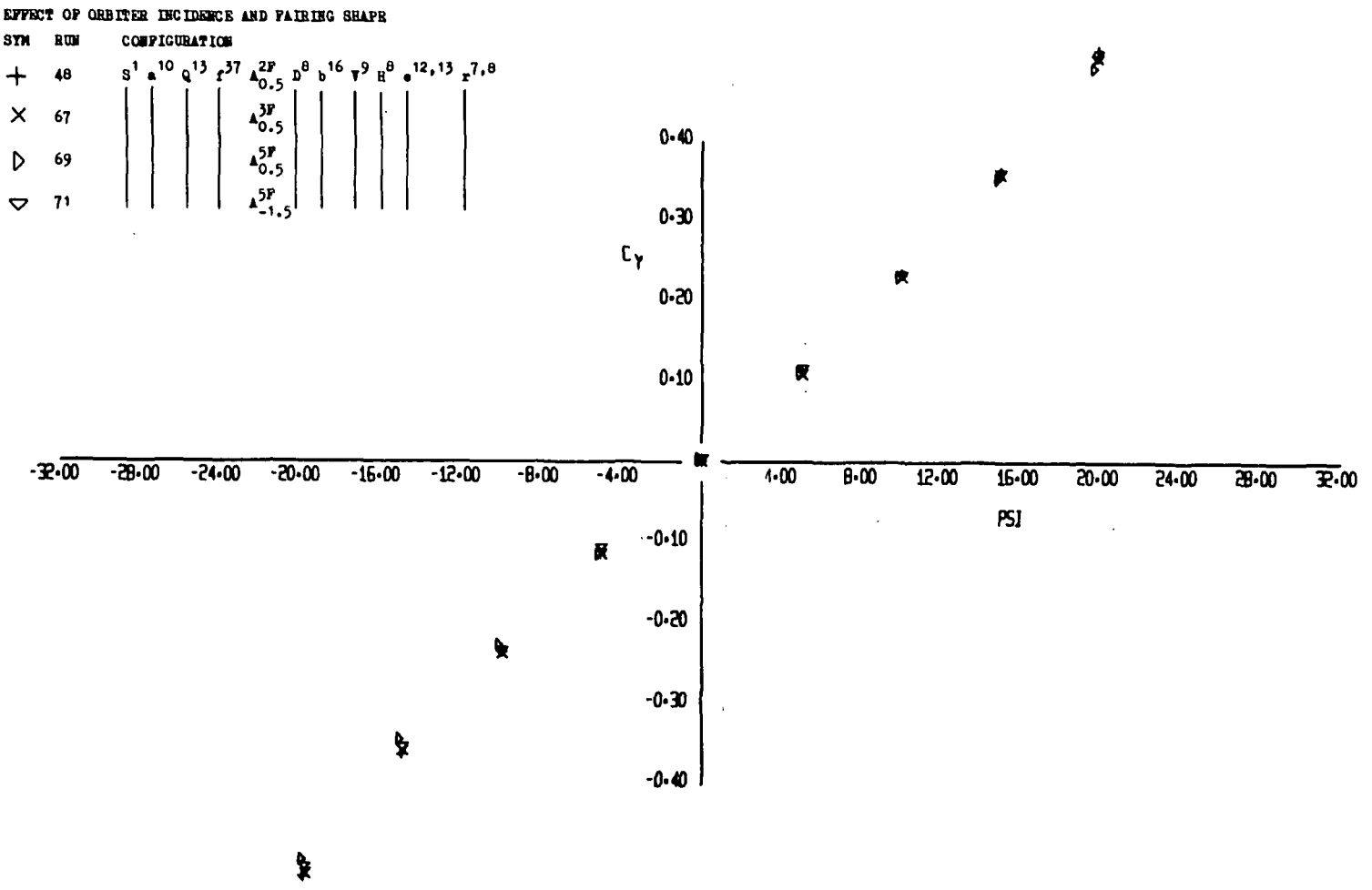

FIGURE 21 (SHEET 4)

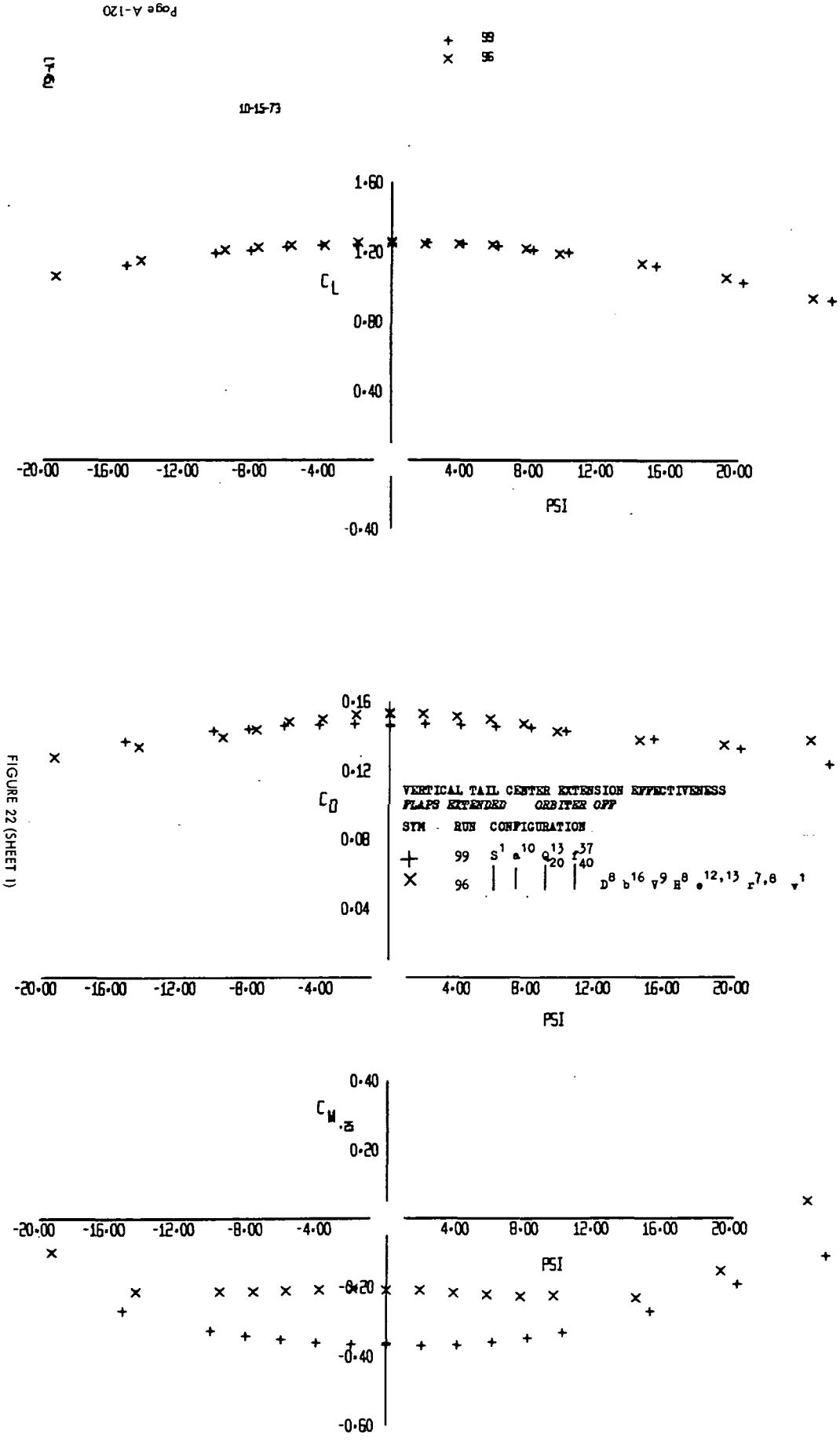

FIGURE 22 (SHEET 1)

VERTICAL TAIL CENTER EXTENSION EFFECTIVENESS
FLAPS EXTENDED ORBITER OFF

SYM	RUN	CONFIGURATION
+	99	$S^{1}\ a^{10}\ Q^{13}_{20}\ f^{37}_{40}$
×	96	$D^{8}\ b^{16}\ V^{9}\ H^{8}\ e^{12,13}\ r^{7,8}\ v^{1}$

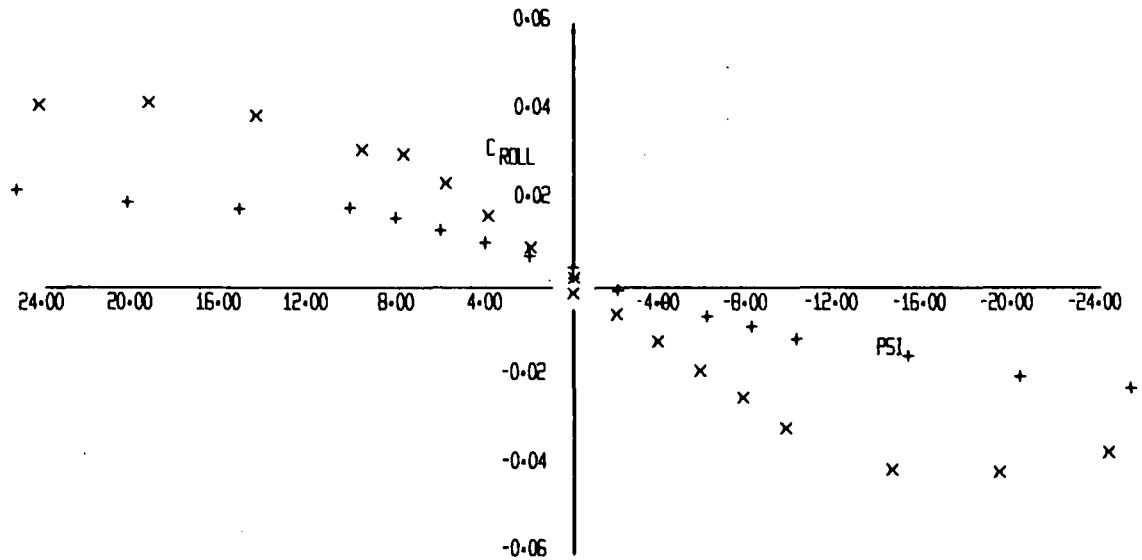

FIGURE 22 (SHEET 2)

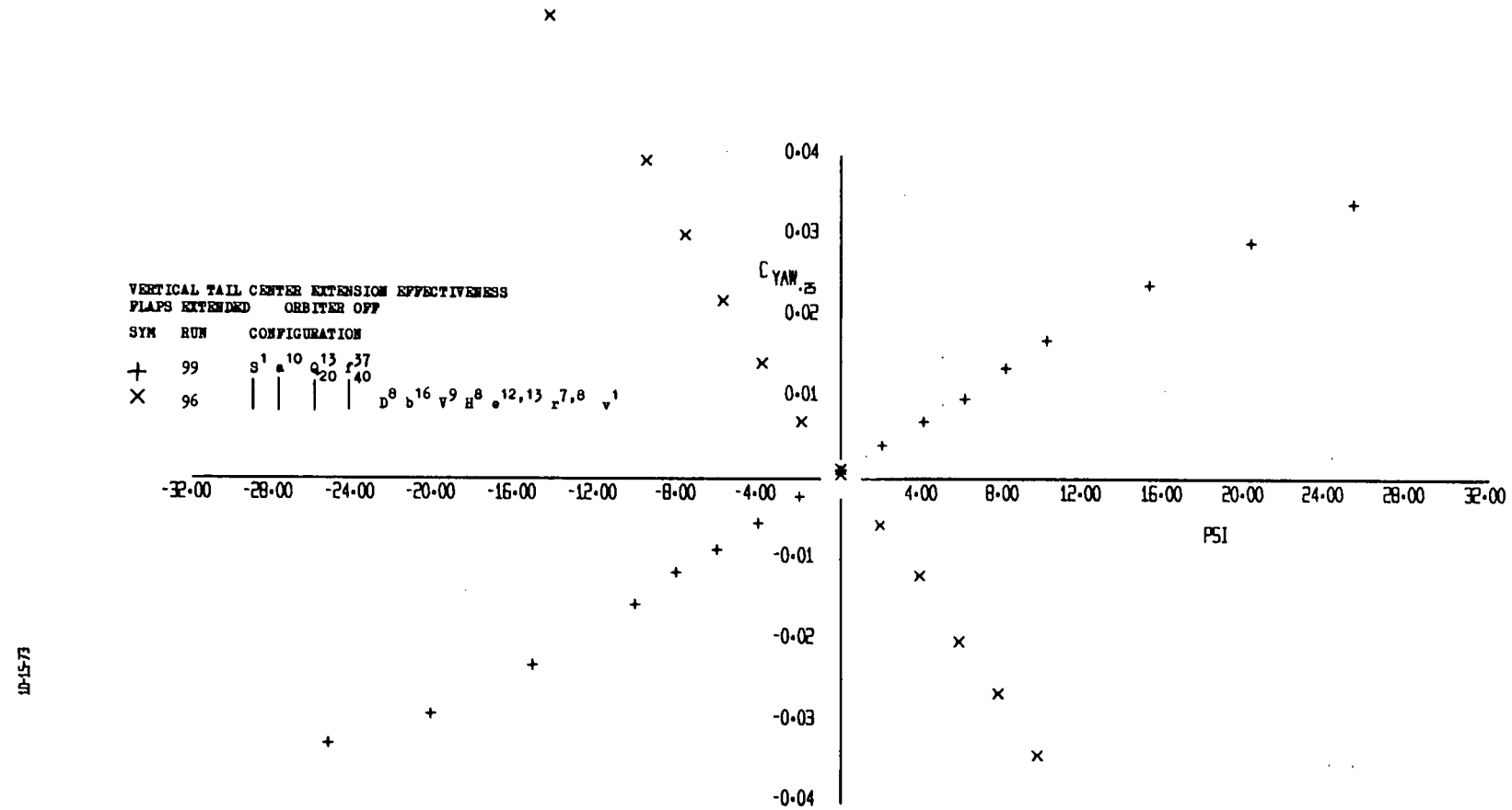

FIGURE 22 (SHEET 3)

VERTICAL TAIL CENTER EXTENSION EFFECTIVENESS
FLAPS EXTENDED ORBITER OFF

SYM	RUN	CONFIGURATION
+	99	S^{1} a^{10} Q^{13}_{20} f^{37}_{40}
×	96	D^{8} b^{16} V^{9} R^{8} $e^{12,13}$ $x^{7,8}$ v^{1}

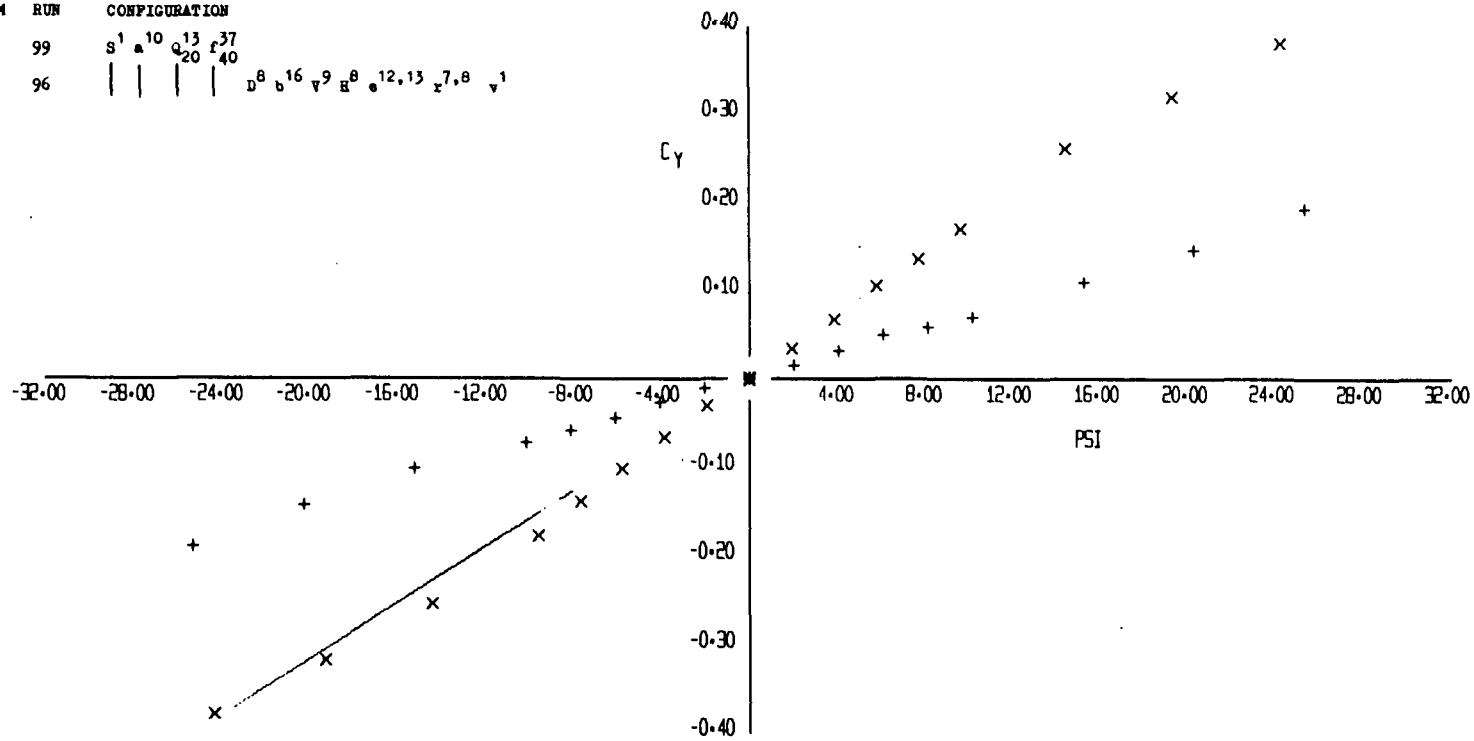

FIGURE 22 (SHEET 4)

VERTICAL TAIL CENTER EXTENSION EFFECTIVENESS
FLAPS EXTENDED ORBITER ON

SYM	RUN	CONFIGURATION
+	87	S^{1} a^{10} g^{13}_{20} f^{37}_{40} $\Delta^{5P}_{0.5}$
×	85	D^{8} b^{16} v^{9} H^{8} $e^{12,13}$ $r^{7,8}$ v^{1}

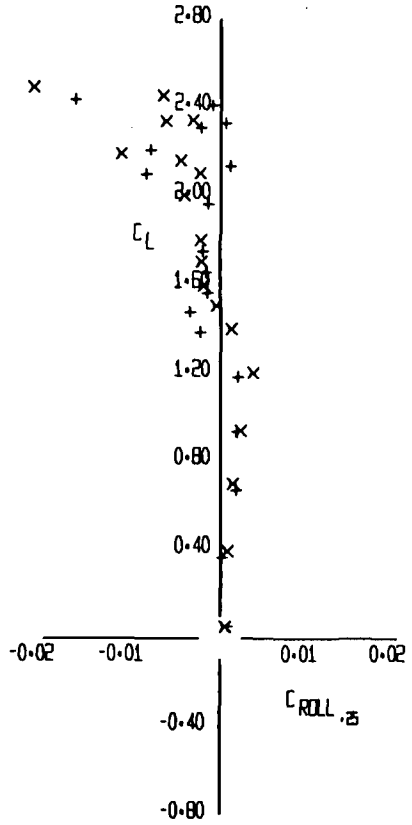

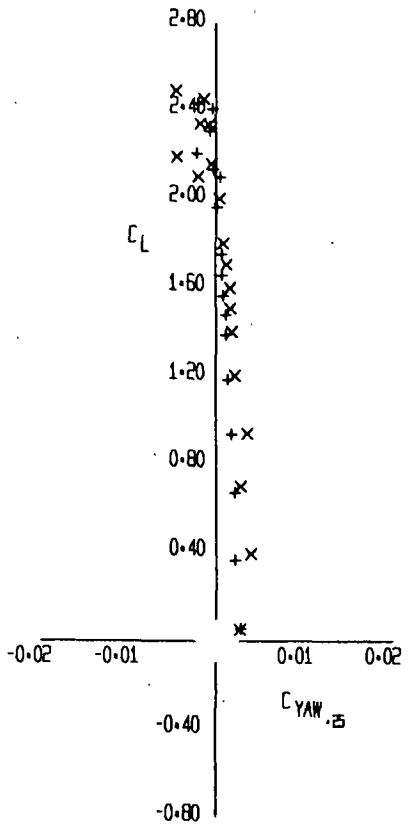

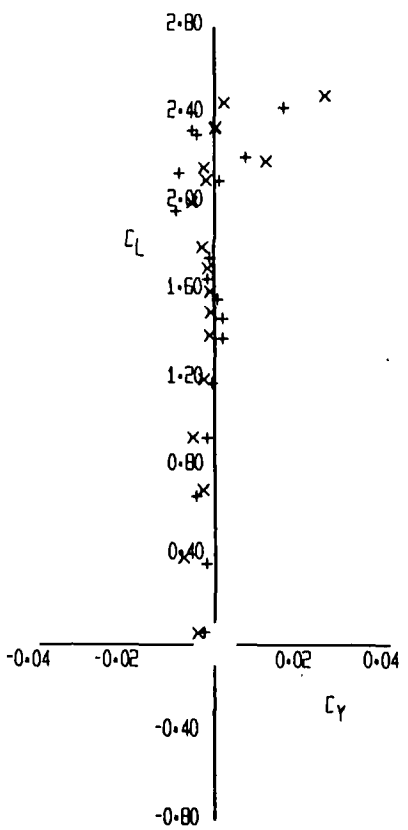

87 85
+ ×

10-15-73

Page A-124

LP-3BH

FIGURE 23 (SHEET 1)

FIGURE 23 (SHEET 2)

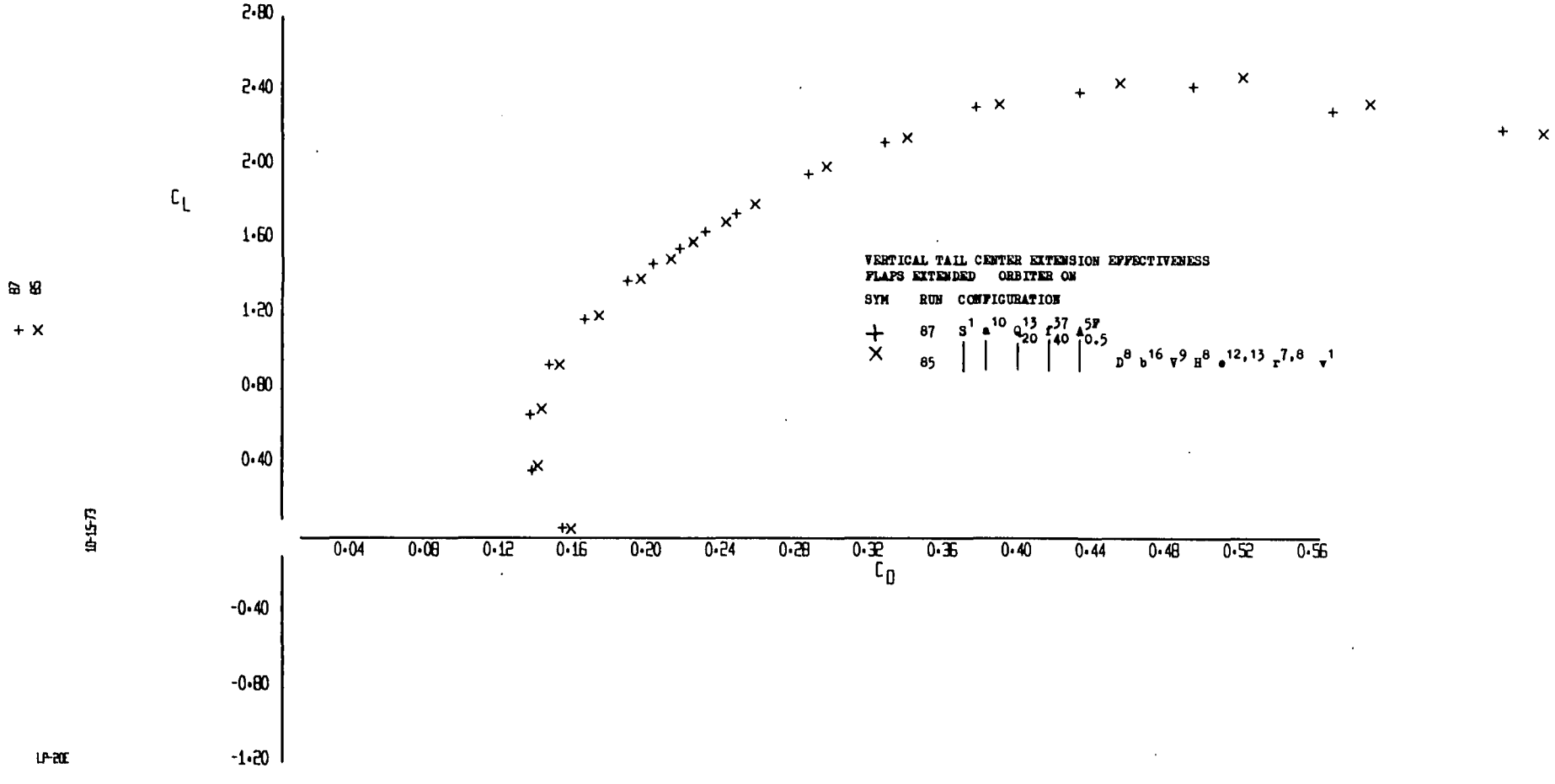

FIGURE 23 (SHEET 3)

VERTICAL TAIL CENTER EXTENSION EFFECTIVENESS
FLAPS EXTENDED ORBITER ON

SYM	RUN	CONFIGURATION
+	87	$S^{1}\ a^{10}\ c^{13}_{20}\ f^{37}_{40}\ \Delta^{5F}_{0.5}\ D^{8}\ b^{16}\ v^{9}\ H^{8}\ e^{12,13}\ r^{7,8}\ w^{1}$
×	85	

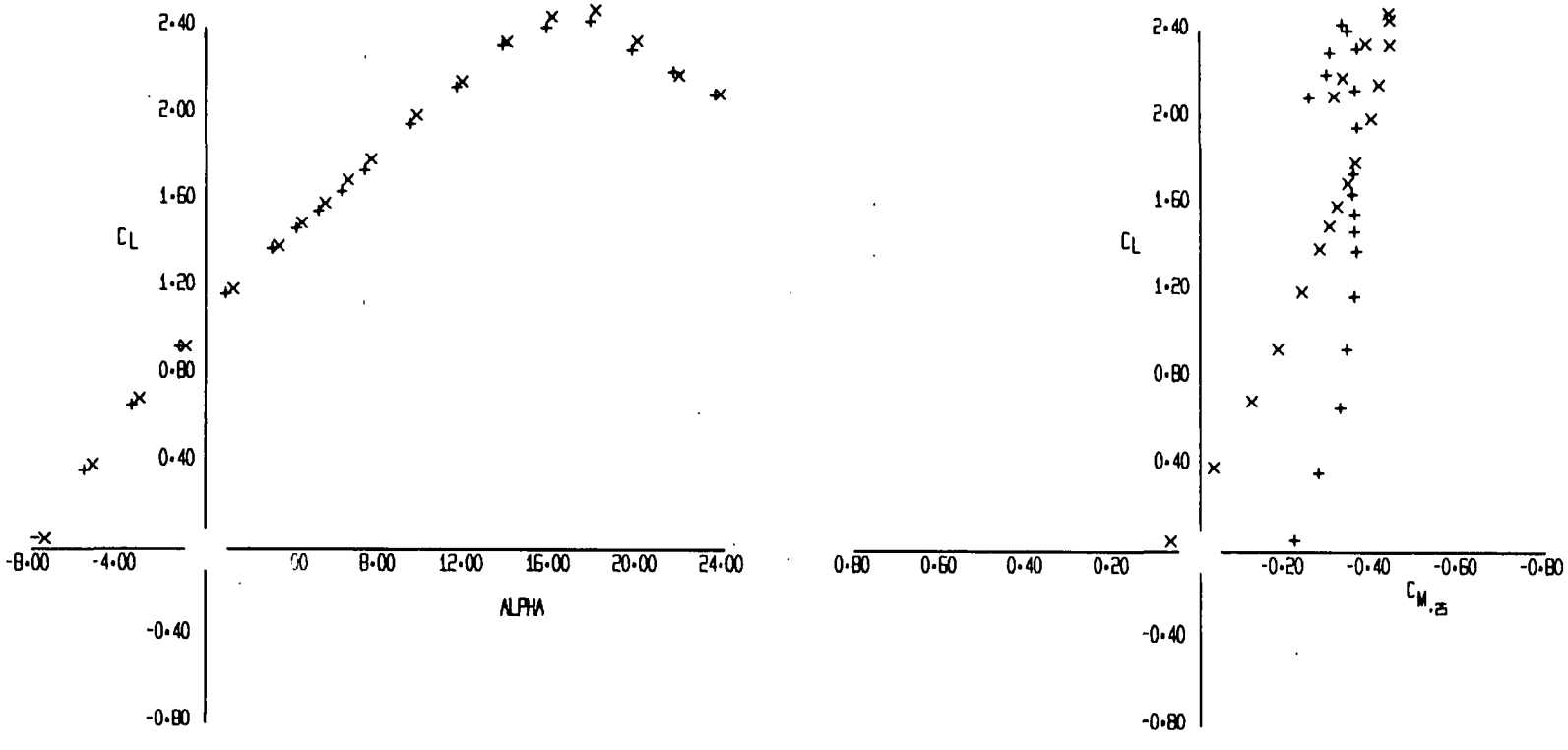

87 85
+ ×

10-15-73

Page A-127

LP-18A

FIGURE 23 (SHEET 4)

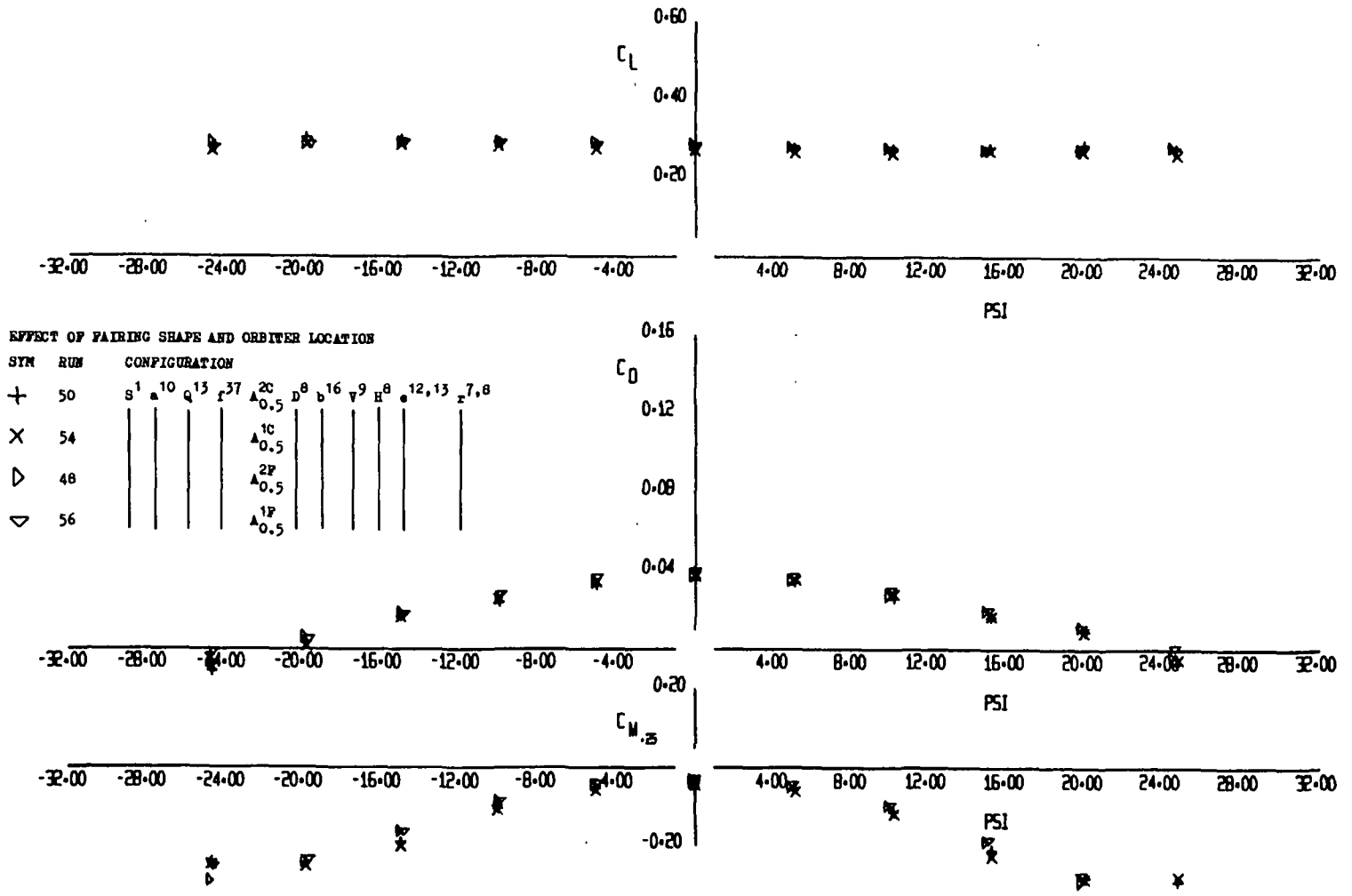

FIGURE 24 (SHEET 1)

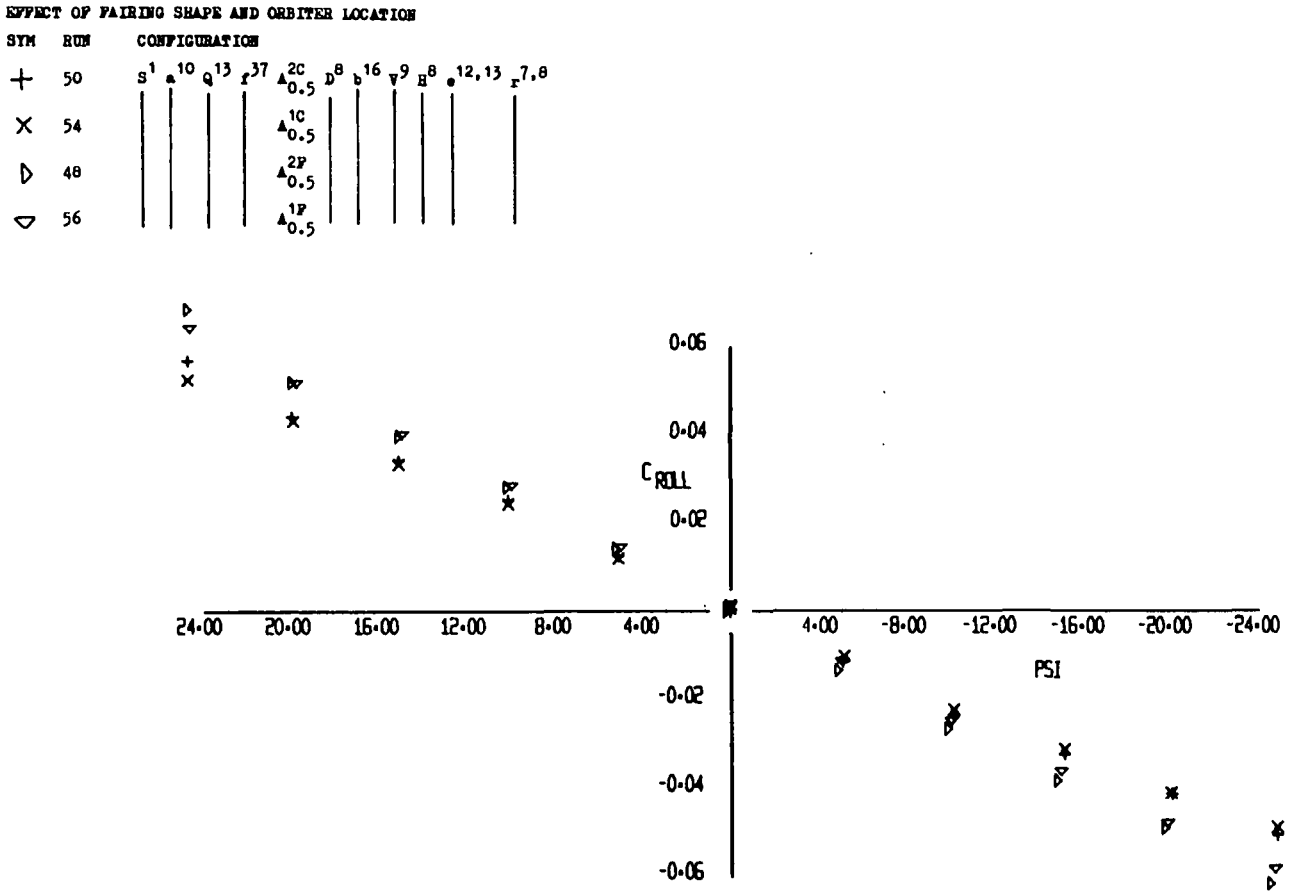

FIGURE 24 (SHEET 2)

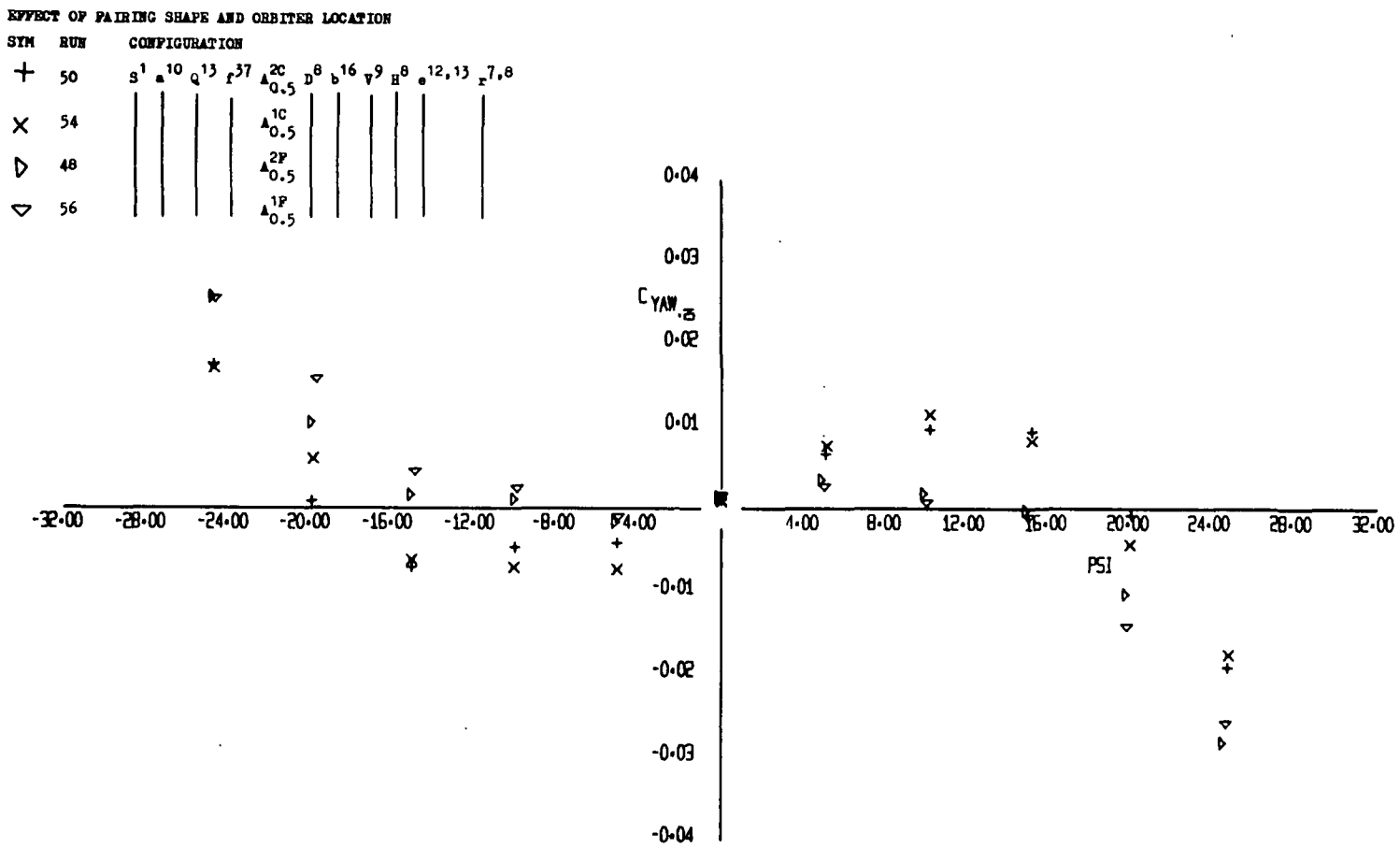

FIGURE 24 (SHEET 3)

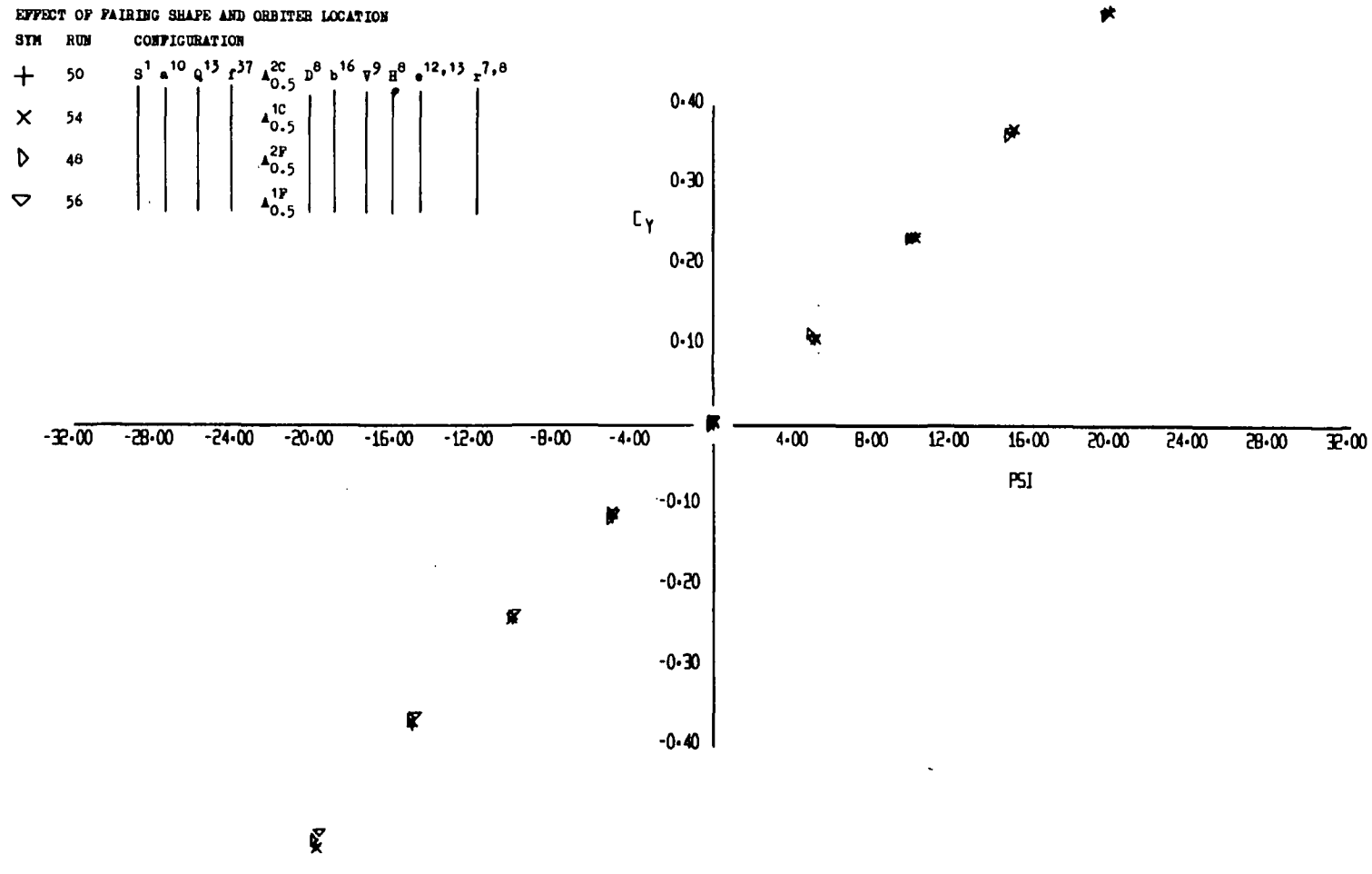

FIGURE 24 (SHEET 4)

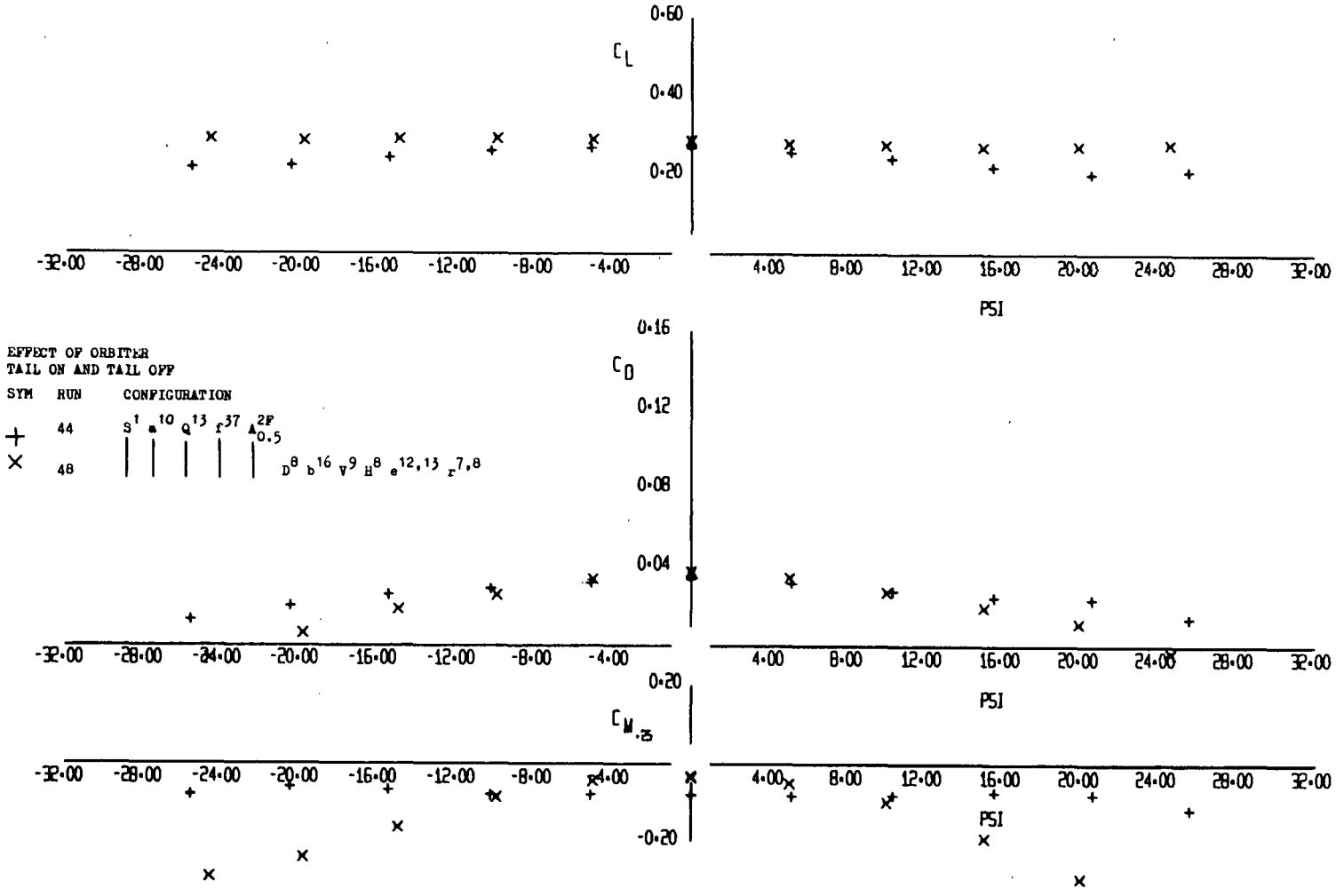

FIGURE 25 (SHEET 1)

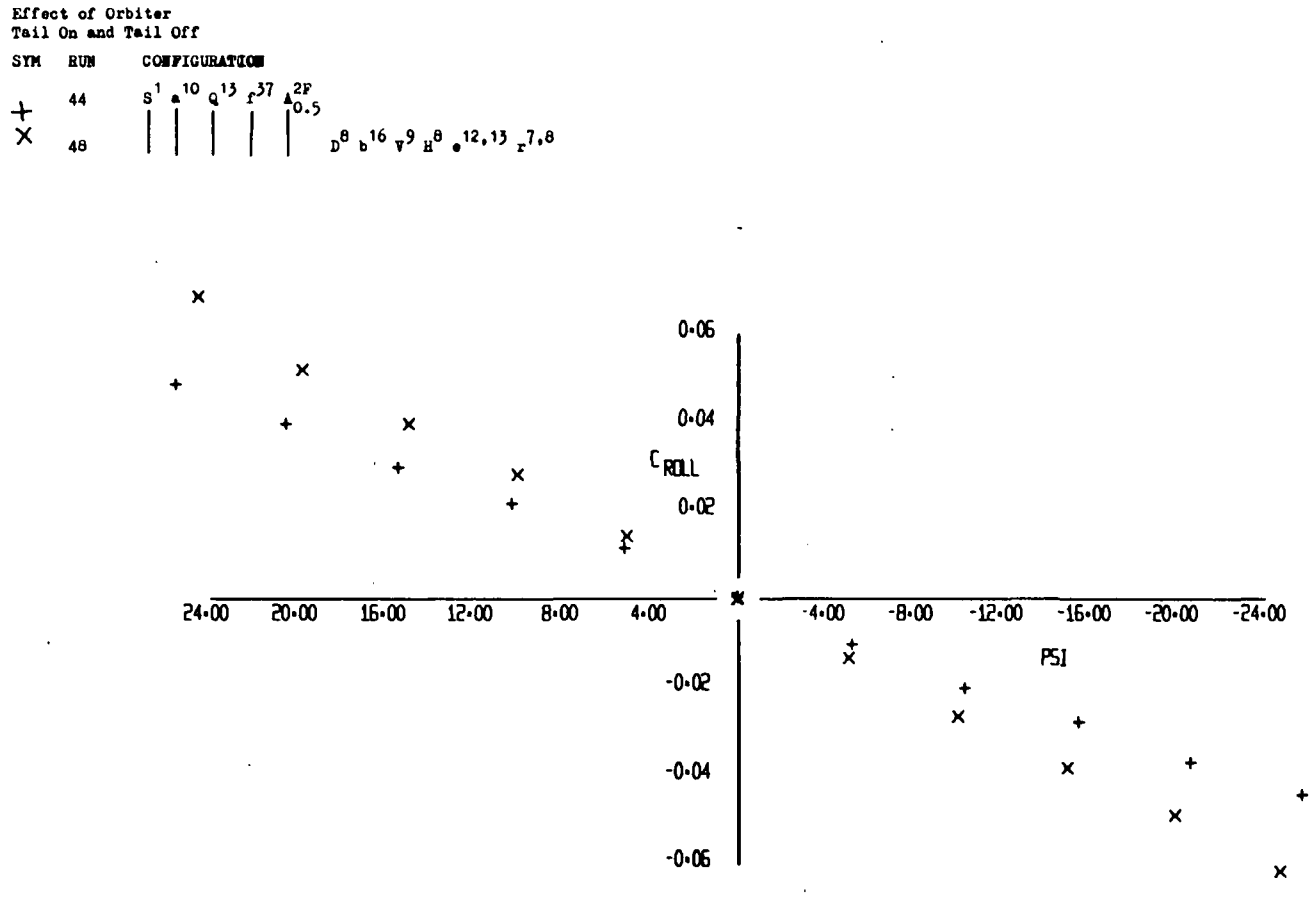

FIGURE 25 (SHEET 2)

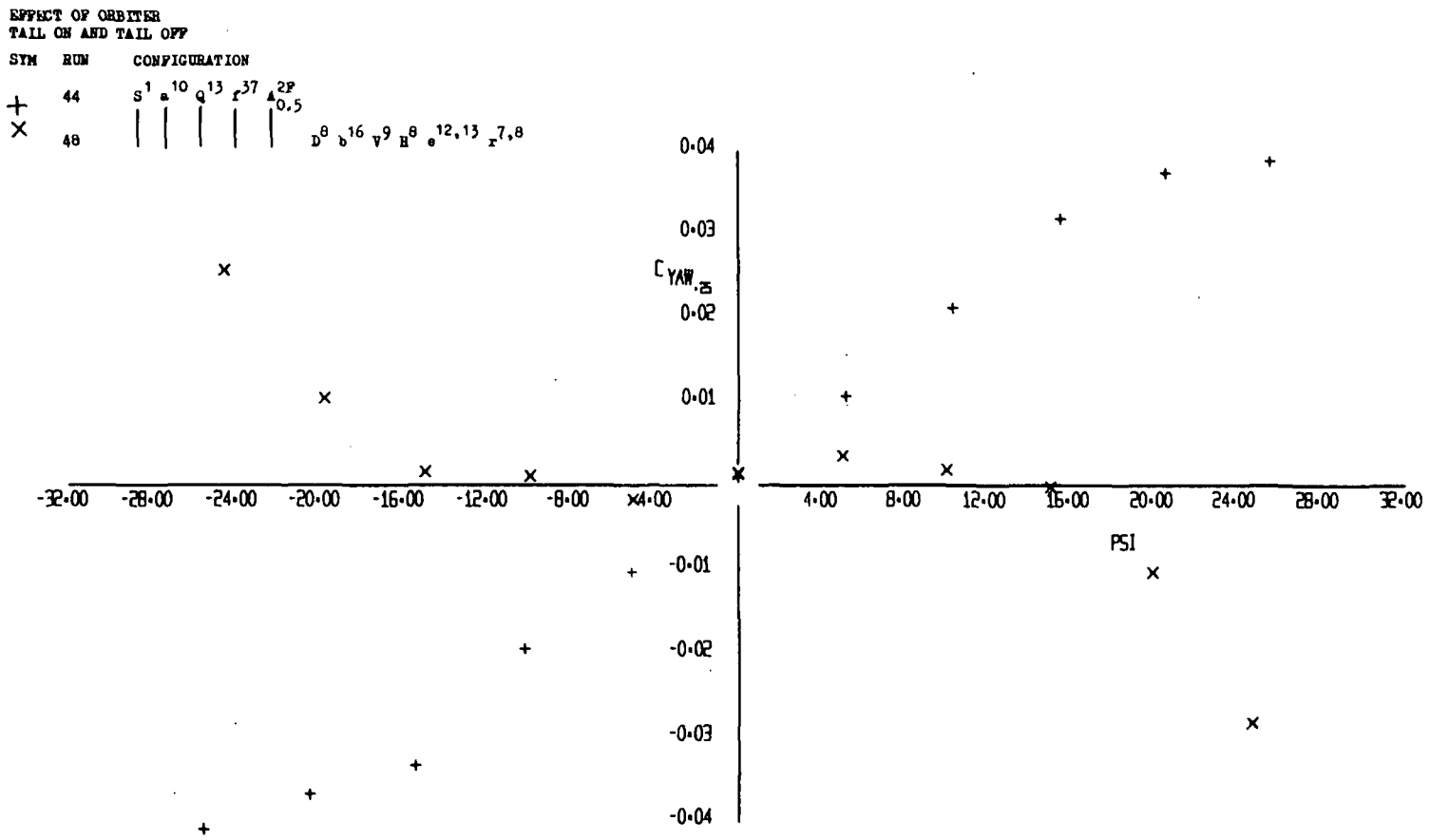

FIGURE 25 (SHEET 3)

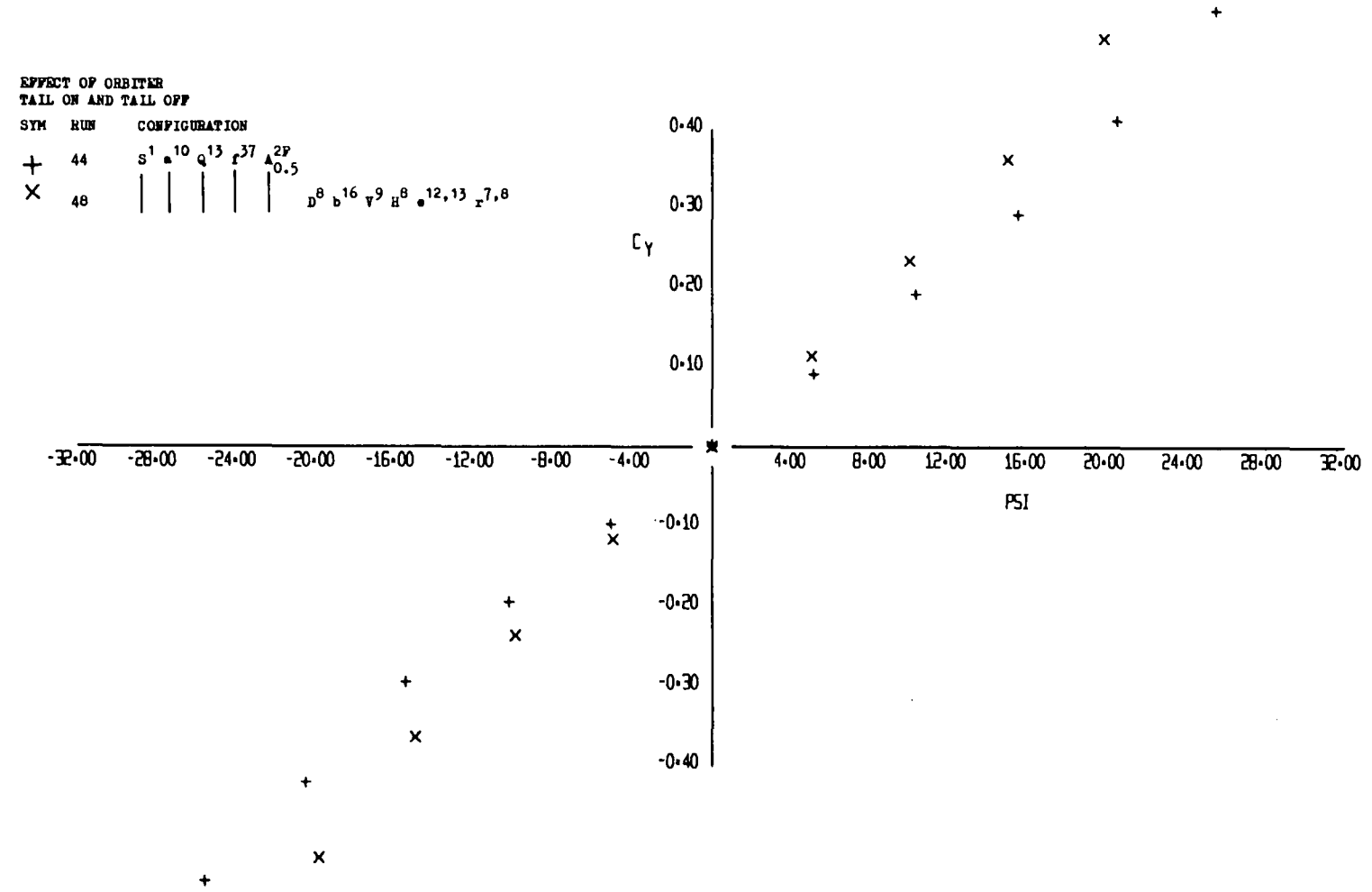

FIGURE 25 (SHEET 4)

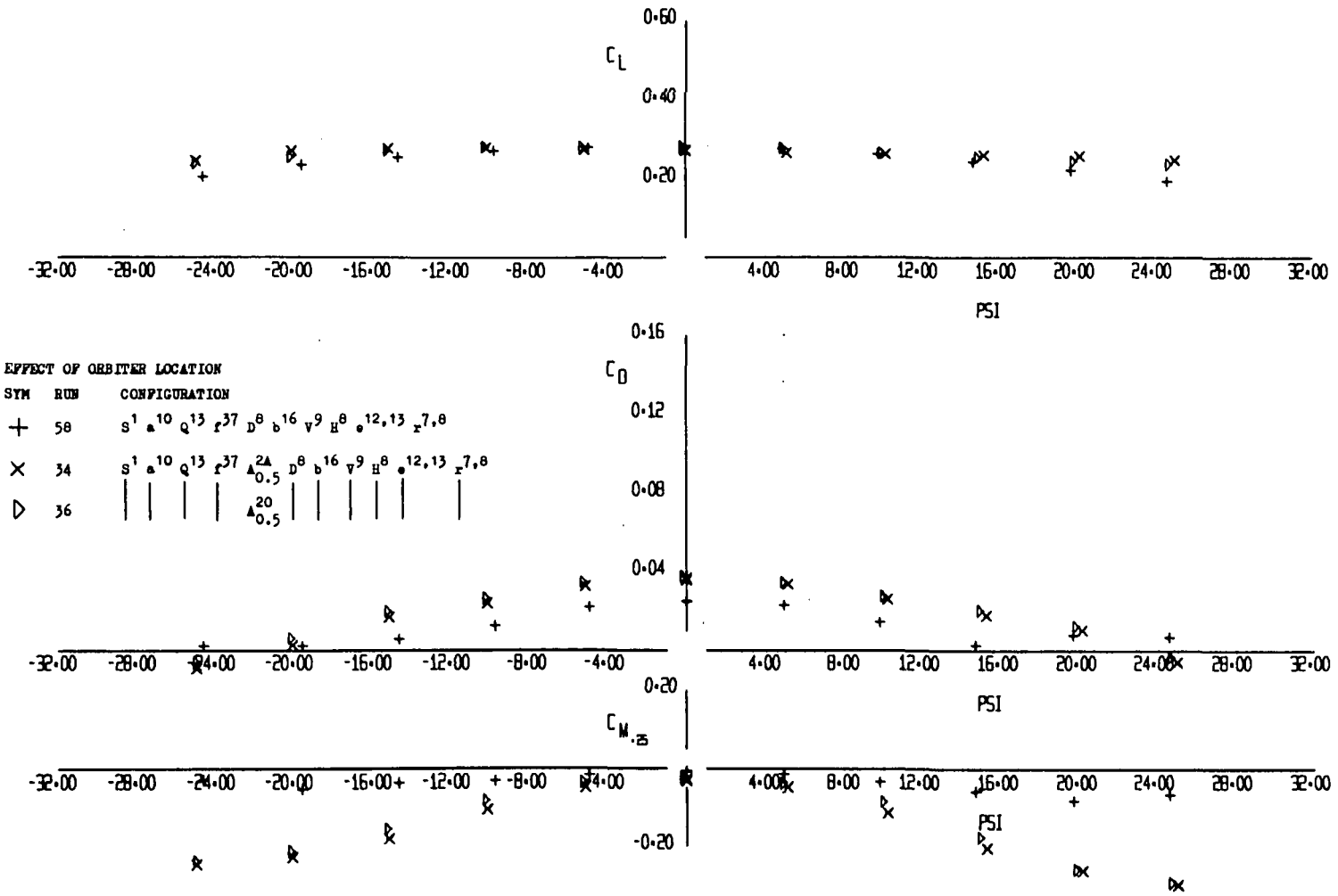

FIGURE 26 (SHEET 1)

EFFECT OF ORBITER LOCATION

SYM	RUN	CONFIGURATION
+	58	$S^{1}\ a^{10}\ Q^{13}\ f^{37}\ D^{8}\ b^{16}\ V^{9}\ H^{8}\ e^{12,13}\ r^{7,8}$
×	34	$S^{1}\ a^{10}\ Q^{13}\ f^{37}\ \blacktriangle^{2A}_{0.5}\ D^{8}\ b^{16}\ V^{9}\ H^{8}\ e^{12,13}\ r^{7,8}$
▷	36	$\blacktriangle^{20}_{0.5}$

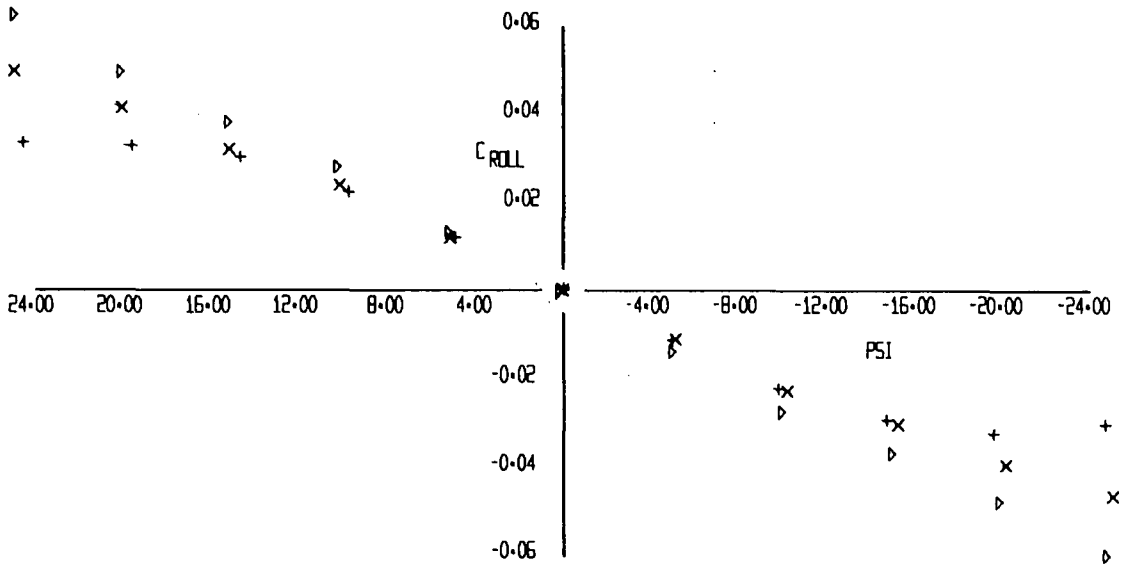

58 34 36

+ × ▷

10-15-73

Page A-137

L7-408

FIGURE 26 (SHEET 2)

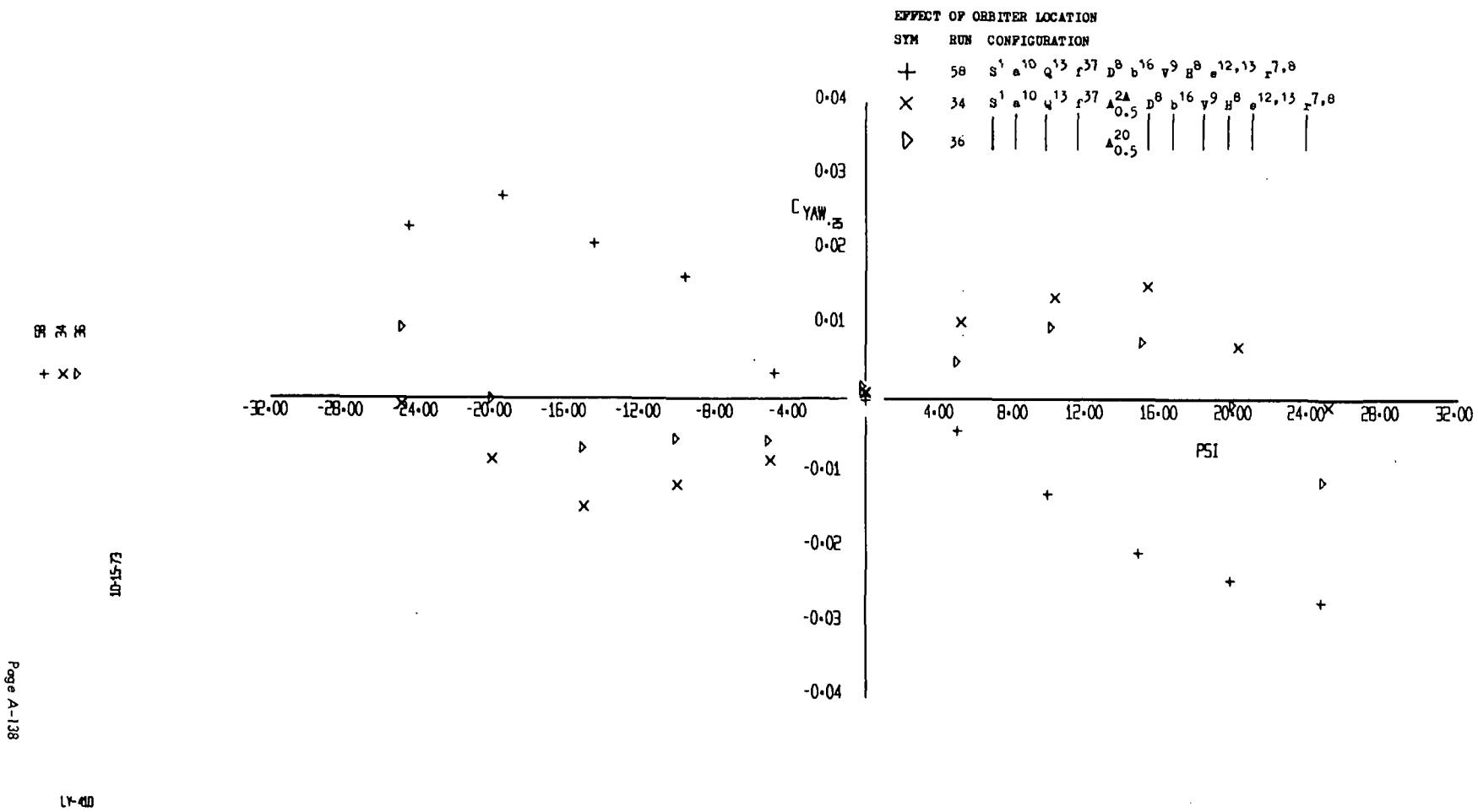

FIGURE 26 (SHEET 3)

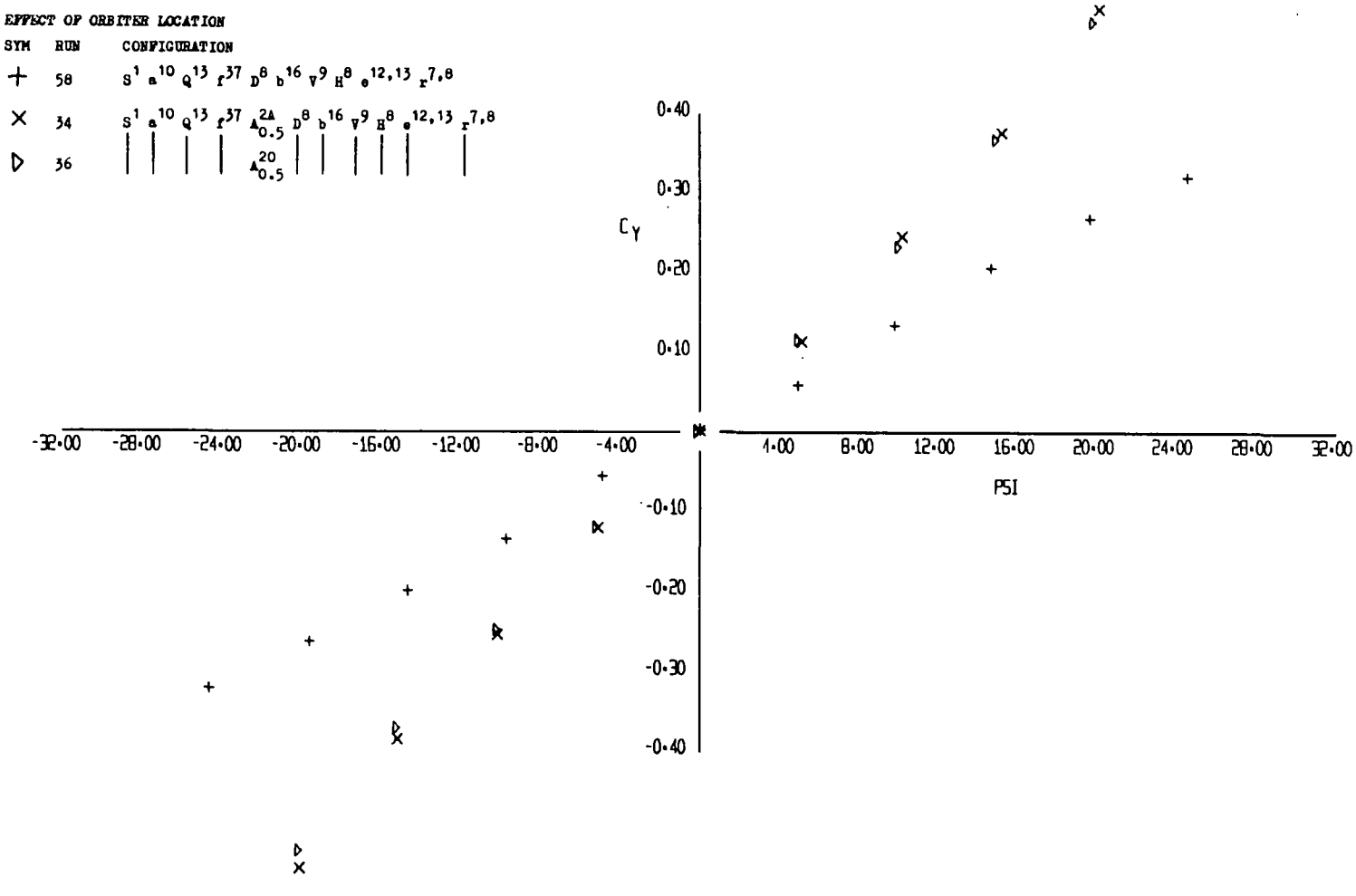

FIGURE 26 (SHEET 4)

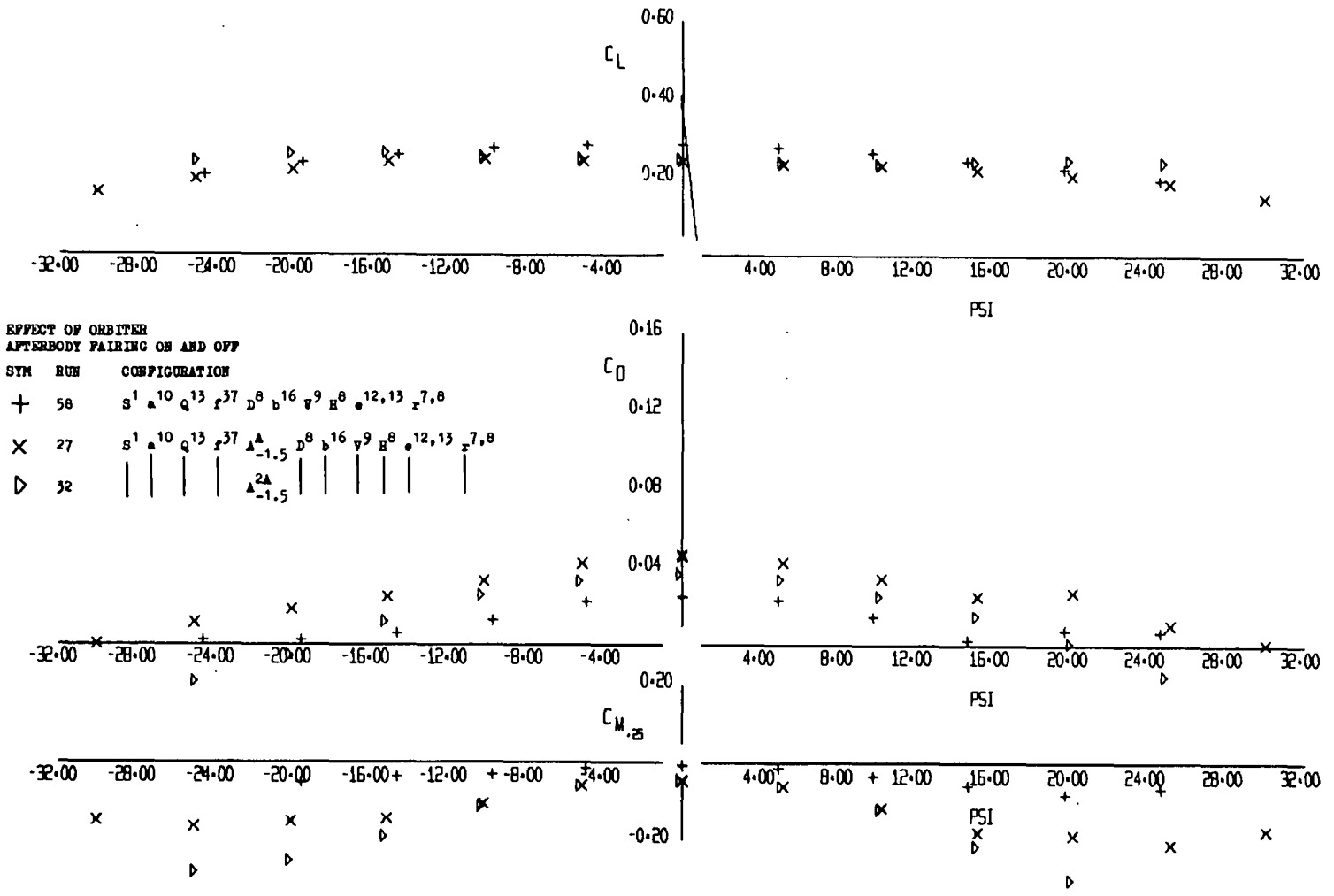

FIGURE 27 (SHEET 1)

EFFECT OF ORBITER
AFTERBODY FAIRING ON AND OFF

SYM	RUN	CONFIGURATION
+	58	$S^{1}\ a^{10}\ Q^{13}\ f^{37}\ D^{8}\ b^{16}\ V^{9}\ H^{8}\ e^{12,13}\ r^{7,8}$
×	27	$S^{1}\ a^{10}\ Q^{13}\ f^{37}\ A^{A}_{-1.5}\ D^{8}\ b^{16}\ V^{9}\ H^{8}\ e^{12,13}\ r^{7,8}$
▷	32	$A^{2A}_{-1.5}$

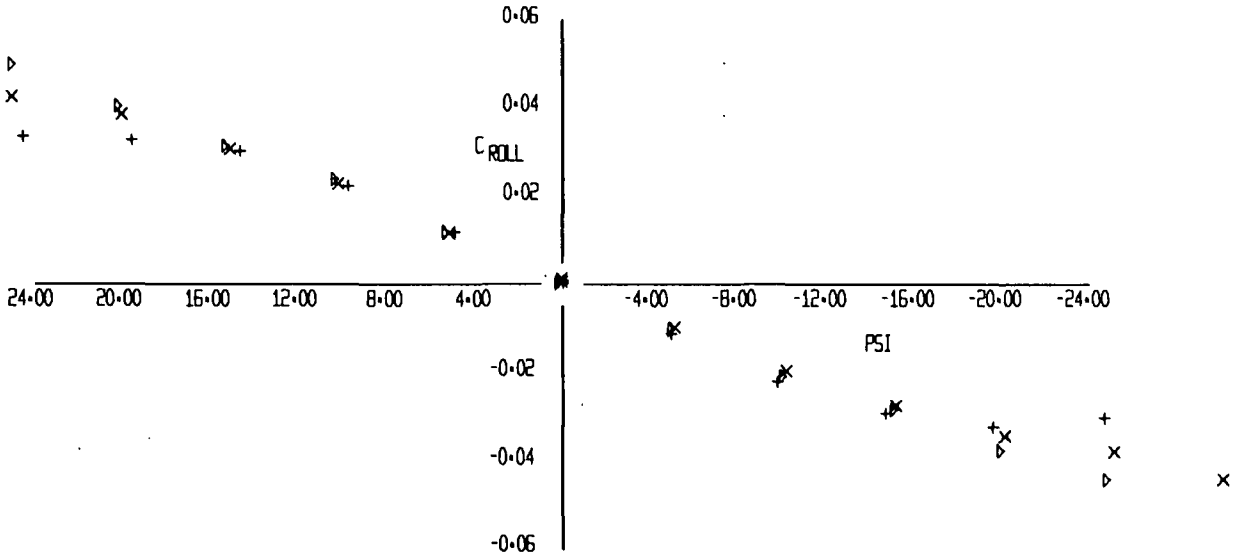

FIGURE 27 (SHEET 2)

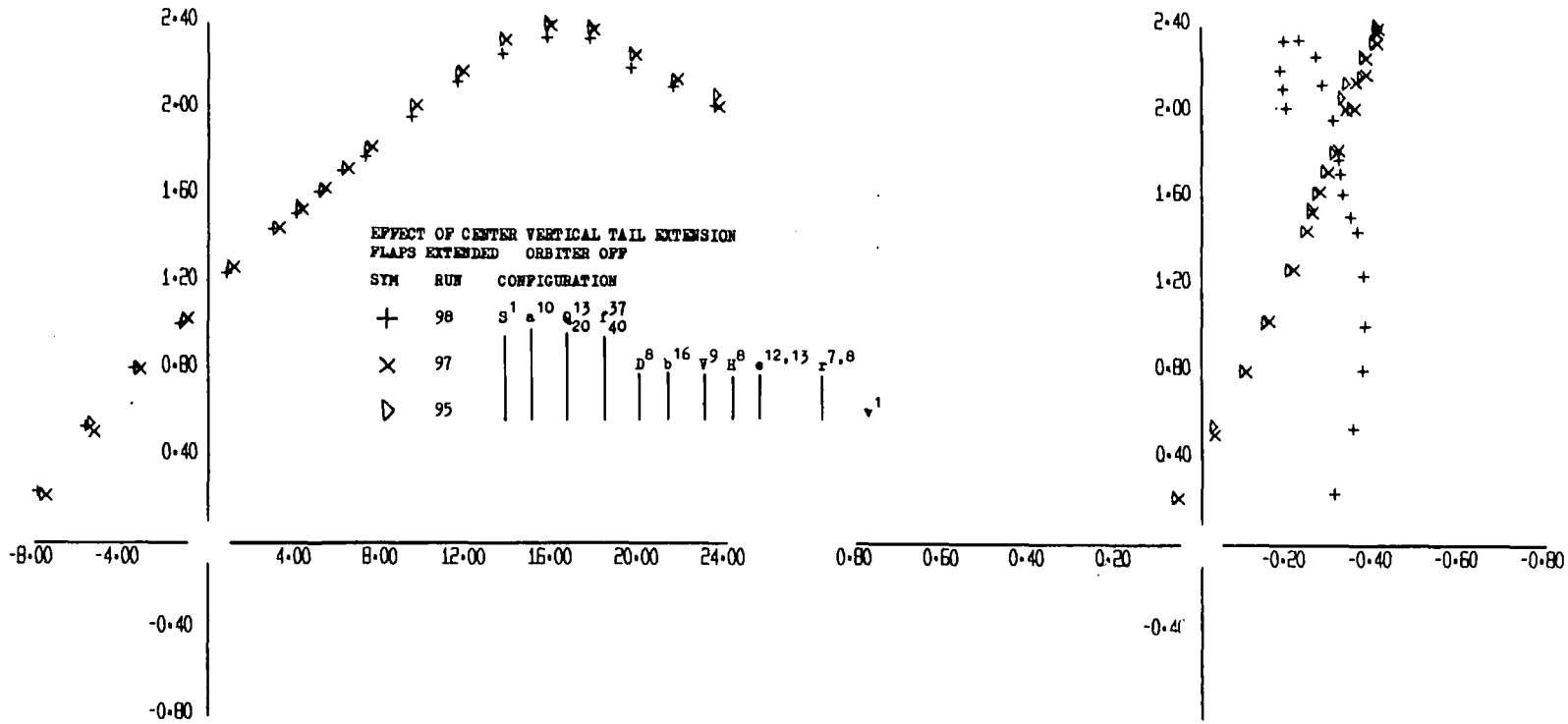

FIGURE 28 (SHEET 1)

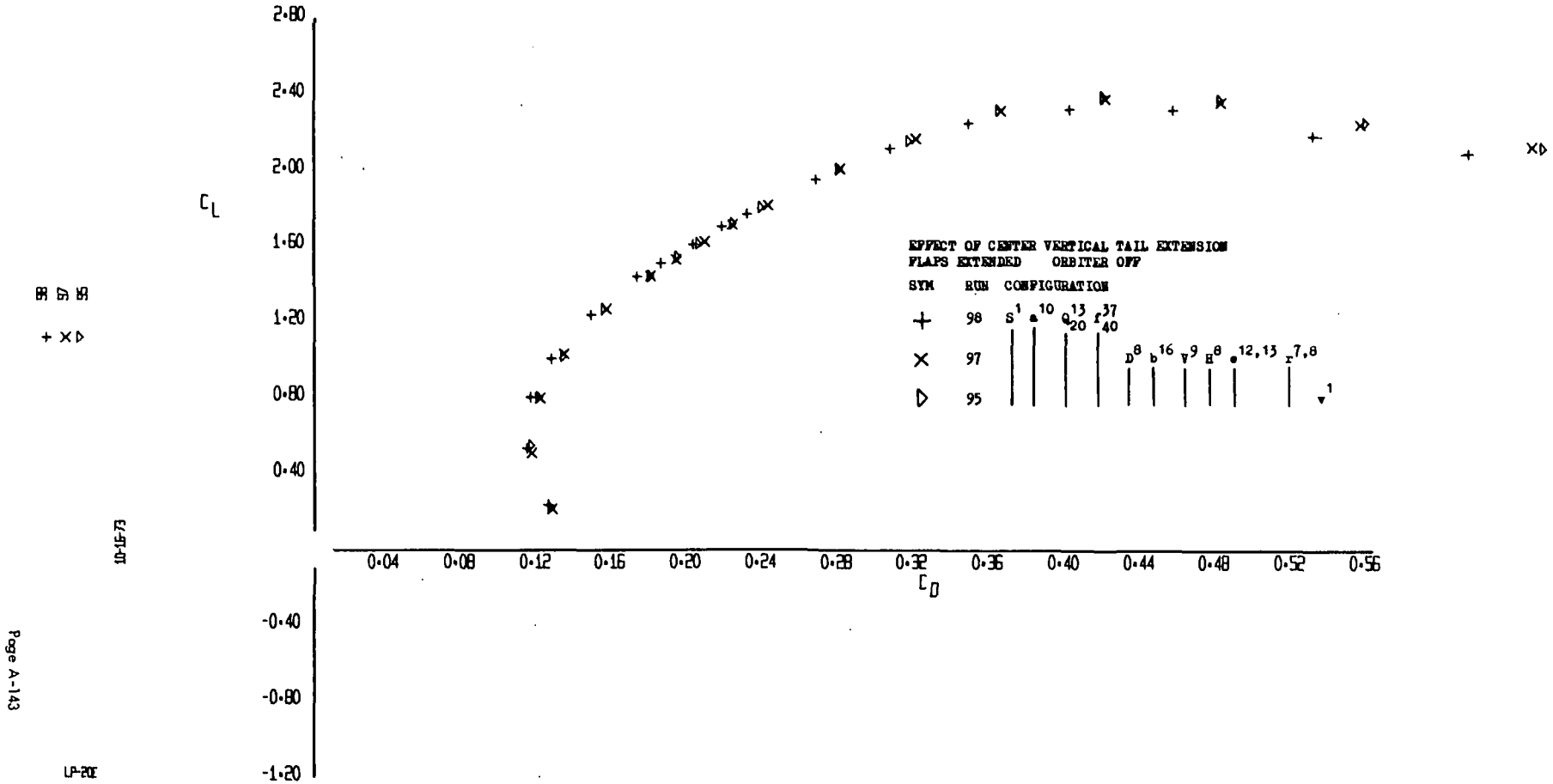

FIGURE 28 (SHEET 2)

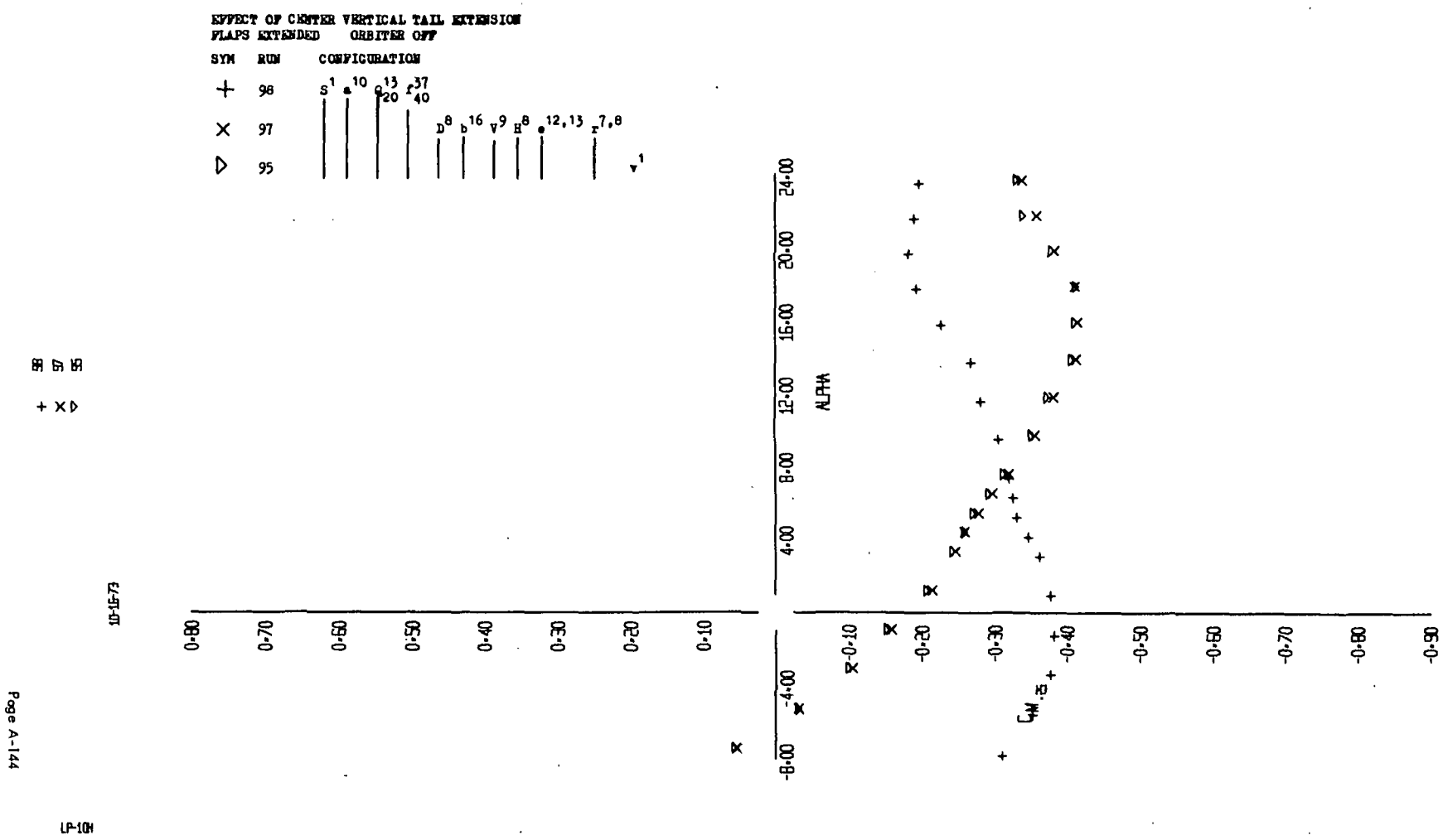

FIGURE 28 (SHEET 3)

EFFECT OF CENTER VERTICAL TAIL EXTENSION
FLAPS EXTENDED ORBITER OFF

SYM	RUN	CONFIGURATION
+	98	S^{1} a^{10} Q^{13}_{20} f^{37}_{40} D^{8} b^{16} V^{9} H^{8} $e^{12,13}$ $r^{7,8}$ v^{1}
×	97	
▷	95	

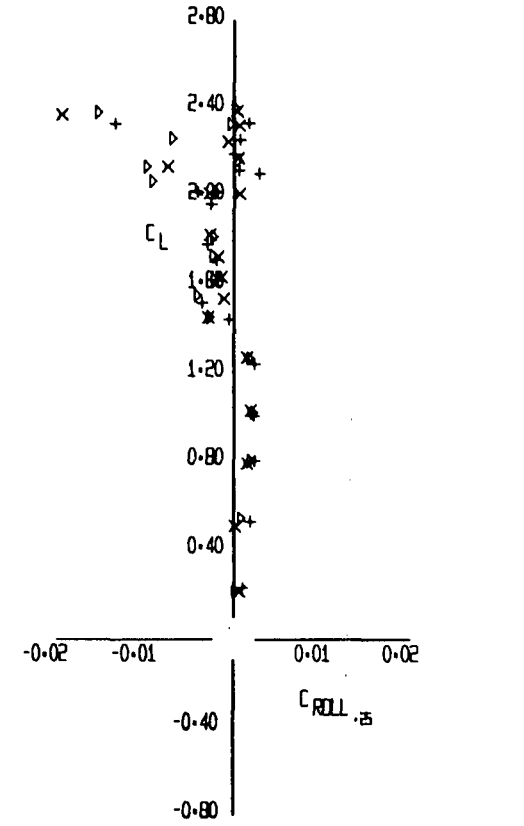

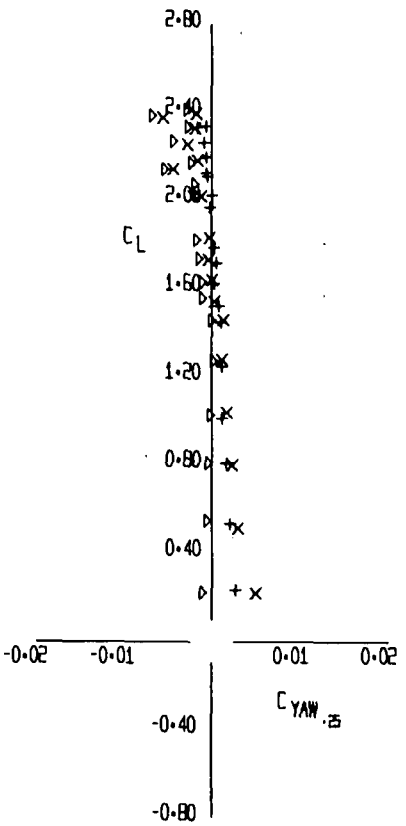

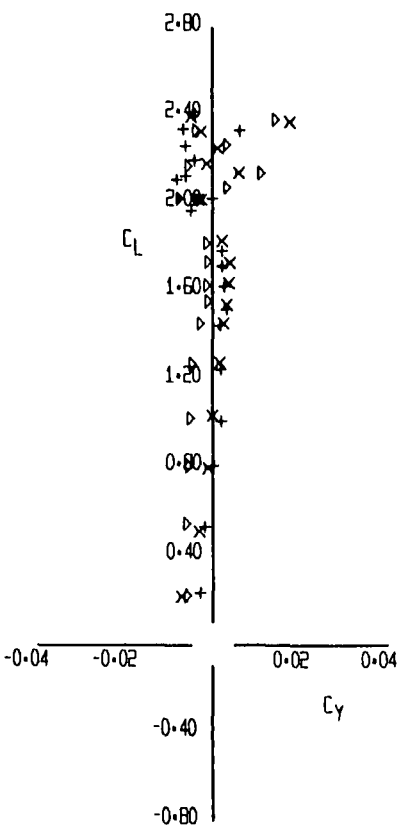

FIGURE 28 (SHEET 4)

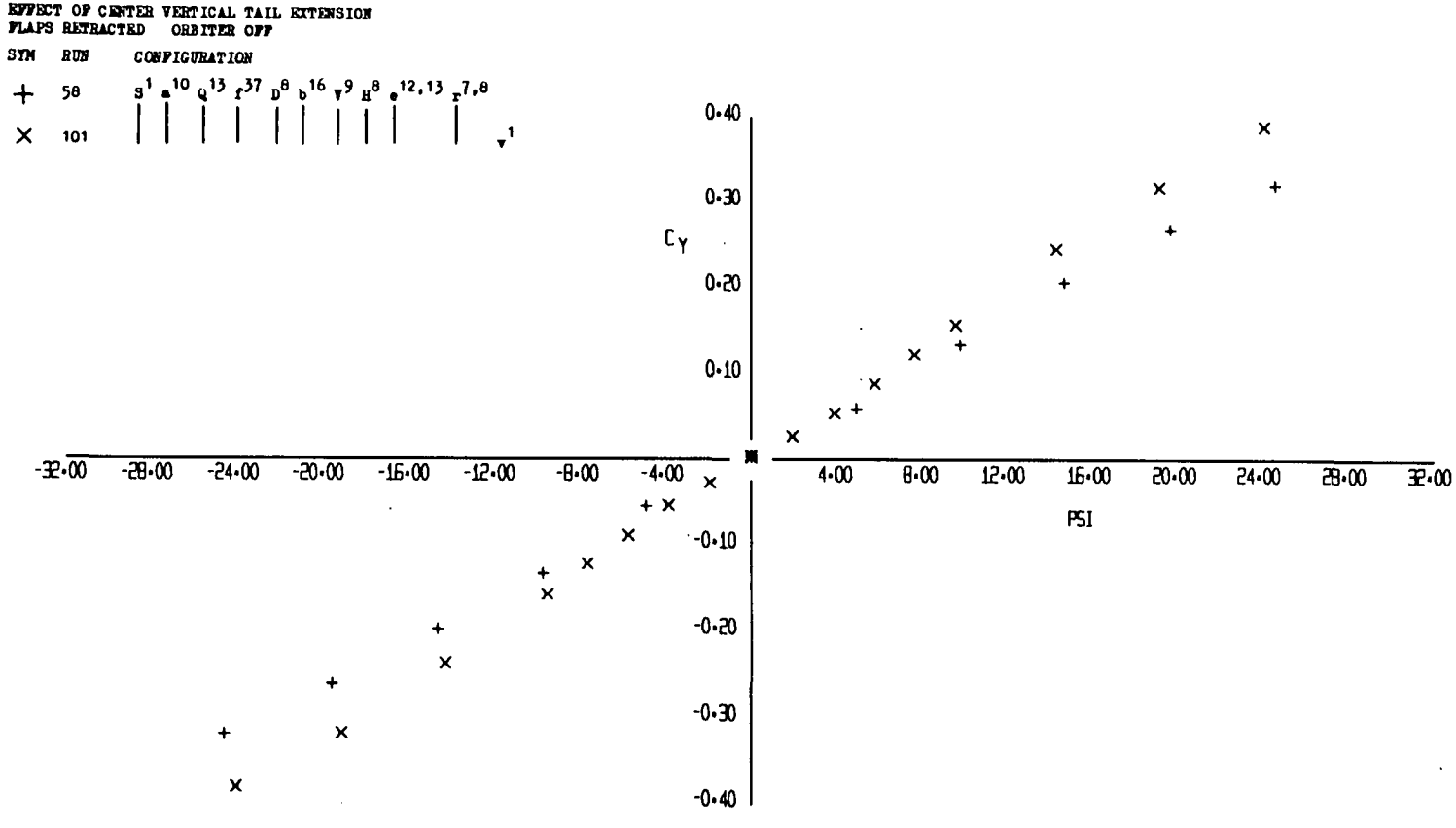

FIGURE 29 (SHEET 1)

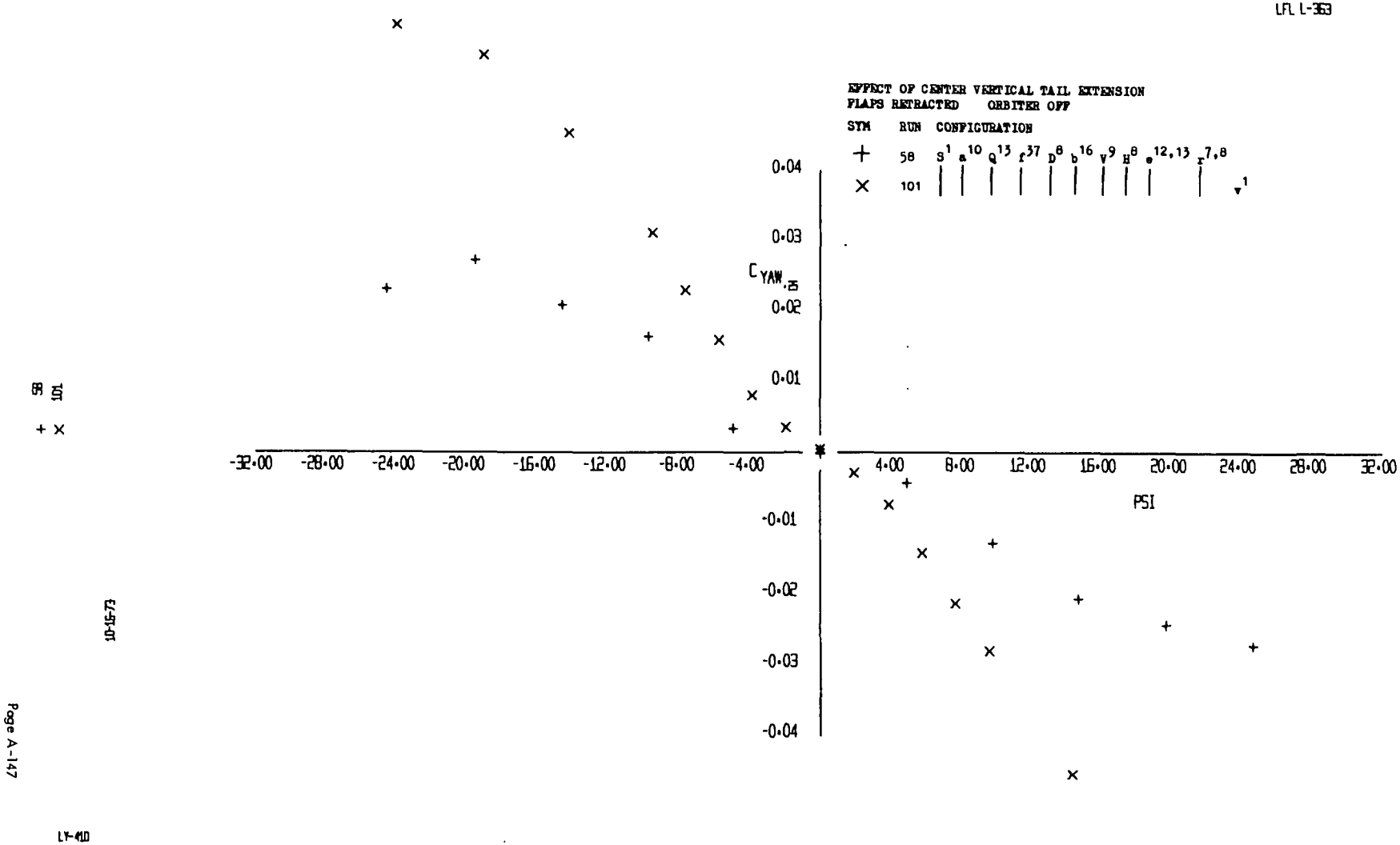

FIGURE 29 (SHEET 2)

EFFECT OF CENTER VERTICAL TAIL EXTENSION
FLAPS RETRACTED ORBITER OFF

SYM	RUN	CONFIGURATION
+	58	S^{1} a^{10} Q^{13} f^{37} D^{8} b^{16} V^{9} B^{8} $\bullet^{12,13}$ $r^{7,8}$
×	101	v^{1}

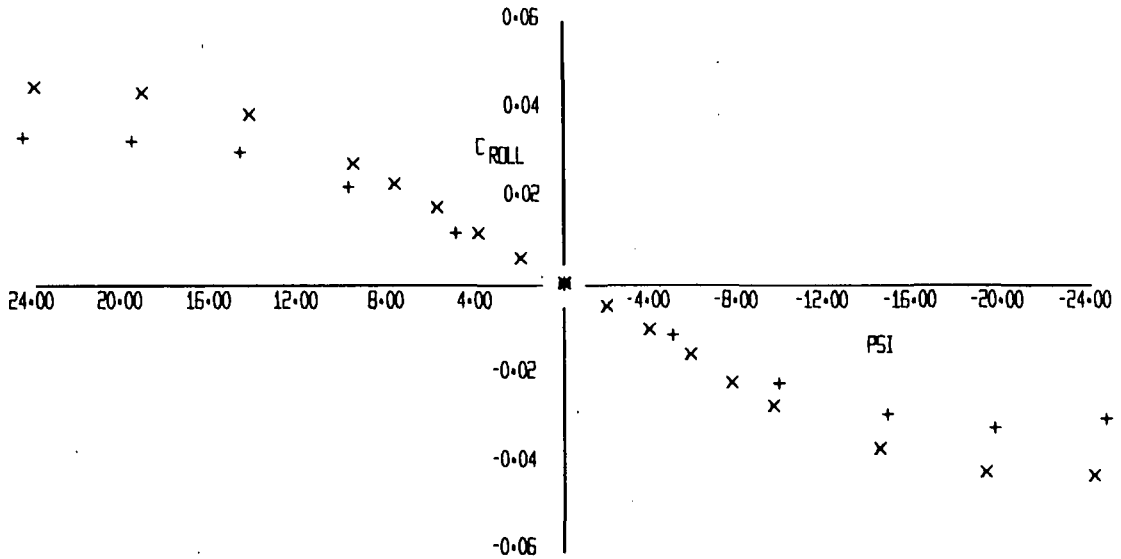

58 101

10-15-73

Page A-148

LF-408

FIGURE 29 (SHEET 3)

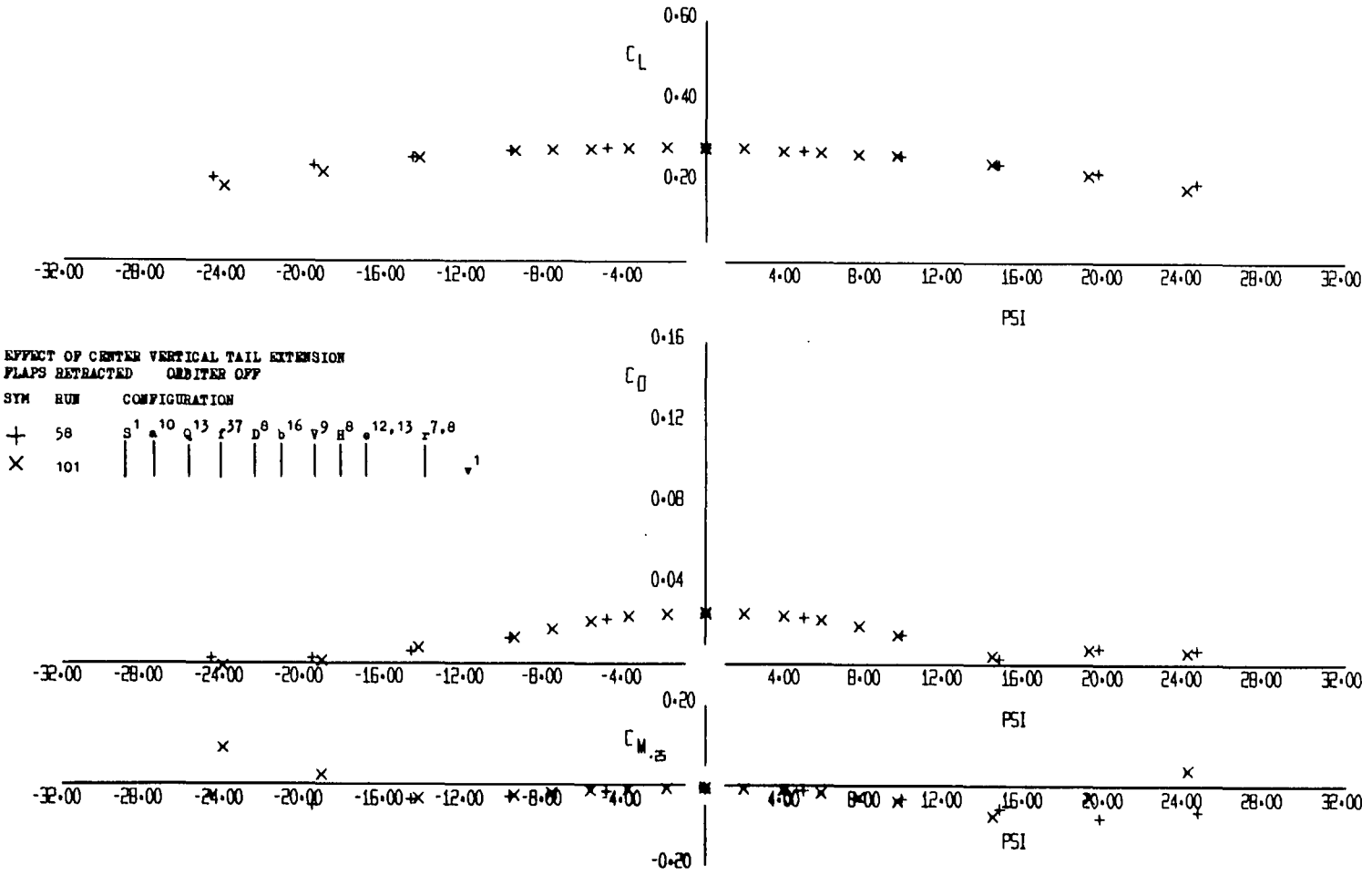

FIGURE 29 (SHEET 4)

FIGURE 29 (SHEET 5)

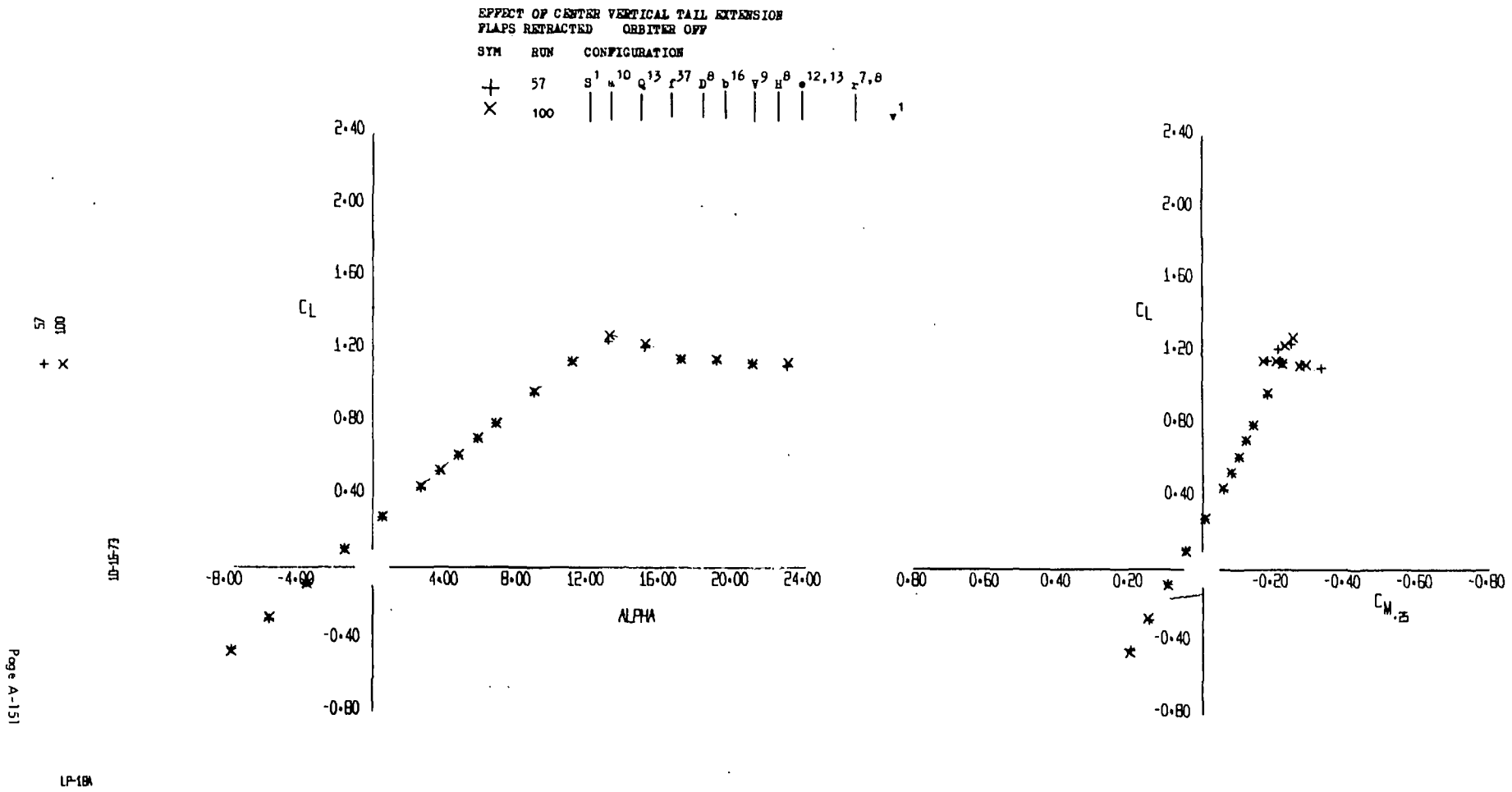

FIGURE 30 (SHEET 1)

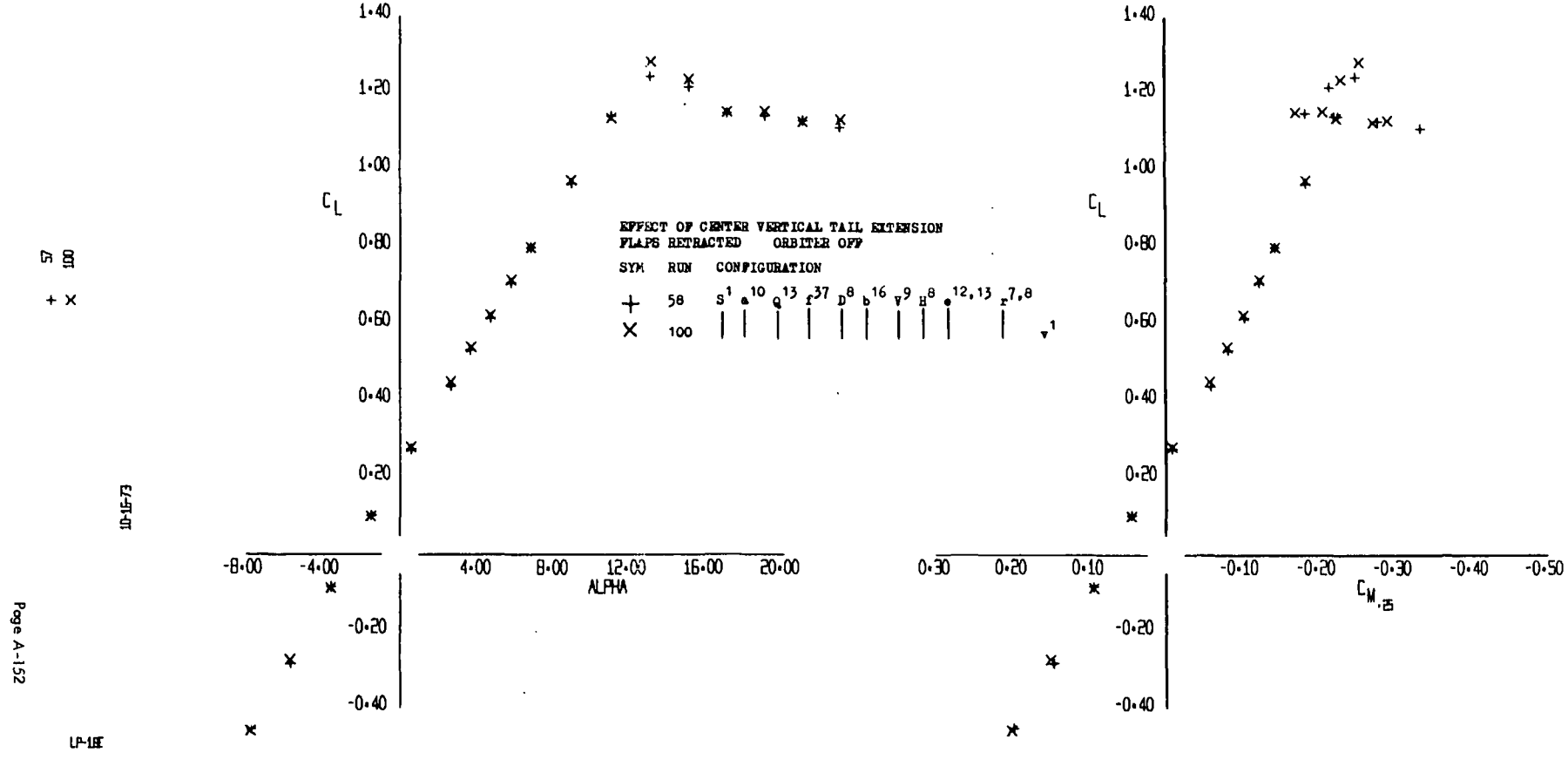

FIGURE 30 (SHEET 2)

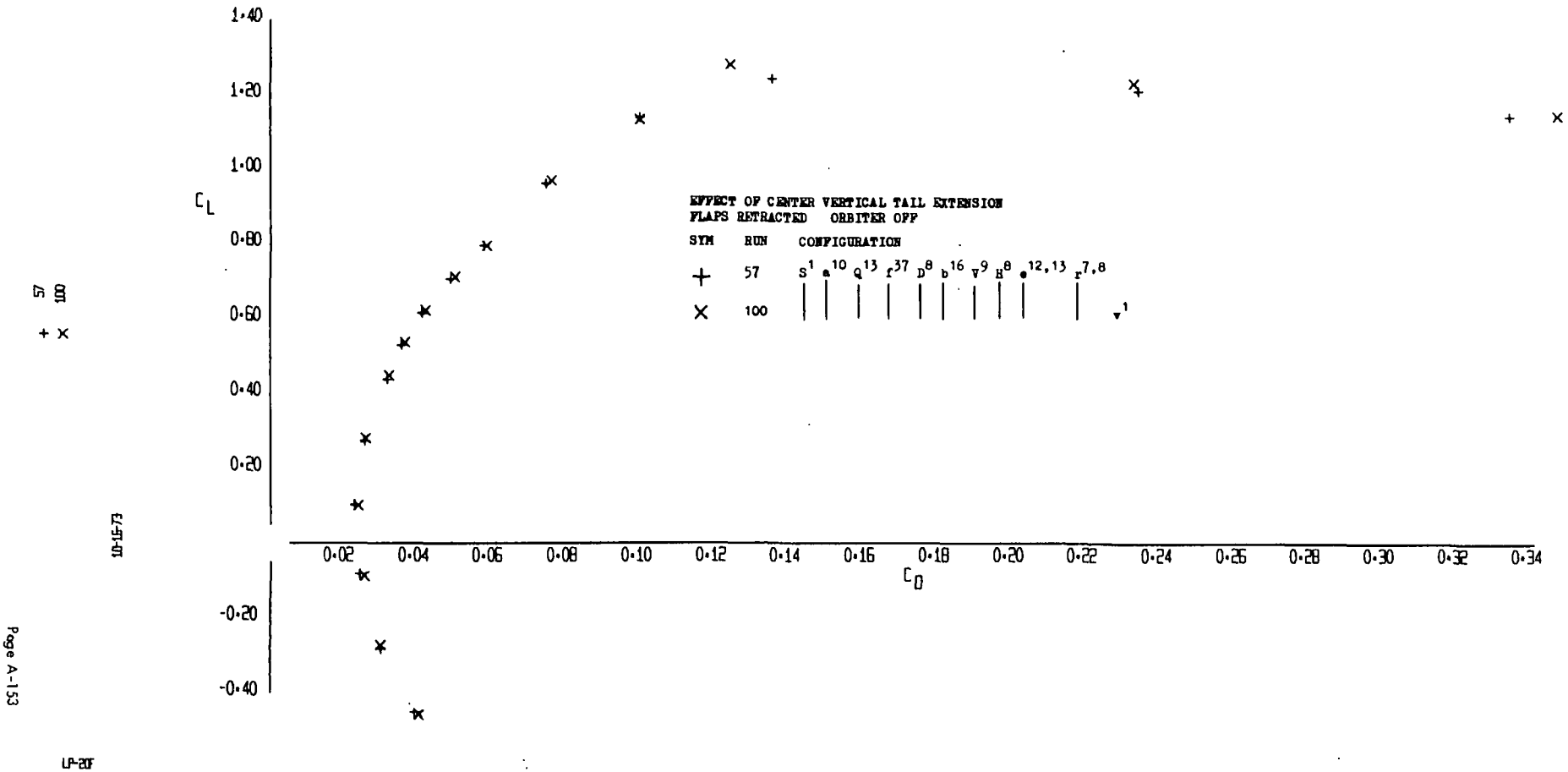

FIGURE 30 (SHEET 3)

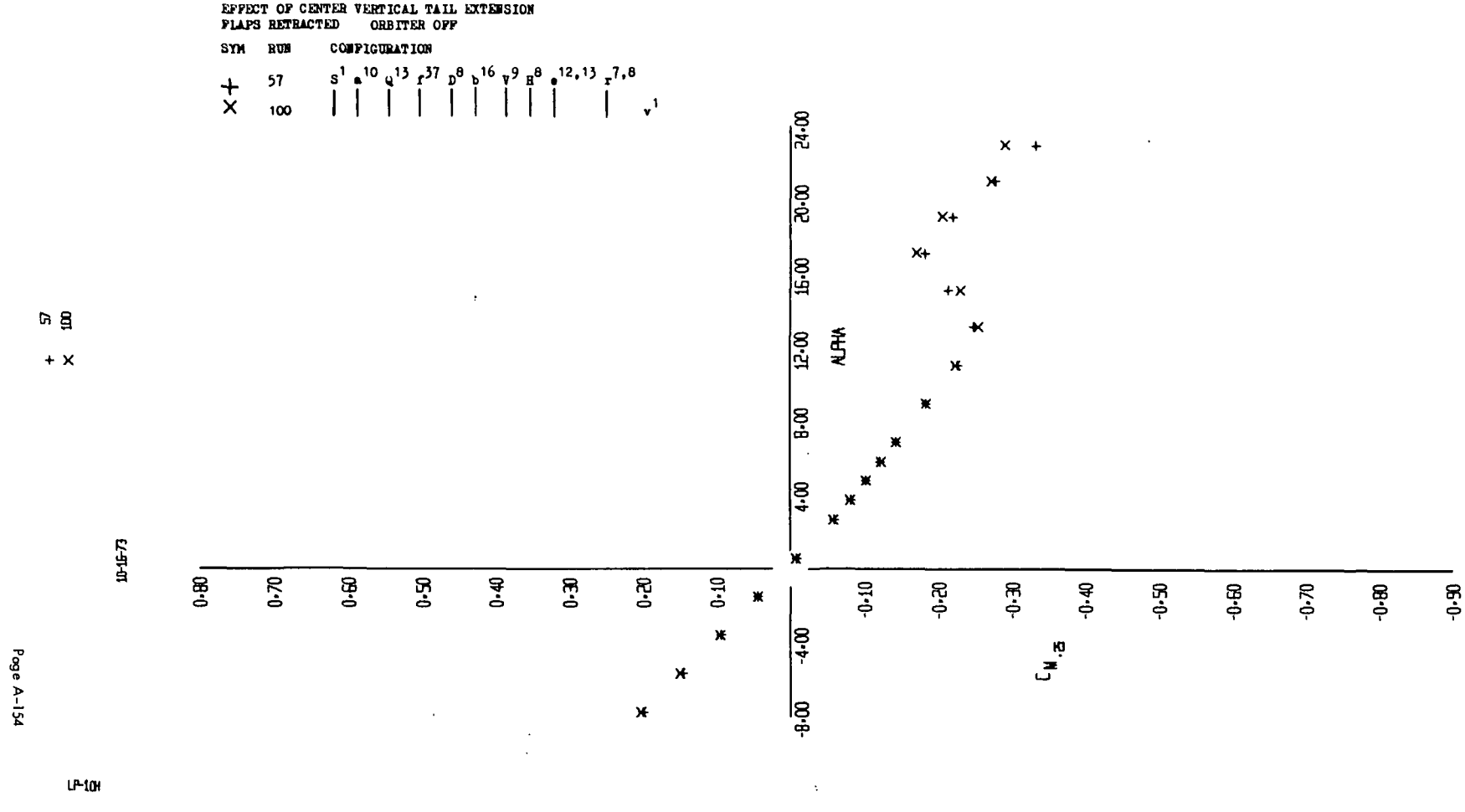

FIGURE 30 (SHEET 4)

EFFECT OF CENTER VERTICAL TAIL EXTENSION
FLAPS RETRACTED ORBITER OFF

SYM	RUN	CONFIGURATION
+	57	S^{1} a^{10} Q^{13} f^{37} D^{8} b^{16} V^{9} H^{8} $\bullet^{12,13}$ $r^{7,8}$
×	100	$\blacktriangledown^{1}$

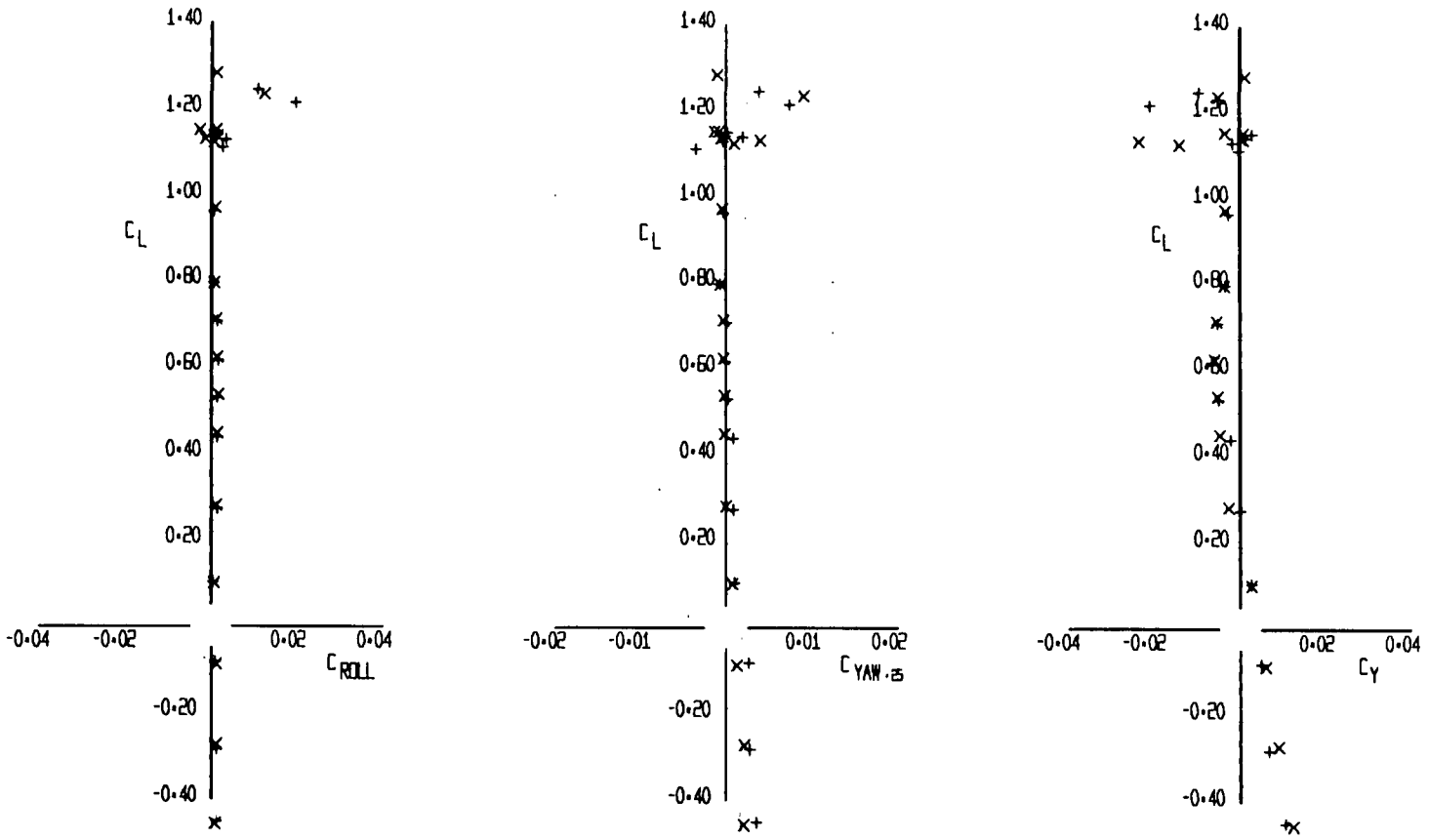

57 100
+ ×

10-15-73

Page A-155

LR-363

FIGURE 30 (SHEET 5)

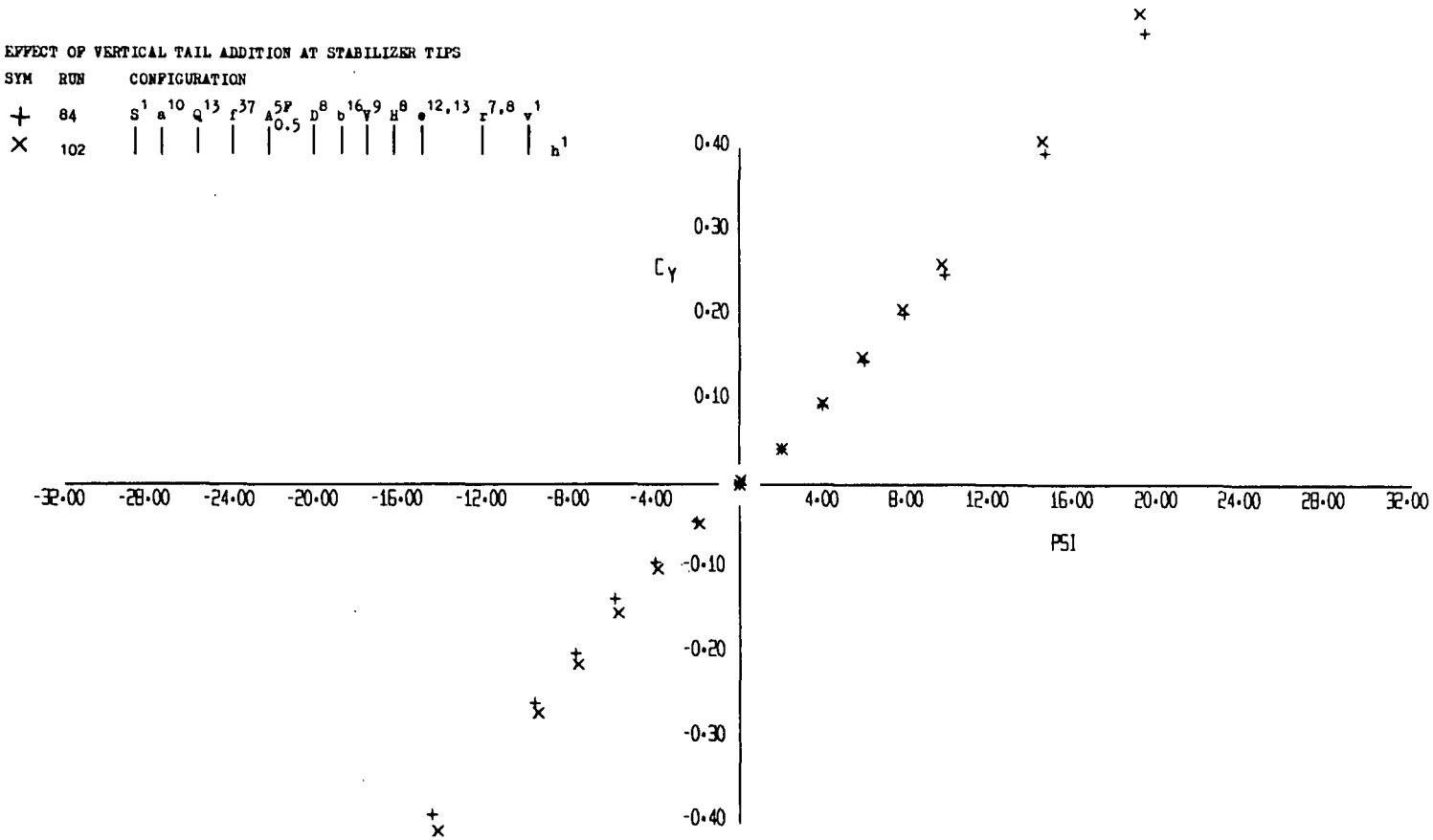

FIGURE 31 (SHEET 1)

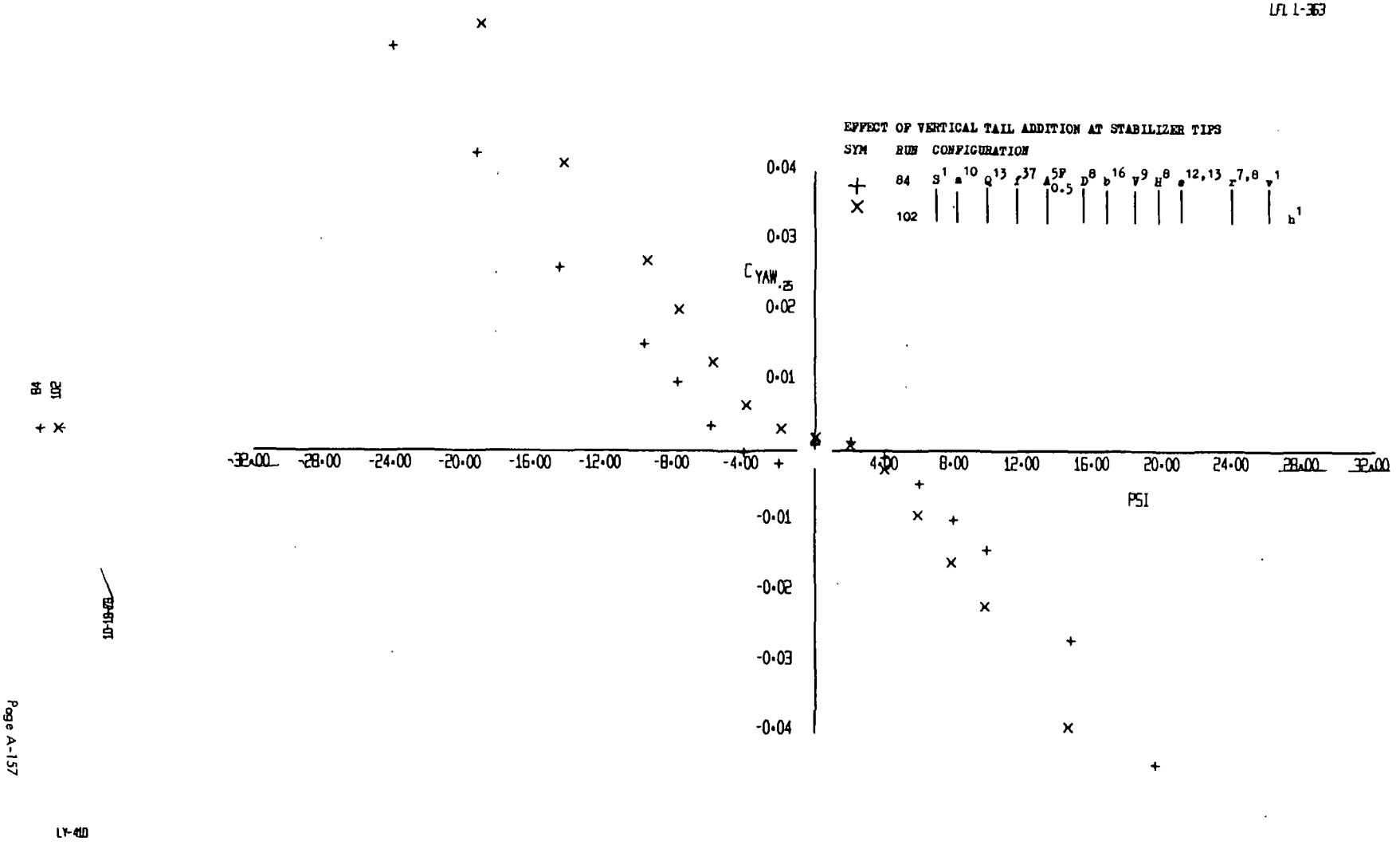

FIGURE 31 (SHEET 2)

LY-410

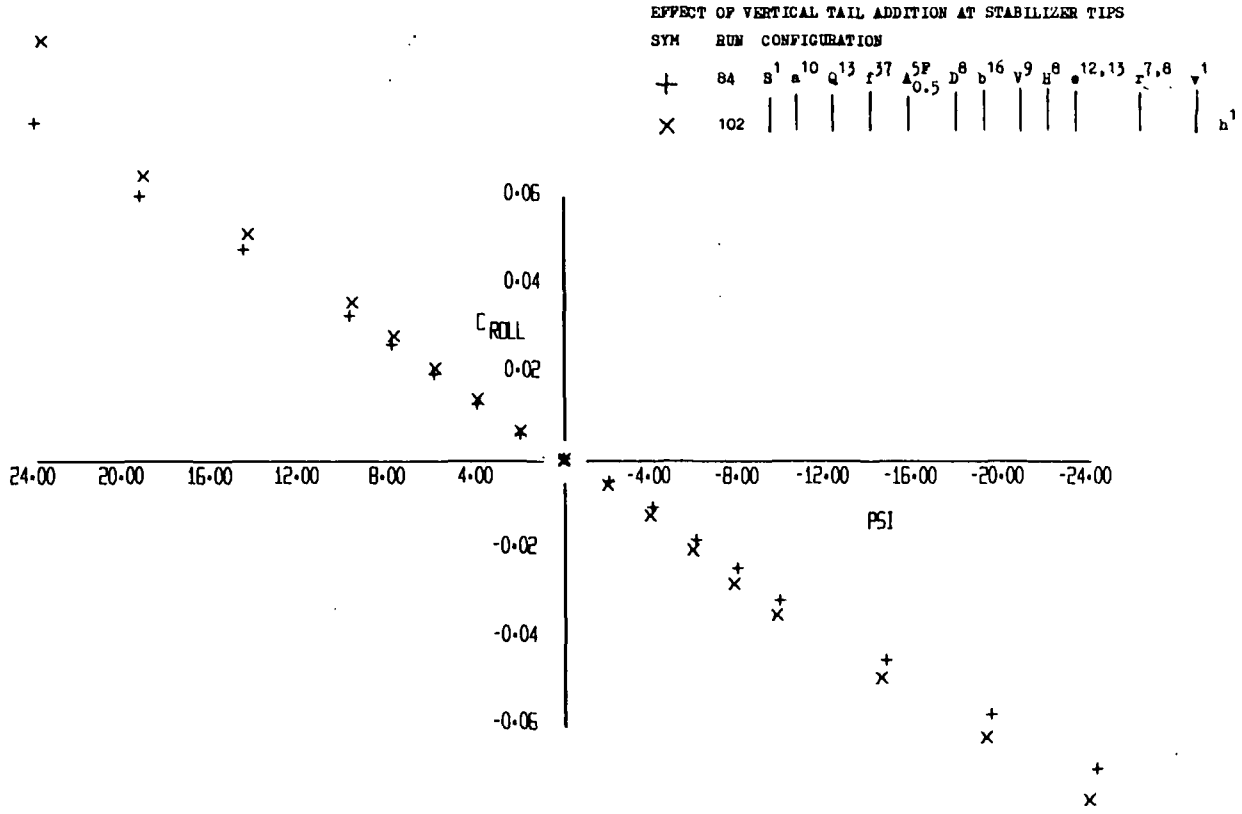

84 102

10-15-73

LY-408

FIGURE 31 (SHEET 3)

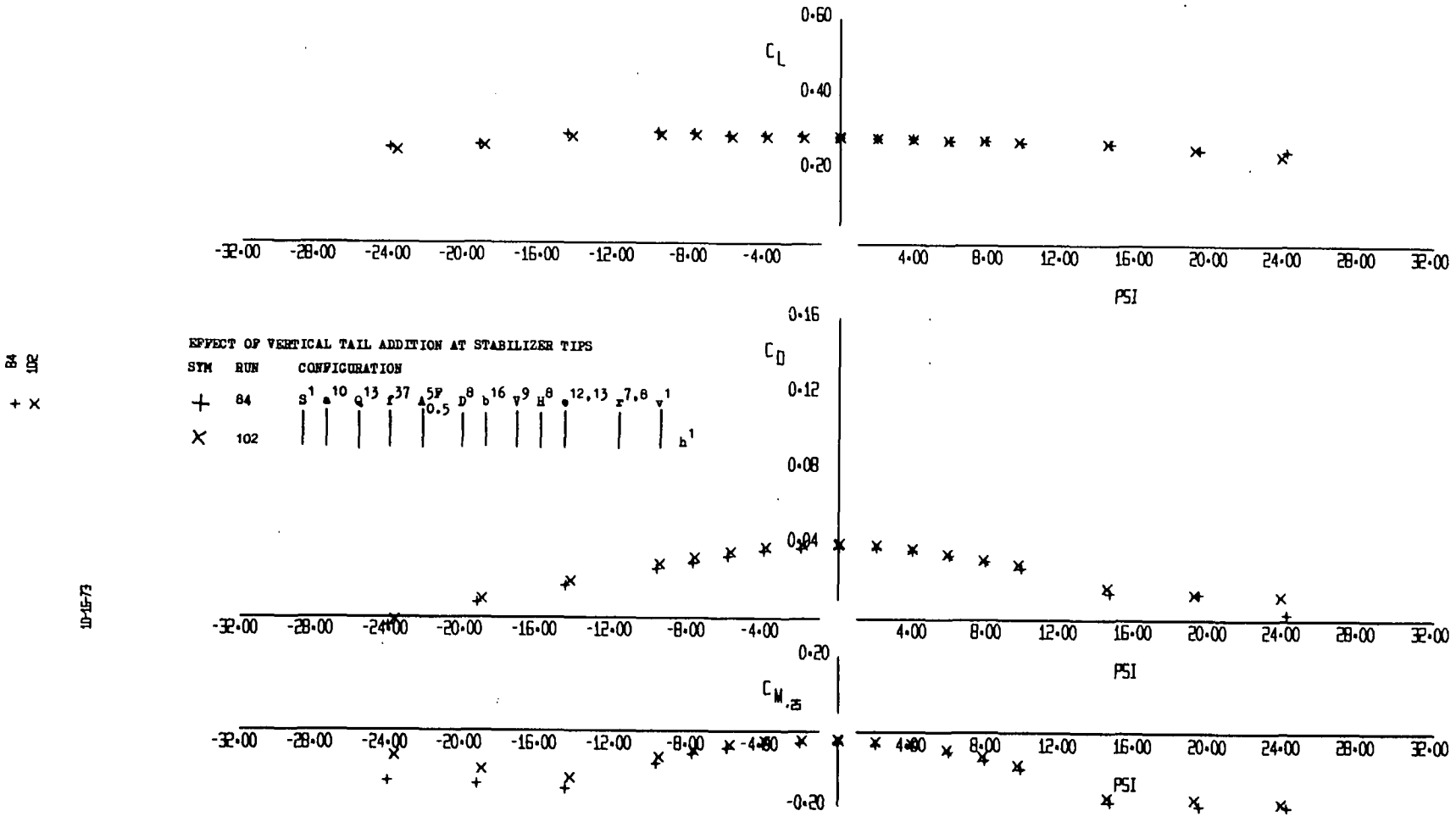

FIGURE 31 (SHEET 4)